The role of oncolytic virus-induced anti-tumour immunity in haematological malignancies

Louise Marie Erika Müller

Submitted in accordance with the requirements for the degree of
Doctor of Philosophy

The University of Leeds
School of Medicine

November 2018

Intellectual Property and Copyright Statement

The candidate confirms that the work submitted is her own and that appropriate credit has been given where reference has been made to the work of others.

Acknowledgements

First and foremost, I would like to thank my supervisor Dr Fiona Errington-Mais for invaluable guidance, advice, and patience during my time as a PhD student. I am forever grateful for your mentorship and for supporting my development as a scientist. I would also like to thank Dr Gina Scott for her advice on most of the practical aspects of this work, for many fruitful discussions, and for providing feedback during the writing of this thesis. In addition, I thank past and present members of Level 5 for their help, advice, and friendship throughout the last three years. In particular, I extend my gratitude to Gemma Migneco for expert assistance with the *in vivo* work performed in this thesis, and to Karen Scott and Emma West for providing access to STORM clinical trial Luminex results. I am also indebted to Professor Gordon Cook who assisted with securing funding for this PhD.

This work could not have been performed without the assistance of dedicated staff in the Haematological Malignancy Diagnostic Service and Haematology Department at St. James's University Hospital. In particular, I extend my gratitude to Dr Richard Kelly, Stewart McConnell, and Catherine Langton for assistance with securing access to patient samples, and to Matthew Cullen for providing diagnostic information and experimental advice. Furthermore, I would like to thank all the patients and healthy donors who have given their time, support, and clinical samples which have been instrumental for this work.

Lastly, I thank my family and friends for their continued support of my endeavours, and Matthew – without you, none of this would be.

Abstract

Haematological malignancies (HM) are a diverse group of relatively rare, but often life-threatening cancers. Over 900 000 people worldwide are expected to receive a HM diagnosis in 2018. Most types of HM have an increasing incidence with age, which is often associated with poor survival due to the inadequate treatment options available. Two types of HM with a particularly poor outlook are acute myeloid leukaemia (AML), which is an acute cancer of immature myeloid blood cells, and multiple myeloma (MM) which is an incurable malignancy with primary focus in the bone marrow (BM).

Oncolytic viruses (OV) preferentially infect and kill malignantly transformed cells. OV therapy (OVT) is a promising treatment strategy which has recently been approved for clinical use in the treatment of melanoma. In addition to direct lytic killing, the induction of an anti-tumour immune response is thought to be essential for efficient OVT with establishment of long-term protection against tumour recurrence. While research efforts into OVT for solid malignancies have seen a surge in recent years, HM remains under-investigated in this context, in particular with regards to the anti-tumour immune response. Thus, the overall aim of this study was to examine the role of OV-induced anti-tumour immunity in HM.

Two OV were evaluated in the context of MM; both reovirus and coxsackievirus A21 (CVA21) were found to induce anti-tumour immune responses *in vitro* comprising cytokine-mediated killing, natural killer cell-mediated cytotoxicity, and the generation of tumour-specific cytotoxic T cells. Moreover, reovirus treatment showed efficacy in an immunocompetent *in vivo* model, along with evidence of the onset of an immune response primarily in the spleen.

Pivotally, this study is the first to evaluate CVA21 as a treatment for AML. CVA21 was able to induce anti-tumour immunity in AML *in vitro* using both AML cell lines and a cohort of primary AML samples, despite resistance to lytic killing. Furthermore, examination of peripheral blood samples from patients with solid malignancies following intravenous administration of CVA21 provided “proof of principle” evidence that CVA21 was able to activate immune cells in the peripheral circulation in a state of malignancy, which is crucial for the future development of CVA21 OVT.

The obtained results also established the cellular mechanisms responsible for CVA21-induced anti-tumour immunity. Plasmacytoid dendritic cells were

identified as the main detectors of CVA21 infection and were responsible for orchestrating both innate and adaptive anti-tumour immune responses. These findings provide novel insights into the immunobiology of CVA21 with importance for the continued clinical development of this OV.

In conclusion, this study has demonstrated that OVT, as a well-tolerated, specific, and long-lasting therapy, has the potential to improve the treatment of both MM and AML through the induction of a multi-component anti-tumour immune response.

Table of Contents

List of Tables

List of Figures

List of Abbreviations

ADCC – antibody-dependent cellular cytotoxicity

ALL – acute lymphocytic leukaemia

AML – acute myeloid leukaemia

ANOVA – analysis of variance

APC – antigen-presenting cell

BiKE – bispecific killer cell engager

BM – bone marrow

CAR – chimeric antigen receptor

CD – cluster of differentiation

cDNA – complementary DNA

CIK – cytokine-induced killer cell

CLL – chronic lymphocytic leukaemia

CM – conditioned cell culture medium

CMC – carboxymethyl cellulose

CML – chronic myeloid leukaemia

CMV – cytomegalovirus

CPE – cytopathic effect

cpm – counts per minute

CTG – Cell Tracker™ Green CMFDA

CTL – cytotoxic T lymphocyte

CTLA-4 – cytotoxic T-lymphocyte-associated protein-4

CVA – coxsackie A virus

CVA21 – coxsackievirus A21

CVB – coxsackie B virus

DAF – decay-accelerating factor

DAMP – danger-associated molecular pattern

DC – dendritic cell (conventional)

DEPC – diethylpyrocarbonate

DMEM – Dulbecco's modified Eagle's medium containing 1% L-glutamine and 4500 mg/L glucose + 10% (v/v) foetal bovine serum

DMSO – dimethyl sulfoxide

DNAM-1 – DNAX accessory molecule-1

dsRNA – double-stranded RNA

dsDNA – double-stranded DNA

EGTA – egtazic acid

ELISA – enzyme-linked immunosorbent assay

E:T – effector:target (ratio)

Fas – First apoptosis signal

FasL – Fas ligand

FBS – foetal bovine serum

Fc – fragment crystallisable

FDA – U.S. Food and Drug Administration

FITC – fluorescein isothiocyanate

FLT3 – FMS-like tyrosine kinase 3

FSC – forward scatter

g – gravitational force

GM-CSF – granulocyte-macrophage colony-stimulating factor

HBSS – Hanks' Balanced Salt Solution

HEV-C – human enterovirus C

HDAC – histone deacetylase

HLA – human leukocyte antigen

HLP – hind limb paralysis

HM – haematological malignancy

hr – hour

HSC – haematopoietic stem cell

HSCT – haematopoietic stem cell transplantation

HSV-1 – herpes simplex virus type 1

ICAM-1 – intercellular adhesion molecule-1

ICP – infected cell protein

iDC – immature dendritic cell

IFN – interferon

Ig – immunoglobulin

IL – interleukin

IMiD – immunomodulatory imide drug

i.p. – intraperitoneal

IRF – interferon regulatory factor

ISG – interferon-stimulated genes

ITD – internal tandem duplication

i.v. – intravenous

JAM-A – junctional adhesion molecule-A

KIR – killer-cell immunoglobulin-like receptors

LAA – leukaemia-associated antigen

LAK – lymphokine-activated killer cell

LN – lymph node

LSA – leukaemia-specific antigen

mAb – monoclonal antibody

MDA5 – melanoma differentiation-associated protein 5

MDS – myelodysplastic syndrome

MDSC – myeloid-derived suppressor cell

MFI – median fluorescence intensity

MGUS – monoclonal gammopathy of undetermined significance

MHC – major histocompatibility complex

mL – millilitre

MM – multiple myeloma

MRD – minimal residual disease

mRNA – messenger RNA

MSC – mesenchymal stem cell

MUK11 – Myeloma UK Eleven clinical trial

MV – measles virus

nAb – neutralizing antibodies

NHL – non-Hodgkin lymphoma

NIS – sodium iodide symporter

NK – natural killer (cell)

NKT – natural killer T cell

n.s – not significant

OV – oncolytic virus

OVT – oncolytic virotherapy

p. – page

PAMP – pathogen-associated molecular pattern

PBMC – peripheral blood mononuclear cells

PBS – phosphate-buffered saline

PCR – polymerase chain reaction

PD-1 – programmed cell death protein-1

pDC – plasmacytoid dendritic cell

PD-L1 – programmed death-ligand-1

PE – phycoerythrin

PerCP – peridinin chlorophyll protein complex

PFA – paraformaldehyde

pfu – plaque-forming unit

pg – picogram

PGE_2 – prostaglandin E2

PHA – phytohaemagglutinin

PKR – protein kinase R

PRAME – preferentially expressed antigen in melanoma

PRR – pattern recognition receptor

PTEN - phosphatase and tensin homolog gene

PVR – poliovirus receptor

RAEB – refractory anaemia with excess blasts

Ras – rat sarcoma viral oncogene

Rb – retinoblastoma protein

RBC – red blood cell

RIG-I – retinoic acid inducible gene-I

ROS – reactive oxygen species

rpm – revolutions per minute

RPMI-1640 – Rosewell Park Memorial Institute-1640 medium containing 1% L-glutamine + 10% (v/v) foetal bovine serum

RT – room temperature

SCID – severe combined immunodeficiency

s.e.m – standard error of the mean

SMM – smouldering multiple myeloma

SSC – side scatter

ssRNA – single-stranded RNA

STAT – signal transducer and activator of transcription

STORM – Systemic Treatment Of Resistant Metastatic Disease clinical trial

T-Vec – talimogene laherparepvec

TAA – tumour-associated antigen

TAM – tumour-associated macrophage

$TCID_{50}$ – 50% tissue culture infective dose

TCR – T cell receptor

T_{EM} – effector memory T cell

TGF-β – transforming growth factor β

T_h1 – Type 1 helper T cell

T_h2 – Type 2 helper T cell

TLR – Toll-like receptor

TME – tumour microenvironment

TNF – tumour necrosis factor

TRAIL – TNF-related apoptosis-inducing ligand

T_{reg} – regulatory T cell

TriKE – trispecific killer cell engager

U – international unit

ULBP – UL16-binding protein

UV – ultraviolet light

VEGF – vascular endothelial growth factor

VSV – vesicular stomatitis virus

WHO – World Health Organisation

WT – wild-type

WT1 – Wilm's tumour antigen 1

Chapter 1
Introduction

Chapter 1
Introduction

1.1 Cancer and the immune system

1.1.1 Background

It has been known for over a hundred years that the immune system is intricately linked to the development of cancer. Early observations of tumour regression following infections with various pathogens, including bacteria and viruses, led William Coley to develop the world's first immunotherapy in the late 1800s. After observing one of his sarcoma patients experience a spontaneous tumour regression following a severe bacterial infection, he developed a preparation of two heat-inactivated bacterial strains as a treatment strategy for cancer patients (1). Coley's toxin demonstrated some therapeutic efficacy and was the start of an intense period of research into the immune system and its involvement in the development and progression of cancer, pioneered by Paul Ehrlich (2). This fundamental research has enabled the development of a range of different cancer immunotherapies which are transforming cancer treatment today and might finally give us a new weapon in this long-standing battle. Cancer immunotherapy aims to activate the immune system to recognise and destroy malignant cells and has the potential to generate long term anti-tumour immunity through the induction of immunological memory.

1.1.2 Immunosurveillance and anti-tumour immunity

Although Ehrlich had made similar hypotheses, the concept that lymphocytes can recognise and destroy nascent malignantly transformed cells was first formally introduced as the immunosurveillance hypothesis by Burnet and Thomas 50 years later. While this hypothesis was met with much scepticism in the beginning, it has been the focus of intense research efforts in the past 20 years and the role of the immune system in cancer development has become ever more apparent. Key experiments using knock-out mice initially highlighted the importance of different components of the immune system in cancer immunosurveillance, including interferon (IFN)-γ, perforin, interleukin (IL)-12, T cells, natural killer T (NKT) cells, and

natural killer (NK) cells (3). Accordingly, both the innate and adaptive immune systems play an integral role in cancer immunosurveillance.

1.1.2.1 Innate immune surveillance

The innate immune system is rapid and efficient and relies on the recognition of a broad range of pathogens via conserved non-self molecules (pathogen-associated molecular patterns), rather than specific antigens. Cells of the innate immune system utilise pattern recognition receptors (PRR), such as Toll-like receptors (TLR), for the detection of foreign pathogens. The cellular innate immune system is mainly comprised of neutrophils, macrophages, NK cells, NKT cells, γδ T cells, and dendritic cells (DC). IFN-γ is a key mediator of both innate and adaptive immune responses. The importance of IFN-γ for anti-tumour immunity was confirmed using murine models genetically deficient in the IFN-γ receptor or the IFN transcription factor STAT-1 (signal transducer and activator of transcription 1), which led to an increased rate of both spontaneous and chemically-induced tumours (4, 5). The source of IFN-γ was identified by a series of experiments utilising mice deficient in effector molecules of NK cells and their respective receptors, or lacking NKT cells, or γδ T cells. The increased tumour frequency observed in these mice confirmed the importance of NK cells, NKT cells, γδ T cells, in cancer immunosurveillance (6, 7).

1.1.2.1.1 NK cells

One of the most important parts of the innate immune system for recognising and destroying malignantly transformed and virally infected cells are the NK cells. NK cells monitor cells around the body for the expression of major histocompatibility complex (MHC) Class I molecules and cell stress markers, relying on the detection of self-molecules rather than foreign antigens for initiation of a response. The main regulator of NK cell cytotoxicity is the critical balance between engagement of activating and inhibitory receptors (Table 1-1). Healthy cells express high levels of MHC Class I and low levels of activating ligands on their surface. According to the “missing self” hypothesis, when tumour cells or virally infected cells down-regulate the expression of MHC Class I molecules on the cell surface, NK cells lose their inhibitory stimulation and their killing instinct is released (8). NKG2D has been identified as a dominant activating receptor on NK cells and ligation to one of its ligands (e.g. MIC A/B, ULBP-1, or ULBP-2) results in target cell lysis, independent of MHC Class I expression. Thus, NKG2D plays an

important role in recognition and killing of nascent tumour cells which manage to maintain the cell surface expression of MHC Class I (9, 10). Type I IFNs (IFN-α and IFN-β) also have a critical role in the recruitment and activation of NK cells in response to viral infection. The role of IFN in NK cell function is discussed in detail below (Section 1.4.1.2.1). The main mechanism of NK cell-mediated killing is a tightly regulated degranulation process resulting in the release of cytotoxic granules directed towards the target cell. Cytotoxic granules contain perforin, a pore-forming glycoprotein, and various proteases, such as granzyme B, which enter cells and induce a proteolytic cascade resulting in cell death (11, 12).

NK cells and the innate immune system should not be considered entirely in isolation. NK cells are able to act as a link between the innate and adaptive immune responses and have been shown to have 'helper' functions by assisting the development of an adaptive anti-tumour T cell response. One example is local secretion of IFN-γ by NK cells at the tumour site which can stimulate DCs, which in turn promote the generation of $CD8^+$ T cell anti-tumour responses (13, 14).

Table 1-1: Human NK cell receptors and their ligands (15).

Receptors	Ligands
Activating Receptors	
NKp30, NKp44, NKp46	Viral haemagglutinins and others undefined
NKG2D	MICA/B and ULBP 1-5
DNAM-1	PVR and Nectin-2
CD16	Immunoglobulin (Ig) G
NKG2C	HLA-E, HLA-C (low affinity)
Inhibitory Receptors	
Killer-cell immunoglobulin-like receptors (KIRs)	MHC Class I (HLA-A,B,C)
NKG2A/CD94	HLA-E

1.1.2.1.2 Dendritic cells (DC)

DC form a heterogenous population of both lymphoid- and myeloid-derived cells with importance for innate, as well as adaptive immune responses. DC are professional antigen-presenting cells (APC) which can prime both naïve T cells and B cells. Immature DC (iDC) reside in peripheral tissues, such as the skin, and continuously sample the local environment to capture antigens (16). While iDC have a high capability for phagocytosis and receptor-mediated endocytosis, their ability to activate T cells is limited, with low expression of MHC Class II, and co-stimulatory molecules CD80 and CD86 on the cell surface (17). Following antigen uptake, the DC matures, which is associated with several phenotypic changes including a redistribution of MHC molecules to the DC surface, down-regulation of antigen internalisation, and an increase in the surface expression of CD80 and CD86. Mature DC migrate to secondary lymphoid organs where the antigen is presented to T cells on MHC molecules (16).

As a result of their extracellular origin, the majority of antigens taken up by DC are presented on MHC Class II molecules to naïve $CD4^+$ T cells. Two main signals are thought to be required for DC activation of naïve $CD4^+$ T cells. The first signal is the engagement of peptide:MHC complexes on DC to a complementary T cell receptor (TCR) on the T cell. The second signal is mediated by the ligation of co-stimulatory molecules, such as CD80 and CD86, to their ligands on T cells (e.g. CD28 and CD40L). Both signals are essential for the differentiation of naïve T cells into mature T helper cells. In addition, a third cytokine signal determines whether the T cell response will be polarized towards a Th_1 or a Th_2 response. In addition to DC cytokine secretion, this often requires a contribution from other innate cells such as NK cells for generation of the appropriate cytokine milieu (18). The functions of T helper cells are further described below (Section 1.1.2.2.1).

Although phagocytosed antigen is normally presented on MHC Class II, adaptation of the endocytic and phagocytic pathways enable DC to also cross-present extracellular antigen on MHC Class I and thereby directly activate $CD8^+$ T cells (19). The cross-presentation of tumour-associated antigen (TAA) on MHC Class I is important for the generation of anti-tumour $CD8^+$ T cell responses (20).

1.1.2.2 Adaptive immune surveillance

The adaptive immune response employs two arms; the cell-mediated T cell response and the humoral B cell response. Unlike the innate immune system, which recognises non-self in an unspecific manner through PRRs, the adaptive immune response relies on specific antigen detection. Foreign antigens are detected by individual T or B cells specific for a single antigen, which results in the development of specific effector responses, and immunological memory with long-lived memory cells reactive to a specific antigen. $CD8^+$ T cells in particular have been identified as key components of cancer immunosurveillance, as mice lacking $CD8^+$ T cells fail to reject a tumour challenge which is rejected by immunocompetent mice, and similarly fail to control dormant tumour cells resulting in nascent malignancy (21-23).

1.1.2.2.1 $CD4^+$ T helper cells

As described above, DC induce activation of naïve $CD4^+$ T cells and stimulate their differentiation into mature helper T cells. Helper T cells provide stimulatory help to $CD8^+$ T cells or B cells to allow for an appropriate immune response depending on the type of infection encountered. Figure 1-1 demonstrates that following antigen presentation, a helper T cell can differentiate into either a Th_1 or a Th_2 cell based on the local cytokine milieu. In the presence of IFN-γ and IL-12, a Th_1 response is mounted. Secretion of IL-2 and IFN-γ from Th_1 cells is crucial for the activation and priming of antigen-specific $CD8^+$ cytotoxic T lymphocytes (CTL). CTLs are able to efficiently kill target cells suffering from an intracellular infection, e.g. a viral infection. In the presence of IL-4 and IL-2, a Th_2 response is generated, where the T cell provides help for the activation of B cells. IL-4 secretion from Th_2 cells is required for isotype switching in B cells, resulting in abundant secretion of antigen-specific antibodies, which are important for clearing extracellular infections, e.g. by bacteria or parasites. Under certain conditions, naïve $CD4^+$ T cells can also differentiate into other T cell subsets, such as regulatory T cells (T_{reg}) and Th_{17} cells (24).

1.1.2.2.2 $CD8^+$ cytotoxic T cells

Upon recognition of intracellular antigen presented on an MHC Class I molecule, naïve $CD8^+$ T cells differentiate into CTL. As described above, due to their high cytotoxic potential, CTLs are tightly regulated and usually require activation help from $CD4^+$ T cells (25). However, DC can also directly cross-present exogenous antigen on MHC Class I to $CD8^+$ T cells (Section 1.1.2.1.2). When CTLs encounter antigen they have been primed against,

they can kill that target cell using a mechanism similar to that of NK cells. Following antigen-specific degranulation, cytotoxic granules containing perforin and granzyme are released, which resulting in the death of the target cell.

The genetic instability of tumour cells often leads to the presentation of mutated, overexpressed, or germline-related proteins which are uniquely related to tumour cells, so called TAA, on MHC molecules. Examples of different types of TAA related to haematological malignancies are presented in Table 1-2. In the case of leukaemia, these can be either leukaemia-specific antigens (LSA), leukaemia-associated antigens (LAA), or cancer-testis/germline antigens (26). LSAs are exclusively expressed on leukaemic cells and are often fusion proteins arising from chromosomal translocations, e.g. AML1-ETO, or tumour-specific mutated proteins such as the internal tandem duplication (ITD) of the FMS-like tyrosine kinase 3 gene (*FLT3*). LSAs are the most ideal targets for development of leukaemia-specific immunotherapies. LAA can be expressed on both normal and leukaemic cells, e.g. Wilms' tumour protein 1 (WT1). In B cell malignancies, including multiple myeloma, the variable regions or idiotypes of immunoglobulin heavy and light chains can serve as tumour-specific antigens following malignant proliferation of a selected B cell clone, with all daughter cells expressing the same idiotype (27). The recognition of TAA by $CD8^+$ T cells can lead to the priming of tumour-specific CTLs, an important function of immunosurveillance.

As discussed below, the identification of TAA and their importance for adaptive anti-tumour immunity has allowed the development of immunotherapeutic strategies such as DC vaccines.

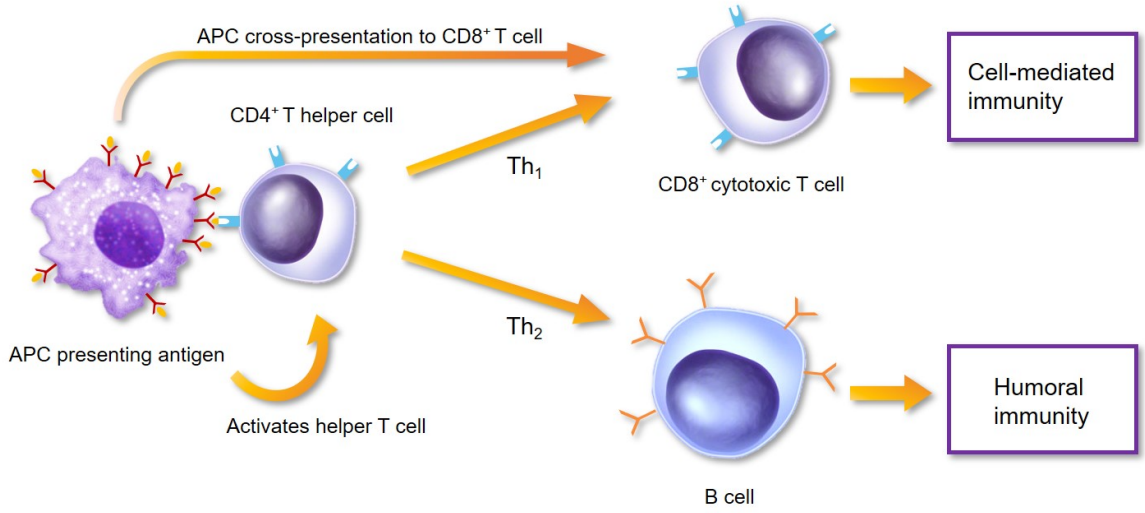

Figure 1-1: T cell responses following antigen presentation.

Following uptake of exogenous antigen in the peripheral tissues, APCs such as DC migrate to secondary lymphoid organs where they present antigen to T cells. DC can either present antigen on MHC Class II to $CD4^+$ T cells, or cross-present antigen directly to $CD8^+$ T cells on MHC Class I. Antigen presentation to naïve $CD4^+$ T cells, in combination with co-stimulatory signals from the APC, results in maturation of naïve cells into T helper cells. Different types of antigens induce different types of cytokine responses from innate immune cells, which determines the differentiation of helper T cells into either Th_1 or Th_2 cells. Through the secretion of IL-2 and IFN-γ, Th_1 cells provide help in the activation and antigen priming of $CD8^+$ cytotoxic T cells which are responsible for T cell-mediated immunity and eradication of cells with an intracellular infection. Through the secretion of IL-4, Th_2 cells provide help to B cells in the production of antigen-specific antibodies as part of humoral immunity and eradication of extracellular infections. APC: antigen-presenting cell.

Table 1-2: Common tumour-associated antigens in haematological malignancies (26, 28).

Disease	Category	Examples
Multiple Myeloma	**Overexpressed genes**	Mucin-1 PRAME hTERT
	Cancer-testis/ germline	MAGE-A1-4 NY-ESO-1 GAGE-1,2 BAGE
Multiple Myeloma & Lymphoma	**Idiotype**	Patient-specific
AML	**Leukaemia-specific (LSA)**	AML1-ETO PML-RARα FLT3-ITD NPM1
	Leukaemia-associated (LAA)	WT1 Mucin-1 Survivin hTERT Bcl-2 RHAMM
	Cancer-testis/ germline	PRAME MAGE RAGE-1

1.1.3 Revised model of immunosurveillance: immunoediting

Although the immune system might protect us against cancer to some extent, we still see tumours forming even in the presence of an intact immune system. Thus, the immunosurveillance hypothesis of interaction between the immune system and malignant cells was expanded on with the immunoediting model. This model, first described by Dunn *et al.*, describes in more detail the effect that the immune system has on cancer progression. Three dynamic processes known as the three Es: elimination, equilibrium, and escape, describe how tumour cells are initially eradicated, but gradually become less immunogenic due to selective pressure, finally resulting in immune escape (3, 29).

1.1.3.1 The three Es of immunoediting

1.1.3.1.1 Elimination

The first step in immunoediting is the elimination phase, which represents the original idea of cancer immunosurveillance. The immune system detects and eliminates nascent malignant cells, and if all transformed cells are eradicated, this completes the immunoediting process without progression to the next phase (3). As described above, immunological rejection of developing tumour cells likely involves both innate and adaptive immune responses (30).

1.1.3.1.2 Equilibrium

As it was observed that tumours, nonetheless, develop in immunocompetent individuals, it was proposed that some tumour cells which avoid immune cell elimination eventually enter the equilibrium phase. In this phase, tumour cells exist in a dynamic equilibrium with the immune system. Immune cells confer a selection pressure on tumour cells which is enough to contain, but not fully eliminate a genetically unstable tumour. This is a delicate balance as although many of the original tumour cells are successfully eliminated, new mutations arise concurrently in progeny cells, resulting in selection of tumour cells with increased resistance to anti-tumour immunity. Eventually, this generates a population of tumour cell clones with reduced immunogenicity and/or the capability of evading the anti-tumour immune response (3).

1.1.3.1.3 Escape

The escape phase details how tumour cells evade anti-tumour immunity and explains how, eventually, tumours arise even in individuals with a fully functional immune system. Tumour variants which have evolved under an immunological selection pressure finally escape immune system control and are able to proliferate uncontrollably in an immunologically intact environment resulting in progression to clinically overt malignant disease (3). Mechanisms of tumour escape are detailed in the following sections.

1.1.4 Tumour immune evasion

As discussed by Hanahan and Weinberg in their Next Generation Hallmarks of Cancer hypothesis, tumour cells acquire an ability to avoid the immune system, escape immunosurveillance and successfully establish an independently growing tumour (31). Tumours evade the immune system by a variety of mechanisms, including 1) reduced immunogenicity, which limits immune recognition, 2) increased resistance to immune-mediated cell death, and 3) induction of immune tolerance.

1.1.4.1 Loss of immunogenicity

One way of evading immune detection is to lose characteristics that are recognised as “non-self” or foreign by the immune system. As discussed above, TAA unique to tumour cells can be presented on MHC Class I molecules and mediate an adaptive anti-tumour immune response. Thus, one way of avoiding this response is to down-regulate the surface expression of classical MHC Class I molecules (HLA-A/B/C), or various components of the antigen presentation machinery (32, 33). However, while escaping adaptive immunity, loss of MHC Class I expression attracts the attention of NK cells and render abnormal cells targets for NK cell cytotoxicity (8). To also escape this response, many tumour cells maintain the expression of non-classical MHC Class I molecules, (e.g. HLA-E and HLA-G) which can protect them from NK cell recognition and immunocytotoxicity (34).

1.1.4.2 Increased resistance to immune cell death

Another way of escaping anti-tumour immunity is to increase resistance to immune-mediated death. Examples of this include manipulating the Fas/Fas ligand (FasL) and TRAIL (tumour necrosis factor-related apoptosis-inducing ligand) apoptotic pathways, modulating immune checkpoint molecules, as well as increased expression of the anti-phagocytosis protein, CD47.

1.1.4.2.1 Apoptosis pathways

Fas (first apoptosis signal) receptor is a death receptor which can be present on different types of cells, including immune cells. Activation of this receptor is mediated by binding to FasL, which results in induction of apoptosis in receptor-expressing cells. FasL can be overexpressed on several types of tumour cells, which enables them to induce apoptosis of immune cells (35). While tumour cells can also express Fas receptor and therefore become susceptible to apoptosis by immune cells, many tumour cells down-regulate the expression of Fas receptor, which in combination with the increased expression of FasL is an efficient strategy for immune evasion (36). In a similar strategy, TRAIL receptors, which also activate the extrinsic apoptosis pathway following binding of their ligand, TRAIL, is down-regulated in many cancers, resulting in a more aggressive phenotype (37, 38). Additionally, the intrinsic apoptosis pathway can be exploited by tumour cells to evade apoptosis. Through overexpression of anti-apoptotic proteins, such as Bcl-2, engagement of the pathways leading to caspase activation is prevented, resulting in increased resistance to apoptosis (39).

1.1.4.2.2 Immune checkpoint molecules

Due to their potency, T cell responses are tightly regulated. Immune checkpoints play an important role in the balance between stimulatory and inhibitory signals in the T cell response. One of the most well-studied inhibitory immune checkpoint molecules is programmed cell-death protein 1 (PD-1) and its ligand (PD-L1). When engaged, PD-1 conducts inhibitory signals in T cells which result in inhibition of both T cell proliferation and secretion of important T cell cytokines like IL-2 and IFN-γ (40, 41). Thus, as an immune evasion strategy, tumour cells upregulate the expression of PD-L1 to limit immune effector cell functions. The importance of immune checkpoint molecules in immunotherapy is discussed further below (Section 1.3.3.4) (42).

1.1.4.2.3 Phagocytosis

Phagocytosis of dead and dying cells, so called programmed cell removal, is another important way for the immune system to remove abnormal cells and thus, evasion of phagocytosis is another strategy for increasing resistance to immune cell-mediated death (43). CD47 is normally expressed on healthy cells to prevent them from being phagocytosed. CD47 binds to its receptor, SIRPα, on macrophages and DCs and inhibits their phagocytic activity. Similarly, by increasing the expression of CD47 on the surface, tumour cells can evade immune cell phagocytosis (44).

1.1.4.3 Induction of immune tolerance

In addition to central tolerance (thymus depletion), which is critical for the development of T and B cells that only react to “non-self” antigen, peripheral tolerance acts as a backup to eliminate or inhibit cells which escaped central tolerance. Peripheral immune tolerance can also be exploited by tumour cells to evade immune attack. The induction of immune tolerance requires a specific, suppressive environment in which antigen-presenting cells are incapable of generating and supporting an effective immune response and instead induce tolerance against specific TAA. Both soluble factors and suppressive cells contribute to generate this local suppressive tumour microenvironment (TME).

1.1.4.3.1 Soluble suppressive factors

Tumour cells can secrete a range of immunosuppressive cytokines in the local microenvironment, including e.g. transforming growth factor β (TGF-β), vascular endothelial growth factor (VEGF), prostaglandin E2 (PGE_2), and IL-10. While TGF-β is a potent inhibitor of proliferation in most cells, many tumour cells have developed mutations to resist this effect. However, as immune cells remain responsive to TGF-β, its secretion can have detrimental effects on the anti-tumour immune response (45). TGF-β also induces the differentiation of T_{regs} (discussed below) (46). VEGF has important implications both as an angiogenic agent to promote tumour growth, but also for recruiting immature myeloid cells to the local environment (47). However, the local immunosuppressive environment induced by e.g. TGF-β, VEGF, and IL-10 suppresses the differentiation and maturation of immature myeloid precursors into professional APCs, such as DCs and macrophages. Ultimately, this results in an impaired adaptive immune response where TAA are not presented efficiently to T cells within the TME (48). The role of IL-10

and its effect on the immune response remains controversial, but similar to PGE_2, a range of effects on cancer progression have been reported. Importantly, secretion of both IL-10 and PGE_2 contributes to tumour-induced suppression of both NK cell function and IFN-γ secretion (49).

1.1.4.3.2 Induction of suppressive cells

A range of different cells have suppressive roles in the immune system with the ultimate goal of protecting the body against auto-immune disease. When hijacked by a tumour, these cells can limit the onset of efficient anti-tumour immune responses. One cell type which is critical for the maintenance of peripheral tolerance against self-antigens is T_{regs}, and many studies have indicated that the presence of T_{regs} in the TME correlates with a worse prognosis in several types of cancers (50-52). T_{regs} inhibit the immune response by multiple mechanisms, including perforin-mediated direct cytotoxicity against $CD4^+$ and $CD8^+$ T cells, monocytes, and DC; secretion of immunosuppressive cytokines which, as discussed above, can have direct suppressive effects on immune cells; as well as the induction of T cell inhibitory receptors on APC, such has B7-H4 (53, 54).

Tumour-associated macrophages (TAM) are macrophages present at high numbers in the TME which often have a tumour-promoting phenotype. Classically, TAMs have been categorised as either M1 or M2 macrophages. M1 macrophages have a pro-inflammatory phenotype and can be both directly cytotoxic through the production of nitric oxide and reactive oxygen species (ROS), or as mediators of a Th_1 response with recruitment of CTL (55). On the contrary, M2 macrophages have an anti-inflammatory and tissue-healing phenotype and are thereby often tumour-promoting. However, according to recent research, these cells are likely forming a much more heterogeneous spectrum depending on the individual tumour and its local environment. TAMs with an M2 phenotype are most prevalent in the TME and can utilise many of the immune evasion strategies previously discussed. For example, they produce IL-10, TGF-β, and PGE_2, and express PD-L1 as well as FasL and TRAIL (56, 57).

Finally, myeloid-derived suppressor cells (MDSC) are a heterogeneous population of cells consisting of both myeloid progenitor cells and immature myeloid cells. Two subsets have been identified; the monocytic MDSCs which are phenotypically and morphologically similar to monocytes, and the granulocytic MDSCs which are more similar to neutrophils. In addition to immunosuppressive effects which promote immune evasion, MDSCs also promote tumour angiogenesis and growth through the secretion of various

cytokines and growth factors (58). MDSCs have several elaborate ways of inhibiting T cell responses including arginine depletion, and production of nitric oxide and ROS. Arginine is crucial for the production of the CD3 ζ-chain, which is an essential part of the TCR (59). Nitric oxide can induce apoptosis in T cells and interfere with IL-2 signalling, critical for T cell activation and proliferation. Through both secreted and membrane-bound TGF-β, MDSCs also suppress the function of NK cells and recruit T_{regs} to the TME (58). Similar to TAMs, a higher level of MDSCs in the peripheral blood is correlated with a worse prognosis in many types of solid and haematological malignancies (58).

With such an extensive range of immune evasion strategies available to tumour cells, identifying methods for reversing tumour-induced immune tolerance and local immunosuppression is critical for the generation of efficient anti-tumour immunity.

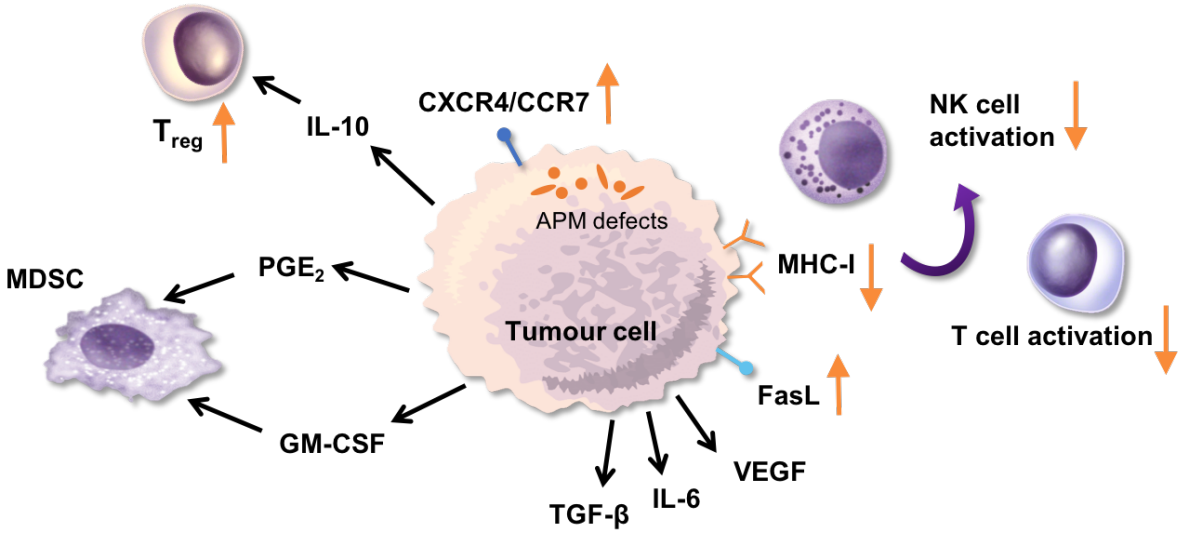

Figure 1-2: Examples of tumour immune evasion strategies.

Tumour cells have many different methods for escaping the immune system, including loss of immunogenicity, increased resistance to immune cell-mediated death, and induction of immune tolerance. Loss of immunogenicity can be mediated by defects in the antigen-processing machinery (APM) and a reduced expression of classical MHC Class I molecules, resulting in T cell escape. Maintained expression of non-classical MHC Class I molecules circumvents NK cell detection. An increased expression of FasL enables tumour cells to induce apoptosis of immune cells. In combination with reduced expression of Fas, the tumour cell can evade eradication attempts from immune cells utilising this pathway, e.g. NK cells. In addition, tumour cells secrete a range of immunosuppressive cytokines in the local TME, such as TGF-β, VEGF, PGE_2, and IL-10. These cytokines can on their own dampen immune cell responses, but can also lead to the recruitment and differentiation of immunosuppressive cells such as T regulatory cells and MDSCs.

1.2 Haematological malignancies

Haematological malignancies (HM) are cancers of the blood and immune cells. An overview of normal human haematopoiesis is provided in Figure 1-3. Typically, HM arise as a result of malignant transformation of immature blast cells during haematopoiesis, but can also arise in terminally differentiated cells such as plasma cells. The HM are a diverse group of diseases as they include both acute and chronic diseases, cells of both myeloid and lymphocytic origin, and various tumour sites, including the peripheral blood, bone marrow (BM), and lymph nodes. As described in Figure 1-4, the three main groups of HM are: leukaemias, which arise from abnormal white blood cells in the blood and BM; lymphomas, which arise from lymphocytes and target the lymphatic system and lymph nodes; and finally, multiple myeloma which is a plasma cell malignancy predominantly residing in the BM.

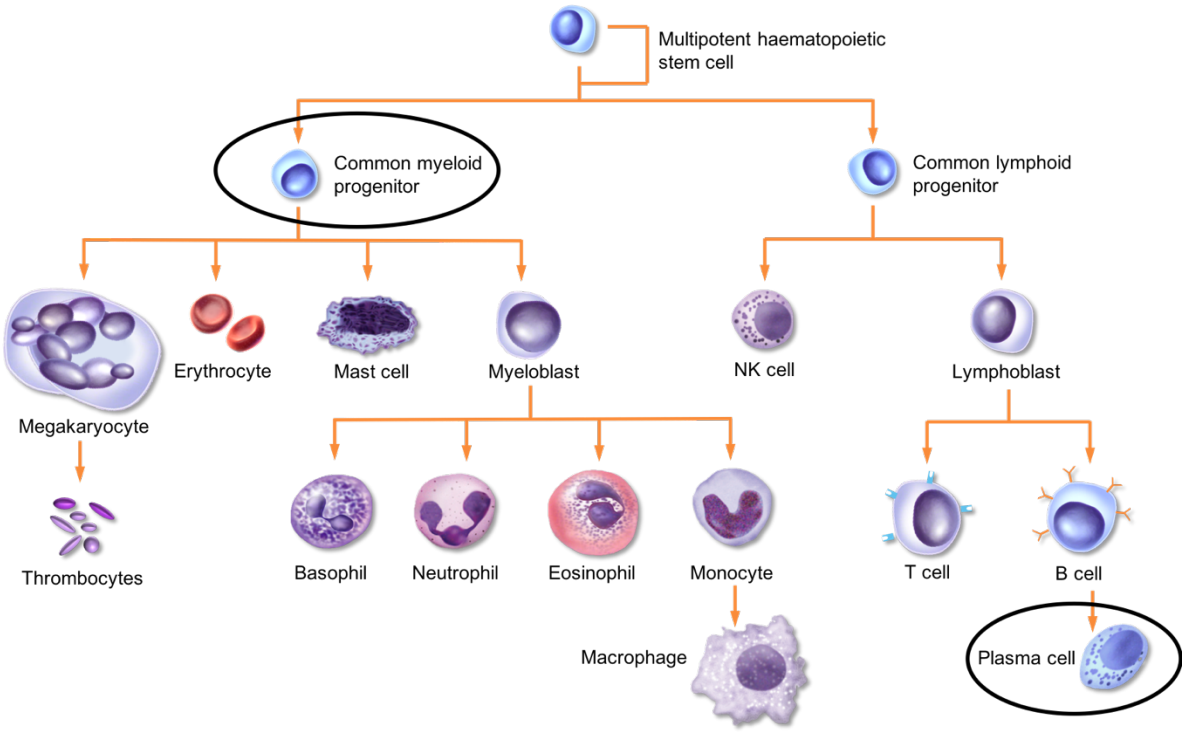

Figure 1-3: Human haematopoiesis.

All haematopoietic cells arise from multipotent haematopoietic stem cells in the BM. Following complex interactions of growth factors, transcription factors, and gene expression patterns, common progenitor cells committed to either the myeloid or lymphoid lineage develop. Within each lineage, the common progenitor cells give rise to a range of different cell types with specialised functions following extensive differentiation. Mutations in common progenitor cells or other immature cells during differentiation can give rise to leukaemia, e.g. acute myeloid leukaemia. Mutations can also occur in terminally differentiated cells, e.g. plasma cells, which give rise to multiple myeloma.

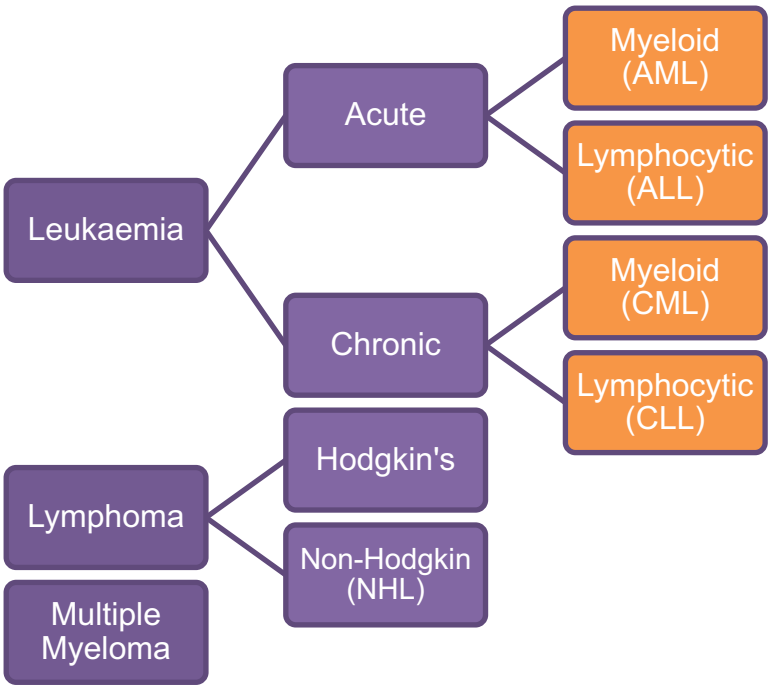

Figure 1-4: Main subtypes of haematological malignancies.

Haematological malignancies have been subdivided based on their haematopoietic origin and tumour location. Leukaemias predominantly reside in the BM and peripheral blood and can be either acute or chronic in their development. Depending on the cell types involved, the leukaemias can be further subdivided into myeloid or lymphocytic, giving four main types (orange). Lymphomas are located to lymph nodes and exclusively involve lymphoid cells. Based on the presence or absence of multinucleated B cell-derived Reed-Sternberg cells, lymphomas are further subdivided into Hodgkin's or non-Hodgkin lymphomas (NHL), respectively. NHL is further subdivided into more than 60 unique subtypes (not shown). Multiple myeloma is a malignancy of terminally differentiated B cells (plasma cells) primarily residing in the BM.

1.2.1 Multiple Myeloma

As discussed, multiple myeloma (MM) is a tumour of terminally differentiated plasma cells (Figure 1-3) which reside and expand in the BM. One of the hallmarks of MM is the onset of osteolytic bone disease due to increased bone resorption by osteoclasts and a complete loss of osteoblast function, resulting in a net loss of bone tissue. This rapid and extensive bone destruction is one of the most debilitating features of MM and often results in bone pain, fractures, hypercalcaemia, and spinal cord compression syndromes, which has extensive impact on the overall quality of life and expected survival (60). Furthermore, like their normal counterparts, MM cells produce large amounts of immunoglobulin, but in MM these proteins (known as paraprotein or M-band) are abnormal and dysfunctional, and largely contribute to the progression of the disease due to their role in the development of kidney and heart disease (61). Two premalignant stages of MM exist; monoclonal gammopathy of undetermined significance (MGUS) and smouldering MM (SMM). While both diseases are asymptomatic with no end-organ damage (hypercalcaemia, renal failure, anaemia, or bone lesions), MGUS has a 1% per year progression rate to MM, compared to 10% for SMM (62).

Another characteristic of MM is the heterogeneous chromosomal aberrations and often numerous mutations in a multitude of genes, which makes therapeutic targeting difficult. The transformation of normal, terminally differentiated plasma cells into proliferating cells requires genetic changes that disrupt the cell cycle arrest, commonly in the cyclin D protein family which regulates the G1/S transition of the cell cycle (62). Chromosomal translocations resulting in activation of cyclin D proteins are one of the most common initiating events of MGUS (62). Several genetic alterations are related to the transition from MGUS to MM, such as mutations in oncogenes Myc, and Ras, as well as further chromosomal deletions and translocations. Overt MM is often characterized by additional mutations in genes such as *KRAS*, *NRAS*, *BRAF*, *TP53*, and *DIS3*. Further progression involves increased genomic instability with an enhanced proliferation rate and decreased dependence on the BM microenvironment, resulting in plasma cell leukaemia and extramedullary metastasis with formation of plasmacytomas. One of the main contributors to BM independence is a constitutive activation of the NF-κB pathway (62, 63).

There is a worldwide incidence of myeloma of about 114 000 cases per year, with an average 5700 cases diagnosed in the UK. It is the second most

common HM, and incidence is expected to increase over the coming decades (64). MM is a chronic disease which is developing slowly and the average five-year survival rate across all age groups in the UK is 47.0%. However, in patients >85 years of age, where incidence is the highest, five-year survival is only 24.0% (64).

While autologous stem cell transplantations have proven successful for prolonging survival in systemic MM and have become an important part of MM management, many patients are ineligible for such radical treatment due to frailty and comorbidities. For chemotherapeutic regimens, first-line treatments include traditional drugs such as melphalan, prednisone/dexamethasone, and thalidomide in combination with more novel therapeutics such as the proteasome inhibitor, bortezomib, immunomodulatory drugs, such as lenalidomide or pomalidomide (Section 1.3.3.2), and monoclonal antibodies (Section 1.3.3.5). After 12-18 months, treatment is usually switched to a consolidation/maintenance strategy. Treatment of relapsed MM is complicated and the therapeutics used depend on initial treatment chosen and resistance patterns. New agents specifically approved for the treatment of relapsed/refractory MM include the proteasome inhibitor, carfilzomib, pomalidomide, and the histone deacetylase (HDAC) inhibitor, parabinostat (65).

However, despite recent advances in treatment which have prolonged overall survival rates, MM remains an incurable disease. With an expected rise in the incidence in an ageing population, it is evident that new treatments which are efficient, durable, and less harsh on elderly patients are urgently required. As described below, several immunotherapeutic strategies, including oncolytic viruses, are being tested in MM and have the potential to prolong survival or even be curative.

1.2.1.1 The bone marrow microenvironment in multiple myeloma

The BM microenvironment is intricately linked to successful establishment of MM lesions and has extensive impact on disease progression and resistance. As a protective niche, the BM microenvironment provides support for MM cell infiltration, growth, proliferation, adhesion, and migration. It also affords a structural and nutritional sustenance for drug-resistant, dormant MM cells (66). As illustrated in Figure 1-5, the BM has a diverse cellular composition. In addition to haematopoietic stem cells (HSC) which are responsible for the continuous production of haematopoietic cells,

mesenchymal stem cells (MSC) are important for regulating bone remodelling and can differentiate into various types of BM cells including osteoblasts, adipocytes, and chondrocytes. Stromal cells such as endothelial cells and fibroblasts provide structural support for the growth of HSCs, together with the extracellular matrix. Normally, the BM is a relatively hypoxic niche, which is imperative for normal haematopoiesis. However, MM cells have been shown to modulate the oxygen supply both by inducing neovascularisation to make the local microenvironment more supportive of tumour expansion and through increased expression of the transcription factor hypoxia-inducible factor (HIF-1α), promoting several cellular changes improving resistance to the effect of hypoxia (67). Moreover, a host of immunomodulatory cells reside in the BM including NK cells, T cells, B cells, T_{regs}, MDSC, and macrophages (68). These cells can provide inflammatory agents such as cytokines, chemokines, adipokine, and growth factors which can contribute to MM cell growth and drug resistance, as well as toxicity against healthy cells. T_{regs} and MDSCs can induce local immunosuppression to further protect MM cells (9). A wide range of soluble factors in the BM microenvironment influence the growth of MM cells in the BM, but IL-6 is of particular importance for MM cell proliferation and survival (69).

Recently, a lot of research has been invested in examining the interaction of MM cells with the BM microenvironment. As a complement to standard treatment, therapies that target the BM microenvironment specifically, such as bisphosphonates, find increasingly more use in MM treatment and demonstrates that targeting the BM niche can be yet another strategy in eradicating MM (70, 71).

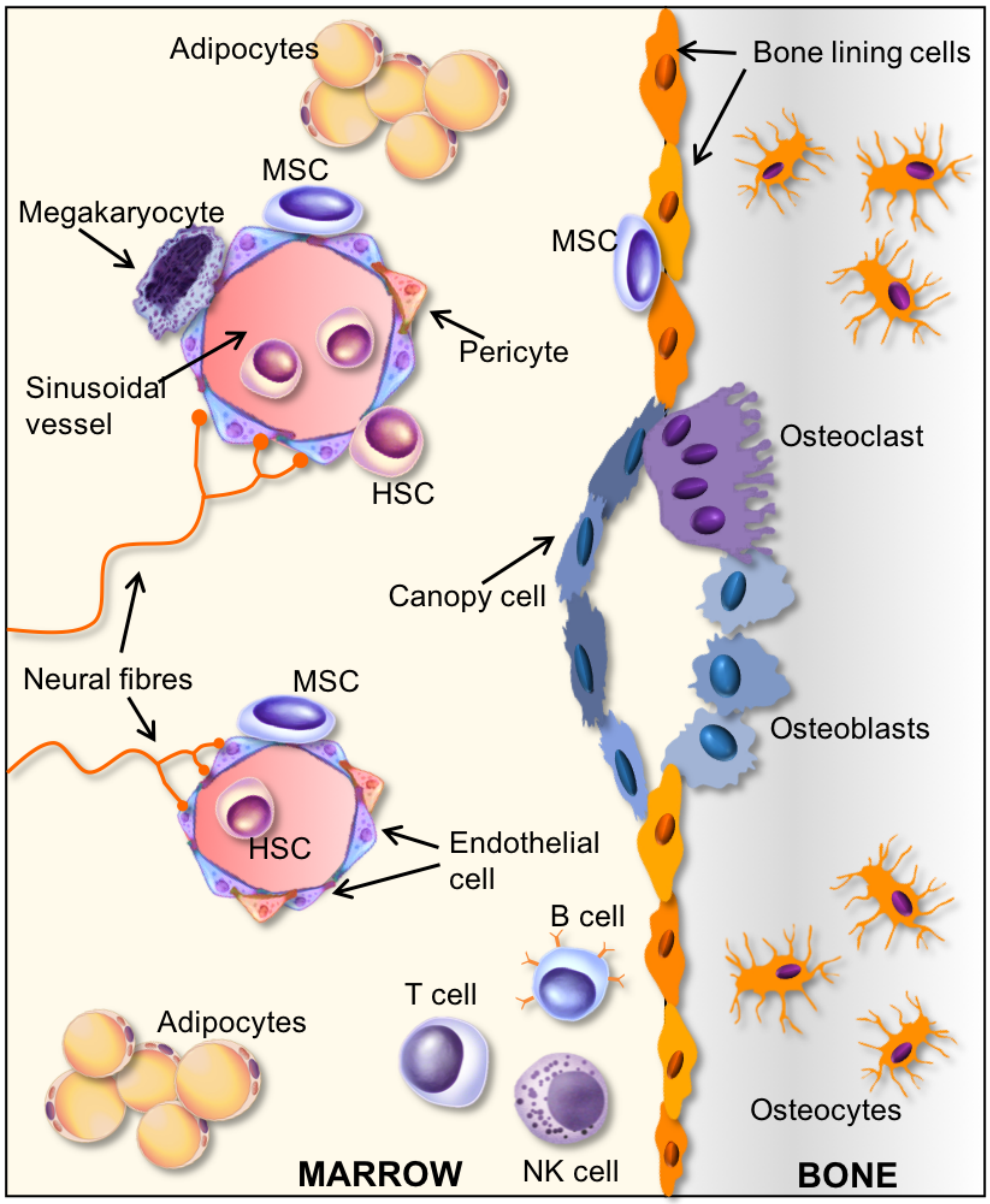

Figure 1-5: Cellular components of the bone marrow microenvironment.

The BM is a microenvironment with a unique cellular composition which provides a protective niche for tumour cells. Stem cells give rise to haematopoietic cells (HSC) and the mesenchymal cells (MSC) such as osteoblasts, adipocytes, and chondrocytes. Immune cells, such as T and B cells return to the BM following maturation in lymphoid organs and contribute to modifying the local environment. Subniches are created within the BM based on the proximity to sinusoids and microvessels, which determines the local level of hypoxia. The BM is encased in solid bone, which similarly is an intricate organ with complicated local homeostasis primarily maintained by osteoblasts and osteoclasts.

1.2.2 Acute Myeloid Leukaemia

Acute myeloid leukaemia (AML) is the collective term for malignant disease of blood precursor cells (blast cells) of the myeloid lineage, which includes granulocytes, erythrocytes, monocytes, and thrombocytes (Figure 1-3). Compared to chronic leukaemia, it has a rapid progression and many patients would only survive a couple of months without treatment intervention. The disease develops in the BM and is characterised by uncontrolled proliferation and accumulation of one or more types of immature blast cells, along with inhibited maturation of normal blasts (72). As opposed to MM, dependence on the BM microenvironment is limited and blast cells are widely present in the peripheral circulation. Myelodysplastic syndromes (MDS) are similar to AML and characterised by BM failure, but with a blast count <20% in the blood and BM. Acute expansion of immature cells along with a decrease in the mature cell populations lead to symptoms of either isolated haematopoietic deficiencies (anaemia, leukopenia, or thrombocytopenia) or pancytopenia, along with common symptoms such as bleeding, bone pain, fatigue, and pallor. The lack of mature immune cells also leads to an impaired immune response, leaving AML patients immunocompromised and susceptible to infections which can be fatal even when caused by commensal pathogens. During later stages of the disease, extramedullary organ infiltration may present as hepatosplenomegaly or lymphadenopathy and may be fatal if involving the brain or lungs (72). Similar to the common dogma of oncogenesis, proliferation, immortality, and impaired differentiation in AML is the combined result of mutations in two different classes of genes (two-hit hypothesis). Class I mutations lead to a proliferative and/or survival advantage in the transforming cells through activating mutations in cell surface receptors (e.g. FLT3 and c-kit). Class II mutations, or fusion of genes, results in impaired differentiation and apoptosis. The genetic makeup of transformed cells in each individual case has great implications for chemotherapy sensitivity and disease outcome (72, 73). A thorough genetic workup is today part of AML diagnostics and routinely examined genes include *FLT3* (FMS-like tyrosine kinase 3), *NPM1* (nucelophosmin-1), *CEBPA* (CCAAT enhancer binding protein), *KIT* (v-kit Hardy-Zuckerman 4 feline sarcoma viral oncogene homolog), *TET2* (Tet methylcytosine dioxygenase 2)*, DNMT3A* (DNA methyltransferase 3A)*, IDH1* (isocitrate dehydrogenase 1), and *IDH2* (74). As an example, an isolated mutation in *NPM1*, or in both alleles of *CEBPA*, improves disease prognosis while an ITD in *FLT3* is associated with poor prognosis (75). The extensive range of cell types, genetic changes, causes, and clinical features involved

in the pathogenesis of AML result in a highly heterogeneous disease with a wide spectrum of unique disease presentations. An overview of the World Health Organisation (WHO) classification of AML is provided in Table 1-3 to illustrate the diversity of the disease.

AML is most common in adults and the elderly with a median age of onset of 70 years. There are around 3100 new cases of AML in the UK every year, making it marginally rarer than MM. However, the average five-year survival in the UK is only 15%, decreasing to just 5% in patients >65 years of age (76). With improved BM transplantation techniques, the survival of young patients has improved significantly, but as for MM, the main patient group is not eligible for such drastic treatment regimens. Chemotherapeutic treatment strategies for AML have only prolonged survival marginally over the past 30 years, with no new drugs being approved for AML treatment until 2017. Following approval of several new therapeutics, the treatment landscape is changing, and some improvement in the survival of elderly patients has been observed (77, 78). Standard treatment consists of two parts; induction and consolidation therapy. Standard induction therapy is given as a 3+7 regimen with three days of intravenous (i.v.) daunorubicin followed by seven days of cytarabine (79). Due to its heterogeneity, treatment strategies are diverse and often need to be tailored specifically to the individual patient. New therapeutics which have recently been approved for combination with standard treatments include the hypomethylating agents, azacytidine and decitabine (Section 1.3.3.3), the multikinase inhibitor midostaurin, IDH inhibitors, enasidenib and ivosidenib, and anti-CD33 monoclonal antibody gemtuzumab ozogamicin (Section 1.3.3.5) (78). Several immunotherapeutic strategies for targeting AML are also currently being explored as detailed below (Section 1.3). When the patient enters remission, consolidation therapy is started with several cycles of high-dose cytarabine or anthracyclines to prevent the return of malignant cells. However, although approximately 50% of all patients enter complete remission, one of the biggest challenges of AML treatment is a high relapse rate (79). Similar to MM, chemotherapy-resistant leukaemic stem cells often find protection in the BM microenvironment. The leukemic cells remaining in the BM following treatment are known as minimal residual disease (MRD) and frequently cause disease relapse at a later stage following reactivation (80).

Although the treatment for AML seems to be improving, much work remains to stratify treatment strategies to disease subtype and individual characteristics and likely, more specialized therapeutics, including immunotherapies, will improve overall survival for AML patients, independent of age, in the coming years.

Table 1-3: World Health Organisation (WHO) classification of AML and related neoplasms.

The table provides an excerpt of the 2016 revised version of the WHO classification of myeloid neoplasms and acute leukaemia (81).

Acute myeloid leukaemia and related neoplasms	
AML with recurrent genetic abnormalities	AML with t(8;21)(q22;q22.1);RUNX1-RUNX1T1
	AML with inv(16)(p13.1q22) or t(16;16)(p13.1;q22);CBFB-MYH11
	APL with PML-RARA
	AML with t(9;11)(p21.3;q23.3);MLLT3-KMT2A
	AML with t(6;9)(p23;q34.1);DEK-NUP214
	AML with inv(3)(q21.3q26.2) or t(3;3)(q21.3;q26.2); GATA2, MECOM
	AML (megakaryoblastic) with t(1;22)(p13.3;q13.3);RBM15-MKL1
	Provisional entity: AML with BCR-ABL1
	AML with mutated NPM1
	AML with biallelic mutations of CEBPA
	Provisional entity: AML with mutated RUNX1
AML with myelodysplasia-related changes	
Therapy-related myeloid neoplasms	
AML, not otherwise specified (NOS)	AML with minimal differentiation
	AML without maturation
	AML with maturation
	Acute myelomonocytic leukaemia
	Acute monoblastic/monocytic leukaemia
	Pure erythroid leukaemia
	Acute megakaryoblastic leukaemia
	Acute basophilic leukaemia
	Acute panmyelosis with myelofibrosis

t: translocation, inv: inversion, APL: Acute promyelocytic leukaemia, PML-RARA: promyelocytic leukaemia/retinoic acid receptor-α fusion, GATA2: GATA-binding factor-2, MECOM: MDS1 and EVI1 complex locus protein EVI1.

1.3 Immunotherapy of haematological malignancies

1.3.1 Background

Cancer immunotherapies are novel treatment strategies which aim to harness the anti-tumour abilities of the immune system by manipulating the patient's own immune system to recognise and kill tumour cells. Successful immunotherapy has the potential to generate immunological memory and thereby induce long-term remission. Initially, ideas for immunotherapies were developed following the observation of the cellular reactions to allogeneic haematopoietic stem cell transplantations (HSCT) in HM. Allogeneic HSCTs take advantage of the generation of graft-versus-tumour effects where donor immune cells recognise and kill recipient tumour cells (82). Immunotherapy strategies exploiting both the functions of immune cells directly, as well as various other ways of stimulating the immune system, have been explored.

1.3.2 Cellular immunotherapy

Cellular immunotherapy takes advantage of the possibility to culture patient immune cells *ex vivo* to potentiate their functions and reverse a suppressed state induced by the TME, followed by re-infusion into the patient to initiate anti-tumour immunity (adoptive transfer). Several different strategies have been explored which are described below.

1.3.2.1 Alloreactive NK cells

NK cells have many characteristics that make them attractive for immunotherapy. In addition. As a part of the innate immune system, they do not depend on specific antigen recognition to initiate an anti-tumour response. The basics of NK cell cytotoxicity regulation was introduced in Section 1.1.2.1. Normally, inhibitory receptors, such as the killer-cell immunoglobulin-like receptors (KIR) interact with HLA molecules on normal cells, which prevents activation of NK cells (Table 1-1). The "missing self" strategy is particularly interesting in relation to allogeneic HSCT, where NK cell immunotherapy has been explored for the induction of a graft-versus-leukaemia response. Intentional KIR ligand mismatch between donors and recipients in AML has generated some remarkable improvements in outcomes following HSCT, generating significantly reduced relapse rates, more frequent progression-free survival at relapse and remission, as well as

a survival advantage (83, 84). One particular benefit of NK cells is that they do not induce the graft-versus-host disease (GVHD) that is often seen as a complication of HSCT due to the presence of donor T cells. Alloreactive NK cells have even been shown to protect against GVHD, which led to the exploration of T cell-depleted allogeneic grafts as a method for preventing GVHD (84, 85). However, as T cell depletion caused an increased mortality rate and risk of relapse, GVHD is now commonly prevented by the use of immunosuppressive drugs which also inhibit the function of NK cells and therefore limit the efficiency of KIR ligand mismatch (8). As many elderly patients are still not eligible for HSCT, adoptive transfer of allogeneic NK cells independent of HSCT has also been explored in AML, but the best strategy for culturing NK cells *ex vivo* has yet to be clarified. A recently completed clinical trial (Phase I) used allogeneic NK cells from related HLA-identical donors, which were activated with a leukaemia cell line lysate before adoptive transfer, which resulted in significantly improved relapse-free survival times (86). A novel strategy to overcome the issues of *ex vivo* culture of NK cells is the development of bispecific and trispecific killer cell engager antibody technology (BiKEs and TriKEs). One of the first BiKEs generated was aimed at AML therapy. With specificity for CD16 and CD33 it could physically link NK cells and tumour cells together *in vivo* and thereby potentiate the cytotoxic effect of NK cells (87). This has been further developed into TriKEs, which additionally can express e.g. IL-15 to stimulate the *in vivo* expansion of NK cells (88).

Various strategies for *ex vivo* activation and expansion of NK cells for MM treatment have been explored. In particular co-culture of autologous NK cells with K562 feeder cells expressing 4-1BB ligand and IL-15 has proven successful with the generation of large numbers of highly cytotoxic NK cells. Encouraging results have been demonstrated following adoptive transfer of *ex vivo* expanded NK cells in early clinical trials of MM (89, 90). One particularly interesting strategy recently presented by Chang *et al*. utilises a combination of *ex vivo* expanded NK cells and carfilzomib treatment, which reduces the expression of HLA Class I on MM cells, thereby making them more attractive targets for NK cell attack (89).

1.3.2.2 Dendritic cell vaccines

DC vaccines are DC-based tumour immunotherapies which exploit the versatile functions of DCs to generate tumour-specific CTLs with the ability to eradicate tumour cells. DCs are either isolated from the patient or

generated *ex vivo* from patient-derived precursor cells. The DCs can then be activated and matured in culture and loaded with TAA before re-introduction into the patient. Overall, clinical trials have demonstrated that DC vaccines are safe and have moderate immunological activity, but only limited clinical efficacy to date (82). DC vaccines have been explored in both MM and AML. One strategy which has been particularly successful in MM is the use of patient-specific idiotype protein as the DC antigen load. As previously discussed, following malignant transformation of plasma cells, all of the malignant clones have the same unique variable region sequences in the heavy and light chains of the secreted immunoglobulins (the idiotype) hence, this can serve as a tumour-specific antigen. In a clinical trial, matured, idiotype-loaded DCs were infused into patients with MM which resulted in the generation of idiotype-specific CTLs in 5/9 patients and five years stable disease in 4/9 patients (91). Similar results have been obtained by pulsing DCs with whole tumour cell lysates (92). In AML, DC vaccines have been explored as a more tolerable form of treatment in the elderly with particular efficacy in MRD and early remission (82). In particular, a DC vaccine generated using DCs electroporated with the LAA, WT1, was tested in a Phase II clinical trial and prevented, or delayed, relapse in 9/13 patients. Moreover, long-term clinical response was correlated with an increased frequency of circulating WT1-specific CTLs (93). Autologous apoptotic leukaemic cells have also been used successfully as antigens, specifically in elderly patients, which is an encouraging development (94). Another antigen, which is currently being tested in a Phase I/II trial as a post-remission therapy in AML, is the germline TAA PRAME (preferentially expressed antigen in melanoma) (95).

1.3.2.3 Lymphokine-activated killer (LAK) cells

Similar to NK cells, LAK cells kill by unspecific mechanisms independent of MHC Class I and therefore provide a good alternative to T cell based-therapies which can generate problems with GVHD. LAK cells are generated *ex vivo* by treating PBMCs with IL-2 and thus, they consist of a heterogenous population of NK, NKT, and T cells, which can then be re-introduced into the patient by adoptive transfer (96). Initial strategies employed adoptive transfer of LAK cells in combination with IL-2 treatment, but this generated systemic IL-2 toxicity in clinical trials and the efficacy was poor (97).

1.3.2.4 Cytokine-induced killer cells

Cytokine-induced killer (CIK) cells are $CD3^+CD56^+$ cells closely related to LAK and NKT cells with a mixed NK- and T cell phenotype. CIK cells were investigated as a development of LAK cell therapy, as the need for systemic IL-2 treatment could be bypassed (98). CIK cells can exert their anti-tumour response using both antigen-dependent and -independent mechanisms. They are terminally differentiated cells which, similar to LAK cells, are generated *ex vivo* by treating PBMCs with IL-2, IFN-γ, IL-1, and anti-CD3 antibodies. CIK cells have been used in both autologous and allogeneic strategies for the treatment of HM with varying results (99). Unfortunately, GVHD remained a problem when allogeneic CIK cells were used in clinical trials and more recently, the focus has been switched to other immunotherapeutic strategies.

1.3.2.5 Chimeric Antigen Receptor (CAR) T cells

One of the major advances in immunotherapy, and in the treatment of HM, is the development of the chimeric antigen receptor (CAR) and CAR-T cells. Briefly, T cells are obtained from patients or healthy donors and then genetically engineered to express a recombinant TCR with specificity for a given TAA. The CAR-T cells are then expanded *ex vivo* and re-introduced into the patient through adoptive transfer where they are destined to find, and destroy, tumour cells expressing the chosen TAA. This is a novel strategy, but so far, it has shown promise in several HM, not least following the development of CAR-T cells with specificity for CD19, which is ubiquitously expressed on immature B cells (100). Encouragingly, CD19-targeted CAR-T cells for the treatment of diffuse large B cell lymphoma and acute lymphoblastic leukaemia (ALL) were approved by the FDA (US Food and Drug Administration) in 2017 as the first CAR-T cell therapies to enter the market (101). As opposed to other B cell malignancies, CD19 is not expressed on malignant plasma cells and other targets have been explored in the MM setting. Early trials of CD138-targeted CAR-T cells showed promising results with stable disease in 4/5 treated patients at the seven month follow-up and no immediate toxicity issues (102). Another dose-escalation trial tested targeting of CAR-T cells to the B cell maturation antigen (BCMA). Following treatment of two patients with MM refractory to chemotherapy and 80-90% malignant plasma cells in the BM prior to treatment, plasma cells remained undetectable in the BM for up to 28 weeks (103). Another target which has recently gained a lot of attention is SLAMF7

which, as described below, is also a promising target for monoclonal antibody therapy in MM (104).

Identifying suitable surface proteins for CAR-T cell targeting in AML has proven more difficult as many of the proteins are not exclusively expressed on haematopoietic cells leading to an elevated risk of off-target effects. Although a large number of targets, including CD33, CD7, CD25, CD123, CD38, and the FLT3 receptor, have been investigated in preclinical studies, translation into clinical studies has been slow (105). Currently, Phase I clinical trials of CD33-, CD38-, and CD56-specific CAR-T cells are on-going with no results published to date (105). Interestingly, oncolytic viruses (OV) have been suggested as a potential novel combination treatment with CAR-T cells to enhance T cell recruitment to the TME, reverse local immunosuppression, and enhance the effector function of CAR-T cells (106).

1.3.2.6 Marrow-infiltrating lymphocytes

Another T cell-based immunotherapy strategy which is specifically aimed at HM, and MM in particular, is the use of marrow-infiltrating lymphocytes (MIL). While the BM is the primary site of the disease, it can also be considered a reservoir of memory T cells. Similar to tumour-infiltrating lymphocytes, MILs are tumour-specific effector T cells which are present in the BM of HM patients and have a greater polyclonal antigen specificity than peripheral blood lymphocytes (107). However, due to the local suppressive environment, MILs are not able to fully eradicate BM disease as a monotherapy. In conjunction with HSCT, MILs are isolated, and then expanded and activated *ex vivo* to promote their potency. Upon transfer back to the patient via adoptive transfer, MILs provide a strategy which is autologous, tumour-specific, and does not require any genetic manipulation. In the first clinical trial in MM it was confirmed that the likelihood of achieving a complete response was associated with greater anti-tumour specificity of activated MILs. Persistence of tumour-specific immunity in the BM for up to one year was also demonstrated (107). Based on these encouraging results, MILs are being further tested in clinical trials for MM (Phase II) and are also gradually expanded to other HM (108, 109).

1.3.3 Drug-based immunotherapy strategies

In addition to cellular therapies, various types of drugs have been explored for their potential to trigger the immune system and generate an anti-tumour immune response. This includes both synthetic compounds and biological therapies, some of which are discussed in more detail below.

1.3.3.1 IFN-α treatment

Early in the era of immunotherapy, the cytotoxic effect of IFN-α on malignant cells was recognised. In addition to direct cytotoxicity and inhibition of proliferation, IFN-α was also shown to have a potentiating effect on the anti-tumour immune response, in particular for the generation of a durable adaptive response (110). IFN-α progressed to Phase III clinical trials as a monotherapy for MM but due to limited improvement in overall survival, as well as high frequency toxicities, interest in continued development subsided (111). Similarly, IFN-α was extensively studied in AML with many clinical trials completed. Although several studies indicated impressive anti-leukaemia activity of IFN-α, there was large variability in the outcomes and an ideal treatment strategy was not identified before interest swayed to other immunotherapies (112). More recently, with a better understanding of anti-tumour immune responses, IFN-α has regained interest in different contexts of AML treatment, for example in the elimination of MRD (113).

1.3.3.2 Immunomodulatory imide drugs (IMiDs)

Immunomodulatory drugs such as lenalidomide and pomalidomide are widely used as part of the standard treatment of MM today. These drugs are analogues of thalidomide, and cereblon has recently been identified as their main target (114). Although the exact mechanisms of action for these drugs are unclear, they have a range of immunostimulatory effects such as reduced secretion of TNF-α, IL-1β, IL-6, and IL-12, along with an increased IL-2 and IFN-γ synthesis, improved T cell priming, enhanced antigen presentation by DCs, and boosted activity of both NK and NKT cells (115-118). More recent research has also implied IMiDs as a potential treatment in AML (119). Early clinical trials using lenalidomide in AML achieved complete response rates of 16-30% (120, 121).

1.3.3.3 Hypomethylating agents

As described above, hypomethylating agents such as azacytidine and decitabine are now part of the standard treatment in AML, in particular for elderly and unfit patients, and chemotherapy refractory AML (122). The main mechanism of action of hypomethylating agents is to induce hypomethylation of tumour suppressor gene promoters by inhibiting DNA methyltransferase, leading to a reactivation of their transcription in tumour cells. However, these agents also have several other effects, including modulation of the immune response. In particular, effects on the adaptive immune response have been demonstrated, including improved antigen expression, processing, and presentation, as well as improved T cell priming and effector functions (123). Hypomethylating agents also upregulate both the PD-1/PD-L1 and CTLA-4/CD80/86 axes and have therefore been suggested in combination treatments with immune checkpoint inhibitors in AML as described below (124).

1.3.3.4 Immune checkpoint inhibitors

The development of immune checkpoint inhibitors is another significant breakthrough in the treatment of cancer. As discussed above, immune checkpoints tightly control the immune response by regulating the balance between stimulatory and inhibitory signals in the T cell response. The two most widely studied immune checkpoints for cancer therapy are the co-inhibitory T cell receptors PD-1 and cytotoxic T-lymphocyte-associated-protein 4 (CTLA-4). The ligands of PD-1 (PD-L1, PD-L2) and CTLA-4 (CD80, CD86) are often overexpressed on tumour cells as an immune evasion strategy. Through the development of monoclonal antibodies, which target the inhibitory receptors and disrupt the suppressive effect of the tumour cells, the immune system can be re-stimulated to generate an anti-tumour immune response. With great success in solid malignancies, in particular melanoma, the use of checkpoint inhibitors is now also being trialled in HM (125). Successful results have been obtained for a range of lymphomas using anti-PD-1 treatment, in particular for Hodgkin's lymphoma. In clinical trials, a response rate of up 87%, with 70% of patients showing a partial response, has been achieved (126). Despite this, the use of checkpoint inhibitors in MM has been disappointing with some clinical trials reporting a complete lack of response to anti-PD-1 monotherapy (127). These results led to other strategies being tested and more positive results were achieved when checkpoint inhibitors were used in combination with standard

therapies, in particular IMiDs (127). Encouragingly, anti-PD-1 treatment in combination with standard therapy is now being tested in several Phase III clinical trials of MM (128, 129).

Various anti-PD-1 and anti-CTLA-4 antibodies have also been tested as monotherapies in AML and MDS with modest results. However, in different combination strategies, e.g. with hypomethylating agents and chemotherapy, more encouraging results have been achieved (125). As discussed, azacytidine treatment can increase the expression of both PD-1, PD-L1, and PD-L2 on tumour cells, including AML blasts. Several clinical trials evaluating anti-PD-1 antibodies in combination with hypomethylating agents are on-going and preliminary results are encouraging (130). As CTLA-4 expression on $CD8^+$ T cells in the TME is thought to induce resistance to anti-PD-1 treatment, and to utilise the distinct molecular mechanisms of action of PD-1 and CTLA-4 blockade, co-treatment with both checkpoint inhibitors is also currently being evaluated in AML (131).

1.3.3.5 Monoclonal antibodies

Monoclonal antibody (mAb) treatment is another immunotherapeutic treatment strategy that was first developed in HM, with anti-CD20 rituximab pioneering the field with its FDA approval for the treatment of chronic lymphocytic leukaemia (CLL) and non-Hodgkin lymphoma (NHL). As opposed to monoclonal checkpoint inhibitor antibodies, these antibodies aim to target proteins specifically expressed on the surface of tumour cells and, via the Fc portion of the antibody, stimulate immune-mediated killing mechanisms such as antibody-dependent cell-mediated cytotoxicity (ADCC), antibody-dependent phagocytosis, and complement-dependent cytotoxicity. mAbs can also block signalling pathways important for cancer progression by binding to selected receptor targets, and deliver conjugated chemotherapeutics directly to the cancer cell. The two main mAbs which have been developed in MM are daratumumab (anti-CD38) and elotuzumab (anti-SLAMF7) which were both approved for clinical use in 2015 and have contributed significantly to advance the treatment of MM (132). While daratumumab has shown good efficacy as a monotherapy, the effect of elotuzumab has been optimised in combination with lenalidomide and dexamethasone. Other possible MM targets for mAbs which are being tested in clinical trials include CD138, CD56, IL-6, and RANK ligand (133).

The mAb strategy has also been explored in AML with the main targets being CD33 and CD123. One anti-CD33 mAb, gemtuzumab ozogamicin, which is conjugated to the cytotoxic agent calicheamicin, was originally approved for the treatment of AML but was withdrawn due to toxicity issues and lack of efficacy. However, following continued research, gemtuzumab ozogamicin was recently re-approved for the treatment of newly diagnosed AML in combination with induction chemotherapy (134). Other strategies include conjugating CD33 to radioactive isotopes. Both treatment with radioactive actinium and bismuth conjugated to a CD33 mAb have shown encouraging results in clinical trials, with good specificity and safety (135). Furthermore, a second generation mAb binding to CD123 has recently been shown to induce potent NK cell-mediated ADCC of AML blasts in a preclinical study and was also proven well-tolerated in a Phase I clinical trial (136, 137). Interestingly, mAb therapy with rituximab has been shown to be potentiated in combination with oncolytic virotherapy (OVT) in preclinical studies of CLL, which indicates the potential for new combination therapy strategies in HM (138).

1.4 Oncolytic virotherapy (OVT)

1.4.1 Background

OVT is a type of biological immunotherapy which has gained increasing attention in recent years. Already in the late 1800s it was noted that viral infection sometimes coincided with tumour regression, in particular in leukaemia patients. At this time, knowledge about both oncology and virology was limited and the therapeutic potential of viruses was not realised. Apart from a brief resurgence in the 1950s and 60s, where several viruses were investigated clinically but abandoned due to efficacy and safety concerns, OVT had not gained significant attention again until the last 10-15 years. With a greater understanding of both virology and molecular techniques, research into the possibility of exploiting the anti-tumour potential of oncolytic viruses (OV) has sky-rocketed (139). Today, OVs are defined as viruses which preferentially infect and kill malignant cells and/or engage the immune system to mount an anti-tumour immune response, while sparing healthy cells due to their inherent antiviral defences. OVs can be naturally occurring, attenuated, or genetically modified; the pioneering OVs first approved for clinical use were genetically engineered. The very first OV to gain approval was the genetically modified adenovirus H101, which was approved in China in 2005 (140). However, it was not until ten years later that another OV was approved for clinical use by the FDA. Talimogene laherparepvec (T-Vec) is a herpes simplex virus-1 (HSV-1) which has been modified to 1) delete the ICP34.5 gene, which limits neurovirulence and replication in normal cells, and 2) express granulocyte-macrophage colony-stimulating factor (GM-CSF), which has an immunostimulatory effect (141, 142). In addition to genetically modified viruses, several wild-type (WT) OV have a natural tropism for tumour cells and generally produce asymptomatic, or mild symptom infection in humans. These include e.g. reovirus, coxsackievirus A21 (CVA21), Newcastle disease virus (NDV), vesicular stomatitis virus (VSV), and parvovirus H1 (143-147). Moreover, naturally attenuated vaccine strains of viruses, such as the Edmonston strain of measles virus (MV), have also been shown to have OV efficacy (148).

1.4.2 Mechanisms of action

It is now well established that OVs have several mechanisms of action, the two most well-defined; direct oncolysis and potentiation of anti-tumour immunity are described in detail below with an overview provided in Figure 1-6. Other mechanisms which contribute to tumour eradication include disruption of tumour-associated vasculature, as well as modulation of the TME (149-151).

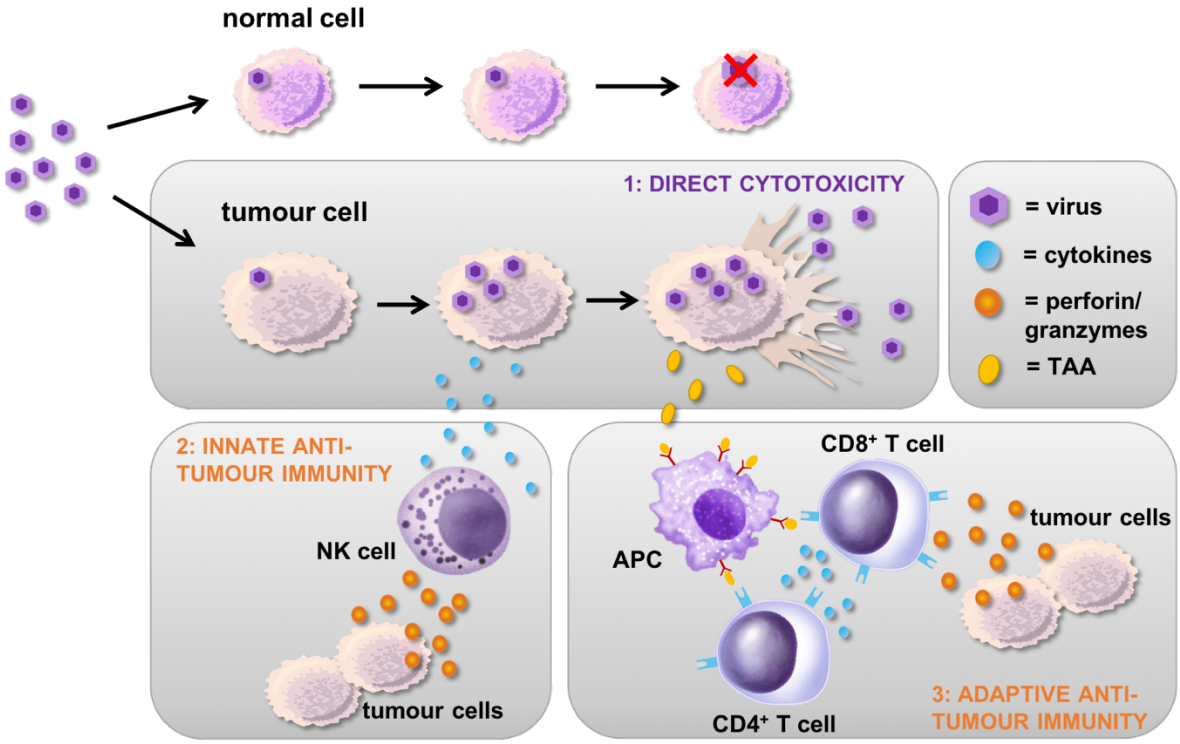

Figure 1-6: Overview of the main mechanisms of action of OV.

In normal cells (dark green), antiviral immune responses limit the replication of viruses following infection and thereby prevent lytic killing. However, tumour cells (orange) often have defective antiviral responses, rendering them susceptible to the effects of OV. OV can eradicate tumour cells through direct cytotoxicity (1) and induction of innate (2) and adaptive (3) anti-tumour immunity. Direct cytotoxicity is the lytic killing resulting from replication of the virus in a host cell, with subsequent spread of new viral progeny to surrounding tumour cells and amplification of the lytic effect. Infection of tumour cells can also lead to the release of both cytokines and TAA which initiate an anti-tumour immune response. Innate anti-tumour immunity can consist of both cytokine-mediated bystander killing and NK cell-mediated cytotoxicity against tumour cells. Adaptive anti-tumour immunity is generated following the phagocytosis of TAA by antigen-presenting cells (APC) and presentation of TAA to either $CD4^+$ or $CD8^+$ T cells, ultimately resulting in the priming of tumour-specific cytotoxic $CD8^+$ T cells.

1.4.2.1 Direct oncolysis

The primary mechanism of action of OVs was initially thought to be direct lysis of tumour cells following replication, resulting in the release of progeny viruses spreading to surrounding cells and perpetuating the oncolytic effect. The preferential replication of OV in tumour cells is due to several cellular defects that arise during malignant transformation which can be exploited by the virus, either naturally or through genetic modification.

1.4.2.1.1 Receptor-targeted viruses

Many OVs take advantage of proteins which are overexpressed on the surface of tumour cells to mediate cell entry, making tumour cells more susceptible than the non-transformed parental cells. In some cases, these proteins are involved in adhesion and migration of tumour cells, such as intercellular adhesion molecule-1 (ICAM-1), decay-accelerating factor (DAF), and junctional adhesion molecule-A (JAM-A). Some OVs have a natural tropism for these proteins, e.g. CVA21 which utilises ICAM-1 and DAF for host cell entry (152). It is also possible to genetically engineer OVs to change their tropism and thereby improve their specificity. For example, adenovirus (serotype 5) has a natural tropism for the coxsackie- and adenovirus receptor (CAR), which has limited expression on tumour cells. Instead, it was engineered to preferentially use cell surface integrins or other adenoviral receptors with higher expression on tumour cells to improve its specificity (153, 154).

1.4.2.1.2 Defects in antiviral responses

1.4.2.1.2.1 *Interferon response*

The interferon (IFN) response is the main cellular defence against viral infection. As described in Figure 1-7, several types of PRRs such as TLRs and retinoic acid-inducible gene-I (RIG-I) can detect pathogen-associated molecular patterns (PAMP) such as viral genomes in healthy cells. The respective signalling pathways of the different receptors converge on the production of type I IFN via activation of interferon inducible factor (IRF)-3 and -7. The secretion of IFN renders the surrounding cells hostile to viral replication through activation of the JAK-STAT signalling pathway. This pathway ultimately leads to the increased expression of cell cycle regulators such as protein kinase R (PKR), which can stop cell division and thereby limit viral replication (Section 1.4.2.1.2.2) (155). Alongside this, many viruses have developed resistance mechanisms to overcome the effects of the IFN

response, such as the ICP0 protein in HSV-1, which can bind and block the effect of IRF3 (156). One of the original hypotheses to explain OV tumour specificity was based on the fact that tumour cells often have defective IFN responses and therefore an increased susceptibility to viral infection (Figure 1-7). Tumour cells can down-regulate the expression of RIG-I, IRF3, and IRF7 which limits their ability to detect viral infection and initiate an IFN response. They can also have defects in the IFN signalling pathway, including down-regulation of both JAK, STAT, and PKR proteins, which reduces the protective effects of the IFN response (155).

Some OVs, such as VSV and NDV, are naturally dependent on defective IFN responses for their replication (157, 158), but viruses can also be engineered to further exploit the inefficient IFN responses to enhance tumour specificity. One example of this would be deletion of the ICP0 gene from HSV-1, rendering the virus susceptible to IFN and unable to infect normal cells while tumour cells with defective IFN signalling pathways become ideal targets (159). Viruses have also been engineered to express IFN genes, such as the VSV-IFN-β, and thereby induce a virus hostile state in normal cells but not tumour cells with defective IFN pathways (160).

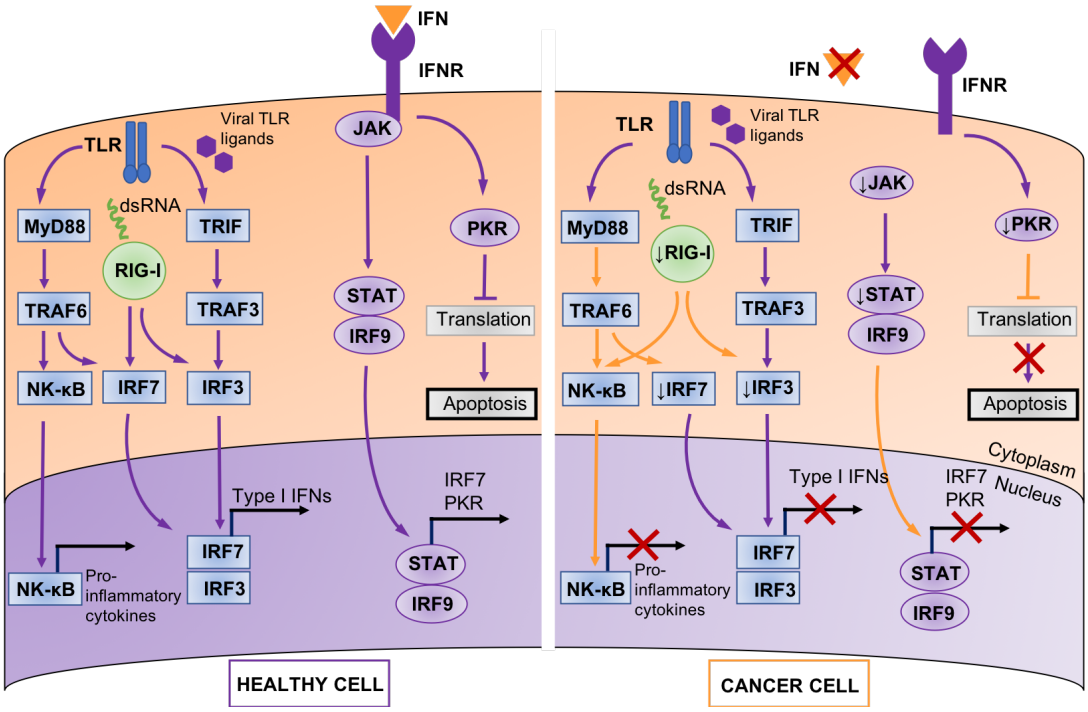

Figure 1-7: Overview of interferon responses in healthy and cancerous cells.

Following detection of viral genomes in healthy cells (left panel), the transcription of type I IFNs is initiated via various signalling pathways converging on IRF3 and -7. Following binding of secreted IFN to the IFN receptor (IFNR), JAK-STAT signalling is initiated in healthy cells, resulting in PKR expression which renders the cell hostile to viral replication. In cancer cells (right panel), many antiviral defence proteins, including PRRs, IRF3 and -7, JAK, STAT, and PKR are down-regulated, leaving the cancer cell susceptible to viral infection. This provides an opportunity for specific targeting of cancer cells using OV, while sparing healthy cells.

1.4.2.1.2.2 Double-stranded RNA-dependent protein kinase

PKR, which is induced by IFN signalling as described above, is a dsRNA-dependent protein kinase which functions as a dsRNA detector and regulator of the cell cycle in the cytosol of healthy cells. When it detects dsRNA, it becomes activated and phosphorylates, thus inhibiting, the translation initiation factor, eIF2, a critical mediator of protein translation. Effectively, this also prevents the translation of viral transcripts and thereby the replication of viruses (161). Mutations activating the Ras pathway, common in many tumour types, prevents phosphorylation of PKR and results in a defective antiviral response, rendering tumour cells particularly susceptible to infection (162, 163). This is exploited naturally by viruses such as reovirus, or through genetic modification, such as ICP34.5 deletion in HSV-1, to prevent the ICP34.5 protein inhibition of PKR activity (163, 164).

1.4.2.1.3 Pro-apoptotic targeting

Another method for enhancing tumour specificity using genetic engineering is to exploit the apoptotic effect of viruses. Many tumour cells acquire mutations in tumour suppressor proteins, such as p53 and pRb, which regulate apoptosis and cell cycle arrest in normal cells, resulting in uncontrolled cell proliferation. Viruses can have a similar effect following infection of normal cells, suppressing the activity of p53 or pRb to delay apoptosis and allow viral replication using the host cell replication machinery. One example of this is adenovirus. The adenovirus E1A proteins can push the infected cell into the S phase of the cell cycle, which is beneficial for viral replication. However, this can lead to an accumulation of p53, which forces the cell into apoptosis before the viral life cycle has been completed. To prevent this, the adenovirus E1B proteins can mediate the degradation of p53, which allows cell replication to continue. This can be exploited to engineer OV with tumour cell specificity. Thus, the E1B-deleted ONYX-15 adenovirus is incapable of disrupting p53-dependent apoptosis, which prevents viral replication as the host cell dies. However, tumour cells with a dysfunctional p53 response would specifically support the continued replication of the E1B-deficient virus as cellular replication ensues with no induction of apoptosis, allowing the viral life cycle to be completed (165-167).

1.4.2.1.4 Transcriptional targeting

It is also possible to use genetic engineering to generate viruses where essential viral genes are under the control of tumour-specific promoters,

thereby creating a virus that exclusively replicates in tumour cells. This method can only be used for DNA viruses, such as adenovirus and HSV. Tumour-specific promoters can be active in several cancer types (e.g. hTERT and survivin), generating a virus with wider specificity, while other promoters such as prostate-specific antigen (PSA) are specific for a single cancer type (168). Adenoviruses have been successfully engineered to be controlled by both hTERT and PSA promoters (169, 170), and more recently, this has also been combined with other genetic modifications to enhance their cytotoxic effects, such as virus-induced TRAIL secretion (171).

1.4.2.2 OV-induced anti-tumour immune responses

More recently, the importance of anti-tumour immunity for successful OV therapy has gained more recognition. The induction of anti-tumour immunity is thought to both have an immediate effect through innate anti-tumour immunity mechanisms and a more long-term protective effect through the generation of immunological memory and adaptive responses. Some of the initial studies pointing out the importance of the immune system for successful OVT were performed by Toda *et al*., demonstrating that HSV treatment was effective in an immunocompetent mouse while the effect was lost in athymic mice, pointing out the importance of T cells for an efficient response (172). Later, both NK cells and $CD8^+$ T cells were also identified as critical mediators for successful VSV therapy (173).

1.4.2.2.1 Innate anti-tumour immunity mechanisms

As described in Figure 1-6, both cytokine secretion as part of an inflammatory response and NK cell activation are important mechanisms for the innate anti-tumour immune response induced by OV. Both immune cells, infected cells, and neighbouring cells can secrete pro-inflammatory cytokines in response to a viral infection. In addition, both PAMPs (viral particles) and danger-associated molecular pattern signals (DAMPs, host cell protein) are released by virally infected and dying tumour cells, which can stimulate activating receptors like TLRs and further propagate the inflammatory response (155). The generation of an inflammatory environment has several effects on tumour cells and the local microenvironment. For example, the immunosuppressive state of the microenvironment induced by the tumour can be reversed to activate immune recognition of transformed cells. Secreted cytokines have also

induced bystander killing of tumour cells through the toxic effect of the cytokines themselves on tumour cells (174, 175). Secretion of cytokines such as TNF-α, IFN-γ, and IL-12 are also important for initiation of the adaptive immune response, as described below.

The recruitment and activation of NK cells as a part of OV therapy is well-described and NK cell-mediated killing is crucial for some viruses to have full effect (173). NK cells can be triggered to kill by OV in various ways. As discussed previously, one of the main NK cell signals for cellular abnormalities is the down-regulation of MHC Class I expression, resulting in reduced presentation of self-antigen (176). In an attempt to avoid adaptive immunity, OVs can decrease the expression of MHC Class I on the surface of infected tumour cells, thereby increasing their visibility to NK cells (177). Additionally, both malignant transformation and viral infection can increase the expression of activating NK cell ligands on the surface of tumour cells (178). Tumours also induce a local immunosuppressive environment which can inhibit NK cells, however, OVs have the potential to stimulate and activate NK cells directly or via cytokine secretion from alternative immune cells (138). In particular type I IFNs, which are widely secreted in response to viral infection, have immense effects on the NK cell response, including NK cell activation, potentiation of cytotoxicity, and induction of TRAIL expression. Both conventional DC, plasmacytoid DC (pDC), and monocytes are common sources of type I IFN for NK cells (179). The main mechanism of NK cell-mediated killing is a tightly regulated degranulation process resulting in the release of cytotoxic granules directed towards the target cell (Section 1.1.2.1). However, another way for NK cells to kill is to engage death receptors on target cells, via FasL or TRAIL expression on the NK cell surface. Death receptor signalling leads to the activation of the caspase cascade resulting in target cell apoptosis (180).

1.4.2.2.2 Adaptive anti-tumour immunity mechanisms

Figure 1-6 also illustrates how, in addition to PAMPs and DAMPs, both TAA and viral antigens are released during OV infection of tumour cells. The secretion of cytokines, as well as PAMPs and DAMPs, as part of the innate response can induce maturation of APCs. As described in Section 1.1.2.2.1, when TAA are phagocytosed by APCs, such as DCs, they can either be presented on MHC Class II to naïve $CD4^+$ T cells, or cross-presented on MHC Class I to naïve $CD8^+$ T cells to activate antigen-specific T cell responses. $CD4^+$ T cells can provide help to $CD8^+$ T cells in their differentiation into tumour-specific CTLs, or $CD8^+$ T cells can be primed

directly following cross-presentation of antigen on DCs (155). Along with tumour-specific CTLs, immunological memory and a durable anti-tumour response are also generated as part of the adaptive response. Long-term protection against tumour recurrence has been demonstrated in several *in vivo* models using e.g. adenovirus, Maraba virus (MG-1), and VSV (181-183). Importantly, the adaptive response is also able to mediate tumour regression at distant sites not directly exposed to virus (155).

1.4.3 Clinical experience with oncolytic viruses

A multitude of WT and genetically modified OVs are in clinical trials today, however, only T-Vec and adenovirus H101, for the treatment of melanoma and head and neck cancers, respectively, have been approved for clinical use. Initially, in line with the hypothesis that direct oncolysis was the most important mechanism of action, virus was administered intratumourally and was thus only considered for solid malignancies. However, following a number of disappointing trials with limited viral spread, i.v. delivery was employed despite the fear of rapidly inducing an antiviral immune response. Several OVs have now been administered i.v. in clinical trials and have been safe and well-tolerated (184, 185). Moreover, results have also indicated that it is possible to achieve therapeutic efficacy despite the onset of an antiviral response. As an example, reovirus was successfully recovered from tumour sites following i.v. administration, despite the presence of neutralizing antibodies (nAb) (186).

Based on results from early clinical trials, as well as the surge in preclinical studies, many recent clinical studies have investigated combination regimens including OV. In particular combinations with checkpoint inhibitors, such as anti-PD-1 and anti-CTLA-4 antibodies, have been the focus of many studies and have generated promising results for example using T-Vec in combination with an anti-CTLA-4 and CVA21 in combination with anti-PD-1 (187).

It remains controversial whether a single, high dose of OV or repeated injections are required to generate an optimal OVT response. Both strategies have been tested, along with prime/boost regimens utilising a combination of two different viruses. In a Phase I trial of MV expressing the thyroidal sodium iodide symporter (NIS), one patient with relapsing drug-refractory MM achieved a complete, durable response with regression of distant plasmacytomas following a single i.v. dose of MV (188). Although a

single-dose regimen would be preferable for patients, most trials are currently employing a repeat-dosing treatment schedule with an initial low dose to induce seroconversion, followed by repeated larger doses until tumour regression (187). Only with continued analysis of clinical trial results, with comparison of different dosing strategies, can the ideal treatment strategy for each OV be devised. Taken together, clinical trials have demonstrated that OVT is safe with limited off-target effects and adverse reactions and has displayed encouraging results in a variety of malignancies.

1.4.4 Oncolytic viruses in the haematological malignancy setting

Since the early observations that influenza and other viruses could induce regression of leukaemia, the progress in OV therapy for HM has been remarkably slow compared to solid malignancies. As discussed above, intratumoural injection, which by nature of the disease are impossible in many HM, were the gold standard administration route. Gradually, as i.v. administration has been proven feasible, more attention has been directed towards HM (184). Sporadic reports of successful OVT in chronic myeloid leukaemia (CML) and in lymphocytic malignancies such as CLL, NHL, and ALL exist, but none of these have progressed to clinical trials (138, 148, 189-192). The studies examining OV for the treatment of MM and AML are detailed below (Table 1-4 and Table 1-5). In addition, most studies have focused on the direct oncolytic effect of OV in HM, with very few investigations of the potential for induction of anti-tumour immunity in this setting. HM are easily accessible through i.v. administration and in immediate proximity to immunological sites such as the blood stream, spleen, and lymph nodes. HM are under-investigated in the field of OVT, despite a requirement for novel treatments, in particular for elderly patients which are the most common patient groups in MM and AML. Therefore, the efficacy of OVT warrants further investigation in this context.

1.4.4.1 Oncolytic virotherapy in multiple myeloma

MM is the HM where most progress with OVT has been made and several Phase I clinical trials have been initiated, but only MV in combination with cyclophosphamide has progressed to Phase II trials so far. An overview of OV tested in MM is provided in Table 1-4. Reovirus, MV, and VSV have been evaluated in MM in clinical trials, while vaccinia virus (VV), myxoma virus, adenovirus, and CVA21 have shown promising results in preclinical studies (193). Only myxoma virus has been evaluated in the context of the immune system and was shown to initiate priming of tumour-specific CTLs *in vivo* (194).

Table 1-4: Overview of oncolytic viruses investigated for the treatment of MM.

Disease	OV	Results	References
Multiple Myeloma	Reovirus	One Phase I clinical trial completed. Phase I trials testing combination with standard chemotherapy initiated. Virus well tolerated following i.v. administration.	(195) (193)
	VSV	VSV-hIFN-β-NIS progressed to Phase I clinical trials (awaiting results). Efficient responses in immunocompetent mouse models.	(196) (197)
	Measles virus	One Phase I clinical trial completed. Virus well tolerated following i.v. administration. One complete response. Phase II trial of MV + cyclophosphamide initiated.	(198) (199)
	Myxoma virus	Rapid oncolysis *in vivo* independent of replication, priming of a CTL-mediated response. Immune cell activation and virus carriage in treated BM transplants.	(194) (200)
	Vaccinia virus	Vaccinia virus induced replicative cell death in myeloma cell lines.	(201)
	CVA21	CVA21 induced replicative cell death in MM cell lines and purged patient BM biopsies of up to 98.7% of $CD138^+$ plasma cells.	(202)
	Adenovirus (AdV)	Efficient oncolysis by Ad5, Ad6, Ad26, and Ad48. Enhanced efficacy with CD40L-expressing AdV.	(203) (204)

1.4.4.2 Oncolytic virotherapy in AML

Only a handful of studies have evaluated OV for the treatment of AML to date. Various viruses have been tested in preclinical studies, including VSV, reovirus, HSV-1, myxoma virus, and adenovirus and an overview of these studies is presented in Table 1-5. Interestingly, NK cell-mediated killing has been shown to contribute to the treatment efficacy of VSV, reovirus, and HSV-1 in AML. Moreover, VSV can also induce priming of tumour-specific CTLs in AML (205). Disappointingly, only one virus so far, VSV-NIS expressing human IFN-β, has been taken forward to clinical trials in AML (Phase I). The outcomes from this trial have not yet been published.

Table 1-5: Overview of oncolytic viruses investigated for the treatment of AML.

Disease	OV	Results	References
Acute Myeloid Leukaemia	VSV	VSV-hIFN-β-NIS progressed to Phase I clinical trials (awaiting results). Dependence on NK cells and priming of CTLs in vivo, which was potentiated in combination with anti-PD-L1 ab.	(196) (205)
	Reovirus	Killing of both AML cell lines and tumour cells, enhancement of NK cell-mediated anti-tumour immunity.	(206)
	HSV-1	Stimulation of NK cell-mediated cytotoxicity against AML cells using UV-inactivated HSV-1.	(207)
	Myxoma virus	Efficient killing of AML cell lines *in vivo* in the absence of replication *in vitro*.	(208)
	Adenovirus (AdV)	Direct cytotoxicity against AML cells using an Ad5/11 chimeric virus expressing IL-24.	(209)
	Measles and mumps virus combination	Enhanced efficacy compared to either virus alone. Significant toxicity *in vivo* and against primary AML blast cells, which was further enhanced in combination with cytarabine.	(210)

1.4.5 Reovirus

1.4.5.1 Background

Respiratory enteric orphan virus (reovirus) is a member of the *Reoviridae* family which is divided into 12 genera based on genome segmentation. All reoviruses are non-enveloped, dsRNA viruses with two concentric icosahedral protein capsids approximately 85 nm in diameter (211). The capsid protects the dsRNA genome which in the orthoreovirus genus comprises a total of 23.5 kbp in ten segments, termed either large (L), medium (M), or small (S) depending on their size, as described in Figure 1-8 (211-213). The genome encodes 12 proteins with some of the most important being μ1 and σ3 which are part of the outer capsid, σ1 and λ2 which are important for attachment and engagement with the host cell entry receptor, and λ3 and μ1 which form subunits of the RNA polymerase (Figure 1-8) (211). Three serotypes of mammalian orthoreovirus have been identified; Type 1 *Lang*, Type 2 *Jones*, and Type 3 *Abney* and *Dearing* (214). Reovirus Type 2 *Jones* was first observed to replicate specifically in malignantly transformed, but not normal, cell lines by Hashiro *et al*. in 1977 (147), but it is the WT reovirus Type 3 *Dearing* strain (T3D), manufactured as Reolysin®, which has now made significant progress as an OV therapeutic agent. Reoviruses are widespread in the environment and as suggested by its full name, it can cause a mild enteric or respiratory illness in young children, but is relatively non-pathogenic in adults (214). Reovirus can kill host cells both through lytic (necrotic, immune-stimulating) killing, induction of apoptosis in infected cells, and via non-apoptotic mechanisms, such as necroptosis (215-217). Apoptosis can be a result of both viral infection or a consequence of the IFN response. Reovirus can manipulate both extrinsic and intrinsic apoptosis pathways, with the mitochondrial pathway augmenting the effect of extrinsic death receptor signalling (218, 219). Infection can lead to secretion of TRAIL with subsequent death receptor activation, as well as translocation of Smac/DIABLO to the cytosol for cleavage of the pro-apoptotic protein, Bid, to its active form as part of the intrinsic pathway (219, 220). Expression of the pro-apoptotic proteins Noxa and Puma are also induced during later stages of reovirus infection as a result of NF-kB pathway stimulation (221, 222).

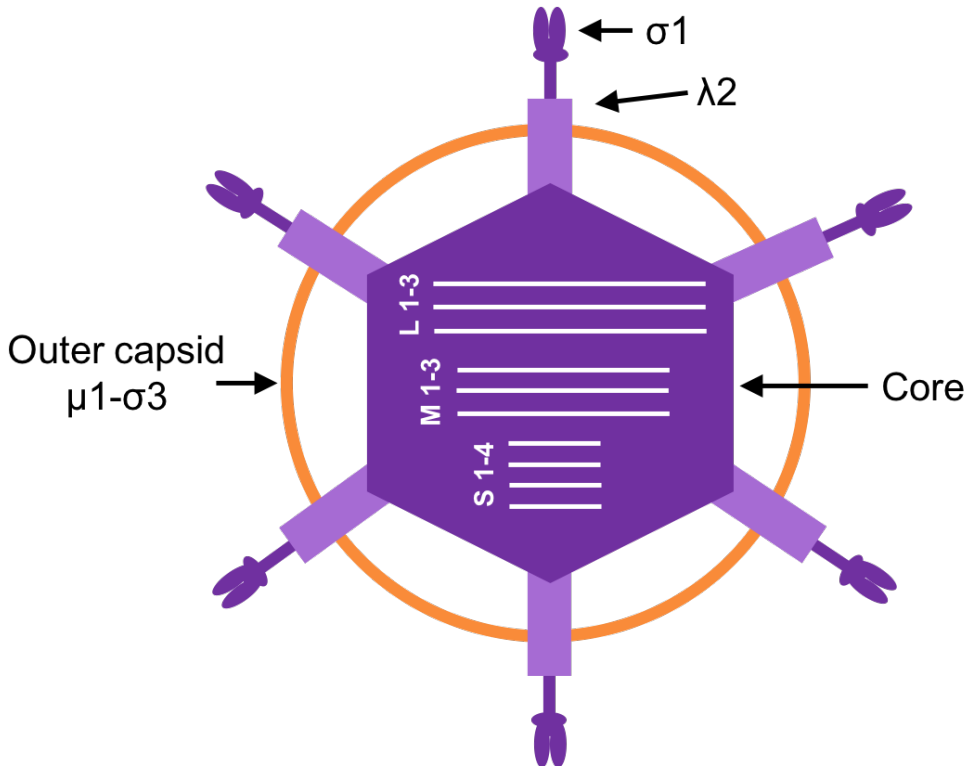

Figure 1-8: Structure of the reovirus virion.

Reoviruses are non-enveloped, dsRNA viruses with two icosahedral protein capsids. The capsid protects a core which harbours the 23.5 kbp genome. The ten genome segments (S1-4, M1-3, L1-3) encode 12 proteins which are required for the virus to propagate. The outer capsid is made up of μ1 and σ3 proteins and σ1 and λ2 proteins facilitate attachment to the entry receptor.

1.4.5.2 Tumour specificity

Reovirus utilises JAM-A as its receptor for entering host cells (223). JAM-A is ubiquitously expressed throughout the body on endothelial and haematological cells, in particular progenitor cells and HSCs (224). JAM-A has several important roles in normal cellular processes such as tight junction formation, leukocyte migration, and angiogenesis. However, JAM-A can also be overexpressed in several types of cancers, including haematological malignancies such as NHL, CLL, AML, and MM (138, 206, 225, 226). When hijacked during cancer transformation, processes like migration and angiogenesis are favourable for tumour progression and JAM-A has been linked to a worse prognosis and reduced survival in several malignancies (227, 228). Following JAM-A engagement, the virus is internalised via receptor-mediated endocytosis, which is dependent on β1 integrin (229). The outer capsid is degraded in the endosome by acid-

dependent cathepsin proteases B and L and thus, both β1 integrin and cathepsin B and L expression are factors which can affect tumour cell susceptibility to reovirus (230, 231). Although JAM-A is important for host cell entry, gain-of-function mutations activating Ras signalling, ubiquitous in malignant cells (232), have also been implicated as a determining factor of the preferential replication of reovirus in cancer cells. Following successful cell entry via JAM-A, Ras transformation can promote three key steps in reovirus replication: uncoating of the virus capsid, generation of progeny with higher infectivity, and sensitising cells to the apoptosis-dependent release of virus progeny (233). These specific characteristics of reovirus contribute to its selective replication in malignant cells and its oncolytic activity has been demonstrated in a variety of malignancies in both pre-clinical and clinical trials (Table 1-6).

1.4.5.3 Reovirus and the immune system

Both innate and adaptive immunity play important roles for the immune response to reovirus. As with most viral infections, the secretion of type I IFN is a key component of the innate response to reovirus. IFNs can be secreted from both infected cells and from immune cells; both DCs and monocytes are important in the detection of reovirus and subsequent secretion of IFN-α (138, 234). As described above, viral dsRNA in the cytoplasm of infected cells is detected by PRRs such as RIG-I, melanoma differentiation-associated protein 5 (MDA5), TLR3, and PKR (235, 236). Binding to PRRs triggers various signalling pathways, which all converge on transcription of type I IFNs. While IFN-α itself is important for NK cell activation in response to reovirus infection (138), a range of other pro-inflammatory cytokines are secreted in response to reovirus, which mediate the recruitment of both NK cells and DC (237, 238). DCs are thought to be one of the key mediators of innate immune cell recruitment during reovirus infection, and reovirus can stimulate DC maturation, causing an upregulation in maturation markers such as CD80, CD86, and MHC Class II. In addition to recruitment, cytokine secretion from DCs in response to reovirus can potentiate the cytotoxic function of NK cells (234). While NK cells are important for the anti-tumour effects of reovirus, they do not limit reovirus infection on their own (239). Neutrophils are also recruited as part of the innate immune response during reovirus infection in the respiratory tract (240).

Reovirus replicates extensively in the respiratory tract of neonatal mice and in tissues of adult SCID mice (lacking T and B lymphocytes), but not in

immunocompetent adult mice, which indicates a role for the adaptive immune system in controlling reovirus infection (241-243). Accordingly, reovirus-specific CTLs with significant cytotoxicity against reovirus-infected target cells have been generated *in vivo* (244). The adaptive immune response also plays an important role in OV efficacy. Similar to NK cells, reovirus-treated DCs can activate T cells and induce antigen-independent cytolysis of target cells (234). Moreover, reovirus treatment of DC can enhance their ability to present TAA with subsequent priming of tumour-specific CTLs (245, 246). Interestingly, it has been proposed that direct reovirus oncolysis might not be necessary to generate adaptive anti-tumour immunity, as tumour-specific CTLs were successfully generated using reovirus-resistant melanoma cells (247).

The humoral arm of adaptive immunity also plays an important role in reovirus infection through the generation of nAb. Due to its widespread presence in the environment, the majority of the population have encountered reovirus and seropositivity between 50 and 100% has been reported (248, 249). While nAb have a positive effect in the immune protection against reovirus, they were previously thought to be detrimental to the reovirus activity with the high seropositivity in the general population being a concern for treatment efficacy. However, both DCs, T cells, and monocytes can act as protective cell carriers of reovirus with efficient hand-off to tumour cells, despite pre-existing antiviral immunity (250-253). Interestingly, when mice were co-treated with reovirus and GM-CSF, the presence of nAb enhanced treatment efficacy (252).

While the immune system has several elaborate ways of protecting the body against reovirus infection, the virus has also developed ways of protecting itself from immune-mediated eradication. For example, the outer capsid protein σ3 can engage with dsRNA and interfere with the binding of PKR to dsRNA, thereby preventing the onset of an IFN response (254). Moreover, Stanifer *et al*. recently showed that one of the non-structural proteins encoded by reovirus, μNS, can sequester the IFN transcription factor IRF3, thereby preventing its translocation to the nucleus and the induction of an IFN response (255).

1.4.5.4 Reovirus clinical trials

As discussed, Reolysin® is a promising candidate for OVT and it has made significant progress in clinical trials. Preference for malignantly transformed cells has been confirmed, and it has demonstrated high tolerability in patients with only low grade adverse effects in clinical trials (256-258). The majority of clinical trials have examined reovirus efficacy in solid malignancies, although early trials for MM have also been initiated (Table 1-6). Most recently, the Myeloma UK *eleven* (MUK11/ViRel/NCT03015922) Phase Ib trial of i.v. administered reovirus in combination with lenalidomide or pomalidomide in refractory MM has been introduced (259). A treatment schedule overview is presented in Figure 3-1A. Both intratumoural and i.v. administration of reovirus have been examined in clinical trials of solid malignancies with successful results. Interestingly, i.v. administration of reovirus in a Phase I trial of heavily pre-treated patients with advanced cancers induced an increase in the populations of both $CD4^+$ T cells, $CD8^+$ T cells, and NK cells, as well as abundant cytokine production, indicating the onset of an anti-tumour immune response (260). Furthermore, in brain tumours, i.v. administration of reovirus led to a local IFN response with recruitment of CTLs and upregulation of PD-1/PD-L1 axis (261). As expected, i.v. administration has been shown to significantly increase nAb titres in clinical trials, but despite this, reovirus could be successfully recovered from tumour sites, such as the liver and from head and neck tumours (186, 262).

Table 1-6: Selected reovirus clinical trials.

Disease	Combinations	Phase	Trial ID	Results
Gliomas	N/A	I	NCT00528684	No DLT, 1/12 patients remained disease free for >6 years (263).
Pancreatic Cancer	Carboplatin/ Paclitaxel	II	NCT01280058	No significant enhancement of PFS with reovirus vs drugs alone (4.9 vs 5.2 months) (264).
Head and Neck Cancers	Carboplatin/ Paclitaxel	II	NCT00753038	4/13 patients had PR, 2/13 had stable disease for >12 weeks (265).
	Carboplatin/ Paclitaxel/ Placebo	III	NCT01166542	Not reported.
Melanoma	N/A	II	NCT00651157	Virus was well tolerated, viral replication was detected in 2/15 patients despite nAb, average PFS 45 days (266).
	Carboplatin/ Paclitaxel	II	NCT00984464	Virus well tolerated, ORR 21%, no complete responses (267).
Multiple Myeloma	N/A	I	NCT01533194	No DLT reported, reovirus localization to BM, SD up to 8 months (195).
	Lenalidomide/ Pomalidomide	I	NCT03015922 MUK11/ViRel	Recruiting (259).
	Dexamethasone/ Carfilzomib	I	NCT02101944	Recruiting (268).
	Dexamethasone/ Bortezomib	I		Evaluating (269).

Lung Cancer	Carboplatin/ Paclitaxel	II	NCT00861627	11/37 partial responses, 20/37 stable diseases, PFS 4 months (270).
		II	NCT00998192	Treatment well tolerated, 12/25 partial responses, 10/25 stable diseases (271).
	Pemetrexed/ Docetaxel	II	NCT01708993	Virus was well tolerated, no enhancement of PFS with reovirus vs drugs alone (2.96 vs 2.83 months) (272).
Prostate Cancer	Docetaxel and Prednisone	II	NCT01619813	Poorer overall survival in virus and drug combination arm, vs drug alone (273).
Breast Cancer	Paclitaxel	II	NCT01656538	Combination arm showed improved overall survival vs drug alone arm (17.4 vs 10.4 months) (274).

All trials included were completed at the time of publication of this thesis except the MM trials. DLT: dose-limiting toxicity, PFS: progression-free survival, PR: partial response, ORR: overall response rate, SD: stable disease.

1.4.6 Coxsackievirus A21

1.4.6.1 Background

Coxsackieviruses belong to the family of *Picornaviridae*, which are non-enveloped, single-stranded (ss), positive-sense RNA viruses. The RNA core of the particle is surrounded by an icosahedral capsid approximately 28 nm in diameter, with a protein coat made up of 60 subunits (275). The prototype picornavirus genome consists of 7000-8000 nucleotides which encode a single polyprotein. As described in Figure 1-9, the polyprotein is cleaved into four structural proteins which make up the capsid subunits, as well as virally encoded proteases, and proteins involved in RNA replication and alteration of the host cell environment (275, 276). The picornavirus family comprises nine heterogenous genera and several well-known human pathogens such as hepatitis A virus, poliovirus, and the coxsackieviruses. The coxsackieviruses belong to the Enterovirus genus. Within this genus, a total of 29 serotypes of coxsackievirus have been identified. For extended classification, the coxsackieviruses were divided into two subgroups (CVA and CVB) based on their pathogenicity in mice (277). Eleven of the CVA serotypes, including coxsackievirus A21 (CVA21), belong to the species of human enterovirus C (HEV-C). Two prototype strains of CVA21 have been identified, *Coe* and *Kuykendall*, with *Kuykendall* being the strain that has been taken forwards as a therapeutic OV. All the CVA in the HEV-C species cause symptoms of the common cold following infection of adults (278).

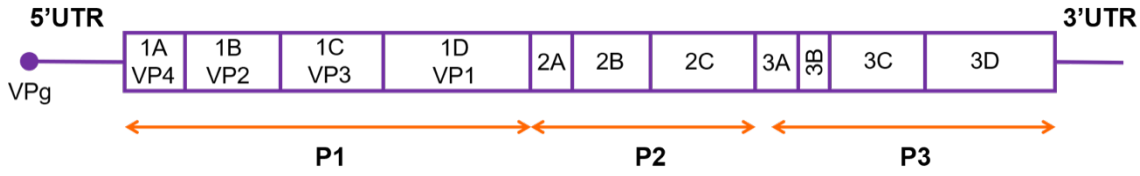

Figure 1-9: Picornavirus genome and polyprotein organisation.

The picornavirus genome is made up of 7000-8000 nucleotides and a single open reading frame. Translation and proteolytic cleavage results in three main polyprotein products, P1-3. The P1 protein is the precursor for the four structural capsid proteins (VP1-4). The P2 and P3 polyproteins contain additional proteins required for genome replication and modification of the host cell environment. UTR: untranslated region.

1.4.6.2 Tumour specificity

CAVATAK™ is a non-manipulated clinical-grade formulation of the CVA21 *Kuykendall* strain. As discussed, both ICAM-1 and DAF are important for mediating host cell entry of CVA21. While DAF acts as the attachment receptor accumulating CVA21 on the cell surface, ICAM-1 is responsible for mediating cell entry (152, 278, 279). DAF alone can mediate cell entry of some clinical isolates of CVA21, but for the *Kuykendall* strain both receptors are required for successful infection and thus, ICAM-1 expression has been defined as the determining factor for tumour cell susceptibility to CVA21 treatment (152, 279). ICAM-1 is a glycoprotein, which belongs to the immunoglobulin family and has widespread functions around the body. As an adhesion molecule, the main function of ICAM-1 is to induce cell-cell adhesion and facilitate cell communication, e.g. in the regulation of leukocyte trafficking across epithelial barriers (280, 281). ICAM-1 is normally expressed on cells involved in immune protection such as leukocytes, epithelial cells, and endothelium, as well as on some haematopoietic cells, including myeloid blasts, monocytic cells, B lymphocytes, and plasma cells (281, 282). More important for the oncolytic effect of CVA21, an increased expression of ICAM-1 has been identified on a range of tumour cells including renal carcinoma (283), malignant melanoma (284), pancreatic cancer (285), and colorectal cancer (286). For the haematological malignancies, high ICAM-1 expression has been observed mainly in B cell malignancies, including MM, CLL, and NHL (202, 287). Furthermore, ICAM-1 is involved in cancer metastasis with increased expression on metastatic disease being reported, which expands the applicability of CVA21 further (284, 288, 289). Other determinants of CVA21 susceptibility, such as factors affecting replication following host cell entry, have yet to be elucidated.

1.4.6.3 CVA21 and the immune system

Very few studies have focused on the specific immunobiology of CVA21 and the exact mechanism for detection of CVA21 by the immune system is not yet known. The interactions of CVB with the immune system have been more widely studied and can provide a generalised picture for all the coxsackieviruses. Coxsackieviruses can be detected by a variety of PRRs, such as MDA5 and TLR3, -7, and -8 (290-294). Recognition on either receptor triggers signalling pathways that induce the production of type I IFNs. Antibody-opsonised CVB3 is detected on TLR7 in the endosomes of pDC, which subsequently secrete large amounts of IFN-α (291). Several

other innate cell types, including NK cells and macrophages, have been shown to be essential for limiting replication of CVB (295, 296). Moreover, the complement system, with C3 opsonisation, has been implicated for the splenic antiviral response against CVB3 (297). As discussed below, antibodies against coxsackieviruses are generated soon after infection as part of the humoral immune response. In addition, it is widely accepted that $CD4^+$ T cells play an important role in CVB protection, while the role of $CD8^+$ T cells is more controversial (298, 299). Coxsackieviruses activate both $CD4^+$ and $CD8^+$ T cells, and $CD8^+$ T cells can limit viral replication, however, efficient priming of CTLs specific for defined epitopes has not been documented (300). The ability of CVA21 to induce anti-tumour immunity has not previously been thoroughly described. However, in a study by Annels *et al.*, CVA21 induced immunogenic apoptosis in bladder cancer cell lines, which resulted in successful tumour vaccination *in vivo*, which was confirmed to be dependent on $CD4^+$ T cells (301).

As discussed for reovirus, the coxsackieviruses are also widely present in the environment, resulting in widespread exposure of the general population with subsequent generation of nAb. In a study from 1959, the prevalence of serum antibodies to a virus identical to the *Coe* strain of CVA21 was examined in the British population, which revealed the presence of nAb in approximately 36.1% of males and 18.4% of females (302, 303). In a more recent small-scale study, pre-existing nAb against CVA21 was present in 14.3% (3 of 21) of samples tested (304). Additionally, early clinical trials indicated that nAb might not develop in patients until Day 7 after i.v. infusion of CVA21 (305). The exact role of nAb for CVA21 treatment remains unknown, but similar to reovirus, monocytes can act as carriers of antibody-neutralised CVA21 with successful delivery to melanoma cells, resulting in oncolytic killing (253). While it is likely that the immune response to CVA21 is similar to those described for CVB, it is evident that documentation on CVA in general, and CVA21 in particular, needs to be expanded so that this virus can be optimally used in OVT.

While the immune system has developed efficient strategies for protection against coxsackievirus infection, the viruses have also developed immune evasion strategies. For example, CVB3 specifically cleaves both MAVS and TRIF, which are downstream adaptor molecules in the signalling pathways of MDA-5 and TLRs, respectively, thereby interfering with the IFN antiviral response pathway (306, 307). Moreover, CVB3 can inhibit antigen presentation through interference with protein trafficking and downregulation

of MHC class I, resulting in evasion of $CD8^+$ T cell immunity, which might also explain the ambiguous evidence regarding $CD8^+$ T cell immune responses against CVB (308). No interference with MHC Class II has been documented, meaning that $CD4^+$ T cell immunity may be unaffected.

1.4.6.4 CVA21 clinical trials

CVA21 is a more novel oncolytic agent than reovirus and has only been tested in Phase I and II clinical trials to date. As shown in Table 1-7, a range of solid malignancies have been included in the clinical trials, but no trials have yet been initiated for HM. CVA21 has made its greatest progress in melanoma where a Phase II trial for late stage melanoma was completed with 63 patients with stage IIIc or IV melanoma receiving 10 intratumoural injections of CAVATAK™ during 18 weeks. In addition, CVA21 is being tested extensively in combination with checkpoint inhibitors, mainly pembrolizumab, for both melanoma, bladder cancer, and lung cancer. Only one clinical trial (STORM/KEYNOTE-200/NCT02043665, Phase I) has investigated i.v. delivery of CVA21 (309). The first part of the study, using CVA21 as a monotherapy, has been completed and was extended with a second part using CVA21 and pembrolizumab in combination. A total of 27 patients with various solid malignancies were recruited to the first part of this trial which employed a non-randomised, open-label, dose escalation study design. Patients were recruited in three cohorts receiving repeated doses of $1x10^8$, $3x10^8$, or $1x10^9$ $TCID_{50}$ CAVATAK™, respectively. A treatment schedule overview is presented in Figure 3-1B. Although a recent addition to the OV family, CVA21 has proven safe and well-tolerated in clinical trials and was recently acquired by Merck & Co. for continued development.

Table 1-7: CVA21 clinical trials initiated to date

Disease	Combinations	Phase	Trial ID	Results
Melanoma	Pembrolizumab	I	NCT02565992 CAPRA	Recruiting, 18/23 disease control rate (310).
	Ipilimumab	I	NCT02307149 MITICI	Recruiting, combination well-tolerated, 14/18 disease control rate (311).
		I	NCT03408587 CLEVER	Recruiting (312).
	N/A	II	NCT01227551 CALM	22/57 immune-related progression-free survival (313).
		I	NCT02043665 STORM KEYNOTE-200	Virus was well-tolerated (305).
Bladder Cancer	Mitomycin C	I	NCT02316171 CANON	Virus was well-tolerated (314).
	Pembrolizumab	I	NCT02043665 STORM Part 2	Recruiting (315).
Lung Cancer	Pembrolizumab	I	NCT02824965	Recruiting (316).
	Pembrolizumab	I	NCT02824965 STORM Part 2	Recruiting (315).

1.5 Conclusions

The immune system has a critical role in reducing the occurrence of cancer, as well as in elimination of already transformed cells. OVT can efficiently exploit the immune system to potentiate anti-tumour immune responses and thereby successfully eradicate tumours. However, HM are under-investigated in the field of OVT, in particular with respect to anti-tumour immunity and in the search for better treatments, OVT needs further investigation in this setting.

1.6 Project hypothesis and aims

The efficacy of OV against HM remains largely underexplored compared to that of solid malignancies. In particular, the role of anti-tumour immunity remains unclear. This is reflected in the limited translation of OV in the haematological setting. In terms of reovirus, the cellular mechanisms by which reovirus activates immune cells have been defined, and a role for direct oncolysis and NK cell-mediated anti-tumour immunity has been reported against AML. However, in the context of MM, whilst the direct oncolytic effects of reovirus have been extensively studied, the role for anti-tumour immunity has not been established. In terms of CVA21, a role for direct oncolysis has been confirmed in MM, but not AML. Moreover, the importance of anti-tumour immunity for CVA21 treatment efficacy has not been defined in either MM or AML and remains to be elucidated also for solid malignancies. Additionally, the specific cellular mechanisms behind CVA21-induced immune cell activation remain largely unknown.

Therefore, this study aimed to develop the understanding of how OV, specifically reovirus and CVA21, may regulate anti-tumour immunity and to do this, the following overlapping but complementary aims were devised:

1. Characterise reovirus and CVA21 direct cytotoxicity and anti-tumour immune responses against human MM and confirm the role for anti-tumour immunity in the context of BM stromal support.
2. Explore reovirus treatment of MM *in vivo*, in particular characterise changes in immune cell populations, and their state of activation, in the spleen and BM following reovirus treatment.
3. Evaluate the potential of CVA21 as a treatment for AML using both AML cell lines and a cohort of primary AML patient samples.
4. Elucidate the cellular mechanisms behind CVA21-mediated anti-tumour immunity.

Chapter 2
Materials & Methods

Chapter 2
Materials & Methods

2.1 Cell culture

2.1.1 Cell culture methods

All cells were maintained in a humidified atmosphere with 5% CO_2 at 37°C using a CO_2 incubator with continuous UV decontamination (Sanyo). Cells were cultured in vented plastic tissue culture flasks and were harvested and washed using serological pipettes (both Corning Costar). Adherent cell lines were passaged near confluence by first washing cells with sterile phosphate-buffered saline (PBS, prepared using Dulbecco's A PBS tablets in dH_2O [Oxoid™]), followed by addition of trypsin at 37°C (10x stock diluted 1:10 in Hanks' Balanced Salt Solution (HBSS), both Sigma-Aldrich). Suspension cell lines were passaged following centrifugation and re-suspension in fresh culture medium. Cells were centrifuged at 400 x*g* for 5 min at room temperature (RT) using an Eppendorf 5810 centrifuge, unless otherwise stated. All cell culture was performed under aseptic conditions using Nuaire Class II Microbiological Safety Cabinets. Cells were counted using trypan blue (0.2% in PBS, Sigma-Aldrich) and an Improved Neubauer haemocytometer. All cell lines were routinely tested for mycoplasma contamination and were found free from infection.

2.1.2 Cell lines

An overview of all cells used and their respective culture medium is available in Table 2-1. All culture media were obtained from Sigma-Aldrich and supplemented with 10% foetal bovine serum (FBS, Gibco®) unless otherwise stated. Additional supplements were also obtained from Sigma-Aldrich. An overview of culture media used for primary cells is available in Table 2-2.

2.1.3 Cryopreservation

In general, cell lines were harvested and resuspended in culture medium + 10% dimethyl sulphoxide (DMSO, Sigma-Aldrich) for freezing. 5TGM1 cells were frozen in culture medium containing 20% FBS and 10% DMSO, PBMC

were frozen in 90% FBS and 10% DMSO. Cells were aliquoted in Nunc™ Cryogenic tubes and frozen to -80°C overnight in a Mr. Frosty™ freezing container (both ThermoFisher Scientific). Subsequently, cells were transferred to the vapour phase of liquid nitrogen for long-term storage. For recovery, cells were rapidly thawed in a 37°C water bath, washed in 10x excess fresh culture medium, and isolated by centrifugation before resuspension in fresh culture medium and transfer to tissue culture flasks.

2.1.4 ICAM-1 transduction

ICAM-1-expressing KG-1 cells were obtained following lentiviral transduction with a vector expressing human ICAM-1, green fluorescent protein (GFP), and puromycin resistance genes under a CMV promoter (GenTarget). KG-1 cells were infected with 0.5 plaque-forming units (pfu)/cell of either an ICAM-1-expressing or empty control vector for 24 hrs in RPMI-1640 with 20% FBS. Stably transduced cells were selected by addition of 2 μg/mL puromycin (Sigma-Aldrich) to the culture medium for up to 6 weeks.

2.1.5 CellTracker™ staining

Cell Tracker™ Green CMFDA (CTG) and Cell Tracker™ Violet BMQC (both Invitrogen™) were used. A 5 mM stock solution of Cell Tracker™ fluorescent dye was prepared in DMSO. A 2.5 μM working dilution was prepared in pre-warmed serum-free RPMI-1640 and cells were stained at 10^6/ml for 30 min at 37°C. Subsequently, cells were washed three times in complete RPMI-1640 (at least three times staining volume/wash) before use in experiments.

Table 2-1: Cell lines and culture media

	CELL LINE	***CELL TYPE***	***SPECIES***	***CULTURE MEDIUM***
AML	KG-1	*Macrophage (BM)*	Human	*Rosewell Park Memorial Institute-1640 medium containing 1% L-glutamine + 10% (v/v) foetal bovine serum (Complete RPMI-1640).*
	HL-60	*Promyeloblast (PB)*	Human	*Complete RPMI-1640*
	THP-1	*Monocyte (PB)*	Human	*Complete RPMI-1640*
	kasumi-1	*Myeloblast (PB)*	Human	*Complete RPMI-1640*
	ML-1	*Myeloblast (PB)*	Human	*Complete RPMI-1640*
	OCI-M2	*Derived from erythroleukemia*	Human	*Iscove's modified Dulbecco's medium containing 1% L-glutamine + 10% (v/v) FBS.*
Multiple myeloma	H929	*IgA_{κ} MM, (BM)*	Human	*Complete RPMI-1640*
	U266B	*IgE_{λ} MM, (PB)*	Human	*Complete RPMI-1640*
	JIM3	*(PE)*	Human	*Complete RPMI-1640*
	OPM2	*IgG_{λ} MM, (PB)*	Human	*Complete RPMI-1640*
	5TGM1	*IgG_{2b} MM, (BM)*	Murine	*Complete RPMI-1640, supplemented with 1mM sodium pyruvate and 100 mM non-essential amino acids.*

BM: bone marrow, PB: peripheral blood, PE: pleural effusion

Table 2-1 continued: Cell lines and culture media

	CELL LINE	***CELL TYPE***	***SPECIES***	***CULTURE MEDIUM***
Bone marrow stroma	HS-5	Fibroblast	Human	*Complete RPMI-1640*
	HS-27	Epithelium	Human	*Complete RPMI-1640*
Additional	K562	Chronic myeloid leukaemia	Human	*Complete RPMI-1640*
	Daudi	Burkitt lymphoma	Human	*Complete RPMI-1640*
	Raji	Non-Hodgkin lymphoma	Human	*Complete RPMI-1640*
	Mel624	Melanoma	Human	*Dulbecco's modified Eagle's medium containing 1% L-glutamine and 4500 mg/L glucose + 10% (v/v) FBS (Complete DMEM).*
	SK-Mel-28	Melanoma	Human	*Complete DMEM*
	L929	Fibroblast	Murine	*Complete DMEM*

Table 2-2: Primary cell culture media

CELL TYPE	*CULTURE MEDIUM*
Monocytes (for iDC generation)	Complete RPMI-1640 containing 1% L-glutamine + 10% (v/v) FBS + 500 U/ml IL-4 + 800 U/ml GM-CSF
CTL priming cultures	RPMI-1640 containing 1% L-glutamine + 7.5% human AB serum + 1 mM sodium pyruvate + 10 mM HEPES + 100 mM non-essential amino acids + 20 μM β-mercaptoethanol + 30 U/mL IL-2 + 5 ng/mL IL-7
Peripheral blood mononuclear cells (PBMC)	Complete RPMI-1640
Primary AML blast cells	Complete RPMI-1640
Murine splenocytes	DMEM + 5% FBS + 1% penicillin/streptomycin + 50μM β-mercaptoethanol

IL-4: BioLegend, GM-CSF: MBL International, IL-2: R&D Systems, β-mercaptoethanol: Sigma-Aldrich, IL-7: BioLegend, human AB serum: GemCell™, Seralabs, penicillin/streptomycin: Sigma-Aldrich.

2.1.6 Stromal cell co-cultures

To investigate the effect of the bone marrow microenvironment on MM cells, MM cell lines H929, U266B, and JIM3 were co-cultured with BM stromal cell lines HS-5 and HS-27, respectively. An overview of the protocol is provided in Figure 2-1. HS-5 and HS-27 cells were seeded and allowed to attach overnight. The following day, MM cell lines were stained with CTG (Section 2.1.5), then added to wells with stromal cells at a 1:1 cell ratio and 1:1 medium ratio, i.e. direct addition of MM cells in an equal volume fresh medium to pre-conditioned stromal medium already in the wells. MM cells and stromal cells were co-cultured for 24 hrs before addition of viral treatments. When used as targets in NK cell and CTL killing assays, MM cells were co-cultured with stromal cells for 48 hrs before inclusion in killing assays.

2.1.7 Cytokine treatments

2.1.7.1 TNF-α for induction of ICAM-1 expression

All cells were treated with human recombinant TNF-α (R&D Systems) for 24 hrs before evaluation of ICAM-1 expression (Section 2.13.2) or subsequent viral treatment. Based on toxicity studies, the TNF-α doses for KG-1 and THP-1 cells were 10, 100, and 1000 U/mL (Low/Intermediate/High). For kasumi-1 cells, the corresponding doses were 1, 10, and 100 U/mL.

2.1.7.2 Cytotoxicity of IFNs

KG-1 and HL-60 cells were treated with human recombinant IFN-α (Peprotech) alone or in combination with human recombinant IFN-γ (R&D Systems) for 96 hrs before evaluation of cell viability by flow cytometry (Section 2.13.1). Cells were either untreated or treated with Low (500 pg/mL), Intermediate (2500 pg/mL), or High (5000 pg/mL) doses of IFN-α. For combination treatment, IFN-γ doses of 500 (Low), 1500 (Interm.), and 3000 (High) pg/mL were used, combining Low IFN-α with Low IFN-γ etc.

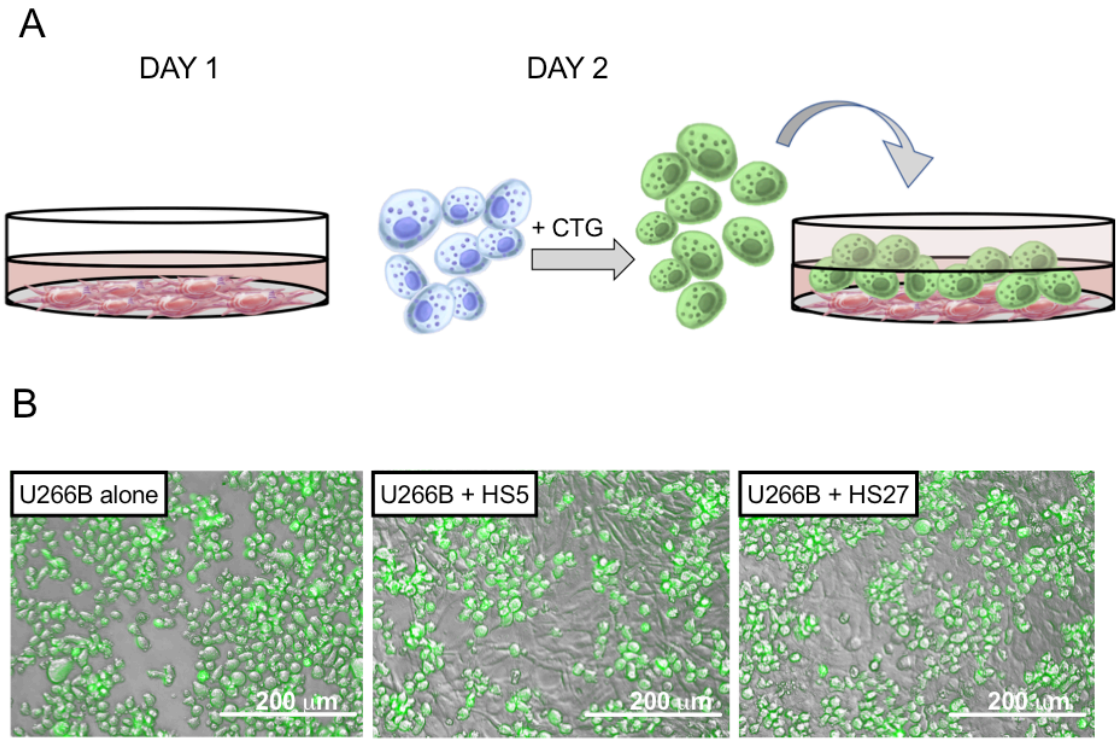

Figure 2-1: Illustration of BM microenvironment co-culture protocol.

A: On Day 1, stromal cells (HS-5 or HS-27) were seeded and allowed to adhere to the cell culture dish. On Day 2, MM cells were stained with Cell Tracker Green (CTG) and added to stromal cells at a 1:1 ratio. Any medium already in the culture wells (conditioned by the stromal cells) was diluted 1:1 with fresh medium on the addition of MM cells. **B**: Representative images of U266B cells cultured alone, or together with HS-5, or HS-27 stromal cells, respectively. Cells were co-cultured for 24 hrs and images taken using an EVOS® FL Cell Imaging System (ThermoFisher Scientific).

2.2 Peripheral blood mononuclear cells (PBMC)

2.2.1 Isolation of human PBMCs

For all AML work, except T cell priming, peripheral blood was collected in K3EDTA-coated Vacuette® blood samples tubes (Greiner Bio-One) from healthy volunteers by peripheral vein phlebotomy after informed consent. For T cell priming experiments (AML+MM), and MM NK cell experiments, healthy donor blood was collected and processed in leukocyte apheresis cones by the National Health Service Blood and Transplant (NHSBT). PBMCs were isolated from donated blood using Lymphoprep™ (Fresenius-Kabi) density gradient centrifugation. Blood from apheresis cones was diluted 1:5 in HBSS prior to layering on the Lymphoprep™ medium at a 2:1 ratio. Following centrifugation for 20 min at 800 x*g* without brake, PBMCs were harvested using a wide-tipped Pasteur pipette (Alpha Laboratories) and washed three times in 50 mL HBSS (1x 400 x*g* for 10 min, 2x 300x*g* for 5 min). PBMCs were seeded at $2x10^6$ cells/mL for all experiments and maintained in complete RPMI-1640 (Table 2-2).

2.2.2 PBMC-conditioned cell culture medium (CM)

To generate CM, PBMCs were seeded at $2x10^6$ cells/mL and treated with 0.1 or 1 pfu/cell of CVA21 or reovirus, or mock treated with PBS. After 48 hrs incubation, cells were removed by centrifugation at 400 x*g* for 5 min, and the culture medium supernatant was sterile filtered using a 0.2 µm syringe filter (Millex®, Merck Millipore) and stored at -20°C until use. For MM experiments, CM was UV irradiated as described below (Section 2.6.3) to inactivate OV. The toxicity of CM was evaluated using MTS assays as described in Section 2.8.

2.3 Primary AML patient samples

Primary leukemic blast cells were obtained from the peripheral blood of patients diagnosed with AML under the care of St. James's University Hospital, Leeds, UK (Table 5-1). The cohort included samples from both newly diagnosed and relapsed patients with a variety of AML subtypes and pre-AML diagnoses (MDS and RAEB). Samples collected both prior to, and during standard treatment were included. The PBMC fraction, including leukemic blasts, was isolated as previously described (Section 2.2.1),

seeded in complete RPMI-1640 and used in experiments immediately. Patient PBMCs were used at a density of $2x10^6$ cells/mL in all experiments. Blast phenotype was determined by flow cytometry (Section 2.13.2) using FITC-conjugated anti-CD45, VioBlue-conjugated anti-CD34 and PE-Vio770-conjugated CD117 antibodies. Details of antibodies used are provided in Table 2-3 along with the gating strategy in Figure 2-2. Written, informed consent was obtained from all patients in accordance with local institutional ethics review and approval, ethics number 06/Q1206/106. Patient-CM was obtained as previously described for CM (Section 2.2.2).

Table 2-3: Flow cytometry antibodies for AML primary samples

The following antibodies were used to identify blast cells in the PBMC fraction of peripheral blood. Additional markers detailed in Table 2-4 were included for immunophenotyping.

Target molecule	Fluorochrome	Volume added	Species of origin	Clone	Supplier
CD45	FITC	2 µL	Mouse	5B1	Miltenyi Biotec
CD34	VioBlue	2 µL	Mouse	AC136	Miltenyi Biotec
CD117	PE-Vio770	2 µL	Mouse	A3C6E2	Miltenyi Biotec

PE: phycoerythrin, FITC: fluorescein isothiocyanate.

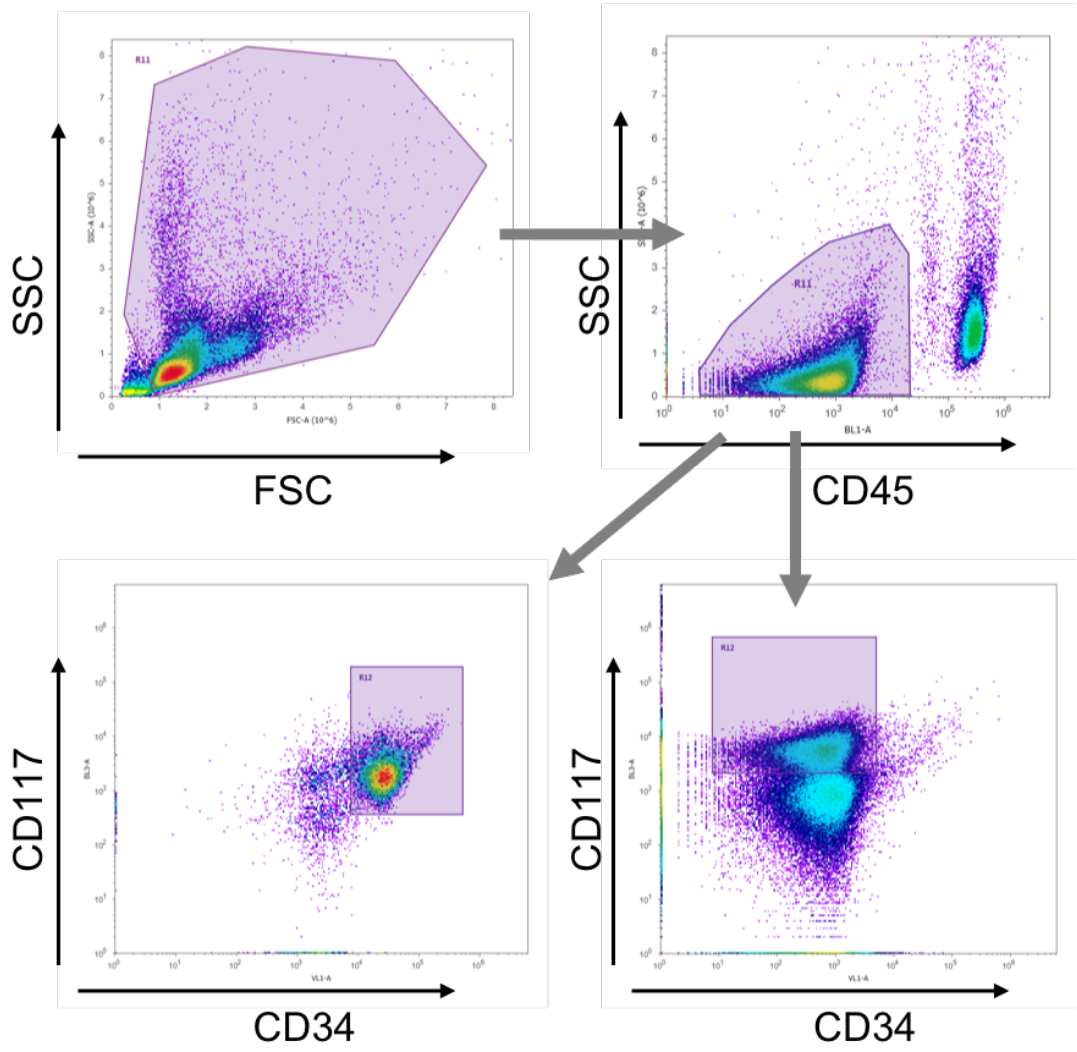

Figure 2-2: AML primary samples gating strategy for blast cell identification.

The phenotype of blast cells in primary AML patent samples was determined by flow cytometry using FITC-conjugated anti-CD45, VioBlue-conjugated anti-CD34 and PE-Vio770-conjugated CD117 antibodies. The bottom panels show samples from two individual AML patients. Blast cells were identified as $CD45^-$ and either $CD34^+CD117^+$ (left panel) or $CD34^-CD117^+$ (right panel) depending on the individual diagnosis. Flow cytometry analysis was performed using Attune™ software (Section 2.13).

2.4 STORM clinical trial patient samples

Peripheral blood samples were obtained from patients taking part in the STORM Phase 1 clinical trial (NCT02043665/Keynote-200/VLA009A). Written, informed consent was obtained from all patients in accordance with local institutional ethics review and approval, ethics number 06/Q1206/106. Five patients were included in this study and received an i.v. infusion of $1x10^8$ or $1x10^9$ $TCID_{50}$ clinical grade CVA21 (Table 3-1) on Day 1, 3 and 5. Peripheral blood samples were taken prior to infusion, then 1 hr, 3 days and 21 days post first infusion (Figure 3-1B). Whole blood samples were treated with BD Pharm Lyse™ buffer (BD Biosciences) according to the manufacturer's instructions to lyse red blood cells before phenotypic analysis of NK cells, $CD4^+$ T cells, and $CD8^+$ T cells using flow cytometry. Relevant antibodies are detailed in Table 2-4.

2.5 Myeloma UK *Eleven* (MUK11) clinical trial patient samples

Peripheral blood samples were obtained from patients taking part in the MUK11 Phase 1b clinical trial (NCT03015922/ViRel). Written, informed consent was obtained from all patients in accordance with local institutional ethics review and approval, ethics number 16/YH/0388. Only one patient was included in this study and peripheral blood samples were taken immediately prior to reovirus infusion (10^{10} $TCID_{50}$), then at 24 hrs, 72 hrs, and seven days post infusion. Blood samples were processed as described in Section 2.2.1 to obtain PBMCs and then the activation of NK cells, $CD4^+$ T cells, and $CD8^+$ T cells was measured by flow cytometry (Section 2.13.2 and Table 2-4).

2.6 Oncolytic viruses

WT coxsackievirus A21, *Kuykendall* strain (CVA21, CAVATAK™), was provided by Viralytics Ltd. or propagated in-house (Section 2.6.2) from WT CVA21 *Kuykendall* strain V-024-001-012 obtained from ATCC® (ATCC®VR-850™). Respiratory enteric orphan virus (reovirus) Type 3 *Dearing* strain (Reolysin®) was provided by Oncolytics Biotech Inc. Both virus stocks were stored long term at -80°C. CVA21 was used immediately after removal from -80°C, whilst reovirus was stored at 4°C for up to two weeks.

2.6.1 *In vitro* virus treatment of cells

MM and AML cell lines were treated at a density of $5x10^5$ cells/mL, healthy donor PBMCs and AML patient samples were treated at a density of $2x10^6$ cells/mL. For stromal cell co-cultures, the viral dose was adjusted for the total number of cells (stroma and MM cells). Both reovirus and CVA21 were diluted in PBS and added to cells at various concentrations. For reovirus, the following doses were used: 0, 0.01, 0.1, 1, and 10 pfu/cell. For CVA21, the following doses were used: 0, 0.01, 0.1, and 1 pfu/cell. Cells and supernatants were harvested at various time points post treatment for determination of cell viability (Section 2.13.1), cytokine/chemokine production (Section 2.12), and generation of CM (Section 2.2.2).

2.6.2 CVA21 propagation

CVA21 was propagated using Mel624 cells. Following CVA21 infection for 24 hrs (0.001 pfu/cell), all supernatants were harvested, filtered (65 μm), and transferred to Thinwall polypropylene tubes (Beckman Coulter). CVA21 in the supernatant was pelleted by centrifugation at 36 000 rpm for 2 hrs at 4°C (SW45 rotor, Optima™ L-80 ultra centrifuge, Beckman Coulter). Virus was harvested and then purified using OptiPrep™ (Sigma-Aldrich) density gradient centrifugation. The OptiPrep™ gradients were prepared in advance using two different solutions; Solution 1: 0.3 M Tris and 0.3 mM EDTA in dH_2O, pH 7.4, Solution 2: 0.1 M NaCl, 50 mM Tris, and 0.5 mM EDTA in dH_2O, pH 7.4. 5 mL of Solution 1 was added to 20 mL 60% OptiPrep™ medium, which was then diluted in Solution 2 to obtain the following concentrations:

- 15%: 3 mL diluted Optiprep™ + 7 mL Solution 2
- 23%: 4 mL diluted Optiprep™ + 6 mL Solution 2
- 28%: 6 mL diluted Optiprep™ + 4 mL Solution 2
- 35%: 7 mL diluted Optiprep™ + 3 mL Solution 2

Starting with the 35% Optiprep™, 2.5 mL of each concentration was gently layered in two Thinwall Ultra-Clear™ open-top tubes (Beckman Coulter). Gradient tubes were stored at 4°C overnight prior to use. The harvested virus pellet was equally distributed across both gradient tubes and

centrifuged at 36 000 rpm for 1.5 hrs at 4°C using an SW41 Ti rotor. Approx. 1 mL of virus-containing solution was harvested, aliquoted, and stored at -80°C until use. Viral titre was determined by plaque assay in Mel624 cells (Section 2.7.2).

2.6.3 Ultraviolet (UV) irradiation of virus and CM

To render viral particles replication incompetent, virus stocks were treated with UV irradiation using a C-1000 UV Crosslinker (UVP). Reovirus stock was UV treated for 2 min (1200 μJ/cm^2) in 100 μL aliquots in an open 48-well plate. CVA21 in PBS was UV treated for 3 min in 100 μL aliquots in an open 48-well plate. CM generated using reovirus was UV treated for 2 min in 2 mL aliquots in an open 6-well plate before addition to susceptible cells. UV inactivation times of up to 10 min were used for CM generated using CVA21.

2.7 Quantification of virus titre

2.7.1 CVA21 $TCID_{50}$ assay

CVA21 replication was determined using a $TCID_{50}$ assay with SK-Mel-28 cells. Samples were prepared by harvesting both cells and supernatants, followed by lysis of the cells using three rounds of freezing in methanol chilled by solid CO_2 (dry ice) and thawing in a 37°C water bath. $6x10^3$ SK-Mel-28 cells in 100 μL complete DMEM were seeded per well in a flat-bottom 96-well plate and allowed to adhere overnight. An additional 100 μL complete DMEM was then added to each well and all samples were diluted 1:10 in complete DMEM before addition in eight replicates to the first column of a plate. Subsequent 10-fold serial dilutions were made across the plate to 10^{-10} using a multi-channel pipette, and cells were incubated for five days. Viral cytopathic effect (CPE) was assessed following methylene blue staining; the culture medium was removed and all wells were washed once in PBS before fixation of remaining cells in 1% paraformaldehyde (PFA) in PBS for 10 min at RT. After removal of the PFA, 30 μL/well of methylene blue (1% methylene blue hydrate [Sigma-Aldrich] in 35% EtOH) was added for 5 min, then plates were rinsed in tap water and air dried. The number of methylene blue negative wells per dilution was counted and the $TCID_{50}$/mL was calculated using the Spearman-Kärber method and the following formula (317):

$$Log_{10}\ TCID_{50}/mL = 10^{1+L+d\ (s-0.5)}$$

Where L = $\log_{10}$ of the lowest dilution with CPE, d = log difference of dilution (i.e. 1 for 10-fold dilutions), s = sum of the ratios of CPE/no CPE per dilution.

2.7.2 Plaque assay

Plaque assays were used to determine stock titres of both CVA21 and reovirus, and to determine reovirus replication. Mel624 cells ($9x10^5$/well in a 6-well plate) were used for the CVA21 plaque assay and L929 cells ($5x10^5$/well in a 6-well plate) were used for reovirus. Cells were seeded on Day 1 and allowed to adhere overnight. On Day 2, 10-fold serial dilutions of virus samples were prepared in serum-free DMEM. Culture medium in all wells was removed and replaced by 500 μL/well serum-free DMEM and 100 μL/well of each virus dilution to be tested (usually 10^{-2} to 10^{-10} dilution range). CVA21 plates were incubated for 2 hrs, then serum-free DMEM was removed and replaced by 2 mL 1:1 2x DMEM (20% FBS) and 3% carboxymethyl cellulose in dH_2O (CMC, Sigma-Aldrich). For reovirus, plates with virus dilutions were incubated for 2.5 hrs and serum-free DMEM was replaced by 2 mL 2:1 1x DMEM (10% FBS) and 1.6% CMC. All plates were incubated for a further 72 hrs. Then, methylene blue staining was performed as described above (Section 2.7.1). 2 mL PBS/well was used to rinse off excess CMC, then 0.5 mL PFA/well was used for fixation and 0.5 mL methylene blue/well was used for staining. Finally, the number of plaques were counted to determine the pfu/mL titre using the following formula:

$$pfu/mL = \frac{no.\ of\ plaques}{d\ x\ V}$$

Where d = the dilution where plaques were counted, and V = the volume of diluted virus added (i.e. 0.1 mL here).

2.8 MTS assay

MTS assays were performed to evaluate cell viability in CM monocultures and the toxicity of UV treated reovirus. $5x10^4$ cells were seeded in 50 μL fresh RPMI-1640 (complete)/well in a flat-bottom 96-well plate. For CM experiments, 50 μL CM was added per well in triplicate (1:1 dilution in fresh medium). For UV-reovirus experiments, UV treated reovirus was added in 50 μL/well RPMI-1640 (complete) to final doses of 0.1 or 1 pfu/cell doses, 50 μL complete RPMI-1640 was used as a negative control. Plates were incubated for 96 hrs, then 20 μL MTS reagent (tetrazolium dye, Abcam) was added to each well followed by 2.5 hrs incubation at 37°C. The optical density of the converted formazan product was measured at 450 nm using a Multiscan EX microplate reader (ThermoFisher Scientific).

2.9 Type I IFN neutralization assay

PBMCs were obtained from healthy donors as previously described (Section 2.2.1). Prior to CVA21 treatment, PBMCs were either treated with a type I IFN blocking antibody mix (1.5% sheep polyclonal anti-human IFN-α, 1.5% sheep polyclonal anti-human IFN-β, and 3% mouse monoclonal anti-human IFN-α/β receptor chain 2, all antibodies from PBL Assay Science), isotype control antibody mix (3% sheep-serum and 3% anti-mouse IgG_{2a} isotype antibody, Sigma-Aldrich and R&D systems, respectively), or left untreated for 30 min at 37°C. Subsequently, the PBMCs were exposed to 0 or 1 pfu/cell CVA21 for 24 hrs before evaluation of NK cell activation and degranulation (Sections 2.13.2 and 2.13.3) with and without IFN neutralization.

2.10 ICAM-1 neutralization assay

PBMCs were obtained from healthy donors as previously described (Section 2.2.1). Prior to CVA21 treatment, PBMCs were either treated with 10 μg/mL LEAF™ purified anti-human ICAM-1-blocking antibody, a mouse $IgG1_κ$ isotype control antibody (both BioLegend), or left untreated for 30 min at 37°C. Subsequently, the PBMCs were exposed to 0, 0.1, or 1 pfu/cell CVA21 for 24 hrs, before evaluation of NK cell activation (Section 2.13.2) with and without ICAM-1 neutralization and collection of culture supernatants for ELISA (Section 2.12.1).

2.11 Magnetic cell sorting

2.11.1 CD14$^+$ cells

CD14$^+$ monocytes were isolated or depleted from whole PBMCs using magnetic cell sorting with MACS® columns and MidiMACS™ separator magnets (Miltenyi Biotec), according to the manufacturer's instructions. Whole PBMCs were labelled with 2 μL/10^6 cells MACS® CD14 MicroBeads (Miltenyi Biotec) in 3 mL MACS buffer (PBS + 1% FBS, 2mM EDTA) for 15 min at 4°C. Then, cells were washed in MACS buffer at 4°C, resuspended in 3 mL MACS buffer, and added to MACS® columns for selection. PBMCs depleted of CD14$^+$ cells were collected following 3x washes of the column with MACS buffer. CD14$^+$ cells were collected by releasing the column from the magnet and flushing with 5 mL MACS buffer. Purity of depleted PBMC was evaluated by flow cytometry and was consistently >95% (data not shown).

2.11.2 pDC

pDC were isolated or depleted from whole PBMC using the pDC Isolation Kit II, MACS® columns, and MidiMACS™ separator magnets (Miltenyi Biotec) according to the manufacturer's instructions. Whole PBMCs were resuspended in 0.5 mL MACS buffer (Section 2.11.1) and labelled with 100 μL/10^8 cells Non-pDC Biotin-Antibody Cocktail for 10 min at 4°C. After a wash in MACS buffer, cells were resuspended in 1 mL MACS buffer and labelled with 100 μL/10^8 cells Non-pDC Microbead Cocktail for 15 min at 4°C. Cells were then washed in MACS buffer at 4°C, resuspended in MACS buffer, and added to MACS® columns for selection. Lin$^-$, BDCA-2$^+$, BDCA-4$^+$, CD123$^+$, CD4$^+$, CD45RA$^+$, BDCA-3^{dim}, BDCA-1$^-$, CD2$^-$ pDC were collected following 3x washes of the column with MACS buffer. PBMCs depleted of pDC were collected by releasing the column from the magnet and flushing with 5 mL MACS buffer. Purity of depleted PBMC was evaluated by flow cytometry and was consistently >95% (data not shown).

2.11.3 Double depletion

To obtain double-depleted PBMCs (without CD14$^+$ cells and pDC), PBMCs were first depleted of CD14$^+$ cells according to the protocol above (Section 2.11.1), followed by a pDC depletion (Section 2.11.2).

2.12 Cytokine detection

2.12.1 Enzyme-linked immunosorbent assay (ELISA)

Flat-bottomed 96-well plates (Nunc Maxisorp®) were coated with capture antibodies diluted in coating buffer (100 nM $NaHCO_3$ in dH_2O) or PBS as indicated in the Appendix (p. 308). Plates were then wrapped in cling film and incubated at 4˚C overnight. Antibody-coated plates were washed three times with PBS-T (0.05% TWEEN® 20 [Sigma-Aldrich] in PBS) using a SkanWasher 300 (Molecular Devices). 200 µL/well blocking solution (PBS-T + 10% FBS) was added for 2 hrs at RT. The plates were washed a further three times with PBS-T before 100 µL of recombinant protein standards (Appendix p. 309) and sample supernatants were added in triplicate. Protein standards were serially diluted (2-fold) seven times and a blank control with culture medium only was included. Plates loaded with samples were wrapped in cling film and incubated at 4˚C overnight. Next, plates were washed six times with PBS-T and diluted biotinylated detection antibodies were added (dilution in blocking buffer according to the table in the Appendix p. 308) and plates were incubated for 2 hrs at RT. Following incubation, plates were washed six times with PBS-T and 100 µL of ExtrAvidin®-alkaline phosphatase conjugate (Sigma-Aldrich), diluted 1:5000 in PBS-T, was added to each well for 1 hr at RT. Plates were then washed three times with PBS-T, followed by three times with dH_2O. 100 µL of substrate solution (1 mg/mL *p*-nitrophenyl phosphate) in 0.2 M TRIS buffer (both Sigma-Aldrich) was added per well and plates were placed in the dark to develop for 10-20 mins. The optical density was determined using a Multiskan EX plate reader (ThermoFisher Scientific) at a wavelength of 405 nm.

2.12.2 Magnetic bead-based multiplex immunoassay (Luminex)

Supernatants from CVA21-treated healthy donor PBMCs were collected 48 hrs post infection. The levels of 48 cytokines and chemokines were assessed using two Luminex plates (Bio-Plex Pro™ Human Cytokine 27-plex and 23-plex Assay, Bio-Rad Laboratories) over consecutive days, as per the manufacturer's instructions. Briefly, the assay plate was first coated with the antibody-conjugated magnetic beads and washed twice with the supplied wash buffer (100 µL/well) using the hand-held magnetic washer accompanying the kit. A standard dilution series for an eight-point curve with a three-fold dilution between each point was prepared using the supplied standard control. Then, 50 µL/well of each standard and sample was added

to the assay plate in duplicate. The plate was incubated on a plate shaker (850 rpm) for 1 hr at RT in the dark. Following incubation, the plate was washed three times with 100 μL/well washing buffer before addition of 25 μL detection antibody. Plates were incubated with the detection antibody on a shaker (850 rpm) for 30 min at RT in the dark. After antibody incubation, the plate was washed three times in wash buffer (100 μL/well) and 50 μL/well Streptavidin-phycoerythrin (SA-PE) was added, followed by incubation on a plate shaker for 10 min at RT in the dark. Following three washes with wash buffer, the beads were resuspended in 125 μL assay buffer per well before analysis on a Bio-Plex 100 plate reader with Bio-Plex Manager™ software (Bio-Rad Laboratories).

2.13 Flow cytometry analysis

All flow cytometry was performed on a 2-laser Attune™ Acoustic Focusing Cytometer (Applied Biosystems®) or on a 4-laser CytoFLEX S (Beckman Coulter). For analysis, Attune™ software and CytExpert software were used, respectively. Details of all antibodies used are provided in Table 2-3, Table 2-4, and Table 2-5.

2.13.1 Cell viability assay using a Live/Dead® discrimination staining kit

Cell viability was evaluated using a LIVE/DEAD® Fixable Yellow Dead Cell Stain Kit (Invitrogen™). Samples were harvested into 5 mL round-bottom FACS tubes (BD Falcon™) and washed in 1 mL PBS by centrifugation at 400 x*g*. Each sample was stained in 500 μL staining mix (LIVE/DEAD dye diluted 1:1000 in PBS) for 30 min at 4°C in the dark. Next, samples were washed with 2 mL PBS and then fixed with 300 μL 1% PFA in PBS, or the LIVE/DEAD® stain was combined with further antibody labelling for phenotyping before fixation.

2.13.2 Cell phenotyping by flow cytometry

For flow cytometry analysis, $5x10^5$-10^6 cells were harvested into FACS tubes and washed in 1 mL FACS buffer (PBS, 1% FBS, 0.1% sodium azide). The cell pellet was resuspended in the residual volume and fluorescently conjugated antibodies relevant to each assay were added according to

Table 2-4. Samples were incubated for 30 mins at 4˚C in the dark and then washed with 2 mL FACS buffer. Following fixation in 300 μL 1% PFA in PBS, cells were stored at 4˚C until data acquisition.

For immunophenotyping of murine cells in Chapter 4, Experiments 1-3 (Table 4-2) were analysed using the Attune™ flow cytometer as described above. For Experiments 4 and 5, samples were stained and acquired in a 96-well plate using the CytoFLEX S flow cytometer (Beckman Coulter). 10^6 cells were added per well, and each well was washed in 200 μL FACS buffer. Antibody master mixes were prepared and added to appropriate wells according to Table 2-5. Following incubation for 30 mins at 4˚C in the dark, wells were topped up with 100 μL FACS buffer, centrifuged for 5 min at 400 x*g*, then washed in an additional 200 μL FACS buffer. Cells were fixed in 100 μL/well 1% PFA in PBS and acquired in a total volume of 250 μL/well.

2.13.3 NK cell and CTL degranulation assay

Lymphocyte degranulation was determined by cell surface expression of CD107a/b. Effector lymphocytes were incubated alone or with target tumour cells at a 2:1 ratio as indicated for each experiment. Cells were added to FACS tubes in a total volume of 400 μL complete RPMI-1640 and were then incubated at 37˚C. After 1 h, antibodies against CD107a, CD107b, and either CD3/CD8 (CTL population) or CD3/CD56 (NK cells) were added to each tube (Table 2-4), along with 10 μg/mL Brefeldin A (BioLegend). Samples were then incubated for a further 4 hrs at 37˚C, washed with 2 mL FACS buffer, fixed in 300 μL 1% PFA and stored at 4ºC until acquisition. For NK cell degranulation assays with AML primary samples and autologous blasts, AML blasts were stained with CTV as described in Section 2.1.5 before inclusion in the degranulation assay.

2.13.4 Intracellular IFN-γ staining

Primed PBMCs were co-cultured with tumour target cells or peptide-loaded $CD14^+$ cells (Section 2.14.2.2) and treated as described for the CD107 degranulation assay (Section 2.13.3), without the addition of CD107 antibodies. Following fixation in 1% PFA in PBS overnight, the cells were washed in 2 mL FACS buffer, then permeabilised in 1 mL 0.3% saponin (Sigma-Aldrich) in FACS buffer for 15 min at RT. Samples were washed in 2 mL FACS buffer and a FITC-conjugated IFN-γ antibody (Table 2-4) was added at a 1:20 dilution in 0.1% saponin (in FACS buffer) for 30 min at 4°C.

Finally, cells were washed in 1 mL 0.1% saponin and resuspended in 300 μL FACS buffer for immediate acquisition and analysis using the Attune™ flow cytometer.

2.13.5 Flow cytometry-based killing assay

Flow cytometry-based killing assays were performed in 96-well round-bottom cell culture plates using the CytoFLEX flow cytometer to examine the ability of primed CTLs to kill target cells, in particular those pre-cultured on BM stromal cells. Target cells were either stained with CTG (Section 2.1.5) immediately prior to the assay, or for target cells pre-cultured with BM stromal cells, CTG staining took place prior to seeding on BM stroma (Section 2.1.6). Cells were cultured on BM stroma for 48 hrs prior to the assay and following harvest, cells were washed once in PBS + 2.5 mM EDTA to disrupt any remaining tumour cell binding to BM stromal cells. Primed CTL effector cells were harvested and added to each well together with CTG-labelled target cells at a 25:1 ratio in a total volume of 250 μL complete RPMI-1640 ($2.5x10^4$ target cells in total). Cells were co-cultured for 5 hrs at 37°C, then cells were pelleted by centrifugation at 400 x*g* for 5 min and the supernatants were discarded. Following a wash in 250 μL/well PBS, cells were stained with the yellow Live/Dead® discrimination staining kit (Section 2.13.1). The Live/Dead® fluorescent dye was diluted 1:500 in PBS and 100 μL of staining mix was added to each well. Plates were incubated for 30 min at 4°C in the dark. Following incubation, cells were washed in PBS and then fixed in 150 μL/well 1% PFA in PBS and stored at 4ºC until acquisition.

Table 2-4: Human flow cytometry antibodies used for immunophenotyping and functional assays.

Target molecule	Fluorochrome	Volume added	Species of origin	Clone	Supplier
NK cell activation					
CD3	PerCP	5 µL	Mouse	SP34-2	BD Biosciences
CD56	PE	2 µL	Mouse	AF13-7H3	Miltenyi Biotec
CD69	FITC	5 µL	Mouse	L78	BD Biosciences
IgG_1	FITC	5 µL	Mouse	MOPC-21	BD Biosciences
NK cell degranulation					
CD3	PerCP	5 µL	Mouse	SP34-2	BD Biosciences
CD56	PE	2 µL	Mouse	AF13-7H3	Miltenyi Biotec
CD107a	FITC	5 µL	Mouse	H4A3	BD Biosciences
CD107b	FITC	5 µL	Mouse	H4B4	BD Biosciences
T cell activation					
CD3	VioBlue	2 µL	Mouse	BW264/56	Miltenyi Biotec
CD4	PE	5 µL	Mouse	SK3	BD Biosciences
CD8	PerCP	2 µL	Mouse	BW135/80	Miltenyi Biotec
CD69	FITC	5 µL	Mouse	L78	BD Biosciences
IgG_1	FITC	5 µL	Mouse	MOPC-21	BD Biosciences
CTL degranulation					
CD3	VioBlue	2 µL	Mouse	BW264/56	Miltenyi Biotec
CD56	PE	2 µL	Mouse	AF13-7H3	Miltenyi Biotec
CD8	PerCP	2 µL	Mouse	BW135/80	Miltenyi Biotec
CD107a	FITC	5 µL	Mouse	H4A3	BD Biosciences
CD107b	FITC	5 µL	Mouse	H4B4	BD Biosciences

Table 2-4 continued: Human flow cytometry antibodies

Target molecule	Fluorochrome	Volume added	Species of origin	Clone	Supplier
NK ligand phenotyping					
MIC A/B	PE	5 µL	Mouse	6D4	BD Biosciences
ULBP-1	PE	5 µL	Mouse	#170818	R&D Systems
ULBP-2/5/6	PE	5 µL	Mouse	#165903	R&D Systems
PVR	PE	5 µL	Mouse	PV404.19	Miltenyi Biotec
Nectin-2	PE	5 µL	Mouse	R2.525	BD Biosciences
HLA A/B/C	PE	5 µL	Mouse	EMR8-5	BD Biosciences
IgG_{2a}	PE	5 µL	Mouse	G155-178	BD Biosciences
IgG_{2b}	PE	5 µL	Mouse	27-35	BD Biosciences
Virus entry receptor phenotyping					
ICAM-1	PE	5 µL	Mouse	LB-2/6D4	BD Biosciences
IgG_{2b}	PE	5 µL	Mouse	27-35	Miltenyi Biotec
JAM-A	PE	5 µL	Mouse	M.Ab.F11	BD Biosciences
IgG_1	PE	5 µL	Mouse	H4B4	BD Biosciences
DC phenotyping					
CD80	PE	5 µL	Mouse	L307.4	BD Biosciences
CD86	FITC	5 µL	Mouse	2331	BD Biosciences
HLA-DR	PerCP	5 µL	Mouse	L243	BD Biosciences
IgG_1	PE	5 µL	Mouse	MOPC-21	BD Biosciences
IgG_1	FITC	5 µL	Mouse	MOPC-21	BD Biosciences
IgG_{2b}	PerCP	5 µL	Mouse	G155-178	BD Biosciences
Intracellular IFN-γ staining (CTL)					
CD3	VioBlue	2 µL	Mouse	BW264/56	Miltenyi Biotec
CD56	PE	2 µL	Mouse	AF13-7H3	Miltenyi Biotec
CD8	PerCP	2 µL	Mouse	BW135/80	Miltenyi Biotec
IFN-γ	FITC	7 µL	Mouse	45-15	Miltenyi Biotec

Table 2-4 continued: Human flow cytometry antibodies

Target molecule	Fluorochrome	Volume added	Species of origin	Clone	Supplier
Additional markers					
BDCA-2 (pDC)	VioBlue	2 µL	Mouse	AC144	Miltenyi Biotec
CD123 (pDC)	FITC	5 µL	Mouse	7G3	BD Biosciences
CD14 (monocytes)	PE	5 µL	Mouse	M5E2	BD Biosciences

PE: phycoerythrin, PerCP: peridinin chlorophyll protein complex, FITC: fluorescein isothiocyanate.

Table 2-5: Murine flow cytometry antibodies used for immunophenotyping.

Target molecule	Fluorochrome	Volume added	Species of origin	Clone	Supplier
Lymphocyte phenotyping					
CD3	PE-Vio770	2 µL	Hamster	145-2C11	Miltenyi Biotec
DX5 (CD49d)	PE	2 µL	Rat	R1-2	Miltenyi Biotec
CD4	VioBlue	2 µL	Rat	GK1.5	Miltenyi Biotec
CD8a	PerCP	2 µL	Rat	53-6.7	Miltenyi Biotec
CD44	FITC	2 µL	Rat	IM7.8.1	Miltenyi Biotec
CD62L	APC	2 µL	Rat	MEL14-H2.100	Miltenyi Biotec
CD69	FITC	2 µL	Hamster	H1.2F3	Miltenyi Biotec
PD-1	APC	2 µL	Rat	HA2-7B1	Miltenyi Biotec
4-1BB	FITC	2 µL	Hamster	17B5-1H1	Miltenyi Biotec
CTLA-4	APC	2 µL	Hamster	UC10-4B9	Miltenyi Biotec
Myeloid cell phenotyping					
CD45	APC-Cy7	2 µL	Mouse	104	BioLegend
F4/80	PE-Vio770	5 µL	REA	REA126	Miltenyi Biotec
CD11b	FITC	5 µL	REA	REA592	Miltenyi Biotec
Ly6C	BV421	1 µL	Rat	HK1.4	BioLegend
Ly6G	PerCP	1 µL	Rat	1A8	BioLegend
CD80	PE	2 µL	Hamster	16-10A1	Miltenyi Biotec
CD86	APC	2 µL	Rat	PO3.3	Miltenyi Biotec
I-A^b (MHC-II)	Alexa 647	1 µL	Mouse	AF6-120.1	BioLegend
Tumour burden					
CD138	PE	2 µL	REA	REA104	Miltenyi Biotec

REA: recombinant antibody

2.14 Priming of tumour-specific cytotoxic T cells

2.14.1 Generation of human myeloid-derived DC

$CD14^+$ monocytes were isolated from whole PBMCs as previously described (Section 2.11.1). $CD14^+$ cells were cultured at $8x10^5$/mL in complete RPMI-1640 containing GM-CSF and IL-4 (Table 2-2) for 5 days to obtain iDC. A proportion of $CD14^+$ cells were frozen for later use in peptide stimulations of primed CTLs (Section 2.14.2.2).

2.14.2 Generation of tumour-specific CTL

PBMCs were obtained from healthy donor leucocyte apheresis cones as previously described (Section 2.2.1). Approx. $2.5x10^8$ PBMC were used for the generation of iDCs as described above (2.14.1) and the remaining PBMCs were frozen in 90% FBS and 10% DMSO (Sigma-Aldrich). Target cells were either left untreated, or treated with 1 pfu/cell reovirus or 0.1 pfu/cell CVA21 for 24 hrs. iDC were loaded with untreated or treated target cells, respectively, at a 3:1 tumour cell:DC ratio and cultured in 50:50 DC medium:RPMI-1640 for 48 hrs. Tumour-loaded DC were then cultured with autologous PBMC (thawed from frozen) at a 1:20-1:30 DC:PBMC ratio in CTL medium (Table 2-2). Cells were incubated in 25 cm^2 flasks (positioned upright) for 7 days at 37˚C; CTL cultures were monitored daily and supplemented with extra CTL medium when required. The remaining frozen PBMC were thawed and used to generate new iDC, which were then cultured with target cells (±OV treatment) to allow re-stimulation of T cells. On Day 7, CTLs were harvested, pelleted by centrifugation, and re-stimulated with fresh target cell-loaded DCs. All CTL culture medium was replenished. Cells were then cultured for another six days before harvesting for use in ^{51}Cr release assays (Section 2.15), CTL degranulation assays (Section 2.13.3), and for intracellular IFN-γ flow cytometry (Section 2.13.4).

2.14.2.1 MHC Class I (HLA-ABC) blockade during CTL degranulation assays

To block HLA-ABC:TCR interaction, target cells were harvested and incubated with 50 μg/mL LEAF™ purified anti-human HLA-ABC (BioLegend), or mouse IgG_{2a} isotype control (R&D Systems) antibodies, for 30-60 min at 37°C before inclusion in CTL degranulation assays as described in Section 2.13.3.

2.14.2.2 Peptide pool stimulation of primed CTLs

PepTivator® Peptide Pools (Miltenyi Biotec) consisting mainly of 15-mer sequences of amino acids with 11 amino acids overlap covering the PRAME, Mucin-1, and MAGE-A1, respectively, proteins were used. All PepTivator® Peptide Pools were reconstituted in dH_2O according to the manufacturer's instructions, resulting in a stock concentration of 30 nmol/mL of each peptide. Aliquots were stored at -80°C. For TAA stimulation of CTLs, autologous $CD14^+$ cells were thawed from frozen, washed in complete RPMI-1640, and allowed to rest for approx. 60 min. $2x10^6$ $CD14^+$ cells were incubated with either peptide pool for 60 min at 37°C at a final concentration of 6 nmol/mL. $CD14^+$ cells incubated in the absence of peptide were used as controls. $CD14^+$ cells were then co-cultured with primed, autologous CTLs at a 2:1 ratio and included in the intracellular IFN-γ assay as described in Section 2.13.4.

2.15 ^{51}Chromium release assay

^{51}Chromium (Cr) release assays were used to examine the cytotoxicity of NK cells and *in vitro* generated CTLs (Section 2.14.2). Target cells were harvested and labelled with 100 µCi $^{51}Cr/10^6$ cells (PerkinElmer) for 1 hr at 37°C. Effector cells were harvested, counted, and added in triplicate to 96-well round-bottom cell culture plates. Serial halving dilutions of effector cells were made in complete RPMI-1640 to create known effector:target (E:T) ratios, starting at 50:1. Following incubation with ^{51}Cr, target cells were washed three times in HBSS by centrifugation, and resuspended in complete RPMI-1640. $5x10^3$ target cells were added to each well of effector cells followed by co-culture for 4 hrs at 37°C. Spontaneous release controls were established using target cells alone in complete RPMI-1640 and target cells alone cultured in 1% Triton-X (Sigma-Aldrich) in complete RPMI-1640 were used as maximum release controls. In CTL assays, unlabelled K562 and Daudi target cells ($5x10^3$ each/well) were added to all wells to mitigate NK cell and LAK cell activity. Following incubation, cells were pelleted and 50 µL of each supernatant was transferred to a LumaPlate™ (PerkinElmer) and left to dry overnight. The level of ^{51}Cr in the supernatant was then measured using a Microbeta^2 scintillation counter (PerkinElmer) and the percentage of target cell lysis was calculated using the following formula (cpm: counts per minute):

$$\%\ lysis = 100\ \times \frac{sample\ cpm - spontaneous\ cpm}{maximum\ cpm - spontaneous\ cpm}$$

2.15.1 EGTA-mediated inhibition of exocytosis in ^{51}Cr assays

As Ca^{2+} is needed for the efficient exocytosis of cytotoxic granules from NK cell and CTLs, the chelating agent EGTA (egtazic acid) was used in ^{51}Cr assays to establish the requirement of exocytosis for target cell lysis. ^{51}Cr assays were set up as described above (Section 2.15), but effector cells were resuspended in complete RPMI-1640 supplemented with 4 mM EGTA prior to addition to 96-well plates. Following the addition of target cells, the final concentration of EGTA during co-cultures was 2 mM. The release of ^{51}Cr into the culture medium was measured as described above (Section 2.15).

2.16 Gene Expression Analysis

2.16.1 Isolation of RNA from cells

RNA was isolated from STORM PBMC samples (pre-CVA21 infusion and three days post-CVA21 infusion) stored in liquid nitrogen, and from murine BM samples stored in RNAprotect Cell Reagent (Qiagen) at -80°C. First, mRNA was isolated using the RNeasy Plus Mini kit (Qiagen) according to the manufacturer's instructions. Briefly, cells were lysed in the provided RLT buffer, then homogenised using QIAshredder columns (Qiagen). Contaminating genomic DNA was removed using gDNA eliminator spin columns from the RNeasy Plus Mini kit. After addition of one volume 70% ethanol (EtOH), the samples were applied to an RNeasy Mini spin column. Following several wash steps to remove contaminants, RNA was eluted in RNase-free water. The final RNA concentration in each sample was measured using a NanoDrop™1000 spectrophotometer (ThermoFisher Scientific).

2.16.2 Isolation of reovirus RNA using TRIzol®

250 μL of reovirus stock was mixed with 1 mL TRIzol® reagent and incubated for 5 min at RT. Next, 200 μL of chloroform (Sigma-Aldrich) was added and the sample was incubated for a further 2-3 min, followed by 15

min centrifugation at 12 000 x*g* at 4°C using an Eppendorf 5415D microcentrifuge. The aqueous phase was aspirated, mixed with 500 µL isopropanol, and incubated for 10 min at RT. RNA was pelleted by centrifugation for 10 min at 12 000 x*g* at 4°C and then washed in 1 mL 70% EtOH by centrifugation for 5 min at 7 500 x*g* at 4°C. The supernatant was aspirated and the pellet air-dried before resuspension in RNase-free water and measurement of RNA concentration using a NanoDrop™1000 spectrophotometer (ThermoFisher Scientific).

2.16.3 Generation of cDNA (STORM samples)

For STORM samples, 0.1 µg purified RNA was converted to cDNA using the SuperScript™ III Reverse Transcriptase kit (ThermoFisher Scientific). All reactions were prepared in individual 0.2 mL PCR tubes. The primer annealing reaction consisted of RNA, 5 µM oligo$(DT)_{20}$, 1 mM dNTP mix, and DEPC-treated water in a total volume of 10 µL which was heated to 65°C for 5 min. The whole primer reaction was used in the cDNA Synthesis Mix, in addition to reagents with the following final concentrations: 1x RT buffer, 5 mM $MgCl_2$, 10 mM DTT, 40 U RNaseOUT™, and 200 U SuperScript™ III reverse transcriptase in a total volume of 20 µL. Reactions were heated to 50°C for 50 min, followed by termination of the reaction at 85°C for 5 min and cooling on ice. Finally, contaminating RNA template was removed by RNase H treatment for 20 min at 37ºC. All heating for DNase treatment and cDNA conversion was performed on a Veriti Thermo Cycler (Applied Biosystems™).

2.16.4 Quantitative real-time polymerase chain reaction (qPCR)

2.16.4.1 TaqMan™ qPCR (STORM samples)

The STORM cDNA was used in a two-step qPCR reaction with TaqMan™ reagents to examine the expression of *18S* RNA, *IFIT1*, *IFI44L,* and *OAS1*. Reactions were prepared in triplicate in 96-well MicroAmp™ Optical Reaction plates (Applied Biosystems™) and consisted of 2 µL cDNA, 1x TaqMan™ Fast Advanced Master Mix (10 µL), 1x TaqMan™ Gene Expression Assay (1 µl), and nuclease-free water in a total volume of 20 µL (all reagents Applied Biosystems™). The following Gene Expression Assays with a FAM™ reporter were used: Hs000356631_g1 (IFIT1), Hs00199115_m1 (IFI44L), Hs009733637_m1 (OAS1), and Hs03003631_g1 (18S). Plates were sealed

with optical adhesive film and then centrifuged briefly to collect the reaction and eliminate air bubbles. Thermal cycling was performed on the QuantStudio™ 5 Real-Time PCR System (Applied Biosystems™) with the following protocol: 2 min at 50°C, 20 sec at 95°C, then 40 cycles of 10 sec at 95°C and 20 sec at 60°C. Results were normalized to 18S RNA and the fold change in expression was calculated using the ΔΔCt method.

2.16.4.2 SYBR™ green reovirus RT-qPCR (murine samples)

The presence of reovirus in murine BM was analysed in a one-step qPCR reaction with SYBR™ green reagents. Reactions were prepared in triplicate in 96-well MicroAmp™ Optical Reaction plates (Applied Biosystems™) using the *Power* SYBR™ Green RNA-to-C_T™ *1-Step* Kit (ThermoFisher Scientific). 0.3 μg RNA was used in each reaction, in addition to 1x *Power* SYBR Green RT-PCR Mix, 1x RT Enzyme Mix, 0.5 μM forward primer, 0.5 μM reverse primer, and RNase-free water to a total volume of 20 μL. Primers used are detailed in Table 2-6. An eight-point 10-fold serial dilution series of reovirus RNA isolated from reovirus stock as described in Section 2.16.2 was included for the quantification of reovirus σ3 RNA. GAPDH expression in each sample was measured to ensure good quality of input RNA. Thermal cycling was performed on the QuantStudio™ 5 Real-Time PCR System (Applied Biosystems™) with the following protocol: 30 min at 48°C, 10 min at 95°C, followed by 40 cycles of 15 sec at 95°C and 60 sec at 60°C.

Table 2-6: Primers used for one-step RT-qPCR

TARGET	*F/R*	*SEQUENCE (5' – 3')*	*T_m (°C)*
Reovirus σ3	F	GGGCTGCACATTACCACTGA	59.3
	R	CTCCTCGCAATACAACTCGT	56.0
GAPDH (mouse)	F	ACTGAGCAAGAGAGGCCCTA	57.7
	R	TATGGGGGTCTGGGATGGAA	57.7

All primers were obtained from Integrated DNA Technologies.

2.17 5TGM1 *in vivo* model

All animal work was approved by the University of Leeds Local Ethical Review Committee and conducted under a project license (PF0BA8592) approved by the UK Home Office. I.v. injections were performed by Dr. Gemma Migneco. C57BL/KaLwRij mice were purchased at age 4-10 weeks from a colony already established at the University of Leeds, which was originally purchased from Harlan Laboratories. From the start of each experiment, mice were housed in individually ventilated, positive pressure ISOcages with a maximum of five mice per cage. All mice had free access to water, standard mouse feed, nesting material, and were subjected to a regulated daylight cycle. All animals were monitored daily and any mice exhibiting hind limb paralysis (HLP), hunched posture, reduced activity levels, skin ulceration, weight loss, difficulty breathing, or other distress were removed from the colony and euthanized by cervical dislocation; at the end of experiments animals were similarly euthanized by cervical dislocation.

2.17.1 *In vivo* passage and bone marrow harvest

To obtain bone-homing 5TGM1 cells, parental 5TGM1 cells were passaged *in vivo* using 8-10 weeks old female mice. $2x10^6$ 5TGM1 cells in 100 μL PBS were injected in the lateral tail vein and upon development of HLP (21-35 days later) mice were sacrificed. Following post-mortem dissection, both femora and tibia were isolated, epiphyses removed and bones flushed with RPMI-1640 supplemented with 10% FBS and 1% penicillin/streptomycin (Sigma-Aldrich) to harvest BM cells. The BM was strained through a 70μm cell strainer (Greiner BioOne) and lymphocytes, including 5TGM1 cells, were isolated from whole BM by density gradient centrifugation on Lympholyte®-M medium (Cedarlane). The recovered cells were washed twice in complete RPMI-1640 and then cultured in complete 5TGM1 medium (Table 2-1) with 1% penicillin/streptomycin. Bone-homing 5TGM1 cells were expanded *in vitro* for up to 7 days and then either re-injected or cryopreserved for future experiments.

2.17.2 Harvest and processing of spleens

Spleens were harvested from all mice in reovirus therapy experiments. Following post-mortem dissection, spleens were immediately processed to obtain splenocytes in suspension. Spleens were crushed through a 70 μm

cell strainer (Greiner BioOne) into splenocyte medium (Table 2-2). Cells were pelleted and red blood cells were lysed in 5 mL ACK buffer (0.15M ammonium chloride, 10mM $KHCO_3$, 0.1mM EDTA, pH 7.2-7.4) for 2 min. Excess cold splenocyte medium was added and cells were centrifuged at 400 x*g* for 5 min. The cell pellet was washed two more times in pre-warmed splenocyte medium and then the splenocytes were counted and included in experiments.

2.17.3 Reovirus therapy experiment – intraperitoneal (i.p) administration

As the reovirus treatment protocol required several repeated injections, i.p. delivery was first tested due to concerns that tail vein scarring would make repeated i.v. injections problematic. 16 female mice aged 6-8 weeks were used and 14 mice were injected with $2x10^6$ bone-homing 5TGM1 cells in 100 μL PBS i.v. on Day 0, while two mice were left tumour- and treatment naïve. Therapy started on Day 13 with i.p. injection of either $2x10^7$ pfu reovirus in 100 μL PBS, or 100 μL PBS alone. Four injections were administered on a Mon/Wed/Fri schedule before development of HLP in PBS mice. Following development of HLP in the first mouse, all mice were sacrificed and bone marrow and spleens were harvested as described above for *in vitro* analysis (Section 2.13.2 and Table 2-5).

2.17.4 Reovirus therapy experiment – intravenous (i.v) administration

Both female and male mice aged 4-8 weeks were used in experiments. An overview of all i.v. experiments performed can be found in Table 4-2, detailing the number of mice used in each experiment, gender, the number of naïve mice included, the number of reovirus doses before HLP, and experimental read-outs used. On Day 0, mice were injected with $2x10^6$ bone-homing 5TGM1 cells in 100 μL PBS in the lateral tail vein (naïve mice left untreated). On Day 7-9, reovirus or control (PBS) treatment was initiated with three weekly injections (Mon/Wed/Fri) of $2x10^7$ pfu/mL reovirus in 100 μL PBS or 100 μL PBS alone, respectively. Treatment continued until development of HLP in PBS-treated mice (20-27 days), then all mice were sacrificed and the BM and spleen were isolated from each mouse. Tumour burden and immunophenotyping was performed as described in (Section 2.13.2 and Table 2-5).

2.17.4.1 Experimental read-outs

Tumour burden in the BM and spleen was examined by flow cytometry using CD138 antibodies as described in Section 2.13.2. NK cells, $CD4^+$ T cells, $CD8^+$ T cells, monocytes, macrophages, and MDSCs were identified and phenotyped as described in Section 2.13.2 using antibodies detailed in Table 2-5. RT-qPCR for reovirus σ3 RNA presence in the BM was performed as described in Section 2.16.4.2. Supernatants for IFN-γ ELISA were generated by co-culture of splenocytes with 5TGM1 cells at a 1:1 ratio for 48 or 72 hrs. Cell-free supernatants were harvested and the secretion of IFN-γ was measured by ELISA according to the protocol in Section 2.12.1.

2.18 Statistical analysis

All statistical analysis was performed using Graphpad Prism 7.0 (GraphPad Software, La Jolla, CA). *p*-values were calculated using either Student's *t*-test with two-tailed distribution for comparing two groups, or one-way analysis of variance (ANOVA) or two-way ANOVA with post-hoc tests and correction for multiple testing when comparing three or more groups. The following post-hoc tests were used:

- Tukey's: multiple pairwise comparisons between all test groups
- Dunnett's: multiple pairwise comparisons of all test groups to a given control group
- Šídák's: multiple pairwise comparisons of selected test groups

Results were considered significantly different from the *null* hypothesis if $p<0.05$. Pearson's r was calculated to evaluate correlation. Details of replicates and numbers of donors are given in each figure legend.

Chapter 3

A comparison of anti-tumour immunity induced by reovirus and coxsackievirus A21 in multiple myeloma

Chapter 3
A comparison of anti-tumour immunity induced by reovirus and coxsackievirus A21 in multiple myeloma

3.1 Introduction

As discussed, MM is a haematological disease which is still considered incurable, and novel, more efficient treatments are urgently needed. The work described in this chapter aimed to compare the anti-tumour immune responses induced by two different OVs, and their role in the treatment of MM. While both Reolysin® (reovirus) and CAVATAK™ (CVA21) have shown preclinical efficacy in MM with regards to direct oncolysis (202, 225, 318-321), no previously published studies have examined the anti-tumour immune response induced by either virus in detail in a MM setting. Reolysin® has progressed to early phase clinical trials (195, 259, 269, 322), while CAVATAK™ remains a novel, and unexplored agent for the treatment of MM.

Early work by Thirukkumaran *et al.*, and Au *et al*. demonstrated that a range of MM cell lines are highly susceptible to the direct lytic effects of both reovirus (320, 323) and CVA21 (202). However, preliminary data generated in earlier projects demonstrated that some cell lines remain resistant to direct oncolysis due to low entry receptor expression, which has also been confirmed in earlier studies (225). Furthermore, the BM microenvironment is well known to induce resistance to chemotherapeutics in MM by providing a protective niche for malignant cells (324). To date, it has not been clarified whether the BM microenvironment can also induce resistance to OVT. The evidence is conflicting regarding the interactions of OV with the local TME, and OV effects on tumour-supportive cells can both aid (150) and oppose therapy (325, 326). However, no studies have investigated the role of the BM microenvironment in OVT of MM, specifically. Therefore, the work presented here examined the effect of the BM microenvironment on OV susceptibility and determines the role for OV-induced anti-tumour immunity for eradication of MM cells. To do this, *in vitro* cell culture models incorporating MM cell co-culture with BM stromal cells, and immunological models of NK cell degranulation and killing, and priming of tumour-specific CTLs were used.

To support the *in vitro* results obtained from healthy donors, primary samples from two different clinical trials were analysed to assess the onset of anti-tumour immunity in a malignant *in vivo* environment. The Myeloma UK *Eleven* (MUK11) Phase Ib trial aimed to evaluate i.v. Reolysin® in combination with lenalidomide or pomalidomide in refractory/relapsed MM; Figure 3-1A shows a treatment schedule overview. The STORM Phase I dose-escalation trial evaluated i.v. infusion of CVA21 in patients with late-stage solid malignancies; Figure 3-1B and Table 3-1 show the treatment schedule overview and patient demographics. Although not from MM patients, the onset of an immune response in the peripheral circulation of immunocompromised cancer patients (327-330) would support the use of OVT in MM.

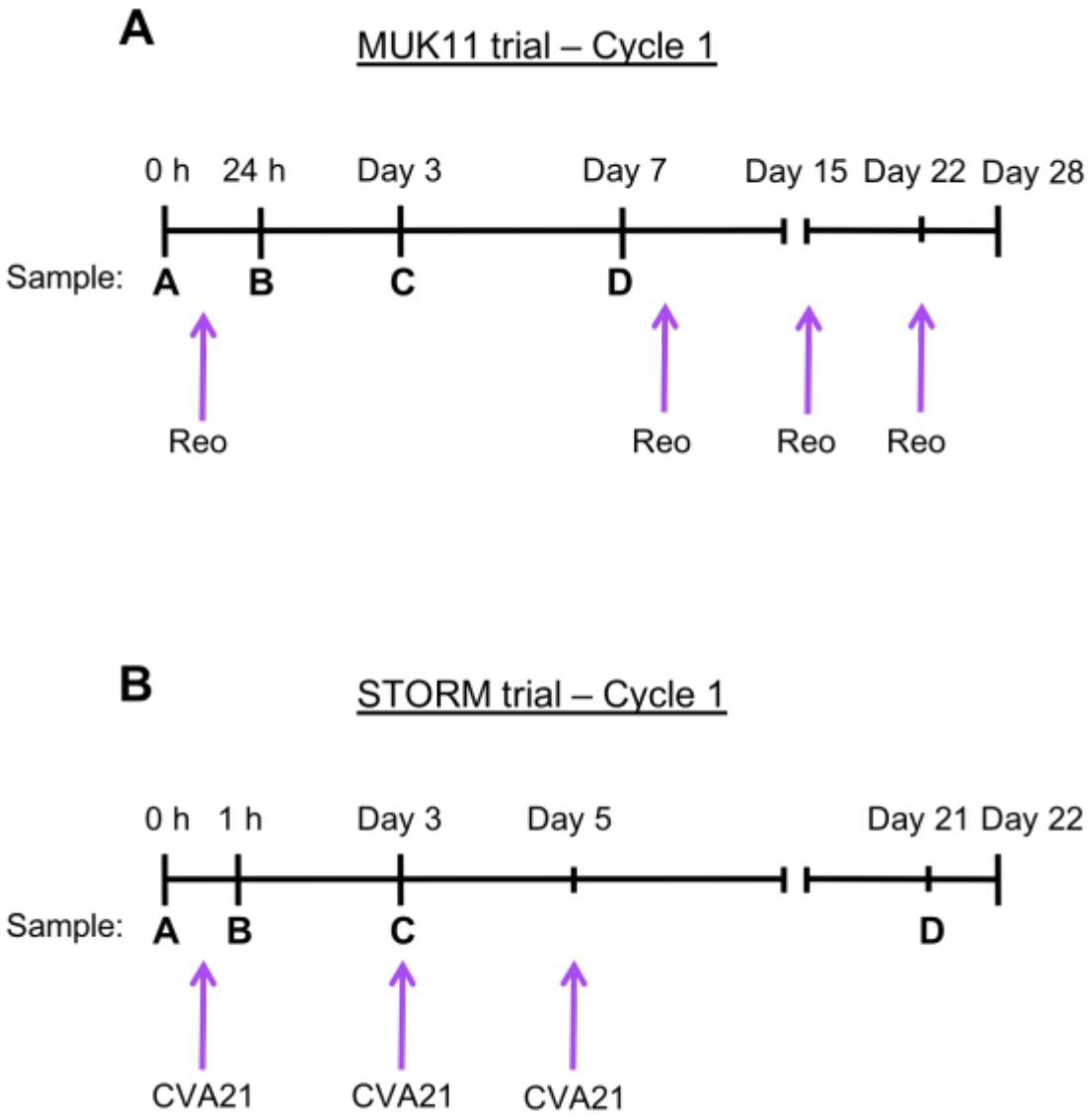

Figure 3-1: Clinical trials treatment schedule overview.

A: MUK11 trial, cycle 1. Patients received Reolysin® i.v. (Patient 2; 10^{10} $TCID_{50}$) on Days 1, 8, 15, and 22, and either lenalidomide (10 mg) or pomalidomide (1 mg) daily. Peripheral blood samples were taken prior to reovirus infusion and then at 24 hrs, 72 hrs , and 7 days post infusion. **B**: STORM trial, cycle 1. Patients received CAVATAK™ i.v. (10^8 or 10^9 $TCID_{50}$) on Days 1, 3, and 5. Peripheral blood samples were taken prior to CVA21 infusion and then at 1 h, 72 hrs, and 21 days post infusion. All samples except sample B were taken prior to the next CVA21 infusion.

Table 3-1: STORM trial patient demographics.

Five patients with late-stage, refractory solid malignancies were recruited to the STORM Phase I dose-escalation trial. All patients had previous treatments as indicated before taking part in the STORM trial. Orange symbols indicate a $1x10^8$ $TCID_{50}$ dose of CAVATAK™ per injection throughout the results section, black symbols indicate a $1x10^9$ $TCID_{50}$ dose.

SAMPLE ID	SYMBOL	MALIGNANCY	STAGE ON RECRUITMENT	PREVIOUS TREATMENTS	CVA21 DOSE	LYMPHOCYTE COUNT (A/B/C/D)
STORM-1	▼	Adenocarcinoma of the lung	Metastatic disease to the lung	CT-322 trial, Erlotinib, Pemetrexed, Gemcitabine, Fiesta trial	$1x10^8$ $TCID_{50}$	**A:** 1.05, **B:** 0.78, **C:** 0.75, **D:** 0.70
STORM-2	▲	Lentigo maligna melanoma	Metastatic disease to the lung, liver, LNs	Excision of primary tumour, Dacarbazine, Ipilimumab	$1x10^8$ $TCID_{50}$	**A:** 1.16, **B:** 0.94, **C:** 1.03, **D:** 1.07
STORM-4	■	Metastatic carcinoma of the prostate	Metastatic disease to LNs and bone	Docetaxel, Abiraterone, Cabazitaxel	$1x10^9$ $TCID_{50}$	**A:** 1.01, **B:** 1.38, **C:** 1.19, **D:** 0.80
STORM-5	◆	Malignant melanoma	Cutaneous, subcutaneous and LN metastases	Multiple surgical excisions, isolated limb perfusion	$1x10^9$ $TCID_{50}$	**A:** 1.39, **B:** 1.17, **C:** 1.10, **D:** 1.07
STORM-6	●	Poorly differentiated squamous cell carcinoma of the lung	Pleural, lung and subcutaneous metastases	Excision of chest wall, MK3475 trial	$1x10^9$ $TCID_{50}$	**A:** 1.02, **B:** 1.89, **C:** 0.79, **D:** 0.94

LN: lymph nodes, Fiesta trial: AZD4547 with gemcitabine and cisplatin, MK3475 trial: pembrolizumab.

Sample A: prior to first infusion, Sample B: one hour post infusion, Sample C: Day 3 post infusion, Sample D: 22 days post infusion.

3.2 Results

3.2.1 Direct oncolysis of multiple myeloma cells

In accordance with previous literature (202, 225), it was confirmed by flow cytometry that a number of MM cell lines (H929, U266B, and JIM3) express both the reovirus entry receptor JAM-A, and the CVA21 entry receptor, ICAM-1 (Figure 3-2 A and B). Overall, ICAM-1 expression was markedly higher than JAM-A expression on both H929, U266B, and JIM3 cells. Interestingly, one cell line, OPM2, was found to be both JAM-A and ICAM-1 negative, with no expression of either receptor above the isotype control (Figure 3-2 A and B). To confirm whether entry receptor expression corresponded with susceptibility to oncolysis, all cell lines were treated with either reovirus or CVA21, and cell viability was assessed by flow cytometry, using a Live/Dead® discrimination kit as described in Section 2.13.1. Following reovirus treatment with up to 10 pfu/cell for 72 and 96 hrs (Figure 3-2C and D), or CVA21 treatment with up to 1 pfu/cell for 48 and 72 hrs (Figure 3-2 E and F), it was confirmed that H929, U266B, and JIM3 cell lines were susceptible to the direct lytic effects of both viruses. CVA21 showed a more pronounced oncolytic effect than reovirus, with >90% of all cells (H929, U266B, and JIM3) dead after 72 hrs treatment with just 0.1 pfu/cell (Figure 3-2F). To achieve a similar level of cell death with reovirus, treatment had to be extended to 96 hrs with a 10 pfu/cell dose, which still only killed 64% of JIM3 cells on average (Figure 3-2D). Thus, the more pronounced oncolytic effect of CVA21 seemed to correlate with the higher expression of ICAM-1. The H929 cell line was the most susceptible to reovirus (Figure 3-2 C and D), while the U266B cell line was the most susceptible to CVA21 (Figure 3-2 E and F). This did not directly correlate with the level of entry receptor expression on individual cell lines, as U266B cells had the highest expression of JAM-A (Figure 3-2A), and JIM3 cells had the highest expression of ICAM-1 (Figure 3-2B). As expected, OPM2 cells, which did not express JAM-A or ICAM-1, remained resistant to direct oncolysis.

To evaluate susceptibility to reovirus and CVA21 in the context of the BM microenvironment, a MM:BM co-culture system was developed using two different types of BM stromal cell lines, HS-5 and HS-27 as described in Section 2.1.6. Co-culture with stromal cells improved the viability of MM cells overall (data not shown) therefore, all results presented in Figure 1-4 were normalised to the untreated control for each co-culture condition. HS-27 stromal cells provided significant protection of both H929, U266B, and JIM3

cells against reovirus direct oncolysis with an average reduction in cell death of 38.2%, 30.7%, and 33.2%, respectively (Figure 3-3 A-C). Moreover, HS-5 stromal cells provided protection against reovirus for H929 and JIM3 cells (Figure 3-3 A and C, an average 35.1% and 20.8% reduction in cell death, respectively). Interestingly, neither stromal cell type was able to significantly protect against CVA21 oncolysis in H929 or U266B cells (Figure 3-3 D and E), while some protection was observed in the JIM3 cells when cultured together with HS-27 cells (Figure 3-3F, average 35.0% reduction in cell death). Based on these results, the HS-27 cells were selected for mimicking the BM microenvironment in subsequent immunological experiments (except for conditioned medium experiments where both stromal cell types were used). Having established the direct oncolytic effects of both viruses, next the induction of anti-tumour immune responses by each virus was examined, along with the ability to exploit these anti-tumour immunity mechanisms for the eradication of MM cells.

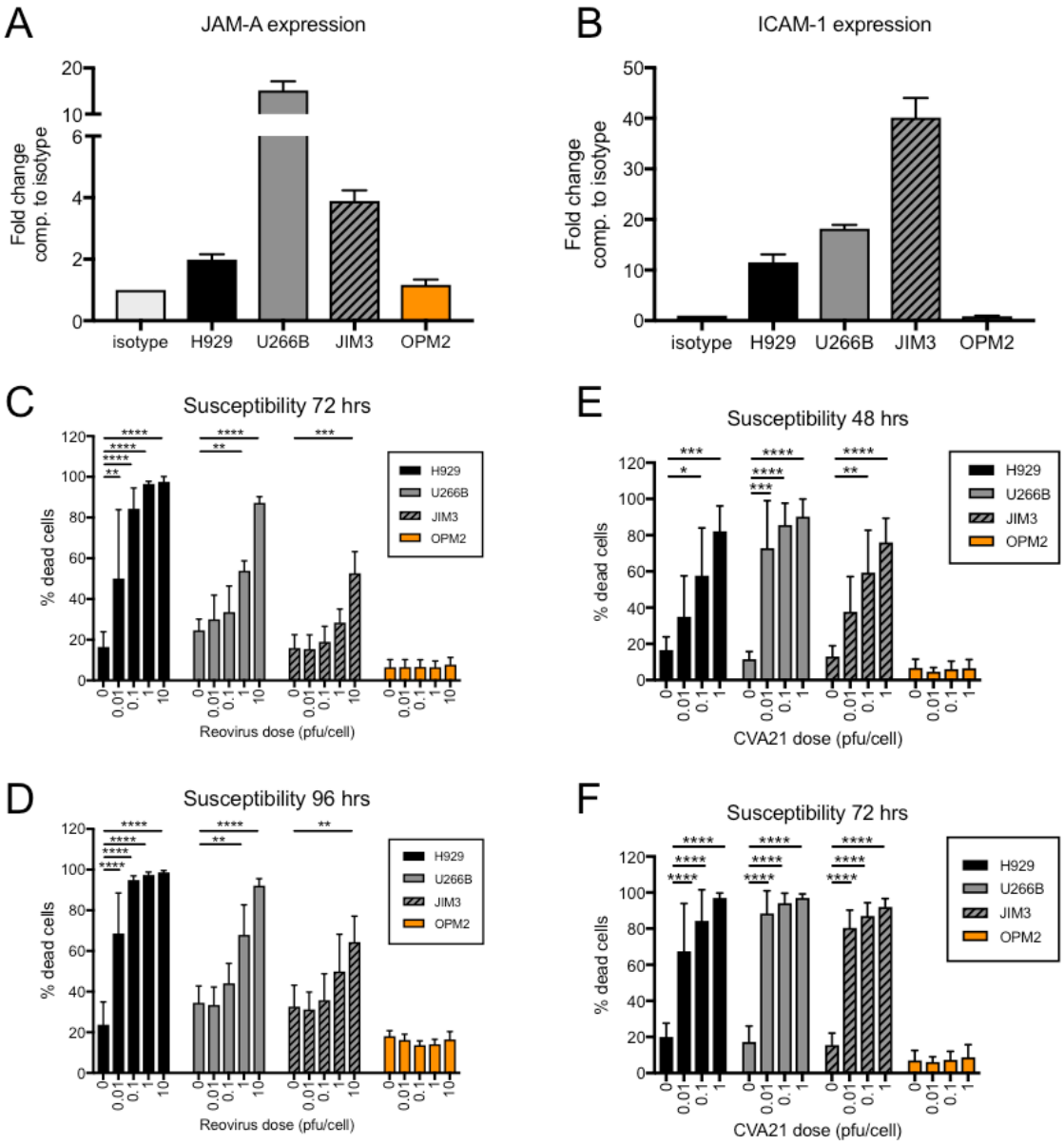

Figure 3-2: MM cell line expression of virus entry receptors and susceptibility to reovirus and CVA21.

MM cell lines H929, U266B, JIM3, and OPM2 were phenotyped for baseline expression of JAM-A (**A**) and ICAM-1 (**B**) using flow cytometry. Expression is shown as the fold change in MFI compared to an isotype control (n=3). **C** and **D**: All cell lines were left untreated (0 pfu/cell) or treated with either 0.01, 0.1, 1, or 10 pfu/cell reovirus for 72 (**C**) or 96 hrs (**D**). **E** and **F**: All cell lines were left untreated (0 pfu/cell) or treated with either 0.01, 0.1, or 1 pfu/cell CVA21 for 48 (**E**) or 72 (**F**) hrs. Cell death was estimated by flow cytometry at each time point, using a Live/Dead® discrimination stain (n=3). Statistical significance was calculated using a two-way ANOVA with Tukey's post-hoc test, * = $p<0.05$, ** = $p<0.01$, *** = $p<0.001$, **** = $p<0.0001$. Error bars indicate s.e.m.

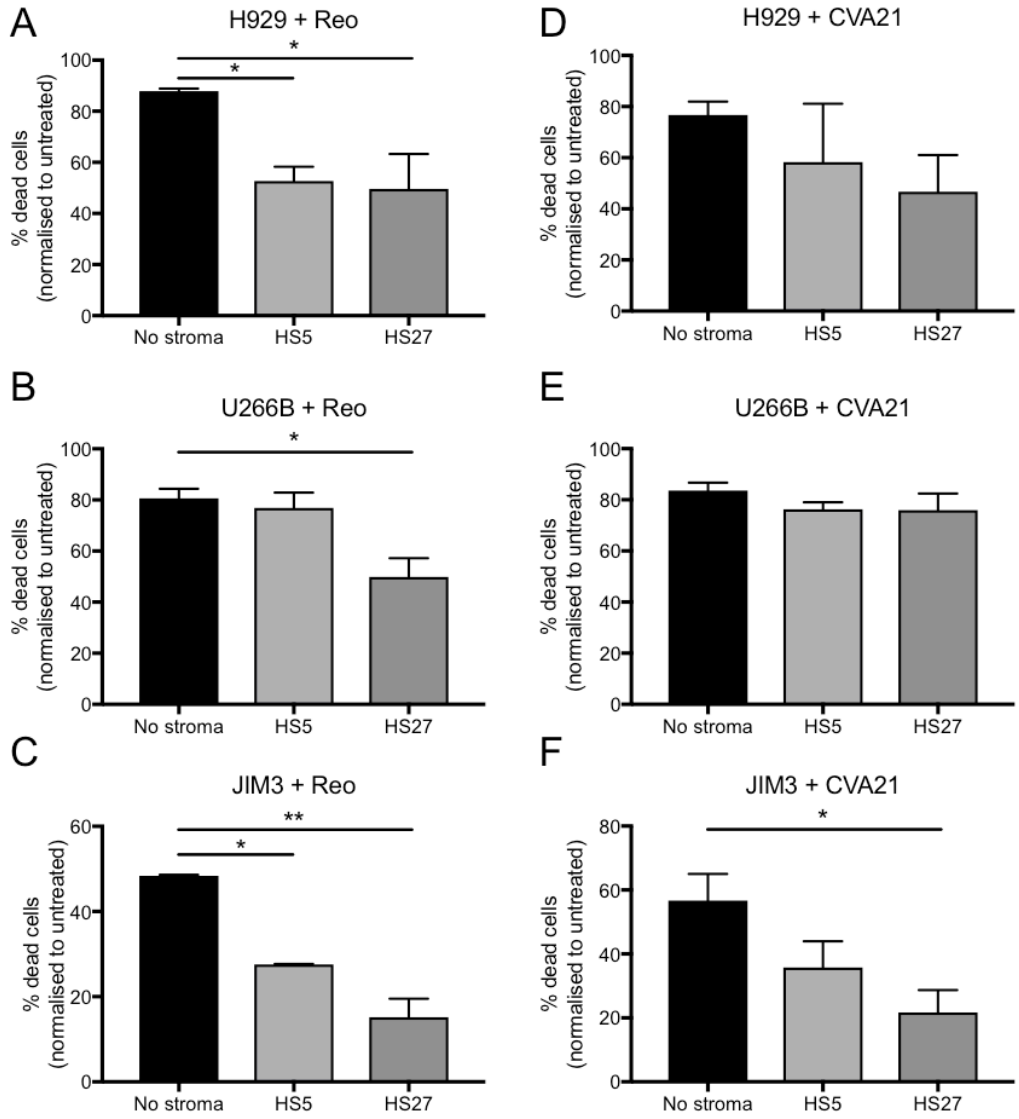

Figure 3-3: Co-culture of MM cells with BM stromal cells can reduce susceptibility to direct oncolysis.

H929, U266B, and JIM3 cells were either treated alone, or co-cultured with HS-5 or HS-27 BM stromal cells at a 1:1 ratio for 24 hrs before treatment with 10 pfu/cell reovirus (**A**-**C**) or 1 pfu/cell CVA21 (**D**-**F**). Cell death was evaluated by flow cytometry using a Live/Dead® discrimination stain, gating on CTG^+ MM cells. Percentages were normalised to the untreated control for each co-culture condition. Statistical significance was calculated using one-way ANOVA with Dunnett's post-hoc test. * = $p<0.05$, ** = $p<0.01$, error bars indicate s.e.m, n=3.

3.2.2 OV-mediated innate and adaptive anti-tumour immunity in multiple myeloma

In order to thoroughly evaluate the induction of anti-tumour immunity in MM, both innate (cytokine-mediated bystander killing, and NK cell-mediated cytotoxicity), and adaptive (priming of tumour-specific cytotoxic CTLs) immune mechanisms were examined.

3.2.2.1 Pro-inflammatory cytokines secreted in response to reovirus or CVA21 treatment induce bystander killing of MM cells

Several cytokines have previously been proposed for the treatment of malignant diseases, the most common being IL-2 and type I IFNs. Both type I and type II IFNs have been implicated as treatments of MM (331-334), and are also an important part of the innate immune response to viral infection. Thus, the secretion of IFN-α and IFN-γ from healthy donor PBMC in response to 48 hrs reovirus or CVA21 treatment (0.1 or 1 pfu/PBMC) was first examined using an ELISA (Section 2.12.1). Significant amounts of IFN-α were secreted in response to both viruses, with absolute levels being higher following reovirus treatment (Figure 3-4 A and B). On average, 11 400 pg/mL IFN-α was secreted in response to treatment with 1 pfu/PBMC reovirus, compared to 2700 pg/mL for CVA21 treatment. Interestingly, the secretion of IFN-γ was more pronounced in response to CVA21 treatment than to reovirus treatment (on average 1000 pg/mL with CVA21, compared to 160 pg/mL with reovirus at the 1 pfu/PBMC dose, Figure 3-4 C and D). IFN secretion in response to CVA21 was further confirmed utilising a Luminex multiplex assay, which measures cytokine secretion in a high throughput manner (Section 2.12.2). Two separate Luminex plates, measuring the secretion of 48 cytokines and chemokines in conditioned medium (CM) were used. This data demonstrated that, in addition to IFNs, CVA21-CM contained several other cytokines and chemokines, such as TRAIL, IL-15, IL-2, TNF-α, GM-CSF, and IP-10 (CXCL10) among others (Figure 3-4E). A significant increase in secretion, compared to untreated PBMC, was seen for IFN-α2, TRAIL, IL-15, CTACK (CCL27), TNF-β, IL-1A, LIF (leukaemia inhibitory factor), Eotaxin, IL-4, and Basic FGF (fibroblast growth factor). Interestingly, secretion of Rantes (CCL5), normally induced by IFN-γ, was reduced in response to CVA21. Along with the IFNs, both TRAIL, IL-2, and GM-CSF have previously been shown to have cytotoxic effects in MM, alone or in combination with other drugs (333, 335-337).

Next, the cytotoxic bystander killing effect of these cytokines, secreted in response to OV treatment, was assessed. CM from PBMC was harvested after 48 hrs of OV treatment, and MM cells were cultured in the CM (diluted 1:1 in fresh medium) for 96 hrs before evaluation of cell viability using an MTS assay (Figure 3-5A and Section 2.8). In an attempt to neutralise the direct cytotoxic effect of the virus on oncolysis-susceptible cell lines, CM was treated with UV-irradiation as described in Section 2.6.3. 2 min of UV irradiation neutralised the majority of reovirus particles when treated in either PBS or CM (Figure 3-5B). However, while 3 min of UV treatment neutralised the majority of CVA21 when treated in PBS, up to 10 min of irradiation had no effect on the replicative potential of CVA21 in CM (Figure 3-5C). Thus, UV-irradiated reovirus-CM was tested on all cell lines, while CVA21-CM could only be tested on OPM2 cells which were resistant to direct CVA21 oncolysis (Figure 3-6). Both reovirus-CM, and CVA21-CM had a significant toxic effect on OPM2 cells after 96 hrs, with reovirus-CM (1 pfu/PBMC) reducing cell viability from 100% (normalised) to 76.9% on average, and CVA21-CM reducing cell viability to 82.5% on average (Figure 3-6A). The UV-treated reovirus-CM was also significantly toxic to H929, U266B, and JIM3 cells (Figure 3-6B). Cell viability was reduced to 44.7%, 62.5%, and 66.1%, respectively, with 1 pfu/PBMC CM, making H929 cells the most susceptible to reovirus-mediated bystander killing. To confirm whether the cell death observed was specifically due to the effect of secreted cytokines, rather than residual toxicity of UV-inactivated virus due to σ1-protein binding to JAM-A or multiplicity reactivation (338, 339), cell death induced by UV-inactivated reovirus particles, in the absence of cytokine-containing medium, was investigated. Figure 3-6C shows that some, but not all, of the toxic effect on H929 and U266B cells at the higher viral dose of 1 pfu/cell may be accounted for by residual toxicity of UV-inactivated viral particles. In contrast, the lower dose of 0.1 pfu/cell of UV-Reo did not induce toxicity, which confirms the bystander killing effect of the cytokines present in the CM at this dose.

After confirming a cytotoxic effect of UV-inactivated reovirus-CM on MM cells grown in isolation, the ability of UV-inactivated CM to kill MM cells in the context of the protective BM microenvironment was evaluated. The co-culture model described in Section 2.1.6 was used, diluting the residual stromal culture medium 1:1 in reovirus-CM instead of fresh medium. Due to the long-term nature of the co-culture model, cells could only be cultured in CM for an additional 72 hrs (compared to 96 hrs in previous experiments) before excessive death of stromal cells due to over-confluency, with

subsequent loss of their protective effect on MM cells. Furthermore, cell viability was evaluated by flow cytometry using a Live/Dead® discrimination stain, rather than an MTS assay, to allow quantification of cell death in the CTG-labelled MM cells only. The results demonstrated that there was no significant difference in H929 viability following culture alone in 1 pfu/PBMC CM, compared to culture in reovirus-CM in the context of HS-27 cells. This indicated that in the case of H929 cells, reovirus-CM could overcome the protective effect induced by HS-27 stromal cells (Figure 3-7A). However, co-culture with HS-5 cells protected H929 cells against the toxic effect of reovirus-CM, similar to the protection observed for direct reovirus oncolysis (Figure 3-3); the percentage of live H929 cells increased from 26.7% to 68.3% following co-culture with HS-5 stromal cells. Similarly, the cytotoxic effect of reovirus-CM was not able to overcome the stromal protection induced in U266B cells as both HS-5 and HS-27 stromal cells protected U266B cells against reovirus-CM to some extent (Figure 3-7B). After 72 hrs culture in 1 pfu/PBMC CM, the percentage of live U266B cells increased from an average 77.4% without stromal protection to 90.0% after co-culture on either stromal cell line. Encouragingly, no protection of JIM3 cells was observed, but the overall cytotoxicity towards these cells was low in the 72 hrs assay (Figure 3-7C). On the contrary, JIM3 cell death was increased by an average 11% (not statistically significant) following co-culture with HS-5 stromal cells, indicating some potentiation of CM-induced death in the context of bone marrow stromal support. As discussed later, HS-5 cells are highly secretory compared to HS-27 cells, raising the question of potential synergistic toxicity between stromal CM and reovirus-CM on JIM3 cells.

Taken together, the results presented in this section demonstrate that cytokines secreted by immune cells in response to both reovirus and CVA21 treatment can generate an inflammatory milieu with a toxic effect on MM cells. Encouragingly, CM showed toxicity against OPM2 cells which were completely resistant to direct oncolysis, and in the case of H929 cells, was able to overcome the protective effect induced by HS-27 stromal cells. However, the experiments performed in this section also indicated that the BM microenvironment can protect MM cells not only against oncolysis, but also against the cytotoxic effects of virus-CM, thus additional anti-tumour immune mechanisms would be required to target these cells.

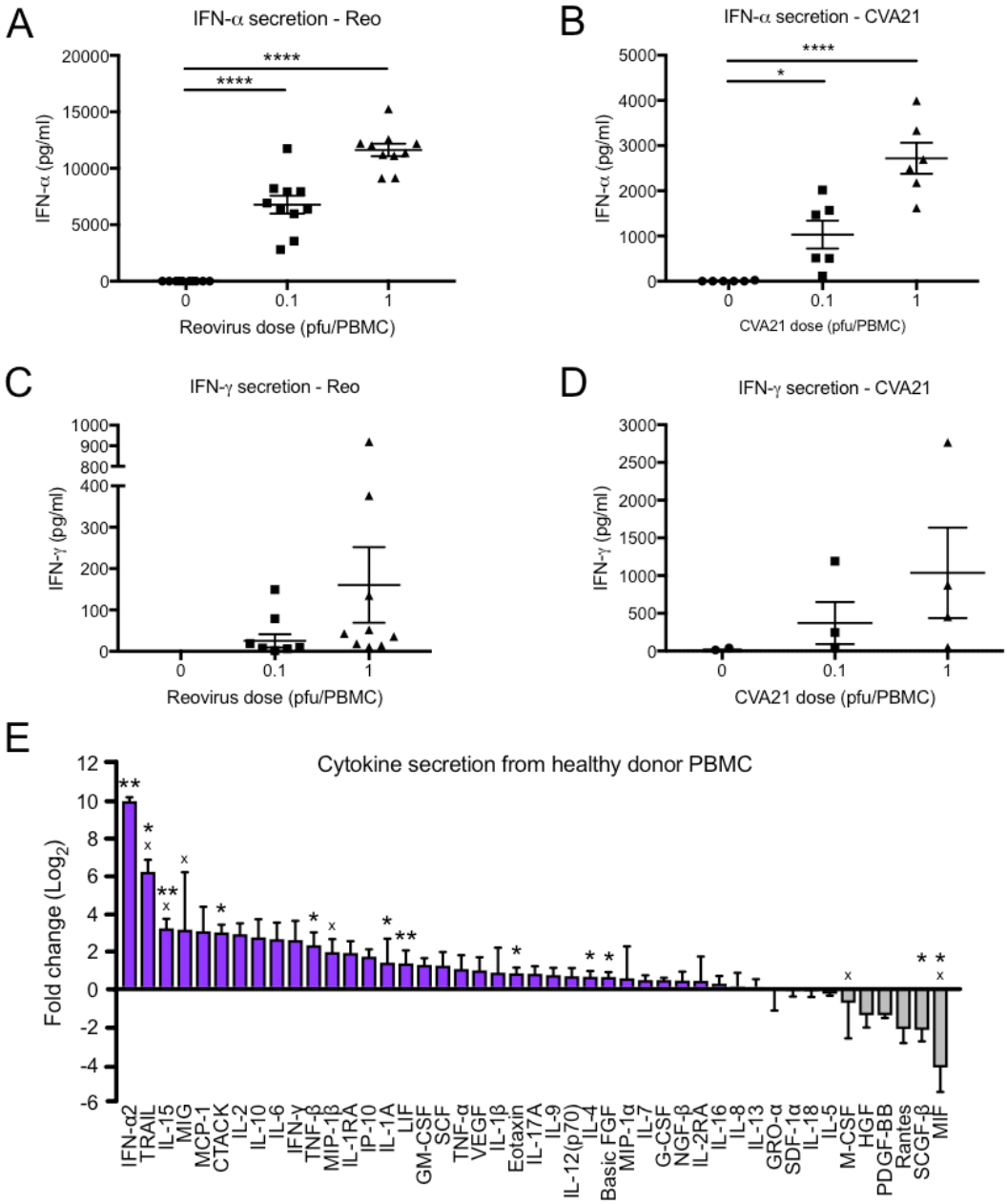

Figure 3-4: Cytokine secretion from healthy donor PBMC in response to reovirus and CVA21.

Healthy donor PBMC were treated for 48 hrs with 0.1 or 1 pfu/cell of reovirus (n=10) or CVA21 (n=6 for IFN-α, n=3 for IFN-γ), respectively. Cell-free supernatants were harvested and secretion of IFN-α (**A** and **B**) and IFN-γ (**C** and **D**) was measured by ELISA. Statistical significance was calculated using one-way ANOVA with Dunnett's post-hoc test. **E**: The secretion of 48 different cytokines was measured in supernatants from PBMC treated with 1 pfu/cell CVA21. The graph shows the mean fold change (n=3) compared to untreated PBMCs. Where a sample reading was out of the detection range, cytokine amounts were estimated using the assay range limits (indicated by x). Statistical significance was calculated using unpaired, two-tailed *t*-tests, comparing the treated to untreated PBMC non-transformed readings. * = $p<0.05$, ** = $p<0.01$, **** = $p<0.0001$. Error bars indicate s.e.m.

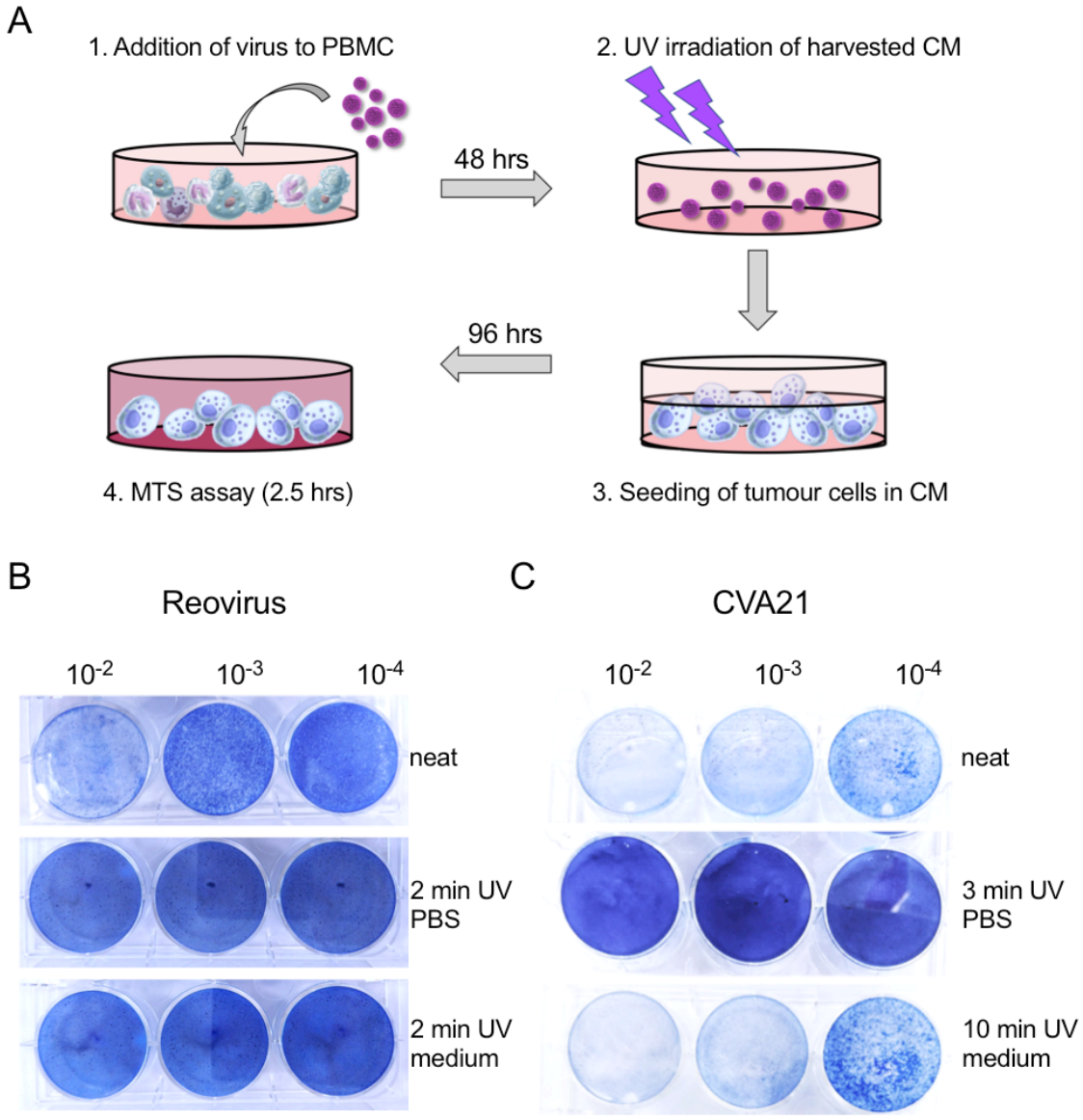

Figure 3-5 Illustration of conditioned medium (CM) culture protocol and UV-inactivation or reovirus and CVA21.

A: CM was harvested from PBMC treated with either 0, 0.1, or 1 pfu/cell of reovirus or CVA21 for 48 hrs (1). Before use on cell lines susceptible to direct oncolysis, reovirus-CM was UV-irradiated for 2 min (2). Cells were resuspended in CM diluted 1:1 in fresh culture medium, each condition was set up in triplicate with a 100% fresh culture medium control (3). After 96 hrs incubation, cell viability was measured using an MTS assay (4). **B** and **C**: Representative plaque assays showing loss of viral replication following UV-irradiation in PBS for 2 (**B**, reovirus) or 3 (**C**, CVA21) min, respectively. 2 min UV-irradiation of reovirus in culture medium resulted in a loss of replication, while up to 10 min UV-irradiation of CVA21 in medium had no effect on replication.

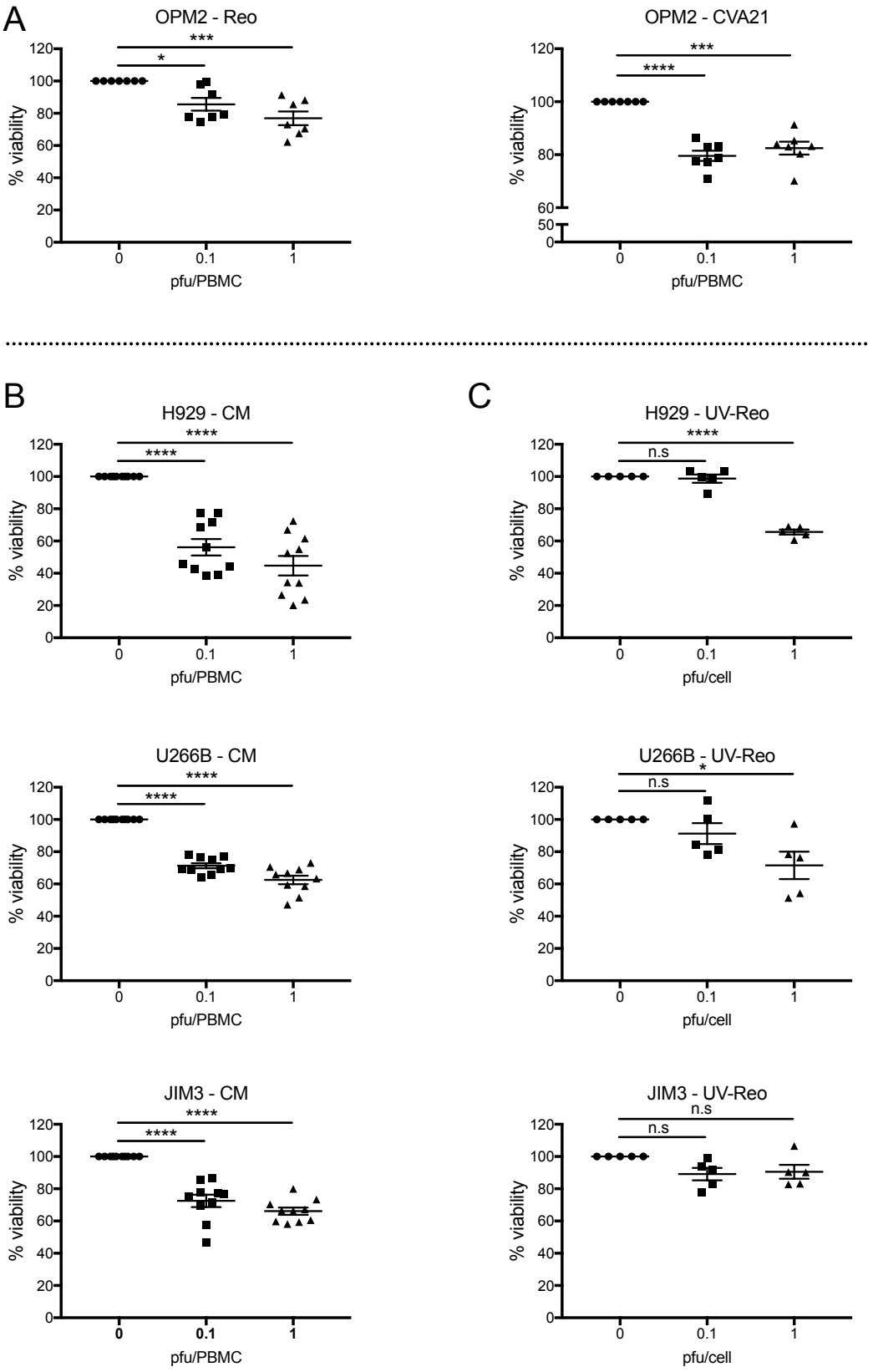
A
OPM2 - Reo
***
*
% viability
120
100
80
60
40
20
0
0
0.1
1
pfu/PBMC
OPM2 - CVA21
***
****
% viability
120
100
80
60
50
0
0
0.1
1
pfu/PBMC
B
H929 - CM
****
****
% viability
pfu/PBMC
U266B - CM
****
****
% viability
pfu/PBMC
JIM3 - CM
****
****
% viability
pfu/PBMC
C
H929 - UV-Reo
****
n.s
% viability
pfu/cell
U266B - UV-Reo
*
n.s
% viability
pfu/cell
JIM3 - UV-Reo
n.s
n.s
% viability
pfu/cell

Figure 3-6: Cytokine-induced bystander killing of MM cells.

Cells were cultured in reovirus- or CVA21-CM for 96 hrs as indicated. All CM was diluted 1:1 in fresh culture medium. After 96 hrs, cell metabolism was measured using an MTS assay and the percentage of viable cells was normalised to 0 pfu/PBMC CM. **A**: Toxicity of reovirus- and CVA21-CM, respectively, to OPM2 cells (n=7). **B**: Toxicity of reovirus-CM to H929, U266B, and JIM3 cells (n=10). **C**: As a control, neat reovirus was UV-inactivated in fresh culture medium for 2 min with reovirus doses equivalent to reovirus-CM. Toxicity of UV-inactivated reovirus against H929, U266B, and JIM3 cells, respectively, was determined using MTS assays after 96 hrs incubation (n=5). Statistical significance was calculated using one-way ANOVA with Dunnett's post-hoc test. * = $p<0.05$, *** = $p<0.001$, **** = $p<0.0001$, n.s = not significant. Error bars indicate s.e.m.

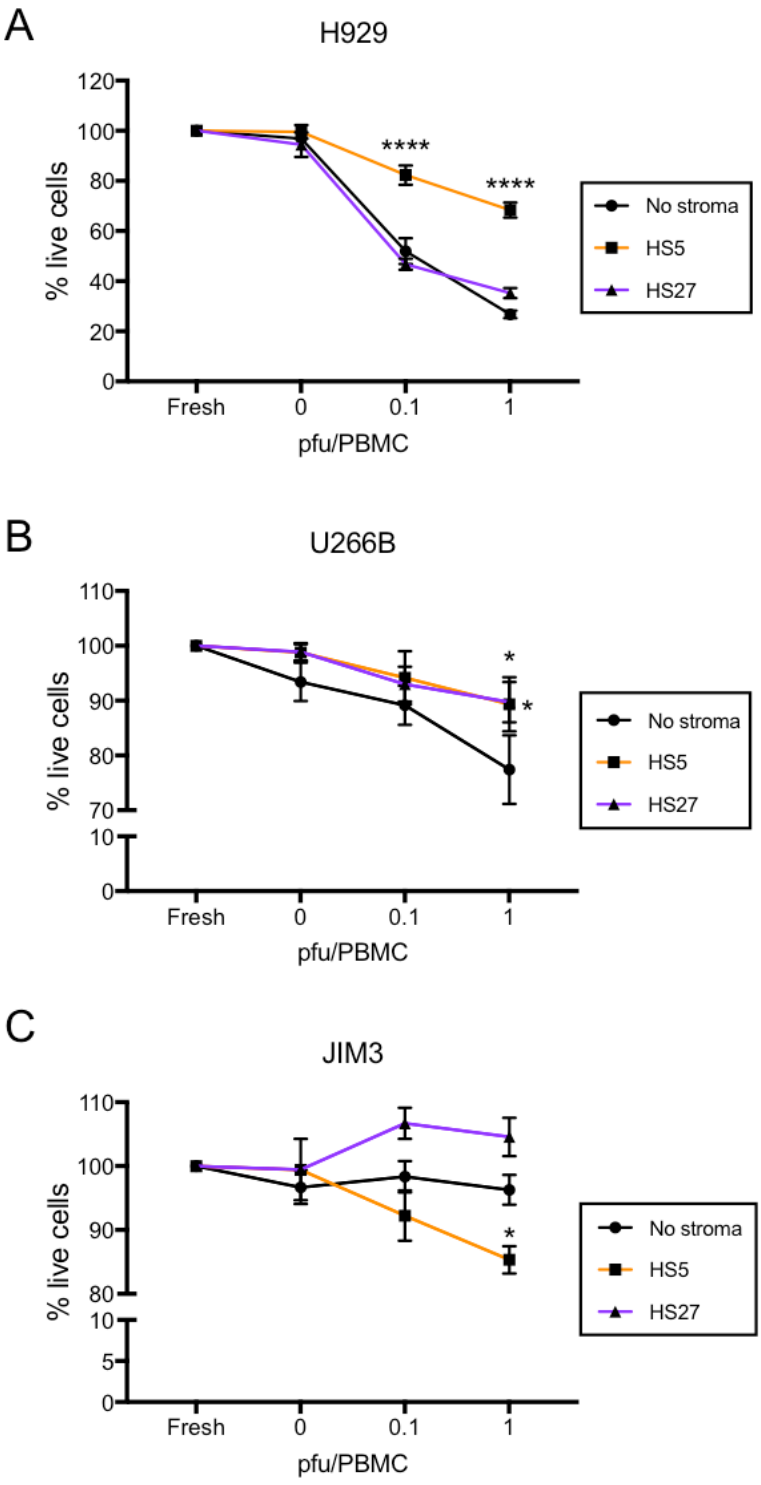

Figure 3-7: Cytokine-mediated killing of MM target cells in the context of BM stroma.

H929 (**A**), U266B (**B**), and JIM3 (**C**) cells were co-cultured at a 1:1 ratio with either HS-5 or HS-27 BM stromal cells for 24 hrs before addition of UV-inactivated reovirus-CM. Reovirus-CM was diluted 1:1 in existing culture medium. After 72 hrs, cell viability was measured by flow cytometry using a Live/Dead® discrimination stain, gating on CTG^+ MM cells. The percentage of live cells was normalised to treatment with 100% fresh medium for each co-culture condition. Statistical significance was calculated using two-way ANOVA with Tukey's post-hoc test. * = $p<0.05$, **** = $p<0.0001$, error bars indicate s.e.m, n=4.

3.2.2.2 OV-activated NK cells show cytotoxicity against MM cells

Pro-inflammatory cytokines, and type I IFNs in particular, secreted as part of the innate immune response have also been shown to be important for the maturation, activation, and function of NK cells (186). Hence, the ability of reovirus and CVA21 to activate NK cells, and potentiate their anti-myeloma cytotoxicity, was next examined. All experiments in this section were performed using PBMC isolated from healthy donors and NK cells were treated with virus as part of the whole PBMC population to mimic important aspects of normal physiology, including cell-cell crosstalk. Using flow cytometry, NK cells were identified as $CD3^{-}CD56^{+}$ cells (Figure 3-8A) and NK cell function following OV treatment was examined through assessment of phenotypic activation, degranulation, and target cell killing.

As shown in Figure 3-8, NK cells significantly up-regulated the expression of the early activation marker CD69 following treatment with either reovirus or CVA21 for 48 hrs, indicating a heightened state of activation in these cells following OV treatment (Figure 3-8 B and C). With reovirus treatment at 0.1 pfu/cell, over 80% of NK cells expressed CD69, and only a 5% enhancement was observed by increasing the dose to 1 pfu/cell (Figure 3-8B). For CVA21 however, a larger difference (15.1%) was detected in the percentage of CD69-positive cells between 0.1 and 1 pfu/cell, resulting in an average 93.3% of NK cells expressing CD69 after treatment with 1 pfu/cell CVA21 (Figure 3-8C). Evaluation of the fold increase in CD69 MFI following treatment with either reovirus or CVA21, compared to untreated NK cells, generated comparable results, with both viruses behaving in a similar way (data not shown). Importantly, in a representative patient from the MUK11 reovirus clinical trial, a peak in CD69 expression was observed on NK cells 72 hrs after reovirus i.v. infusion (Figure 3-8D). In addition, a small increase in CD69 positive NK cells was detected 24 hrs post reovirus infusion and by Day 7, the percentage of CD69 positive NK cells had decreased to a similar level, still above that prior to infusion. Similarly, 72 hrs after CVA21 i.v. infusion, the expression of CD69 was also increased on NK cells in the peripheral blood of patients taking part in the STORM clinical trial, in particular, those who received the highefr dose ($1x10^{9}$ $TCID_{50}$) of CVA21 (Figure 3-8E). No change in CD69 expression was detected on NK cells from patients receiving the lower dose of CVA21, and there was no difference in the level of CD69 positive NK cells at the 1 hr or 21-day time points, compared to pre-infusion. Degranulation and release of cytotoxic granules is required for NK cells to kill target cells upon recognition. Thus,

NK cell degranulation against MM target cells was examined using a flow cytometry-based degranulation assay as described in Section 2.13.3. PBMC from healthy donors were pre-activated with either reovirus or CVA21 for 48 hrs, and their propensity for degranulating against MM target cells compared to untreated NK cells was examined when cultured at a 2:1 effector:target ratio. Figure 3-9A shows representative flow cytometry plots from a degranulation assay using reovirus-activated NK cells challenged with U266B target cells. Spontaneous degranulation (no targets) was low, with only 1.3% $CD107^+$ NK cells (left panel). Similarly, without any reovirus treatment, degranulation in response to U266B targets was only 5.2% (middle panel), increasing to 18.9% $CD107^+$ NK cells following pre-activation with reovirus (right panel). This trend was similar for H929, JIM3, and OPM2 target cells, with a significant enhancement in NK cell degranulation following reovirus pre-treatment of PBMC (Figure 3-9B). For all target cells, except JIM3, a higher level of NK cell degranulation was observed following treatment with 1 pfu/PBMC, compared to 0.1 pfu/PBMC reovirus. For H929, U266B, and JIM3 cell targets the levels of NK cell degranulation were similar (average 9.3% increase with 0.1 pfu/PBMC reovirus treatment), with very low degranulation in the absence of virus treatment. Encouragingly, a significant increase in NK cells degranulation was also observed against the oncolysis-resistant target cells OPM2. While baseline degranulation against these targets without any reovirus pre-activation was higher (average 17.5% $CD107^+$ NK cells), the relative potentiation with reovirus treatment was similar to that for other targets tested (average 7.1% increase with 0.1 pfu/PBMC reovirus).

Pre-treatment of PBMC with CVA21 had a similar effect on NK cell degranulation, with a significant enhancement observed against all MM target cells tested (Figure 3-9C). For CVA21 treatment, a maximum level of degranulation was reached with 0.1 pfu/PBMC treatment, with CD107 expression decreasing at the higher dose of 1 pfu/cell. The levels of degranulation achieved against H929, U266B, and JIM3 targets cells were slightly lower with CVA21 treatment compared to reovirus treatment (average 6.7% increase with 0.1 pfu/PBMC CVA21 treatment). As observed in the reovirus experiment, baseline NK cell degranulation against OPM2 targets without CVA21 pre-treatment was high, but still increased to a similar extent as for the other target cells (average 5.4%).

Next, the cytotoxic functionality of virus-activated NK cells was tested using a flow-cytometry based killing assay (Section 2.13.5). NK cells were pre-

activated with either virus and subsequently challenged with MM target cells (H929, U266B, JIM3, or OPM2) at a 25:1 effector:target ratio. Overall, killing of all target cells was significantly enhanced after pre-treatment of PBMC with either reovirus (Figure 3-9D) or CVA21 (Figure 3-9E). The cytotoxic effect was most pronounced against H929 cells and, notably, OPM2 cells. With reovirus treatment (1 pfu/PBMC) the average killing of these target cells increased to 26.1% compared to untreated NK cells. With CVA21 treatment (1 pfu/PBMC), an average 43.7% and 35.5% increase in the killing of H929 and OPM2 targets, respectively, was observed, suggesting that CVA21 was the more potent agent for enhancing NK cell-mediated cytotoxicity, despite the lower induction of NK cell degranulation (Figure 3-9). Importantly, this demonstrated that the enhanced degranulation following OV treatment was correlated with an enhanced cytotoxic function of the NK cells.

To examine the ability of NK cells to overcome the protection of MM cells induced by the BM microenvironment, the stromal cell co-culture model was used as described previously (Section 2.1.6). As co-culture with HS-27 stromal cells induced the greatest protection against direct oncolysis overall (Section 3.2.1), this stromal cell line was chosen for the NK cell killing assays. H929, U266B, and JIM3 cells stained with CTG were co-cultured with HS-27 stromal cells for 48 hrs to generate MM cells with reduced susceptibility to direct oncolysis, then cells were harvested and used as targets in NK cell killing assays. Despite some reduction in the NK cell cytotoxicity observed (for U266B target cells particularly), importantly, there was no significant decrease in the ability of reovirus-activated NK cells to kill MM cells cultured on HS-27 cells, compared to MM target cells alone (Figure 3-10 A-C). This was also true for CVA21-treated NK cells, with no significant difference in the levels of NK cell-mediated killing observed for either H929, U266B, or JIM3 cells cultured on HS-27 stromal cells, compared to each cell type alone (Figure 3-10 D-F). Although not significant, H929 cells appeared to be less affected by co-culture with BM stroma, compared to U266B and JIM3 cells, with identical levels of cell death with and without stromal cell support (Figure 3-10A and D).

The results presented in this section show that NK cells activated with either reovirus or CVA21 can degranulate against, and kill, MM cells, including those completely resistant to direct oncolysis (OPM2) and those with reduced susceptibility to oncolysis in the BM niche. Together with the experiments presented in Section 3.2.2.1 on the cytotoxicity of CM, these

results indicate a role for innate anti-tumour immune mechanisms in the eradication of MM cells.

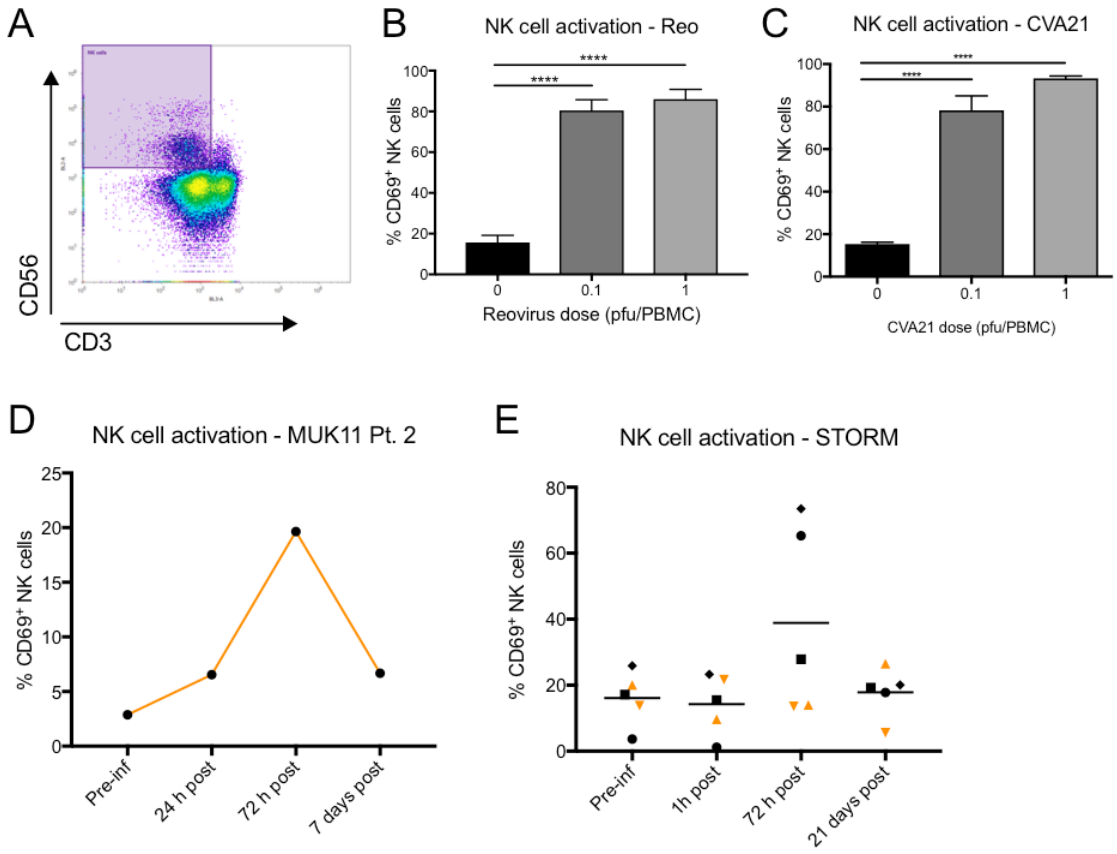

Figure 3-8: Reovirus and CVA21 activate NK cells *in vitro* and *in vivo* following i.v. administration.

A: NK cell flow cytometry gating strategy. For all NK cell experiments, NK cells were treated with virus in the context of whole PBMC and identified by flow cytometry as the $CD3^{-}CD56^{+}$ population. **B** and **C**: PBMCs from healthy donors were treated with 0.1 or 1 pfu/cell of reovirus (**B**) or CVA21 (**C**) for 48 hrs. CD69 expression was measured by flow cytometry on $CD3^{-}CD56^{+}$ NK cells and is presented as the percentage of $CD69^{+}$ cells (n=4). Statistical significance was calculated using one-way ANOVA with Tukey's post-hoc test, **** = $p<0.0001$. Error bars indicate s.e.m. **D**: CD69 expression on NK cells from one patient treated with i.v. reovirus as part of the MUK11clinical trial. Peripheral blood samples were taken prior to infusion, then 24 hrs, 72 hrs, and 7 days post infusion. **E**: CD69 expression on NK cells from five patients treated with i.v. CVA21 as part of the STORM trial. Peripheral blood samples were taken prior to viral infusion, then at 1 h, 72 hrs, and 21 days post infusion. Bars indicate the mean CD69 expression, orange = 10^{8} $TCID_{50}$ CVA21, black = 10^{9} $TCID_{50}$ CVA21 (Table 3-1).

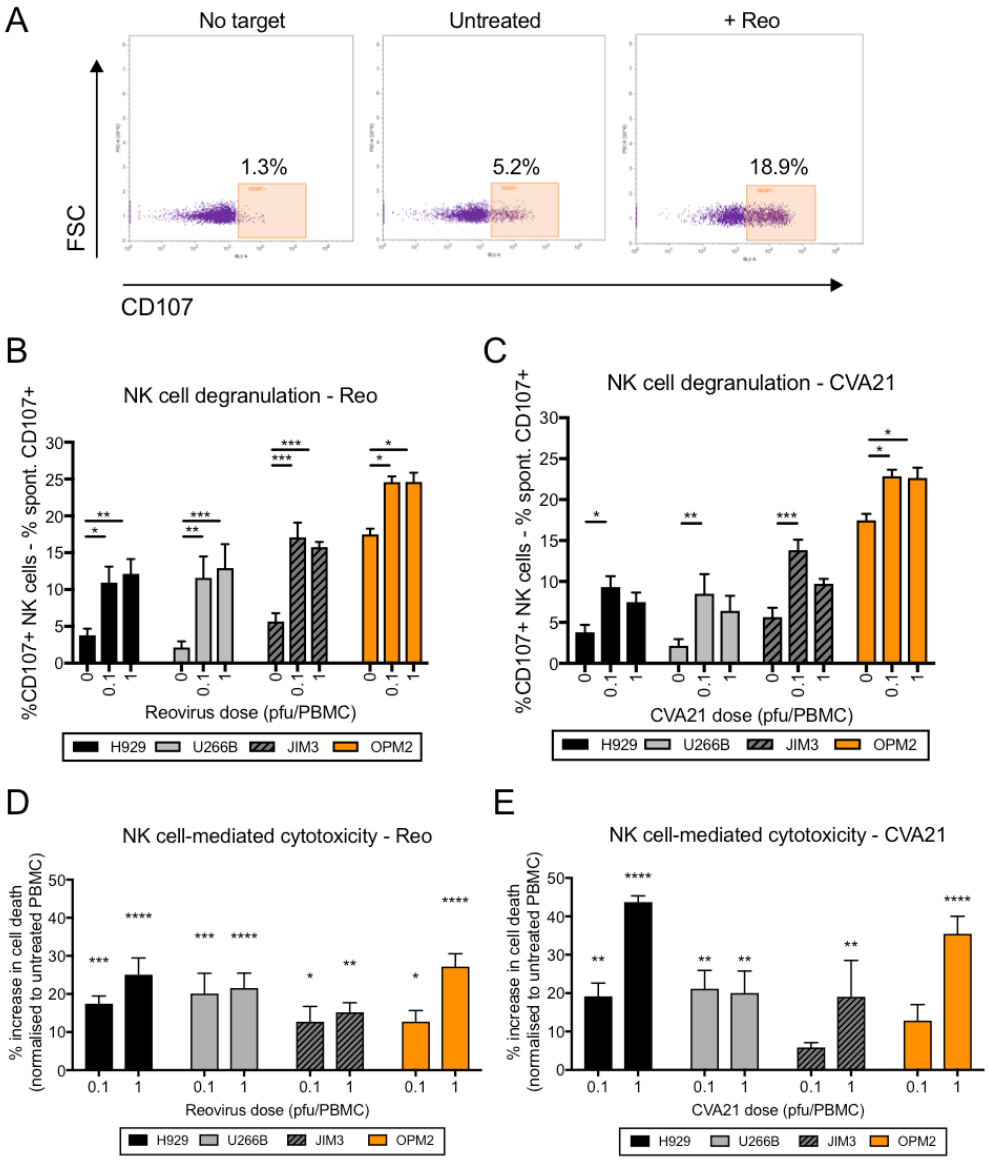

Figure 3-9: NK cell degranulation against, and killing of, MM target cells following activation with reovirus or CVA21.

For NK cell degranulation assays, whole PBMC were pre-activated with either 0.1 or 1pfu/cell reovirus or CVA21, respectively, for 48 hrs. PBMC were co-cultured with MM target cells at a 2:1 effector:target ratio for 1 h, followed by another 4 hrs incubation in the presence of Brefeldin A. Surface expression of CD107a/b was measured by flow cytometry on $CD3^{-}CD56^{+}$ NK cells. **A**: Representative flow cytometry plots showing CD107a/b expression on NK cells in the absence of target cells (left panel), and in the presence of U266B targets cells, after co-culture with untreated- (middle panel) and reovirus-treated PBMC (right panel), respectively. **B**: CD107a/b expression on NK cells pre-activated with reovirus following co-culture with H929, U266B, JIM3, or OPM2 cells. **C**: CD107a/b expression on NK cells pre-activated with CVA21 following co-culture with H929, U266B, JIM3, or OPM2 cells. **D** and **E**: For NK cell killing assays, MM target cells were labelled with CTG and co-cultured with reovirus (**D**) or CVA21 (**E**) pre-activated PBMC at a 25:1 effector:target ratio for 5 hrs, before staining with a Live/Dead® discrimination stain. Percentage cell death is shown as the increase in death with OV-activated NK cells, compared to untreated NK cells. Statistical significance was calculated using one-way ANOVA with Tukey's post-hoc test, * = $p<0.05$, ** = $p<0.01$, *** = $p<0.001$, **** = $p<0.0001$. Error bars indicate s.e.m, n=4.

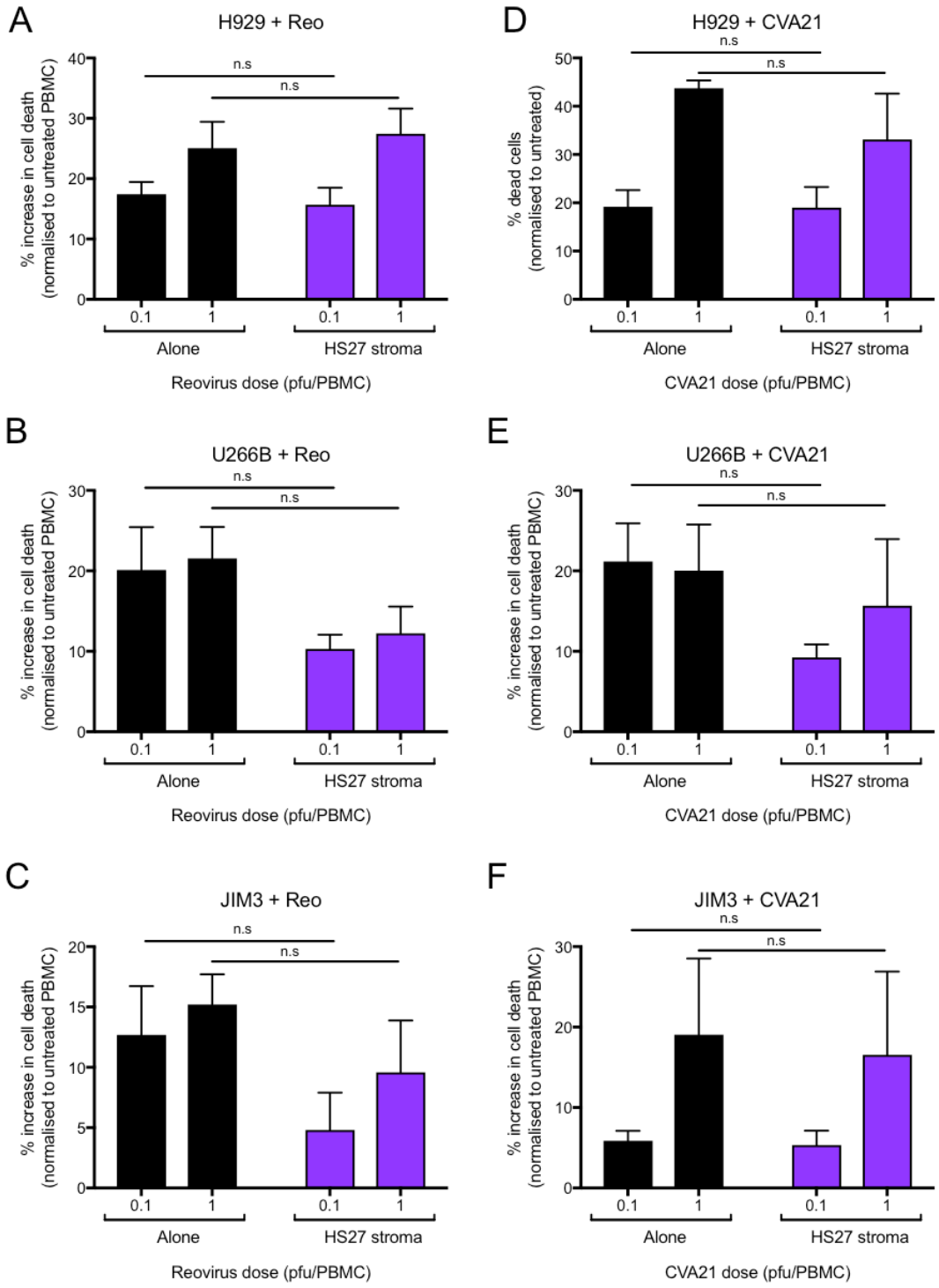

Figure 3-10: NK cell-mediated killing of MM target cells with reduced susceptibility to direct oncolysis after culture on BM stromal cells.

MM target cells (H929, U266B, and JIM3) were co-cultured with HS-27 BM stromal cells for 48 hrs before inclusion in a flow cytometry-based NK cell killing assay. PBMC treated with either 0.1 or 1 pfu/cell of reovirus (**A**-**C**) or CVA21 (**D**-**F**) were co-cultured with either target cells alone (black) or target cells pre-cultured on HS-27 (purple) for 5 hrs before staining with a Live/Dead® discrimination stain. Cell death was measured on CTG^+ MM cells and was normalised to an untreated PBMC control. Statistical significance was calculated using two-way ANOVA with Šídák's post-hoc test, error bars indicate s.e.m, n=4, n.s. = not significant.

3.2.2.3 Both reovirus and CVA21 can induce priming of MM-specific cytotoxic T cells

Further analysis of PBMC from the MUK11 and STORM trials showed significant upregulation of CD69 on both $CD4^+$ (Figure 3-11 A and B) and $CD8^+$ (Figure 3-11 C and D) T cells following i.v. infusion of reovirus or CVA21, respectively. By 72 hrs, the percentage of CD69-positive $CD4^+$ T cells increased from 0.7% to 16.0% in the patient receiving Reolysin® (Figure 3-11A). The response was similar in patients receiving CVA21, with a significant increase in CD69 expression on $CD4^+$ T cells 72 hrs after CVA21 infusion (Figure 3-11B). Interestingly, up-regulation of CD69 was seen in response to both the higher and the lower dose of CVA21, and for patients STORM-2, -4, and -6, the elevated CD69 expression was sustained until the 21-day time point. Activation of $CD8^+$ T cells was detected 24 hrs after reovirus infusion, with a 22.0% increase in the number of CD69 positive $CD8^+$ T cells (Figure 3-11C). Activation was sustained until the 72 hrs time point and reduced by Day 7. Similarly, $CD8^+$ T cells from patients in the STORM trial showed an increase in CD69 expression 72 hrs after CVA21 treatment (Figure 3-11D). However, $CD8^+$ T cell activation was predominantly seen in patients receiving the higher dose (10^9 $TCID_{50}$) of CVA21. Activation of T cells in the peripheral circulation of patients in response to virus administration was encouraging for subsequent studies investigating the ability of reovirus and CVA21 to induce an adaptive CTL immune response *in vitro*.

Mature DCs display a high expression of T cell co-stimulatory molecules CD80 and CD86, as well as MHC Class II, and are pivotal for the generation of functional CTL responses (340-342), while iDCs (low expression of CD80, CD86, and MHC Class II) are generally tolerogenic (Section 1.1.2.1.2). Thus, the next step in the evaluation of the potential for successful CTL priming was to examine the response of iDC to reovirus and CVA21, respectively. iDC differentiated from $CD14^+$ cells were treated with reovirus or CVA21 for 24 hrs, and the expression of CD80, CD86, and HLA-DR, was analysed by flow cytometry. Interestingly, reovirus treatment induced a more pronounced upregulation of CD80, CD86, and HLA-DR on DCs (Figure 3-12A), compared to 24 hrs CVA21 treatment (Figure 3-12B). Increasing treatment time to 48 hrs with CVA21 did not enhance the DC maturation (data not shown). Although significant, upregulation of CD80 and CD86 was less than two-fold following CVA21 treatment (1 pfu/DC), compared to three-fold and 27-fold, respectively, following reovirus treatment. As reovirus was

more capable of maturing DCs, it was also hypothesized that this OV may be more effective in the priming of MM-specific CTLs than CVA21.

A protocol for priming of tumour-specific CTL in a haematological context was adapted from a protocol developed for melanoma (246). The protocol involved loading of iDCs with virus-treated MM target cells and subsequent co-culture of DCs with autologous PBMC, including the T cells. Following a re-stimulation of the T cells with target-loaded DCs, the primed CTLs were evaluated for their ability to kill the (relevant) MM targets cells used for priming, and for their antigen specificity, using irrelevant target cells and TAA peptide stimulation (protocol overview in Appendix, Figure A-1). Based on susceptibility to oncolysis (Figure 3-2), 1 pfu/cell reovirus and 0.1 pfu/cell CVA21 were chosen for the pre-treatment of target cells. Target cells were treated for 24 hrs to allow tumour cell infection without excessive cell death. First, CTLs were generated in the presence of OV-loaded U266B cells, and their ability to kill relevant and irrelevant target cells was evaluated using chromium release assays (Section 2.15). Figure 3-13 demonstrates the ability of CTLs generated in the presence of either reovirus (Figure 3-13A) or CVA21 (Figure 3-13B) to specifically kill relevant U266B targets (purple), with no enhanced killing of irrelevant myeloid target cells (KG-1, orange). CTLs primed using reovirus were more efficient at killing U266B targets cells than those primed using CVA21 with an average 65.0% of U266B cells lysed using reovirus, compared to 50.8% using CVA21 at a 50:1 E:T ratio. No CTLs with cytotoxicity against U266B targets could be generated without virus present during the priming.

CTLs rely on the Ca^{2+}-dependent exocytosis of cytotoxic granules for the killing of target cells (Section 1.1.2.2.2). Thus, the first step in confirming that target cell killing was mediated by MM-specific CTLs was to include a chelating agent (egtazic acid, EGTA) during the killing assay to prevent Ca^{2+}-dependent exocytosis. In the presence of 2mM EGTA, killing of U266B cells in the chromium release assay was completely abrogated (Figure 3-13 C and D), indicating that death was mediated through the exocytosis of cytotoxic granules from CTLs. It is worth noting that in these experiments, the level of target cell killing was similar independent of which OV was used for priming, demonstrating that these experiments are susceptible to large donor variation.

To also examine the ability of CTLs to target MM cells protected against oncolysis by the BM niche, CTL killing was evaluated using U266B target cells pre-cultured on HS-27 stromal cells. As demonstrated in previous

sections, co-culture with HS-27 induced protection against reovirus-mediated oncolysis and CM cytotoxicity in U266B but was not able to protect against NK cell-mediated killing. CTLs were generated in the presence of reovirus- (Figure 3-14A) or CVA21-loaded (Figure 3-14B) U266B cells, then target cell killing was measured using a flow cytometry-based killing assay, comparing U266B cells alone as targets with U266B cells co-cultured with HS-27 stromal cells for 48 hrs. Encouragingly, there was no significant reduction in the killing of U266B target cells with prior co-culture on HS-27 stromal cells, regardless of the virus used for CTL priming. Interestingly, CTLs primed against U266B using CVA21 were also able to kill OPM2 target cells inherently resistant to oncolysis (Figure 3-14C) with an average increase in cell death of 11.8% at a 25:1 E:T ratio, compared to CTLs primed without CVA21.

To further characterise the cells generated using the priming protocol, and to confirm the importance of CTLs in the eradication of relevant target cells, the specific response of $CD8^+$ T cells to relevant and irrelevant target cells was evaluated using flow cytometry. First, CTL degranulation against relevant and irrelevant targets was measured after 5 hrs co-culture as described in Section 2.13.3. Figure 3-15A shows that when using CTLs primed in the presence of reovirus, degranulation against relevant U266B target cells, but not irrelevant cells, was significantly enhanced compared to CTLs generated without virus. This further confirmed the results in Figure 3-13C, which indicated that target cell killing was mediated by a Ca^{2+}-dependent mechanism. Interestingly, CTLs generated using CVA21 showed very low levels of degranulation against relevant targets, only 1.4% CD107-positive CTLs generated against relevant targets, compared to 5.0% using reovirus (Figure 3-15B), again indicating reovirus as the more efficient agent in the CTL priming context. The generation of antigen specific CTLs was further evaluated by blocking the interaction of CD8 with MHC Class I, which is essential for antigen recognition and activation of CTL cytotoxicity (343). U266B target cells were pre-labelled with an MHC Class I-blocking antibody or an isotype control, and then included in the degranulation assay as previously described. Using CTLs primed in the presence of reovirus, co-culture with U266B target cells without any antibody labelling stimulated approximately 6.2% of CTLs to transport CD107 to the cell surface. However, this degranulation was completely abrogated when MHC Class I on the target cells was blocked. Following labelling of target cells with an isotype control antibody, the degranulation response was restored to 6.1% (Figure 3-15C). This confirmed the importance of MHC-I:CD8 interaction for

the degranulation of primed CTLs and implicated that successful antigen recognition was required to generate an efficient CTL response. As the degranulation of CTLs generated in the presence of CVA21 was negligible, no response to MHC Class I blockade was expected. However, while not significant, the overall response indicated a similar trend for CTLs primed using CVA21-loaded U266B, with a reduction in the percentage of CD107-positive cells following MHC Class I blockade, which was restored following labelling with an isotype control (Figure 3-15D).

IFN-γ is important for CTL activation and proliferation, and is secreted in large amounts upon antigen recognition by CTL, and also by NK cells, and Th_1 $CD4^+$ T cells (344, 345). Thus, the next step in characterising the primed CTL response was to examine the secretion of this cytokine. First, an ELISA was used to confirm abundant secretion of IFN-γ in both reovirus and CVA21 priming cultures with an average 25 600 pg/mL secreted in reovirus cultures (Figure 3-16A) and 13 100 pg/mL secreted in CVA21 cultures (Figure 3-16B), suggestive of the generation of a T_h1-skewed immune response, as expected during priming of CTLs (346, 347). To confirm that IFN-γ was truly secreted by CTLs in response to antigen recognition, rather than as an innate response to virus, IFN-γ production was next examined using intracellular flow cytometry. CTLs primed using OV-loaded U266B cells were co-cultured with relevant (U266B) or irrelevant (KG-1) target cells for 5 hrs. Then, cells were fixed, permeabilised, and stained with an anti-IFN-γ antibody as described in Section 2.13.4. These data demonstrated that CTLs primed using either reovirus (Figure 3-16C) or CVA21 (Figure 3-16D) produced IFN-γ specifically against relevant, but not irrelevant, target cells. Interestingly, the percentage of IFN-γ-positive CTLs was similar in CTLs primed using both reovirus (4.0%) and CVA21 (3.0%), suggesting that CTLs primed using CVA21 can also mount an efficient response in an antigen-dependent manner, despite the lack of DC maturation seen in response to CVA21 treatment (Figure 3-12B). In keeping with the results presented in Figure 3-14C, showing that CTLs primed against U266B target cells using CVA21 could also kill OPM2, it was confirmed that CTLs, while not producing IFN-γ in response to an irrelevant myeloid target, did produce IFN-γ upon recognition of OPM2 cells (Figure 3-16F). IFN-γ production in response to OPM2 in CTLs primed against U266B using reovirus was not statistically significant due to donor variability but did indicate an increase compared to CTLs primed without reovirus (Figure 3-16E). These results suggest the possibility of shared antigens between U266B and OPM2 cells,

and the potential of CTLs primed against a CVA21-susceptible target to also eliminate CVA21-resistant targets, depending on the antigen repertoire.

To confirm the antigen specificity of primed CTL discussed above, the IFN-γ response was further explored by challenging CTLs with TAA peptide pools generated from TAA expressed in MM; PRAME, Mucin-1, and MAGE-A1. As discussed (Section 1.1.2.2.2), these TAA are some of the most commonly expressed in MM, both on primary cells and MM cell lines (28). Autologous $CD14^+$ APCs were loaded with either peptide pool and then co-cultured with primed CTLs for 5 hrs as previously described. CTLs generated against U266B in the presence of reovirus showed significantly enhanced production of IFN-γ in response to both PRAME and MAGE-A1 peptides (Figure 3-17A), with the increase in the number of IFN-γ-producing CTLs being approximately 3.0% and 4.0%, respectively. The responses were variable depending on the donor, and some donors also showed a response, although not significant, against Mucin-1 peptides. CTLs primed against U266B in the presence of CVA21 showed significantly enhanced production of IFN-γ in response to Mucin-1 and MAGE-A1 peptides (3.1% and 5.4% increase, respectively), with some donors also responding favourably to PRAME peptides (Figure 3-17B). These findings are particularly encouraging as they demonstrate that both reovirus and CVA21 can be used to prime CTLs specific not only for non-self/allo-antigen, but for well-recognised and reported TAA in MM.

To demonstrate the broad applicability of this approach, and further examine whether there was a role of anti-tumour immunity in the absence of direct oncolysis, the priming assay was next performed using H929 cells, susceptible to reovirus and CVA21, and OPM2 cells, which were resistant to both viruses. Using chromium release assays, the ability of primed cells to kill relevant (H929 or OPM2) and irrelevant (KG-1) cells was assessed. As shown in Figure 3-18, CTLs that specifically killed relevant, but not irrelevant target cells, could be primed using H929 cells in the presence of either virus (Figure 3-18 A and B). Using reovirus, the level of H929 target cell lysis was comparable to that seen with CTLs primed against U266B (average 68.2% at a 50:1 effector:target cell ratio). The efficacy was again lower when CTLs were primed using CVA21 (average 40.7% lysis). When priming CTLs against resistant OPM2 cells using reovirus, a small improvement in killing of target cells was seen (maximum 10.2% lysis of target cells at 50:1 effector:target cell ratio), compared to using reovirus-susceptible cells (Figure 3-18C). Furthermore, no successful priming was possible using

CVA21, resulting in no difference in the lysis of relevant and irrelevant target cells (Figure 3-18D). The fact that CTLs primed using U266B cells were in fact able to kill OPM2 cells in an antigen-dependent manner (Figure 3-14C and Figure 3-16F), suggests that the inefficient priming against OPM2 cells might be due to absence of viral replication rather than resistance to CTL-mediated killing (225).

Taken together, the findings presented in this section demonstrated that treatment of MM cells with either reovirus or CVA21 could induce efficient priming of MM-specific CTLs. While both viruses generated CTLs with high cytotoxicity against relevant, but not irrelevant, targets and specificity to well-recognised TAA in MM, reovirus constantly generated a more potent response. However, it was possible to prime efficient CTLs using CVA21, despite limited maturation of DC following CVA21 treatment. Importantly, there was no difference in the levels of target cell killing when target cells were subjected to the protective effects of the BM niche. This section demonstrates the generation of adaptive anti-tumour immunity and together with the data presented previously, demonstrates that both innate and adaptive anti-tumour immune responses could play a role in the eradication of MM following OV treatment.

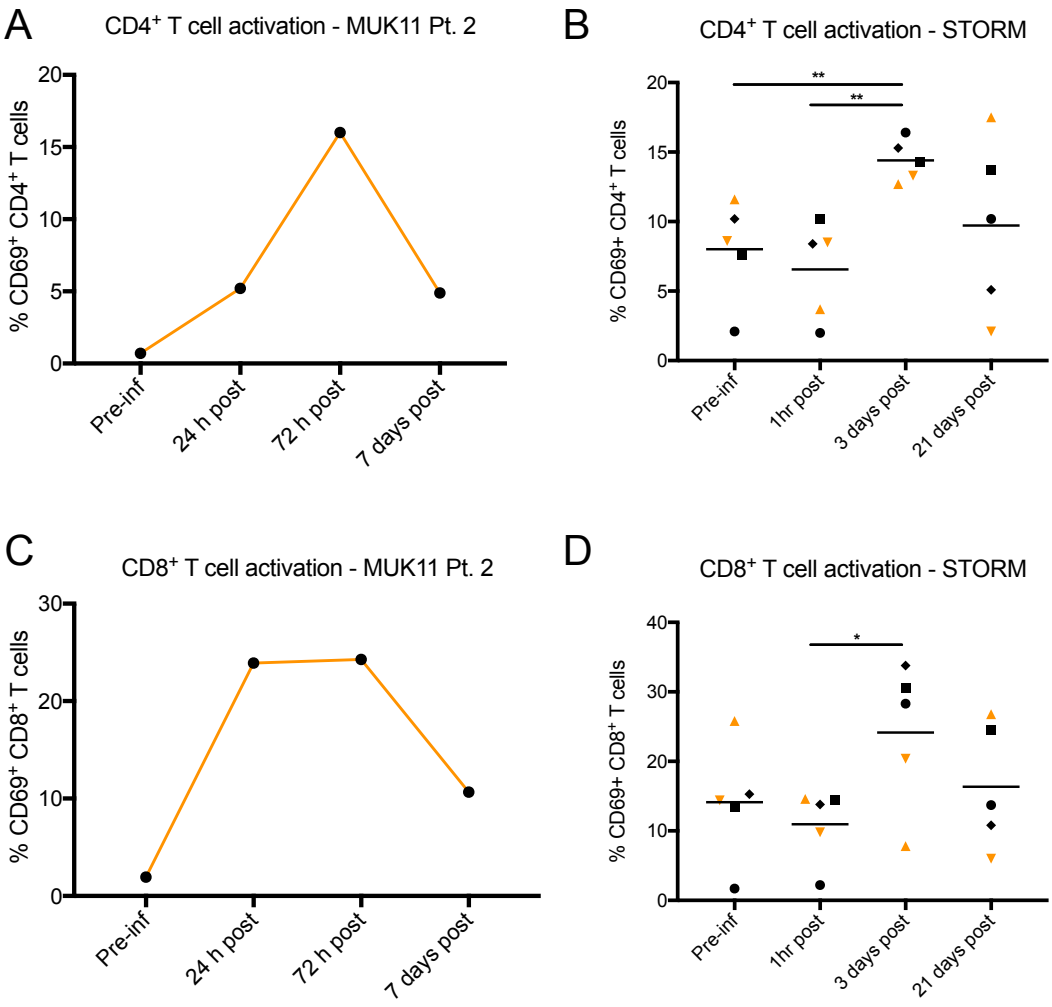

Figure 3-11: T cell activation after i.v. infusion of reovirus or CVA21.

CD69 expression was evaluated by flow cytometry on $CD4^+$ (**A** and **B**) and $CD8^+$ (**C** and **D**) T cells from one patient treated with i.v. reovirus as part of the MUK11 trial (**A** and **C**), and five patients treated with i.v. CVA21 as part of the STORM trial (**B** and **D**). Peripheral blood samples were taken prior to infusion, then 24 hrs, 72 hrs, and 7 days post infusion for MUK11 patients and prior to infusion, then at 1 h, 72 hrs, and 21 days post infusion for STORM patients. Bars indicate the mean CD69 expression, orange = 10^8 $TCID_{50}$ CVA21, black = 10^9 $TCID_{50}$ CVA21 (Table 3-1). Statistical significance was calculated using one-way ANOVA with Tukey's post-hoc test, * = $p<0.05$, ** = $p<0.01$.

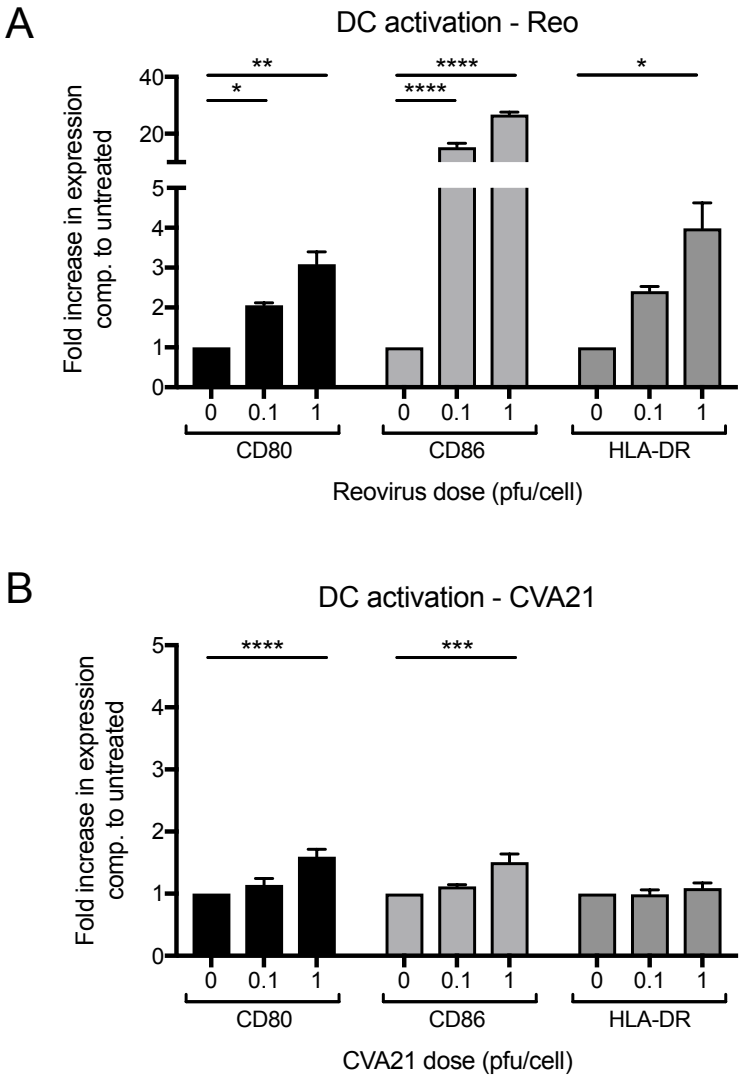

Figure 3-12: Reovirus and CVA21 treatment increase the expression of T cell co-stimulatory molecules on DCs.

iDCs were differentiated from $CD14^+$ cells obtained from healthy donor PBMC by MACS cell separation (n=4). Following differentiation, DCs were treated with 0.1 or 1 pfu/cell of reovirus (**A**) or CVA21 (**B**) for 24 hrs and the expression of CD80, CD86, and MHC Class II (HLA-DR) was evaluated by flow cytometry. Expression is shown as the fold increase in MFI compared to untreated DCs. Statistical significance was calculated using one-way ANOVA with Tukey's post-hoc test, * = $p<0.05$, ** = $p<0.01$, *** = $p<0.001$, **** = $p<0.0001$. Error bars indicate s.e.m.

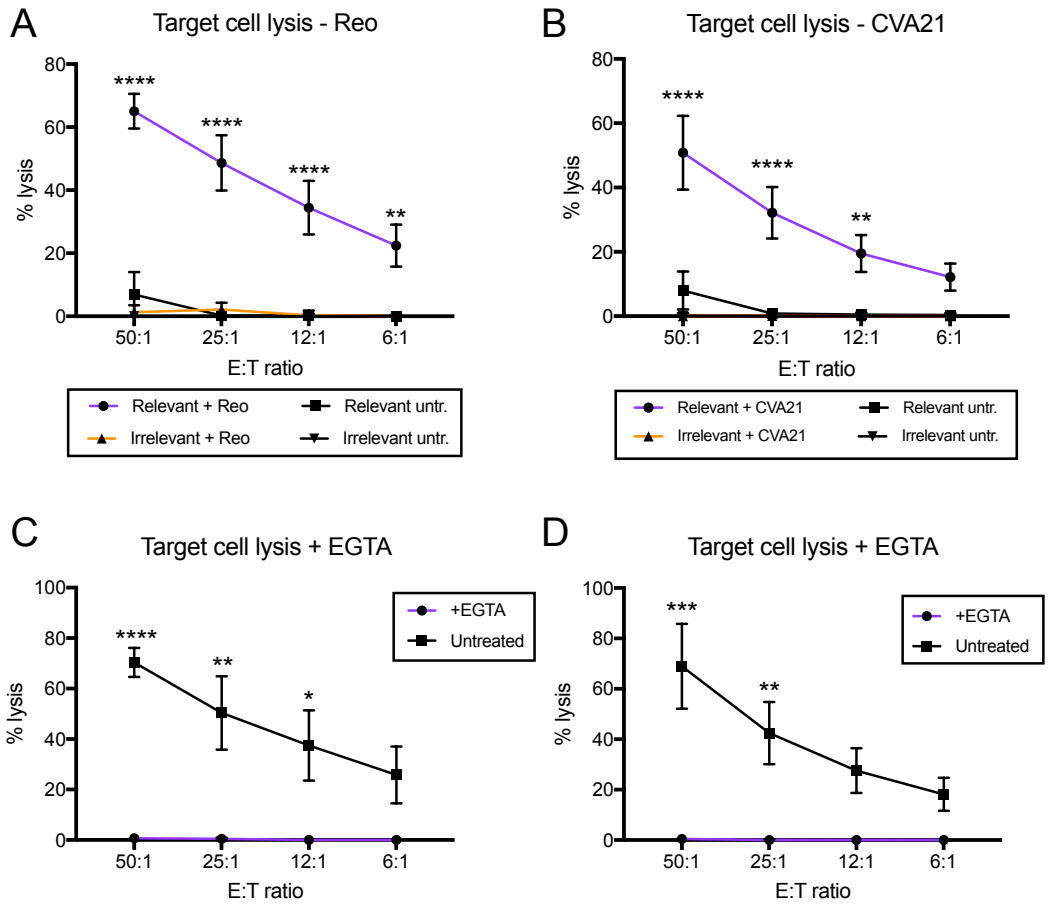

Figure 3-13: Killing of relevant, but not irrelevant, MM target cells following CTL priming.

Primed CTLs were generated after co-culturing PBMC with autologous DC, pre-loaded with U266B cells treated with either 1 pfu/cell reovirus (**A**), or 0.1 pfu/cell CVA21 for 24 hrs (**B**). Following one re-stimulation with OV-U266B-loaded DC, CTL generated with or without reovirus or CVA21, were co-cultured with ^{51}Cr-labelled relevant (U266B) and irrelevant (KG-1) target cells for 4 hours at different effector:target ratios. The percentage of cell lysis was determined after 4 hours (n=6). **C** and **D**: CTLs were co-cultured with relevant target cells in the presence or absence of 2 mM EGTA (untreated), n=3. **C**: CTLs generated using reovirus-loaded U266B cells. **D**: CTLs generated using CVA21-loaded U266B cells. Statistical significance was calculated using two-way ANOVA with Tukey's post-hoc test and refers to comparison between Relevant + virus and Irrelevant + virus, * = p<0.05, ** = p<0.01, *** = p<0.001, **** = p<0.0001. Error bars indicate s.e.m.

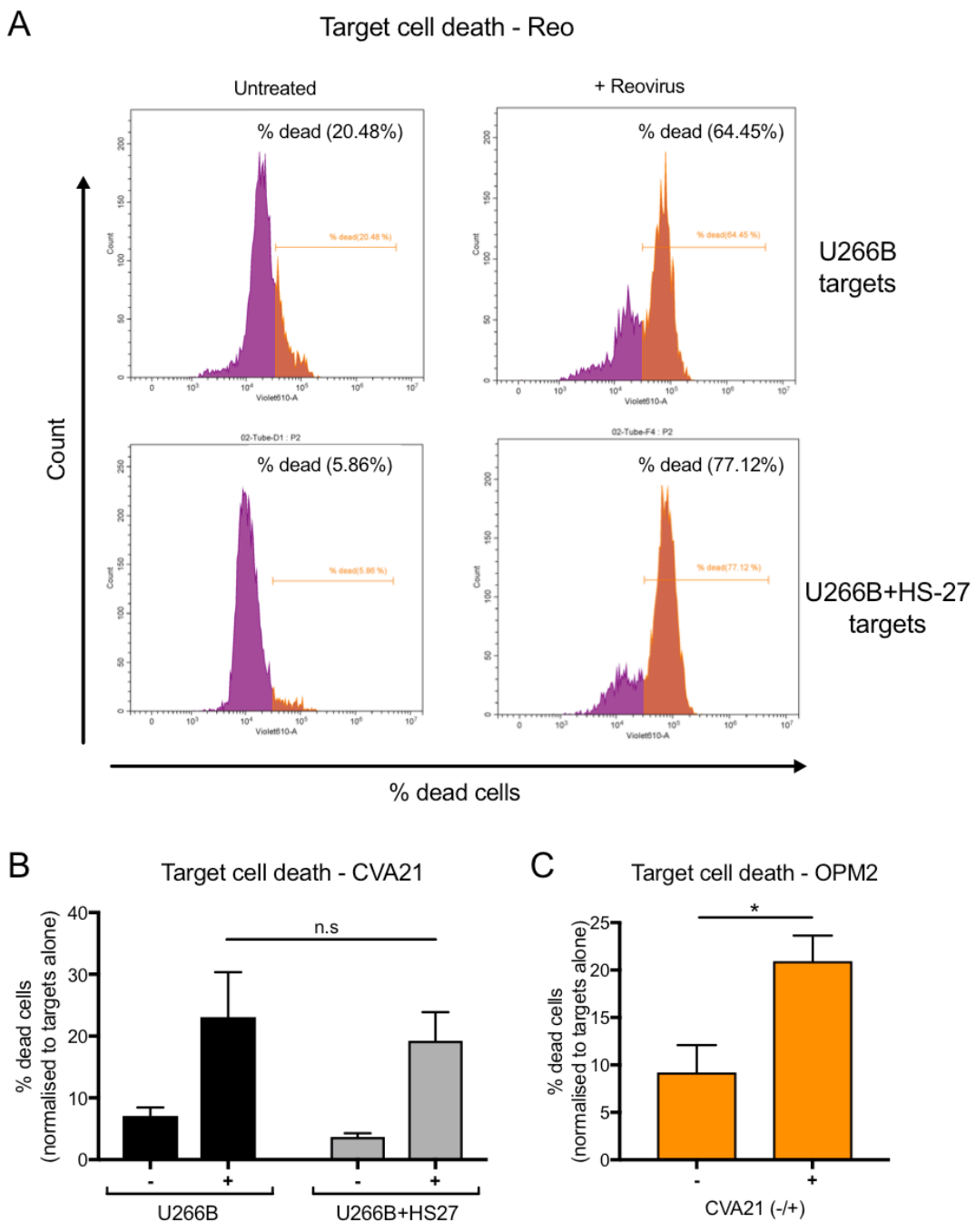
A
Target cell death - Reo
Untreated
+ Reovirus
% dead (20.48%)
% dead (64.45%)
% dead (5.86%)
% dead (77.12%)
U266B targets
U266B+HS-27 targets
Count
% dead cells
B
Target cell death - CVA21
% dead cells (normalised to targets alone)
n.s
U266B
U266B+HS27
C
Target cell death - OPM2
% dead cells (normalised to targets alone)
*
CVA21 (-/+)

Figure 3-14: CTL-mediated killing of MM target cells with reduced susceptibility to direct oncolysis.

A and **B**: U266B CTLs, primed using either reovirus (**A**) or CVA21 (**B**), were co-cultured with CTG-stained U266B target cells alone, or CTG-stained U266B cells pre-cultured on HS-27 stromal cells for 48 hrs, at a 25:1 effector:target ratio for 5 hrs before staining with a Live/Dead® discrimination stain. **A**: Representative flow cytometry plots using cells primed in the presence (right panels) or absence (left panels) of reovirus. The percentage of dead cells (orange gate) is indicated in each plot. Top plots: U266B targets alone. Bottom plots: U266B cells pre-cultured with HS-27 stromal cells (n=1). **B**: CTLs primed in the presence of CVA21 (n=3). Cell death was measured on CTG^+ U266B cells and was normalised to the viability of the respective target cell alone. Statistical significance in **A** and **B** was calculated using one-way ANOVA with Šídák's post-hoc test. **C**: CTLs primed in the presence of CVA21 (n=3) were co-cultured with CTG-stained OPM2 target cells. Target cell death was measured as described for A and B, and normalised to the viability of OPM2 cells alone. Statistical significance in **C** was calculated using paired, two-tailed *t*-tests, * = $p<0.05$, n.s = not significant. Error bars indicate s.e.m.

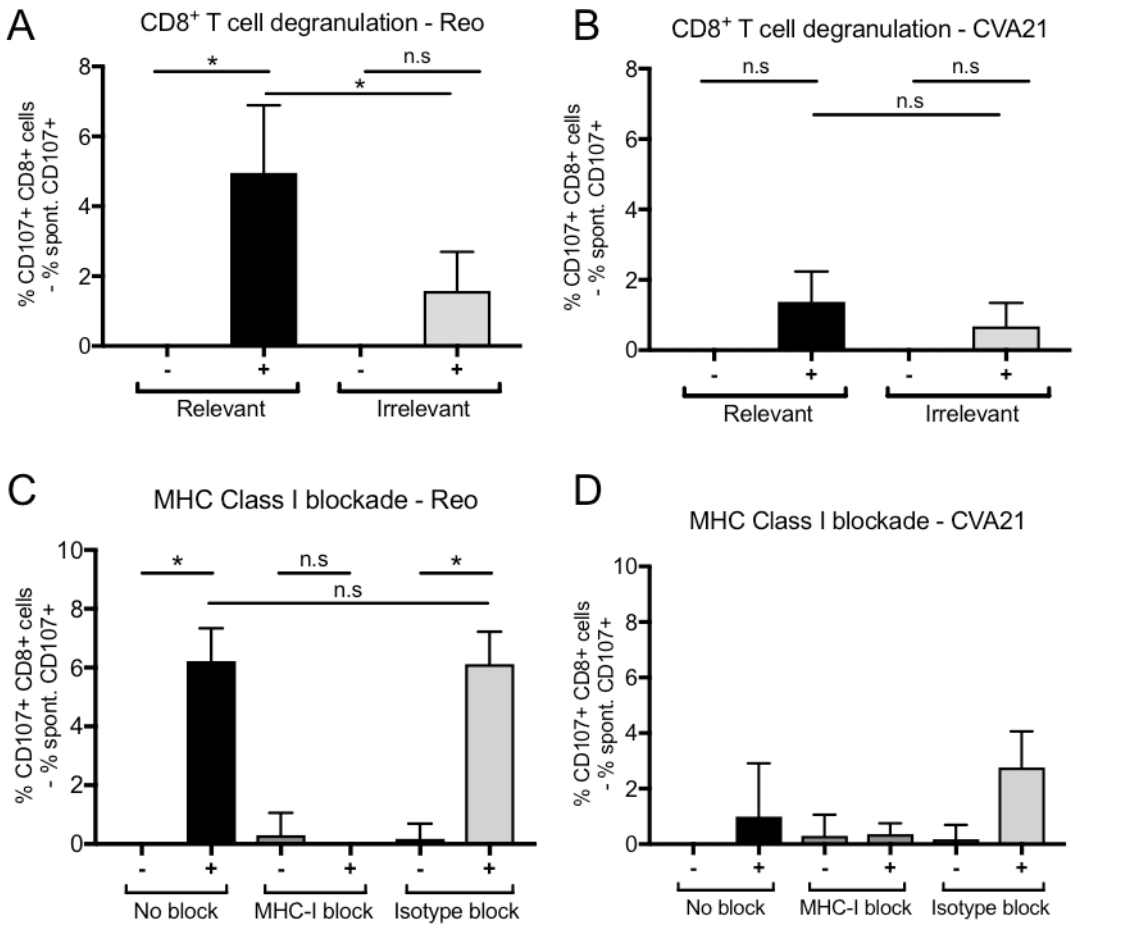

Figure 3-15: For CTLs primed using reovirus, degranulation against relevant targets is dependent on CD8:MHC-I interaction

PBMCs primed in the presence of reovirus (**A**) or CVA21 (**B**) were co-cultured with relevant (U266B) or irrelevant (KG-) target cells at a 2:1 effector:target ratio for 1 h, followed by another 4 hrs incubation in the presence of Brefeldin A. Surface expression of CD107a/b was measured by flow cytometry on $CD3^+CD8^+$ CTL (n=8). **C** and **D**: U266B targets were pre-labelled with either an MHC Class I-blocking antibody or an isotype control for 30 min at 37°C before inclusion in the CTL degranulation assay (n=3). **C**: CTLs generated using reovirus. **D**: CTLs generated using CVA21. Statistical significance was calculated using one-way ANOVA with Tukey's post-hoc test, * = $p<0.05$, n.s = not significant. Error bars indicate s.e.m.

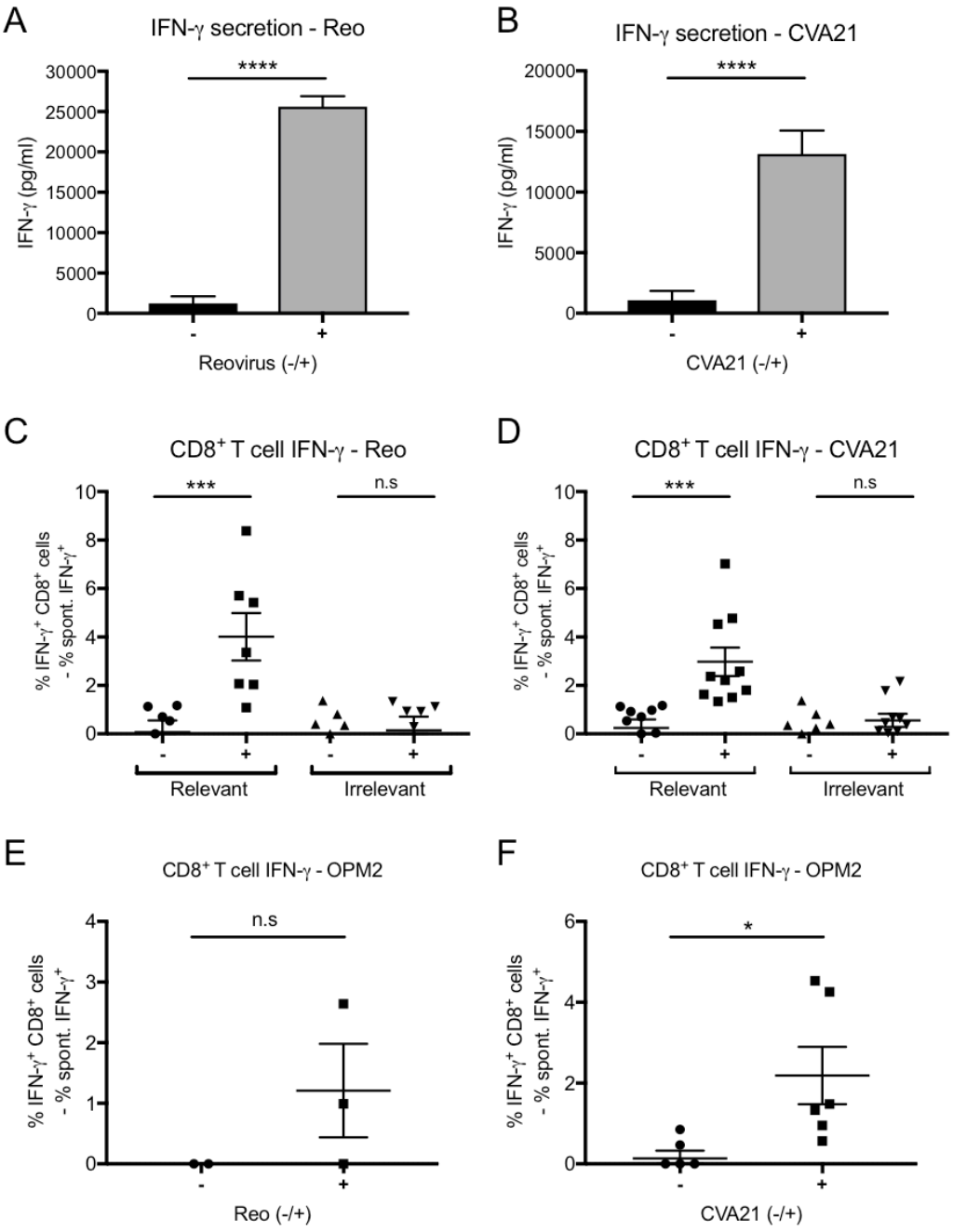

Figure 3-16: Primed CTL secrete IFN-γ in response to relevant, but not irrelevant, target cells.

A and **B**: IFN-γ secretion into culture medium was measured at the end of the priming protocol using an ELISA with matched paired antibodies (n=6). **C**-**E**: Intracellular IFN-γ in CTLs generated using reovirus- or CVA21-treated U266B cells was measured by flow cytometry after permeabilization of cells with saponin and staining with an anti-IFN-γ antibody. **C** and **D**: PBMCs primed in the presence of reovirus (**C**, n=7) or CVA21 (**D**, n=10) were co-cultured with relevant (U266B) or irrelevant (KG-1) target cells at a 2:1 effector:target ratio for 1 h, followed by another 4 hrs incubation in the presence of Brefeldin A. **E**: PBMCs primed in the presence (+) or absence (-) of reovirus (n=3) were co-cultured with OPM2 target cells as described for C and D. **F:** PBMCs primed in the presence (+) or absence (-) of CVA21 (n=6) were co-cultured with OPM2 target cells as described for C and D. Statistical significance was calculated using paired, two-tailed *t*-tests, * = $p<0.05$, *** = $p<0.001$, **** = $p<0.0001$, n.s = not significant. Error bars indicate s.e.m

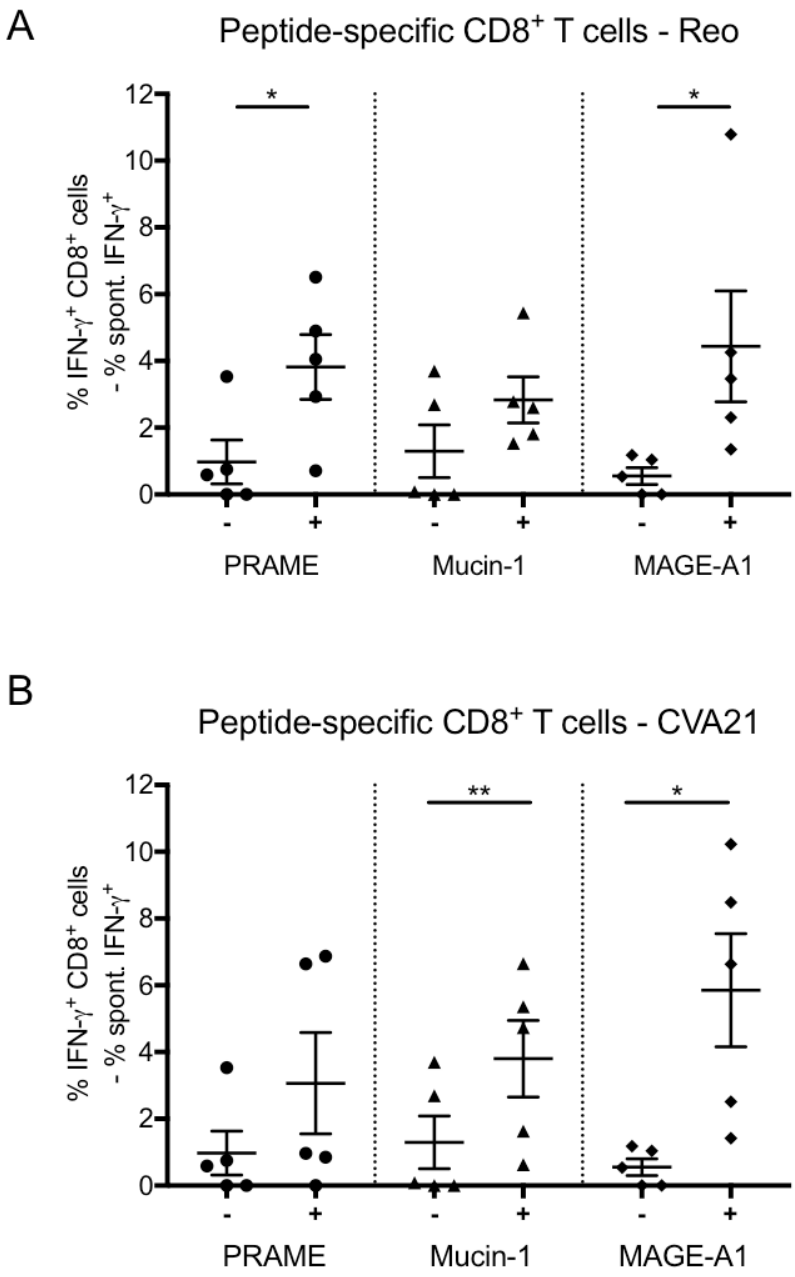

Figure 3-17: Primed CTL secrete IFN-γ in response to MM-associated antigen peptide pools.

Autologous $CD14^+$ cells were loaded with PRAME, Mucin-1, and MAGE-A1 peptide pools, respectively (1 hr at 37°C), and co-cultured with PBMC primed in the presence of either reovirus (**A**) or CVA21 (**B**). Cells were co-cultured at a 2:1 effector:target ratio for 1 h, followed by another 4 hrs incubation in the presence of Brefeldin A. Intracellular IFN-γ was measured by flow cytometry after fixation of cells in 1% PFA, permeabilization with saponin, and staining with an anti-IFN-γ antibody (n=5). Statistical significance was calculated using paired, two-tailed *t*-tests, * = $p<0.05$, *** = $p<0.001$, **** = $p<0.0001$, n.s = not significant. Error bars indicate s.e.m.

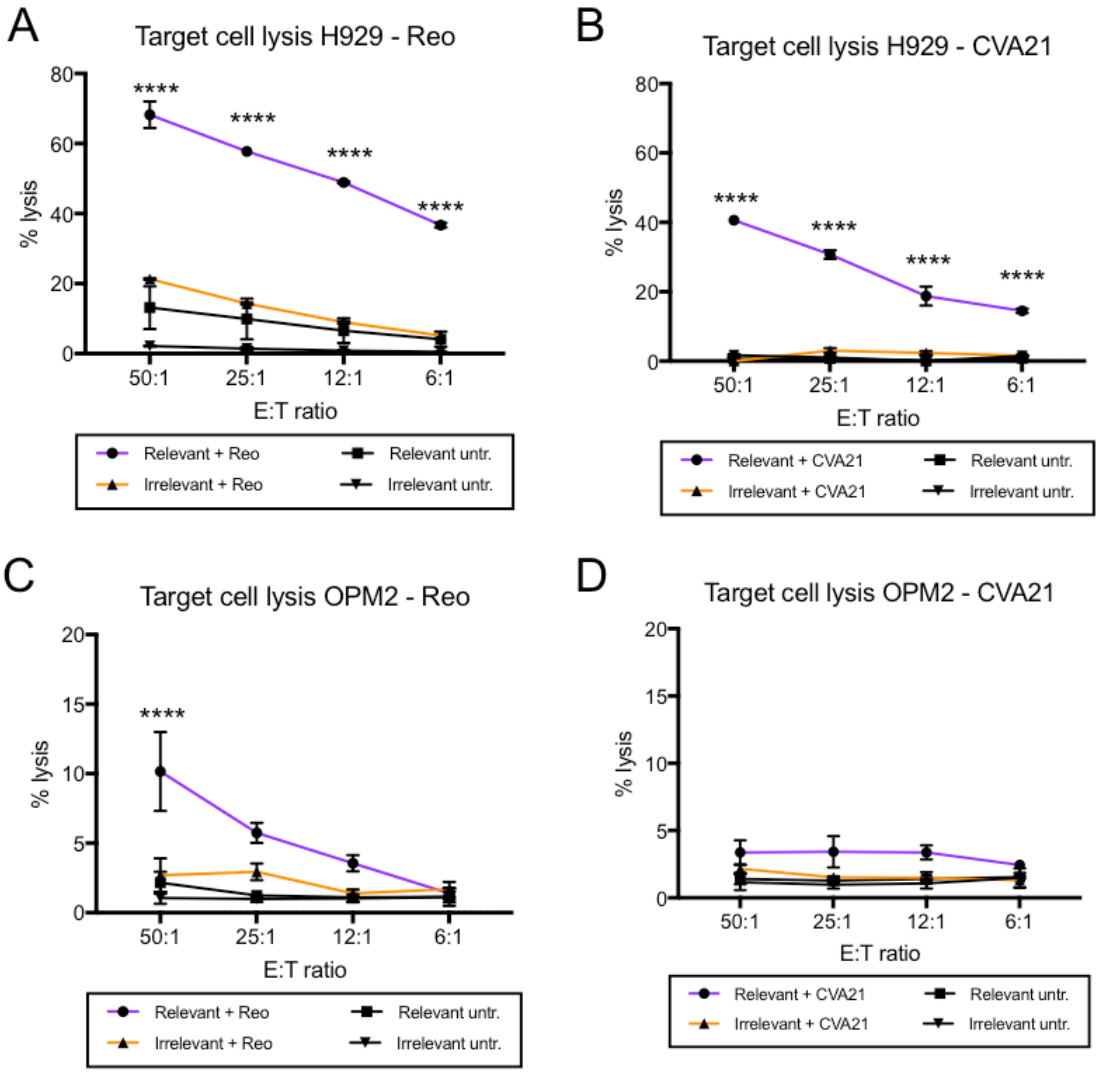

Figure 3-18: Priming of CTLs using virus-susceptible H929 cells and virus-resistant OPM2 cells.

CTL priming was performed as previously described using H929 cells pre-treated with either reovirus (**A**) or CVA21 (**B**) as target cells. The ability of primed cells to lyse relevant (H929) and irrelevant (KG-1) target cells was evaluated using a chromium release assay at various effector:target (E:T) ratios (n=3). **C** and **D**: CTL priming using virus resistant OPM2 target cells treated with reovirus (**C**) or CVA21 (**D**), respectively (n=3). Statistical significance in was calculated using two-way ANOVA with Tukey's post-hoc test and refers to comparison between Relevant + virus and Irrelevant + virus, **** = p<0.0001. Error bars indicate s.e.m.

3.3 Summary & Discussion

This chapter has compared and evaluated reovirus and CVA21 as oncolytic agents in MM. While the main focus was on the induction of anti-tumour immunity, a screen for the susceptibility of MM cell lines to the direct oncolytic effect of each virus was introduced in Figure 3-2. This confirmed, in agreement with previous studies (202, 318, 320, 323), that MM cell lines H929 and U266B are susceptible to the direct oncolytic effect of both reovirus and CVA21. While these cell lines have been commonly used in previous studies, it is the first time that susceptibility to reovirus and CVA21 has been shown in JIM3 cells. A range of other MM cell lines have also been shown to be susceptible to reovirus (RPMI-8226, MM1S, LP-1, KMS-18-BM, SKMM-2, and L363) (225, 318, 319, 323, 348) and CVA21 (RPMI-8226, Kas6/1) (202, 349). However, in accordance with the findings published by Kelly *et al.*, the results presented in this chapter also demonstrated that MM cell line OPM2 was completely resistant to reovirus-mediated oncolysis (225), and additionally, to CVA21-mediated oncolysis. Kelly *et al.* suggested that reovirus resistance was likely due to low expression of the viral entry receptor, JAM-A, on the surface of OPM2 cells, which was also confirmed in this chapter (Figure 3-2A). Interestingly, Kelly *et al.* also reported that overexpression of JAM-A could sensitise OPM2 cells to reovirus oncolysis (225).

While many MM cell lines are susceptible to reovirus and CVA21 in isolation, the data presented in Figure 3-3 demonstrated that the susceptibility of cells that are normally permissive to infection can be reduced in the context of the BM microenvironment. Co-culture of MM cell lines with BM stromal cells HS-27 for 24 hrs before viral treatment significantly reduced the susceptibility of both H929, U266B, and JIM3 cells to reovirus, and also protected JIM3 cells against CVA21-mediated oncolysis. While it is the first time that the BM microenvironment has been shown to induce protection against OVs in MM, it is commonly known that the protective BM niche induces resistance to several common chemotherapeutic agents in MM, including bortezomib, melphalan, and dexamethasone (350-352). BM-induced resistance can be mediated both by the secretion of soluble mediators and by cell-cell contacts (353). As shown in Table 2-1, HS-5 cells are fibroblastoid, while HS-27 are epithelial-like cells, both derived from normal BM stroma (354). In this study, HS-27 cells induced the largest overall protection against OV in MM cells. HS-5 cells have been shown to be more secretory, with abundant secretion of several haematopoietic growth factors and IL-6 (354). This could lead to

enhanced proliferation of MM cells, resulting in less protection against virus-mediated death. Furthermore, interaction of MM cells with stroma has been shown to modify the expression of pro- and anti-apoptotic proteins, ultimately making MM cells more resistant to apoptosis induced by chemotherapeutics (355-357). The co-culture model used in this study is a simple 2D model and not entirely representative of the complexity of the BM microenvironment (Figure 2-1), and it can only be assumed to underestimate the actual protective effect against direct oncolysis (358). While BM-induced drug resistance remains a concern for successful treatment, the data presented in this chapter show that induction of anti-tumour immunity by OVs may have an important role in eradicating MM cells resistant to oncolysis due to low expression of entry receptors, or resistance mechanisms induced in MM cells residing in close proximity to BM stromal cell compartments. Many more advanced *in vitro* 3D models of the BM microenvironment exist, taking into account the various subniches, hypoxic gradients, and local milieu established by a multitude of cell types, but developing such models was beyond the scope of this study. Another concern for efficient therapy in MM is therapeutic access to the BM. In a Phase I clinical trial, it was confirmed that reovirus can access the BM following i.v. administration also in the presence of nAb (195). In addition, several studies have documented the ability of reovirus to interact with PBMC, facilitating the trafficking of replication-competent reovirus to tumours and metastatic sites (186, 250, 251). Such cellular hijacking could be a way for OVs to target MM cells within the BM niche, a prospect which warrants further investigation. Early *in vitro* studies have also confirmed successful cell carriage of CVA21, resulting in protection from antiviral nAb and OV delivery to target cells (253).

This study is the first to examine the onset of anti-tumour immunity in response to both reovirus and CVA21 in MM, and has confirmed that an anti-myeloma response can be induced by both viruses. The anti-myeloma response consisted of both innate and adaptive immune mechanisms including 1) cytokine-mediated bystander killing, 2) NK cell-mediated cellular cytotoxicity, and 3) priming of MM-specific CTLs.

Both reovirus and CVA21 were able to induce the secretion of cytokines from PBMC, which in turn induced a bystander killing effect on MM cells (Figure 3-4 and Figure 3-6). It was particularly encouraging that culture of OPM2 cells in either reovirus-CM or CVA21-CM could kill a significant

proportion of these oncolysis-resistant cells (Figure 3-6A). Similarly, reovirus-CM was able to overcome the protective effect induced following co-culture of H929 cells with HS-27 stromal cells (Figure 3-7A). A number of cytokines have been suggested as part of immunotherapy alone, or to enhance the efficacy of chemotherapeutics in MM, including IFN-α, IL-2, IL-12, GM-CSF, and TRAIL (111, 333, 335-337, 359). The results presented in Figure 3-6 suggest that in a mixed cocktail, these cytokines can have significant anti-tumour effects on their own. As expected, IFN-α was one of the abundantly secreted cytokines in response to both reovirus and CVA21 (Figure 3-4 A and B). Secretion of IFN-α from PBMC in response to reovirus, but not CVA21, has been previously documented in chronic lymphocytic leukaemia (CLL) (138). The role of IFN-α in OVT is controversial, as it has both been shown to have anti-tumour effects in several haematological malignancies, including MM (111, 113, 360, 361), however, it is also one of the main antiviral cytokines as discussed in Section 1.4.2.1.2.1. Interestingly, OVs have been engineered to function as delivery vectors for local delivery of cytokines, including IFN-β, to facilitate the generation of an anti-tumour immune response within the TME (197, 362-364). Under the assumption that malignantly transformed cells frequently possess a dysfunctional IFN signalling response (155, 365), secretion of IFN within the TME improves the specificity of OVT, as viral replication occurs in malignant, but not normal, cells regardless of the presence of IFN (362). Thus, overall the anti-tumour effects of IFN-α are believed to outweigh its antiviral effects, in particular as anti-tumour immunity is now considered pivotal for the long-term success of OVT.

The interplay between cytokines, viruses, tumour cells, and immune cells is complex. Several cytokines identified in the Luminex screen of CVA21 (Figure 3-4E) have been shown to have pro-tumour effects, with IL-6 being particularly important in the MM setting with its proliferative and anti-apoptotic effect. However, IL-6 in the TME has also been shown to sensitise tumour cells to certain OVs (366). Similarly, a synergistic anti-tumour effect was suggested following co-culture of JIM3 cells with HS-5 stromal cells in reovirus-CM (Figure 3-7C), indicating that cytokine release from the BM niche might, under certain circumstances, synergise with cytokines secreted from immune cells as a response to OV. Additionally, while the majority of cytokines secreted in response to viral infection have downstream activating effects on the immune system, others, such as IL-10, can also have an immunosuppressive effect (367, 368). Thus, while the toxic effect of the cytokine milieu induced in response to OVT is positive, off-target and

downstream effects will require careful future analysis to ensure the anti-tumour effects of OV-induced cytokines outweigh any pro-tumour effects.

Another important aspect of innate anti-tumour immunity is the enhanced cytotoxic function of NK cells. Figure 3-8 demonstrated that both reovirus and CVA21 treatment leads to the activation of NK cells, both *in vitro*, and following i.v. infusion as part of the MUK11 and STORM trials, respectively. In Figure 3-9, it was confirmed that activation of NK cells resulted in enhanced degranulation and killing of MM target cells, including the oncolysis-resistant OPM2 cells. Susceptibility of OPM2 cells to NK cell-mediated killing has previously been reported by Garg *et al*. and van Rhee *et al*. (369, 370). Importantly, there was no significant reduction in the ability of virus-activated NK cells to kill MM cells that had been pre-cultured on BM stromal cells HS-27 (Figure 3-10), compared to MM target cells alone. Reovirus-induced potentiation of NK cell-mediated cytotoxicity has previously been demonstrated in several disease settings, including AML and chronic lymphocytic leukaemia (CLL) (138, 206, 234, 371), while this is the first study to report the effect of CVA21 on NK cells. As discussed in Section 1.4.4.1, other OVs, including MV and myxoma virus, have been evaluated as therapies for MM, however; no studies have documented induction of NK cell cytotoxicity in MM in response to other OVs. Interestingly, when comparing reovirus and CVA21, reovirus seemed to have a more stimulating effect on NK cells overall with the highest stimulation of NK cell activation and degranulation (Figure 3-8 and Figure 3-9), but CVA21 induced the largest enhancement in NK cell-mediated killing (Figure 3-9). This dichotomy is interesting and warrants further exploration. Possible mechanisms could be induction of a more cytotoxic subpopulation of NK cells in response to the CVA21-induced cytokine secretion or an enhanced killing via degranulation-independent mechanisms such as Fas- or TRAIL-mediated killing induced by CVA21.

The prospect of enhancing anti-tumour immunity induced by OVs using various combination treatments is an interesting avenue to develop to 1) enhance their anti-myeloma activity, and 2) better tailor therapies to the individual patient. One option for such combination therapies is monoclonal antibodies. Reovirus has previously been shown to enhance rituximab-induced NK cell-mediated ADCC of malignant B cells in CLL (138). Two monoclonal antibodies targeting plasma cells have recently been approved for the treatment of MM, anti-CD38 daratumumab and anti-SLAMF7/CD319 elotuzumab (372). Encouragingly, elotuzumab can enhance ADCC of

oncolysis-resistant OPM2 cells (369), but neither antibody has been tested in combination with OVs to date. Another interesting option for combination with OVs is the histone deacetylase inhibitor, valproate (VPA), which has previously been implicated as a treatment for MM (373-375). VPA can increase the expression of activating NK ligands on MM cells, making them more attractive targets for NK cells (376) and thus, could be an interesting combination with OVT which, as demonstrated here, boosts the cytotoxic effect of NK cells.

Adaptive anti-tumour immunity was introduced in Section 3.2.2.3 with the successful priming of MM-specific CTLs using both reovirus- and CVA21-loaded MM target cells. Figure 3-13 demonstrated that cells primed in the presence of either reovirus or CVA21 were highly cytotoxic towards relevant, but not irrelevant, target cells. Importantly, primed CTLs were equally effective at killing MM targets cells when they had been pre-cultured on BM stromal cells HS-27, and CTLs primed against oncolysis-susceptible target cells U266B were able to recognise and kill oncolysis-resistant OPM2 cells (Figure 3-14). The data presented in subsequent figures characterised the primed cells and confirmed their specificity towards MM target cells and well-known TAA peptides. CTLs primed in the presence of reovirus degranulated specifically towards relevant, but not irrelevant targets, and CTL degranulation was shown to be dependent on CD8:MHC-I interaction (Figure 3-15). Furthermore, CTLs primed using either virus secreted IFN-γ specifically upon recognition of relevant, but not irrelevant target cells (Figure 3-16). Importantly, CTLs were able to recognise peptides from common TAAs in MM (PRAME, Mucin-1, and MAGE-A1) when presented on autologous APCs (Figure 3-17). As opposed to CTLs primed using reovirus, antigen-specificity of CTLs primed using CVA21 did not seem correlate with an enhanced degranulation against relevant target cells (Figure 3-15). However, while the percentage of degranulation was low, the overall trend was similar to CTLs primed using reovirus, with specific degranulation against relevant, but not irrelevant, target cells. It is possible that, with an increased number of donors tested, variability will be reduced to generate a statistically significant result, and that even low levels of degranulation are sufficient for successful target cell killing. Interestingly, sporadic studies have indicated the possibility for antigen-specific CTL-mediated killing through the Fas/FasL pathway, independent of CTL degranulation, which again could

indicate a role for Fas/FasL in CVA21-mediated anti-tumour immunity (377, 378).

In the experiments presented here, reovirus generated the more potent response overall compared to CVA21. However, in the EGTA experiment (Figure 3-13), levels of target cell death were similar, independent of which virus was used for priming, indicating that these experiments are susceptible to donor variation. It is possible that with continued experimental repetition, differences in performance between the viruses would be less pronounced. It is also interesting to consider if a given virus performs better in a subset of donors depending on the individual immunological landscape. It is also important to note that CVA21 was able to prime efficient CTLs despite limited DC maturation (Figure 3-12B). Additionally, while it was possible to successfully prime CTLs using two reovirus- and CVA21-susceptible cell lines (U266B and H929), this proved more challenging using oncolysis-resistant OPM2 cells. A minor increase in killing of relevant, but not irrelevant, target cells was observed at high E:T ratios following priming in the presence of reovirus, but no priming was evident using CVA21 (Figure 3-18), posing the question whether successful oncolysis is required to kick start an anti-tumour immune response. These observations will be investigated in more detail in the next chapters. Similar to NK cell-mediated anti-tumour immunity, the priming of myeloma-specific CTLs has not been investigated using other OVs. Reovirus has previously been shown to enhance the priming of tumour-specific CTLs in other malignancies, including ovarian cancer and several studies of melanoma (246, 250, 379, 380), but no such data exists for CVA21 to date. Several studies have documented the successful priming of CTLs specific for Mucin-1 and MAGE-A1 *in vitro*, as well as demonstrated the presence of CTLs specific for these antigens at high frequencies in MM patients (28, 381-384).

Interestingly, CTLs primed against U266B cells using CVA21 were able to kill not only U266B cells, while ignoring irrelevant myeloid target cells, but also OPM2 cells (Figure 3-14C). The onset of IFN-γ production in CTLs challenged with OPM2 cells (Figure 3-16F) suggested that killing occurred in an antigen-specific manner and was not due to non-specific innate killing by residual PBMCs in priming cultures. These results suggest that, while CTLs could not be primed directly against virus-resistant cells, shared antigens between susceptible and resistant cells could result in the eradication of virus-resistant cells by primed CTLs. Priming of such pan-myeloma CTLs have previously also been documented by Lu *et al* (385), and both U266B

cells and OPM2 have been shown to express MGUS-related antigen OFD1 (386).

Albeit anecdotal, important signs of immune cell activation was shown *in vivo* following i.v. infusion of either virus as part of the MUK11 (reovirus) and STORM (CVA21) clinical trials throughout this chapter. Only samples from one patient were analysed on the MUK11 MM trial as part of this study, but these showed a convincing peak in activation of both NK cells, $CD4^+$, and $CD8^+$ T cells 72 hrs after reovirus infusion (Figure 3-8 and Figure 3-11). Importantly, this was in a patient with myeloma refractory to standard immunomodulatory treatment (lenalidomide/pomalidomide). While patients included in this trial are refractory to the anti-tumour effect of IMiDs, preliminary studies have indicated that combination of reovirus with lenalidomide might potentiate the anti-tumour immune response, providing another interesting avenue for combination treatments in MM (387). The lymphocyte activation observed in the present study is also in accordance with previously published literature demonstrating that reovirus can activate immune effector cells following i.v. administration (186, 261, 388). The previously completed Phase I clinical trial evaluating reovirus in MM did not examine immune cell responses in treated patients (195). None of the patients analysed as part of the STORM clinical trial had MM, but they all had late stage solid malignancies known to induce an immunocompromised physiological state, like MM (327-330). Thus, it is an encouraging first step towards clinical applicability that both NK cells, $CD4^+$, and $CD8^+$ T cells in the peripheral circulation were activated in response to i.v. administration of CVA21 (Figure 3-8 and Figure 3-11). I.v. administration is the preferred route of delivery in MM where direct access to tumours residing in the BM is challenging. The ability of reovirus to induce a local immune response in the BM following i.v. administration *in vivo* is examined in Chapter 4. Interestingly, two patients on the STORM CVA21 trial received checkpoint inhibitor treatment prior to taking part in the STORM trial. Patient STORM-6 received pembrolizumab and patient STORM-2 received ipilimumab. Both patients showed good responses to CVA21 treatment, with patient STORM-6, who also received the higher dose of CVA21, displaying the most potent response. Checkpoint blockade (anti-PD1) initially seemed to have little effect in MM, but has more recently shown promise when combined with IMiDs (389, 390). In a Phase II clinical trial, an objective response rate of 60% was documented, with 8% of participants achieving a complete

response (390). Unfortunately, several clinical trials have been suspended due to safety concerns with the checkpoint inhibitor. As demonstrated in this chapter, OVs can, like both IMiDs and checkpoint inhibitors, have an immunomodulatory effect in MM. CVA21 is already being successfully trialled in combination with pembrolizumab for melanoma (391), while reovirus has been shown to upregulate the expression of PD-L1 on tumour cells in both MM and other malignancies, with subsequent potentiation of both anti-PD1 and anti-PD-L1 treatments (261, 392, 393). Hence, both reovirus and CVA21 in combination with anti-PD1, or anti-PD-L1 antibodies might be interesting options for synergistic combination therapies with favourable safety profiles in MM.

Based on the results demonstrated throughout this chapter, comparing reovirus and CVA21 in the MM setting, CVA21 appears to have a more pronounced oncolytic effect than reovirus, while both viruses show some immunogenic character. CVA21 was able to induce a higher level of NK cell-mediated killing despite low NK cell degranulation while reovirus induced the more potent adaptive response overall. While tumour cell killing by primed CTL was comparable using both viruses, it is interesting to note that CTLs primed in the presence of CVA21, similar to NK cells, also showed very low levels of CTL degranulation. Previous immunological studies in other malignancies have shown onset of anti-tumour immunity using reovirus alone (237, 394), while most studies on CVA21 have chosen to enhance anti-tumour immunity using combination treatments (301, 395). Reovirus has also made significant progress in several clinical trials, including early trials for MM. However, as discussed, its ability to induce anti-tumour immunity in this setting has not been thoroughly documented. CVA21 has mainly made progress in clinical trials for melanoma in combination with immune checkpoint inhibitors, and has not been taken forward in the MM setting. Taken together, the results presented in this chapter indicate that CVA21 could also be a useful agent in MM and future pre-clinical studies, as well as clinical trials, will be required to determine its fate in this context. As discussed previously (Section 1.4.5.3), reovirus is recognised by immune cells through both RIG-I and MDA5 pathways, and subsequent NK cell activation is thought to be dependent on IFN-α secretion from $CD14^+$ monocytes (138, 394, 396), while very little is known about the immunobiology of CVA21. The experiments performed in Chapter 5 will examine the immune recognition and response to CVA21 in more detail. In

addition, the work presented in Chapter 4 has examined the use of reovirus in an *in vivo* model of MM to further characterise the anti-tumour immune response induced by this virus.

Chapter 4
Effects of reovirus in an *in vivo* model of multiple myeloma

Chapter 4
Effects of reovirus in an *in vivo* model of multiple myeloma

4.1 Introduction

The experiments outlined in Chapter 3 provided evidence that both reovirus and CVA21 can induce an anti-tumour immune response against MM *in vitro*. It was previously hypothesised that CVA21 is dependent on human ICAM-1 for entering host cells and accordingly, does not naturally infect murine cells (397). This has necessitated the use of xenograft models to study CVA21 and so far, no suitable immunocompetent model has been described. In line with this, the work performed in this chapter aimed to establish whether an anti-tumour immune response could be induced following reovirus treatment of an immunocompetent *in vivo* model of MM.

The majority of *in vivo* studies previously published utilising reovirus and MM have been performed using immunocompromised models with humanised xenografts (318-320, 323). A range of different immunocompetent models exist as well, including both transgenic and syngeneic models, which all represent different features and stages of MM, and resemble human MM to varying extents (398). The most common syngeneic *in vivo* model of MM is the 5T series, comprising a series of cell line subclones established from 5T cells first isolated from the BM of aging C57Bl/KaLwRij mice (398). Around 0.5% of C57Bl/KaLwRij mice spontaneously develop a myeloma-like disease with age (399). The 5T series includes 5T2, 5T7, 5T8, 5T13, 5T14, 5T21, 5T33, and 5T41 cell lines which all have different growth characteristics. In addition, stroma-independent subclones, such as 5TGM1 (derived from 5T33), have been established, which enable *in vitro* passage of cells after isolation from the bone marrow following *in vivo* passages (398, 400).

Along with a fully competent immune system, similar to that of WT C57Bl/6 mice, the 5TGM1 model produces a disease which mimics many features of human MM, such as secretion of paraprotein, hypercalcaemia, and generation of lytic bone disease with decreased bone mineral density (401, 402). Moreover, the disease is largely confined to the BM and the spleen, which has haematopoietic capacity in mice. Taking all these features

together, the 5TGM1 model allows considerable flexibility and is well suited to answer the questions posed in this chapter.

While the model has been used for many studies of MM before, including for the development of IFN-β-expressing oncolytic VSV, it has only been reported on twice before in the context of reovirus treatment (197, 403). Kelly *et al.* first demonstrated efficacy of reovirus in combination with bortezomib in the 5TGM1 model (318). More recently, this was expanded to an immunological study demonstrating that reovirus treatment increased the expression of PD-L1 on MM cells, with subsequent potentiation of therapeutic efficacy when used in combination with an anti-PD-L1 antibody (392). However, to date, the cellular mechanisms responsible for tumour eradication in response to reovirus treatment alone, or in combination therapy strategies, have not been reported. Thus, the work described in this chapter aimed to characterise the immune response to reovirus treatment in the 5TGM1 model, and establish the contribution of anti-tumour immunity to reovirus treatment efficacy.

4.2 Results

4.2.1 *Ex vivo* reovirus and CVA21 susceptibility of 5TGM1 cells

Before inclusion in *in vivo* experimentation, the susceptibility of 5TGM1 to reovirus and CVA21 *in vitro* was established (Figure 4-1). 5TGM1 cells were treated with either reovirus or CVA21 for 48 (Figure 4-1A) or 72 hrs (Figure 4-1B) and cell death was analysed by flow cytometry. After 48 hrs of reovirus treatment, a dose-dependent response was seen with a maximum of 86.6% cell death at the 10 pfu/cell dose. Following 72 hrs of treatment, over 95% of 5TGM1 cells were eradicated, even at the lowest dose of 0.01 pfu/cell (Figure 4-1B). As expected, this experiment further confirmed the CVA21 dependency on human ICAM-1 for host cell infection as no changes in 5TGM1 cell viability were observed following treatment for 48 or 72 hrs. As direct oncolysis might not be strictly necessary to study anti-tumour immunity, the potential for using CVA21 in the 5TGM1 model was further explored. It was hypothesised that CVA21 might still be able to elicit an immune response in a murine model through engagement with PRRs. To test this, splenocytes from WT C57Bl/6 mice were isolated and treated with CVA21 *ex vivo*. Splenocyte activation in response to CVA21 was measured by flow cytometry and confirmed that, in addition to the lack of direct oncolysis, CVA21 also had no activating effect on murine splenic immune cells (data not shown). As a result, reovirus was chosen as the preferred agent to use in the subsequent *in vivo* experiments.

4.2.2 Optimisation of an *in vivo* reovirus treatment protocol

After *in vitro* propagation, 5TGM1 cells were passaged *in vivo* to obtain bone-homing 5TGM1 cells. Following re-injection i.v., bone-homing 5TGM1 cells generated bone disease within a more reliable timeframe (described in Section 2.17.1). As expected (404), 5TGM1 cells disseminated to the skeleton following i.v. injection and untreated mice developed HLP within 21-25 days. Next, an optimised protocol for reovirus treatment was developed.

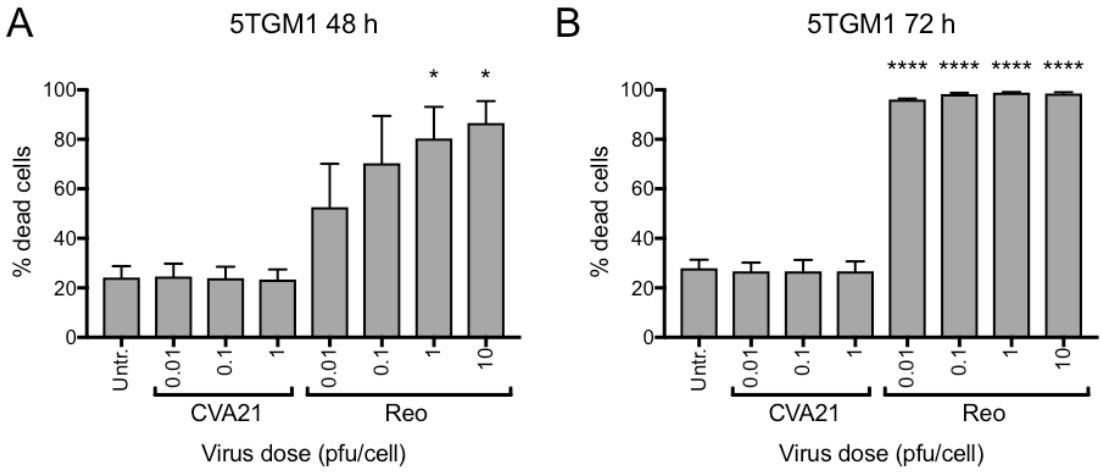

Figure 4-1: *Ex vivo* susceptibility of 5TGM1 to reovirus and CVA21.

Murine MM cells 5TGM1 were either left untreated (Untr.) or treated with reovirus (0.01, 0.1, 1, or 10 pfu/cell) or CVA21 (0.01, 0.1. or 1 pfu/cell) for 48 (**A**) or 72 (**B**) hrs (n=3). Cell viability was measured by flow cytometry at each time point using a Live/Dead® discrimination stain. Statistical significance was calculated using one-way ANOVA with Dunnett's post-hoc test, * = $p<0.05$, **** = $p<0.0001$. Error bars indicate s.e.m.

4.2.2.1 Reovirus treatment with intraperitoneal administration

As described in Section 2.17.3, all *in vivo* experiments started with the injection of $2x10^6$ 5TGM1 cells in the tail vein of C57Bl/KaLwRij mice. As intraperitoneal (i.p.) delivery is the preferred systemic route of delivery for repeated injections in mice, a treatment schedule with four i.p. injections of $2x10^7$ pfu reovirus/injection before development of HLP was first tested (Figure 1-2A). A total of 16 female mice, aged 6-8 weeks old, were randomised, age-matched, between Naïve (2), PBS (7), and Reo (7) treatment groups and treatment efficacy was evaluated by examining the presence of tumour cells in the BM and spleen. Upon sacrifice, the BM and spleen were harvested and the percentage of $CD138^+$ 5TGM1 cells at each site was evaluated by flow cytometry. Disappointingly, there was no significant reduction in tumour burden in either the BM or the spleen following reovirus treatment. In the BM, the percentage of $CD138^+$ cells was reduced from an average 81.5% to 64.4% (Figure 1-2B), indicating that reovirus treatment did have some effect, however, these data suggested that the treatment schedule required further optimisation. Some variability in the tumour burden in both the BM and spleen of PBS-treated mice was observed, ranging from 3.4% to 82.8% in the BM and from 4.4% to 23.9% in the spleen, suggesting that large group sizes were required to perform well powered experiments.

Next, the potential for the induction of an anti-tumour immune response induced by reovirus in the BM of treated mice was examined. An overview of all phenotypic markers used in the *in vivo* experiments throughout this chapter is provided in Table 4-1. First, the presence of NK cells and $CD4^+$ T cells in the BM, with and without reovirus treatment, was assessed. While not significant, some enlargement of the NK cell and $CD4^+$ T cell populations in the BM was observed in reovirus-treated mice compared to PBS treatment. The percentage of NK cells increased by an average 0.5%, and the percentage of $CD4^+$ T cells increased by 0.4% (Figure 4-2D). Significant variation within the groups made comparison to the naïve control mice difficult. However, a significant negative correlation between the tumour burden in the BM and both the size of the NK cell ($p<0.0001$, Pearson's $r=-0.99$) and $CD4^+$ T cell ($p=0.010$, Pearson's $r=-0.87$) populations was identified, indicating that the BM might be repopulated with immune cells as the tumour burden is reduced.

Next, immune cell activation in response to reovirus treatment was evaluated by measuring the expression of the activation marker CD69 on NK

cells and $CD4^+$ T cells (Figure 4-2E). As described in Chapter 3 and in several previous studies, CD69 is a common marker of both NK and T cell activation (405). However, no significant increase in CD69 expression was detected on either NK or $CD4^+$ T cells in this experiment. To better mimic the human clinical scenario, and provide a more relevant treatment schedule to examine reovirus efficacy, and its *in vivo* mechanism of action, the protocol was next adapted to i.v. delivery.

Table 4-1: Overview of phenotypic markers used in *in vivo* experiments.

ANTIBODY	*TARGET NAME*	*FUNCTION/PURPOSE*
CD138	Syndecan-1	MM cell identification
CD3	T cell co-receptor	T cell identification
DX5 (CD49b)	Integrin-α2	NK cell identification
CD4	T cell co-receptor	$CD4^+$ T cell/helper T cell identification
CD8	T cell co-receptor	$CD8^+$ T cell/cytotoxic T cell identification
CD44	CD44	Effector-memory T cell identification, up-regulated in response to T cell activation
CD62L	L-selectin	Naïve T cell identification, required for T cell homing to secondary lymphoid tissues
CD69	CD69	Early activation of lymphocytes, C-type lectin
4-1BB (CD137)	4-1BB	T and NK cells activation, marker of antigen-recognition in CTLs
PD-1 (CD279)	Programmed cell death protein-1	Immune checkpoint, prevents autoimmunity, marker of T cell activation and exhaustion
CTLA-4 (CD152)	Cytotoxic T Lymphocyte Antigen-4	Immune checkpoint, induced on activated T cells, negative regulator of activation
CD80	B7-1	CD28 and CTLA-4 ligand on APCs, provides co-stimulation for T cells; monocyte and macrophage activation
CD86	B7-2	See CD80 (above)
$I\text{-}A^b$	MHC Class II	Extracellular antigen-presentation molecule on professional APCs

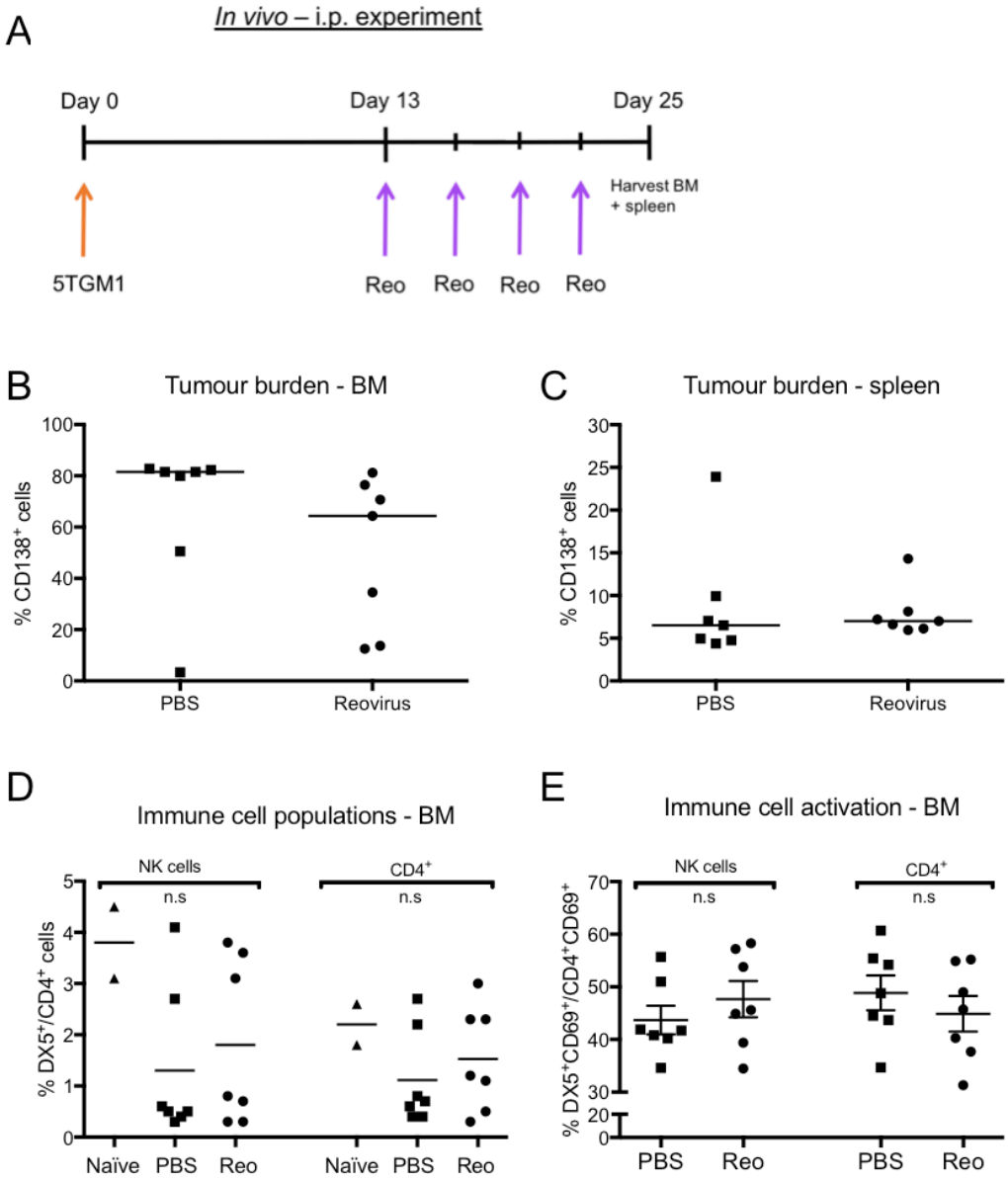

Figure 4-2: Effects of reovirus treatment administered i.p.

A: Schematic demonstrating the *in vivo* treatment schedule. 16 mice were injected with $2x10^6$ 5TGM1 cells i.v. on Day 0 (orange). Reovirus (or PBS vehicle) therapy ($2x10^7$ pfu) was started on Day 13 (purple). Four injections were administered before development of HLP in control mice. Following sacrifice, the BM and spleen were harvested from all mice. **B** and **C**: The tumour burden in the BM (**B**) and spleen (**C**) after PBS or reovirus treatment was measured by flow cytometry and was estimated as the percentage of $CD138^+$ cells. **D**: The percentage of NK cells and $CD4^+$ T cells in the BM following PBS or reovirus treatment, respectively, was measured by flow cytometry. NK cells were identified as $CD3^-DX5^+$, $CD4^+$ T cells were identified as $CD3^+CD4^+$. Naïve mice were non-tumour bearing and untreated. **E**: The activation state of NK cells and $CD4^+$ T cells following PBS or reovirus treatment was estimated by CD69 expression, measured by flow cytometry. The percentage of $CD69^+$ cells is shown. In **B**, **C**, and **E** statistical significance was calculated using two-tailed, unpaired *t*-tests. In **D,** a one-way ANOVA with Tukey's post-hoc test was used. n.s = not significant, error bars indicate s.e.m.

4.2.2.2 *In vivo* eradication of MM tumours following i.v. treatment with reovirus

As i.v. delivery is the preferred route of administration in MM patients, the efficacy of i.v. reovirus was next tested *in vivo*. Early pilot experiments in our lab using this model, and results in the studies by Kelly *et al.* indicated that i.v. administration can provide good efficacy for reovirus treatment (318, 392, 406). In an attempt to enhance efficacy compared to the i.p. experiment (Section 4.2.2.1), reovirus treatment was started earlier in subsequent experiments (Day 7-9 after tumour administration). After establishment of tumours, mice received reovirus or PBS i.v. according to a Mon/Wed/Fri schedule until development of HLP in PBS control groups (Figure 4-3A). The data presented within this section show the combined result of several repeated experiments, as indicated in figure legends and Table 4-2, to enable reproducible changes to be identified. Both female and male mice were included in the experiments. While all mice received the same tumour challenge at the start of each experiment ($2x10^6$ 5TGM1 cells i.v.) and the same reovirus dose ($2x10^7$ pfu/injection), treatment continued until development of HLP in each individual control group, resulting in a different number of injections given in different experiments (Table 4-2). In particular one experimental repeat stood out as mice received up to eight injections (eight injections for males, seven for females) compared to the average five. As the mice in this experiment responded particularly well to reovirus treatment, these mice have been highlighted in purple (both males and females) on the relevant figures. Including these mice in the overall evaluation did not change the decision to accept or reject the *null* hypothesis for any variable. Additionally, the flow cytometry phenotyping protocol was gradually developed with each individual experiment, resulting in variations in the number of mice included between markers. For all experiments, the BM and spleen were harvested after sacrifice, and tumour burden, along with the size of immune cell populations, and their respective activation state, was evaluated at both sites.

Using i.v. injections, reovirus treatment resulted in a significant reduction in tumour burden in both the BM and the spleen, compared to PBS treatment (Figure 4-3 B and C). Tumour burden in the BM decreased from an average 47.9% to 23.9% with reovirus treatment (Figure 4-3B). However, the effect was more pronounced in Expt. 2 (purple symbols), where male mice received eight reovirus injections (seven for females), with an average reduction in $CD138^+$ cells in the BM from 59.5% to 9.9%. The homing of

tumour cells to the spleen was more variable, but overall, reovirus treatment resulted in an average 4.8% decrease in tumour burden in the spleen (Figure 4-3C). While these results were encouraging, it was uncertain whether the reduction in tumour burden was due to direct oncolysis or the activation of an anti-tumour immune response hence, this was next examined in more detail.

The presence of reovirus in the BM at the time of sacrifice was examined by RT-qPCR, using the reovirus σ3 capsid gene as a marker of reovirus particles. BM was harvested on average three days after the last reovirus injection and no reovirus could be detected in the BM at that time point (Figure 4-3D). Interestingly, the absence of reovirus at this time point could indicate that direct oncolysis has subsided and the virus has been cleared by the development of antiviral immune mechanism, however, it could also suggest that reovirus efficacy was mediated through the induction of an anti-tumour immune response.

Table 4-2: Overview of *in vivo* experiments with i.v. administration of reovirus.

In figures throughout sections 4.2.2.2-4.2.2.4 results from several individual *in vivo* experiments detailed below were pooled. All mice received $2x10^7$ pfu/injection reovirus i.v. however, the number of injections varied depending on the time required for development of HLP in control mice. Details of the cohorts for each individual experiment, including the number of injections and age of the mice are shown. The phenotyping done for each experiment is also described.

EXPT. NUMBER	*NO. OF MICE*	*MOUSE AGE (WEEKS)*	*DAYS TO HLP*	*NO. OF INJECTIONS*	*PHENOTYPING DONE*
1	10 (F)	4-6	20	5	CD138, CD69, 4-1BB
2	8 (F) 8 (M) (+4 naïve)	6-8	25 (F) 27 (M)	7 (F) 8 (M)	CD138, CD69, CD25 (not shown), CD44 (not shown), RT-qPCR
3	10 (F) (+3 naïve)	6-8	23	6	CD138, CD69, 4-1BB, PD-1, CTLA-4, naïve/memory T cells
4	10 (F) 6 (M)	6-8	21	5	CD138, CD69, 4-1BB, PD-1, CTLA-4, naïve/memory T cells, myeloid cells CD80, CD86, MHC Class II, RT-qPCR

F: female, M: male, naïve: non-tumour bearing and untreated, HLP: hind limb paralysis.

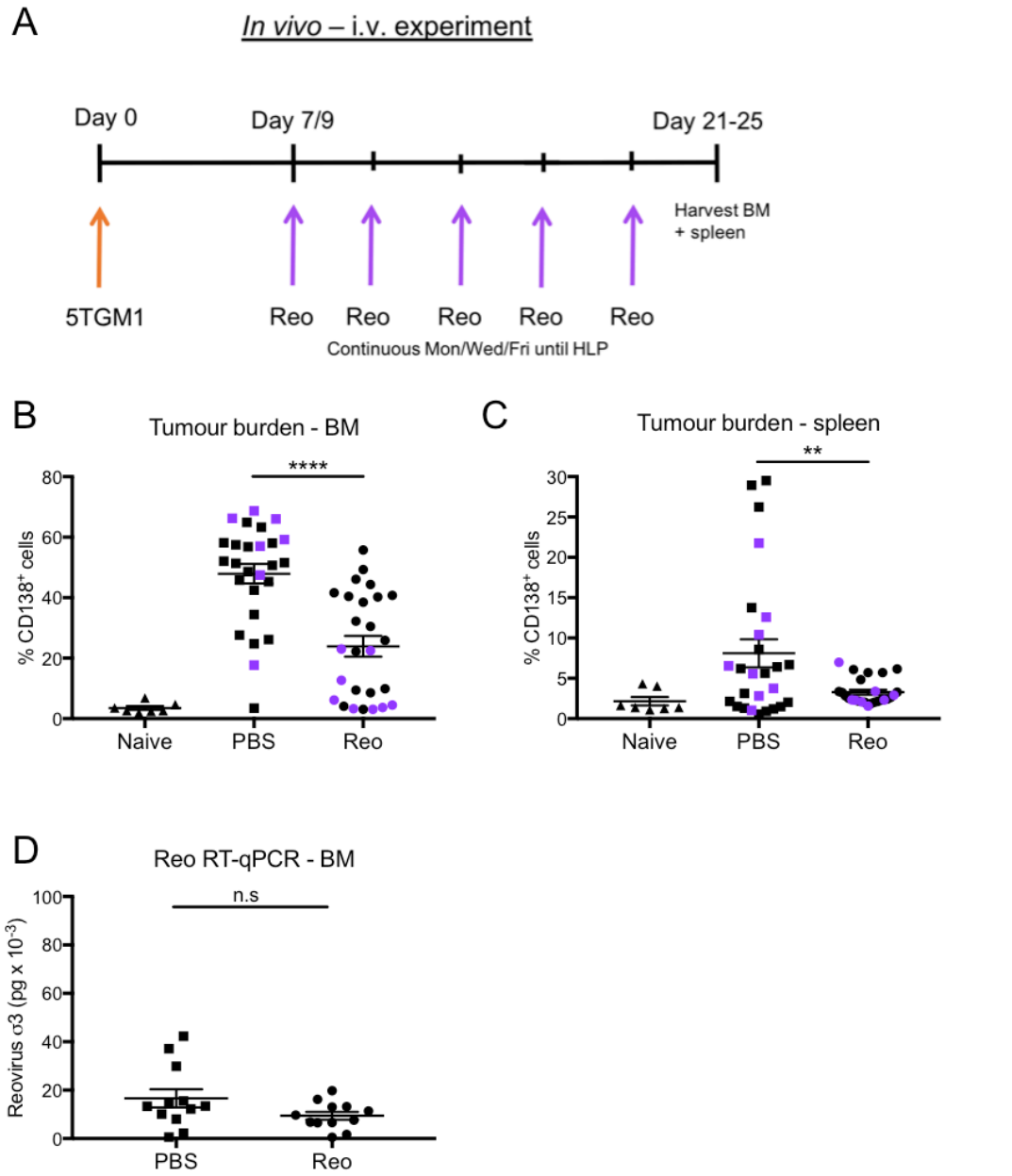

Figure 4-3: Reduction in tumour burden following i.v. treatment with reovirus.

A: Schematic demonstrating the *in vivo* treatment schedule. Mice were injected with $2x10^6$ 5TGM1 cells i.v. on Day 0 (orange). Reovirus (or PBS vehicle) therapy ($2x10^7$ pfu) was started on Day 7-9 (purple) and continued three times weekly until development of HLP in control mice (Day 21-25). Following sacrifice, the BM and spleen were harvested from all mice. **B** and **C**: The tumour burden in the BM (**B**) and spleen (**C**) after PBS or reovirus treatment was measured by flow cytometry and was estimated as the percentage of $CD138^+$ cells (n=26 per group). Naïve mice were non-tumour bearing and untreated (n=7). **D**: The presence of reovirus in the BM on termination of experiments was examined by RT-qPCR using reovirus σ3 primers (n=12 per group). RNA was isolated using the RNEasy Mini Kit. Results were quantified using a standard curve method. Statistical significance was calculated using two-tailed, unpaired *t*-tests, ** = $p<0.01$, **** = $p<0.0001$, n.s = not significant, error bars indicate s.e.m. Purple symbols indicate mice from Expt. 2 (Table 4-2).

4.2.2.3 Normalisation of immune cell populations in the BM and spleen following reovirus treatment i.v.

As i.v. treatment with reovirus generated a significant reduction in tumour burden, the next step was to examine the possible onset of anti-tumour immunity. A multitude of immune mechanisms have the potential to be involved in an anti-tumour immune response generated by reovirus *in vivo*. As the *in vitro* experiments performed in Chapter 3 indicated a role for both NK cells and T cells in anti-myeloma immunity, these cell types were the main focus of the initial phenotyping experiments *in vivo*. First, the proportions of NK cells, $CD4^+$, and $CD8^+$ T cells in the BM and spleen were measured by flow cytometry to evaluate the potential for immune cell recruitment in response to reovirus treatment. In the BM, there was a significant enlargement of the NK cell, $CD4^+$, and $CD8^+$ T cell populations following reovirus treatment (Figure 4-4 A-C) compared to PBS treatment. On average, populations increased by 1.0%, 1.2%, and 1.7%, respectively. In the spleen, only the $CD8^+$ T cell population was significantly enlarged in response to reovirus treatment (1.7%, comparable to the naïve BM), compared to PBS treatment (Figure 4-5C). While there was suggestion of an increase in the populations of both NK cells and $CD4^+$ T cells compared to PBS treatment, neither was statistically significant (Figure 4-5 A and B). For all cell types in both locations, there was no significant difference in the population sizes between naïve mice and mice treated with reovirus, which may suggest a normalisation or reconstitution of the BM compartment, rather than recruitment of effector cells as part of an antiviral or anti-tumour immune response. Thus, the T cells in the BM and spleen were next characterised further to evaluate whether they were naïve T cells (part of a reconstitution) or effector cells (anti-tumour or antiviral T cells).

The T cell populations were examined by evaluating the proportion of naïve ($CD44^-CD62L^+$) T cells to effector memory T cells (T_{EM}, $CD44^+CD62L^-$). While naïve T cells have yet to encounter antigen, T_{EM} have been primed against antigen, typically display rapid effector functions, and carry cytotoxic granules necessary for eradication of cells in an antigen-specific manner (407). Interestingly, while both $CD4^+$ and $CD8^+$ T cell populations in the BM were enlarged in response to reovirus treatment (Figure 4-4), there was no significant change in the proportion of naïve or T_{EM} populations (Figure 4-6 A and B). In the spleen however, a significant increase in the T_{EM} population (both $CD4^+$ and $CD8^+$) was observed in response to reovirus, along with a decrease in the population of naïve T cells (Figure 4-7 A and B). $CD4^+$ T_{EM}

increased from 25.2% to 35.7% and $CD8^+$ T_{EM} from 14.0% to 41.1%. Importantly, the size of the T_{EM} populations increased beyond the level of naïve (non-tumour bearing) mice (28.9% and 20.0% T_{EM}, respectively) in response to reovirus. Furthermore, a significant negative correlation was identified between the size of the $CD8^+$ T_{EM} population in the spleen and the population of $CD138^+$ tumour cells in the BM (p=0.023, Pearson's r=-0.62), suggesting a role of $CD8^+$ T cells for the eradication of MM cells within the BM. Taken together, the results presented in this section demonstrate a normalisation of immune cell populations in the BM and spleen following reovirus treatment. Importantly, evidence of T_{EM} was observed in the spleen, indicating that priming of either anti-tumour or antiviral cytotoxic $CD8^+$ T cells might have occurred.

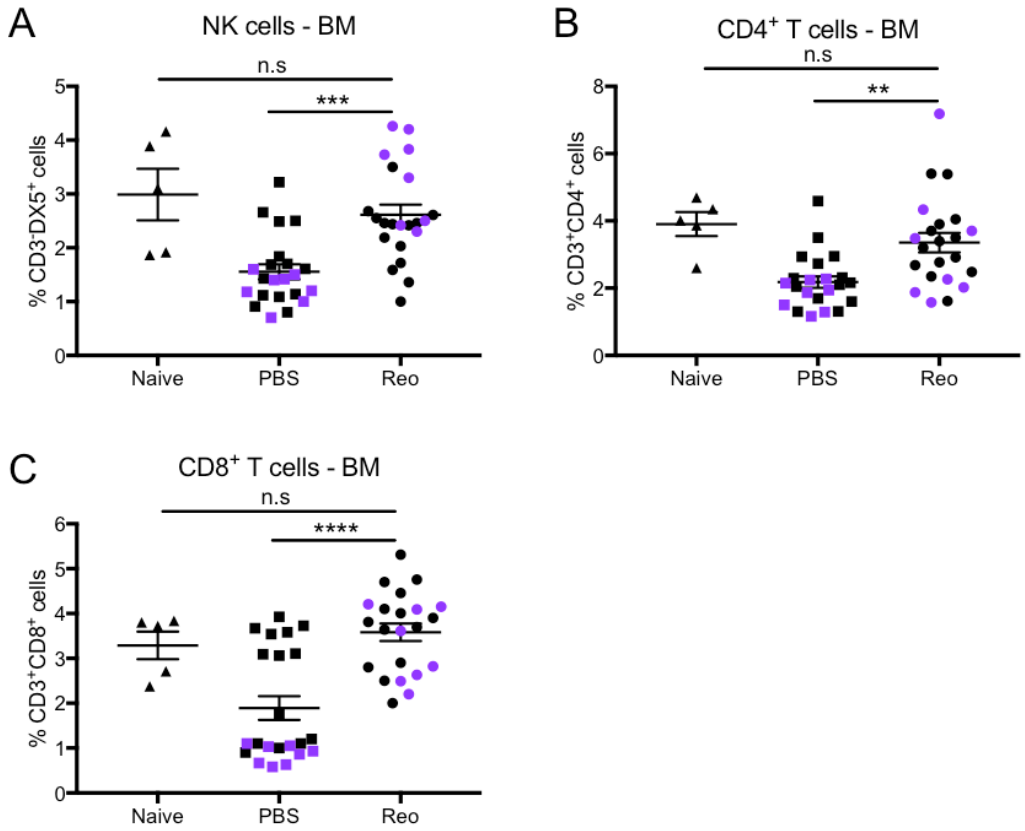

Figure 4-4: Normalisation of immune cell populations in the BM following reovirus treatment i.v.

The percentage of NK cells (**A**), $CD4^+$ T cells (**B**), and $CD8^+$ T cells (**C**) in the BM was measured by flow cytometry following repetitive PBS or reovirus treatment as previously described (n=22 per group). Naïve control mice were non-tumour bearing and untreated (n=5). NK cells were identified as $CD3^-DX5^+$, $CD4^+$ T cells as $CD3^+CD4^+$, and $CD8^+$ T cells as $CD3^+CD8^+$. Purple symbols indicate mice from Expt. 2 (Table 4-2). Statistical significance was calculated using one-way ANOVA with Tukey's post-hoc test, ** = $p<0.01$, *** = $p<0.001$, **** = $p<0.0001$, n.s = not significant, error bars indicate s.e.m.

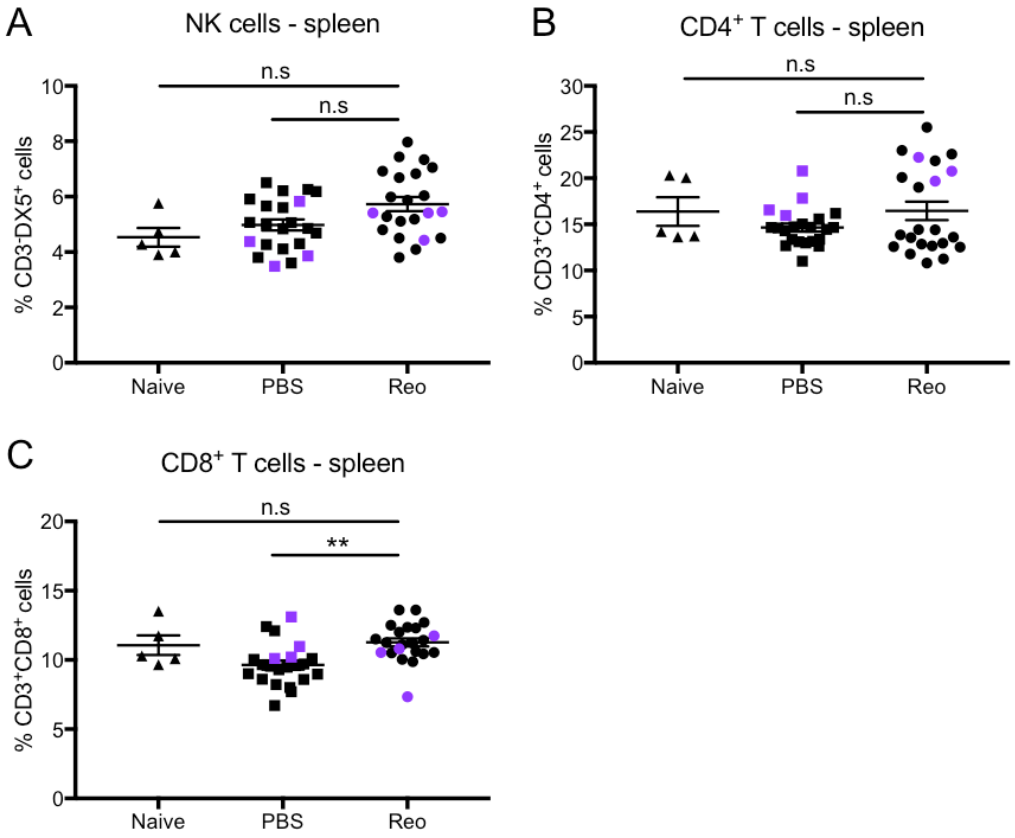

Figure 4-5: Normalisation of immune cell populations in the spleen following reovirus treatment i.v.

The percentage of NK cells (**A**), $CD4^+$ T cells (**B**), and $CD8^+$ T cells (**C**) in the spleen was measured by flow cytometry following repeated PBS or reovirus treatment as previously described (n=22 per group). Naïve control mice were non-tumour bearing and untreated (n=5). NK cells were identified as $CD3^-DX5^+$, $CD4^+$ T cells as $CD3^+CD4^+$, and $CD8^+$ T cells as $CD3^+CD8^+$. Purple symbols indicate mice from Expt. 2 (Table 4-2). Statistical significance was calculated using one-way ANOVA with Tukey's post-hoc test, ** = $p<0.01$, n.s = not significant, error bars indicate s.e.m.

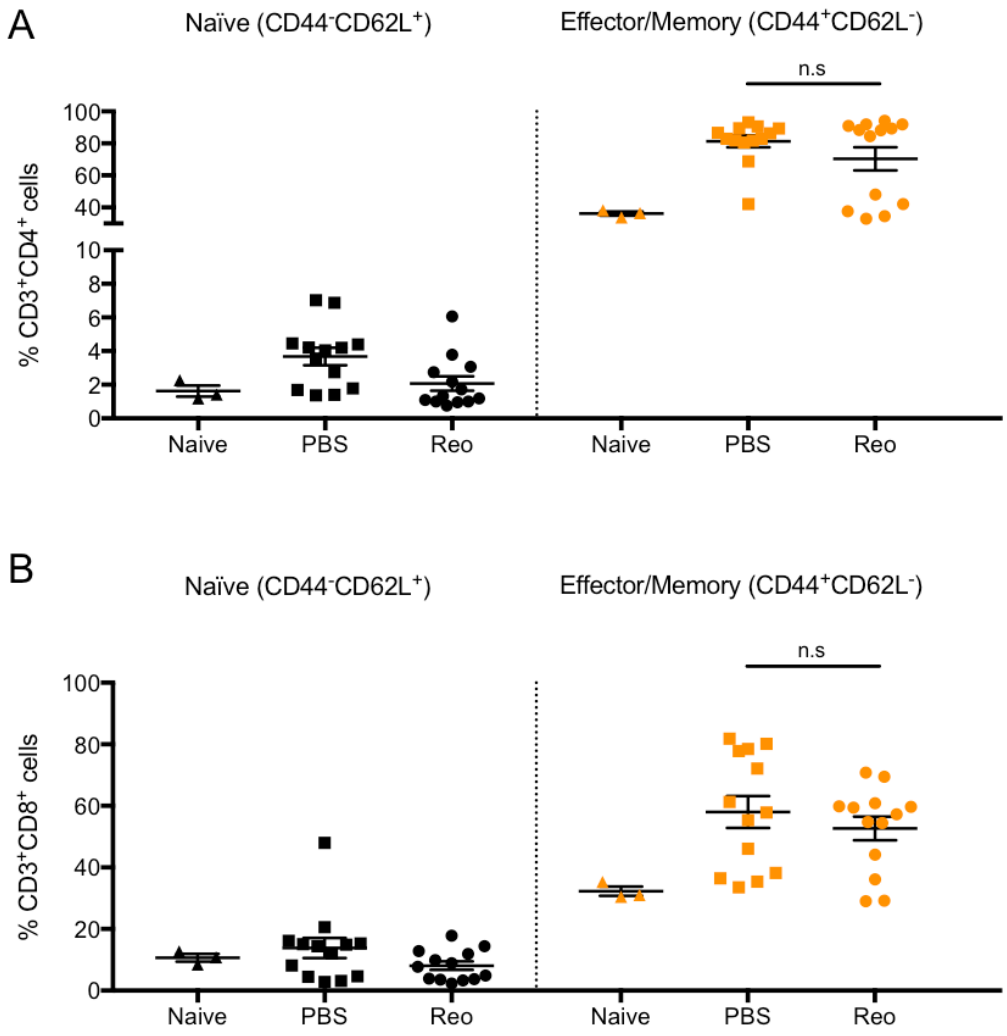

Figure 4-6: Naïve and effector/memory T cell populations in the BM following reovirus treatment i.v.

Following repeated reovirus or PBS treatment, the BM was harvested and the percentage of naïve T cells ($CD44^-CD62L^+$, black symbols) and effector/memory T cells (T_{EM}, $CD44^+CD62L^-$, orange symbols) was evaluated by flow cytometry (n=13 per group). Naïve control mice were non-tumour bearing and untreated (n=3) **A**: $CD4^+$ naïve T cells and T_{EM}. **B**: $CD8^+$ naïve T cells and T_{EM}. Statistical significance was calculated using one-way ANOVA with Tukey's post-hoc test, n.s = not significant, error bars indicate s.e.m.

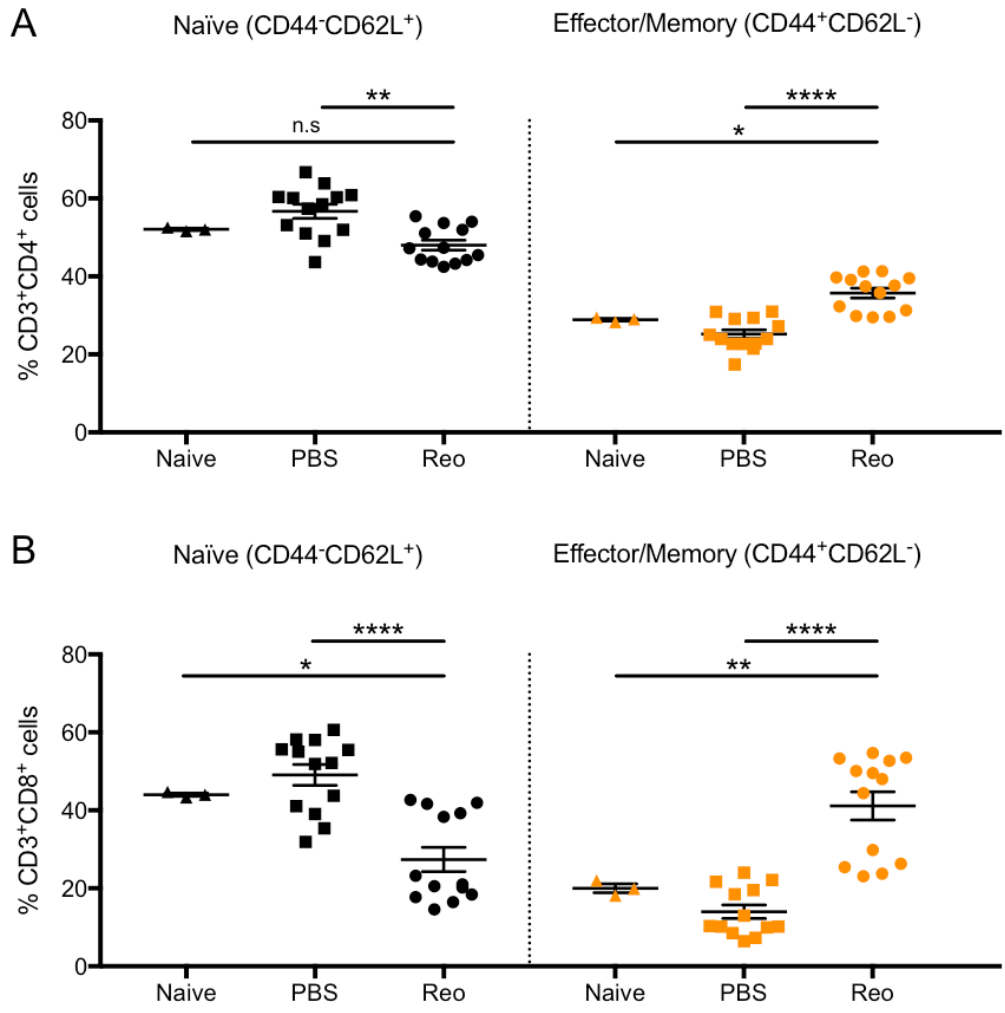

Figure 4-7: Naïve and effector/memory T cell populations in the spleen following reovirus treatment i.v.

Following repeated reovirus or PBS treatment, the spleen was harvested and processed, and the percentage of naïve T cells ($CD44^-CD62L^+$, black symbols) and effector/memory T cells (T_{EM}, $CD44^+CD62L^-$, orange symbols) was evaluated by flow cytometry (n=13 per group). Naïve control mice were non-tumour bearing and untreated (n=3) **A**: $CD4^+$ naïve T cells and T_{EM}. **B**: $CD8^+$ naïve T cells and T_{EM}. Statistical significance was calculated using one-way ANOVA with Tukey's post-hoc test, * = $p<0.05$, ** = $p<0.01$, **** = $p<0.0001$, n.s = not significant, error bars indicate s.e.m.

4.2.2.4 Lymphocyte phenotyping following reovirus treatment i.v.

Next, NK cells, $CD4^+$, and $CD8^+$ T cells were interrogated with a phenotyping panel consisting of CD69, 4-1BB, PD-1, and CTLA-4. As described in Table 4-1, CD69 is a marker of lymphocyte activation (405), 4-1BB is a marker of antigen recognition on T cells (and activation of NK cells) (408-410), and both PD-1 and CTLA-4 are known immune checkpoints which can be up-regulated both in response to T cell activation and exhaustion (411-414). Overall, few phenotypic changes were detected in both NK cells (Figure 4-8), $CD4^+$ T cells (Figure 4-9), and $CD8^+$ T cells (Figure 4-10) in the BM in response to reovirus treatment. Figure 4-8 shows that only the expression of PD-1 on NK cells was significantly changed, with a 1.5% reduction in PD-1-positive cells (Figure 4-8C). No significant changes in the expression of either CD69, 4-1BB, PD-1, or CTLA-4 were detected on $CD4^+$ T cells in the BM in response to reovirus treatment (Figure 4-9). Similar to the NK cells but more pronounced, the only significantly changed marker on $CD8^+$ T cells was PD-1, with a 21.3% reduction in PD-1-positive cells (Figure 4-10C). The overall $CD8^+$ T cell expression of CD69, 4-1BB, and CTLA-4 was also decreased, but these changes were not statistically significant.

Upon examination of immune cell populations in the spleen, the changes in response to reovirus treatment were again more notable. On splenic NK cells, 4-1BB expression was up-regulated with reovirus treatment (Figure 4-11B). Previously, 4-1BB has been reported to be upregulated on NK cells following activation, but its involvement in the cytotoxic function of NK cells remains unclear (408, 409). Similar to the BM, the percentage of PD-1-expressing NK cells was significantly reduced by 0.7% (Figure 4-11C). Moreover, on $CD4^+$ T cells both immune checkpoint molecules, PD-1 and CTLA-4, were up-regulated following reovirus treatment (Figure 4-12 C and D). Up-regulation of several negative regulators might indicate a state of exhaustion in $CD4^+$ T cells, in particular in response to chronic viral infections (415, 416). Examining responses in $CD8^+$ T cells, PD-1 expression was also up-regulated, with an average increase in PD-1-positive $CD8^+$ T cells from 11.8% to 26.7% (Figure 4-13C). Importantly, expression of the activation marker CD69 was also significantly enhanced on $CD8^+$ T cells in the spleen following reovirus treatment (Figure 4-13A). The dual expression of these markers may indicate an overall activation of $CD8^+$ T cells in the spleen, which is encouraging in the light of the expanded T_{EM} population (Figure 4-7). Disappointingly, there was no significant correlation between either CD69 or PD-1 expression on $CD8^+$ T cells in the spleen and

a favourable outcome in terms of BM tumour burden. In an attempt to further clarify the involvement of tumour-specific CTLs in the reduction of tumour burden in response to reovirus treatment, splenocytes were re-challenged with 5TGM1 cells *ex vivo* to evaluate CTL antigen specificity; no increase in IFN-γ secretion from splenocytes could be detected using an ELISA and a 1:1 ratio of splenocytes to 5TGM1 cells for 24 or 48 hrs (data not shown). Further optimisation of these experiments, and complementary experiments evaluating the IFN-γ response upon splenocyte stimulation with 5TGM1 cells, MM antigens or reovirus by intracellular flow cytometry and ELISpot assays is required to establish the nature of the effector T cells present in the spleen following reovirus treatment.

In summary, this section has evaluated the phenotype of lymphocytes (NK cells, $CD4^+$, and $CD8^+$ T cells) following reovirus treatment i.v. An overview of the phenotypic changes in each cell type with reovirus treatment is shown in Table 4-3. Phenotypic changes in the BM were modest, however, the reduction in PD-1 expression on NK cells and $CD8^+$ T cells was encouraging and could indicate a disruption of the local immunosuppressive environment. The phenotypic effects of reovirus treatment were more pronounced in the spleen. Overall, the changes observed on NK cells and $CD8^+$ T cells (increased expression of 4-1BB on NK cells and of CD69 and PD-1 on $CD8^+$ T cells) in the spleen suggested that these cell populations were activated in response to reovirus treatment. In particular the $CD8^+$ T cell response was encouraging considering the increased population of $CD8^+$ T cells in the spleen, which was associated with an increased $CD8^+$ T_{EM} population, and a decrease in naïve $CD8^+$ T cells (Section 4.2.2.3). Taken together, these findings demonstrate immunological changes in reovirus-treated mice, however the nature of these changes with regards to their anti-tumour or antiviral character requires further investigations.

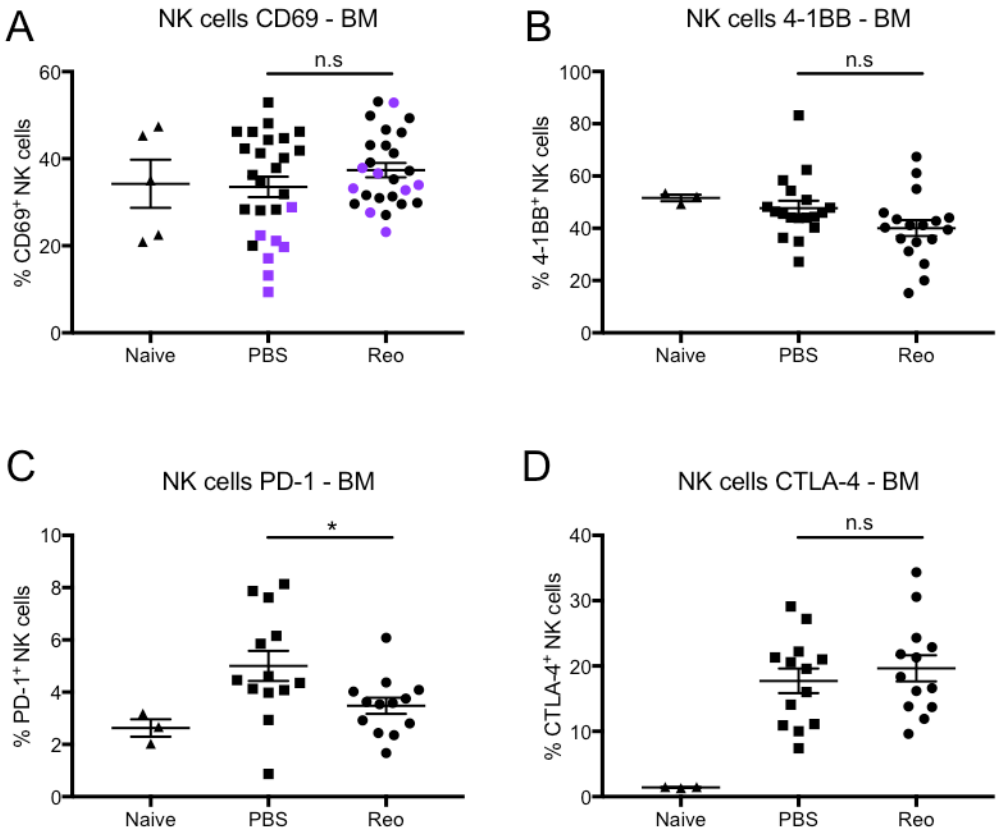

Figure 4-8: Phenotyping of NK cells in the BM following reovirus treatment i.v.

Following repeated treatment with either PBS or reovirus, the BM was harvested and NK cells ($CD3^{-}DX5^{+}$) were phenotyped for the expression of activation markers and immune checkpoint molecules by flow cytometry. Naïve control mice were non-tumour bearing and untreated. Results are shown as the percentage positive cells determined using a fluorescence minus one control. **A**: CD69 expression. Purple symbols indicate mice from Expt 2 (Table 4-2), n=26 per group, naïve=5. **B**: 4-1BB/CD137 expression (n=18 per group, naïve=3). **C**: PD-1/CD279 expression (n=13 per group, naïve=3). **D**: CTLA-4/CD152 expression (n=13 per group, naïve=3). Statistical significance was calculated using one-way ANOVA with Tukey's post-hoc test, * = $p<0.05$, n.s = not significant, error bars indicate s.e.m.

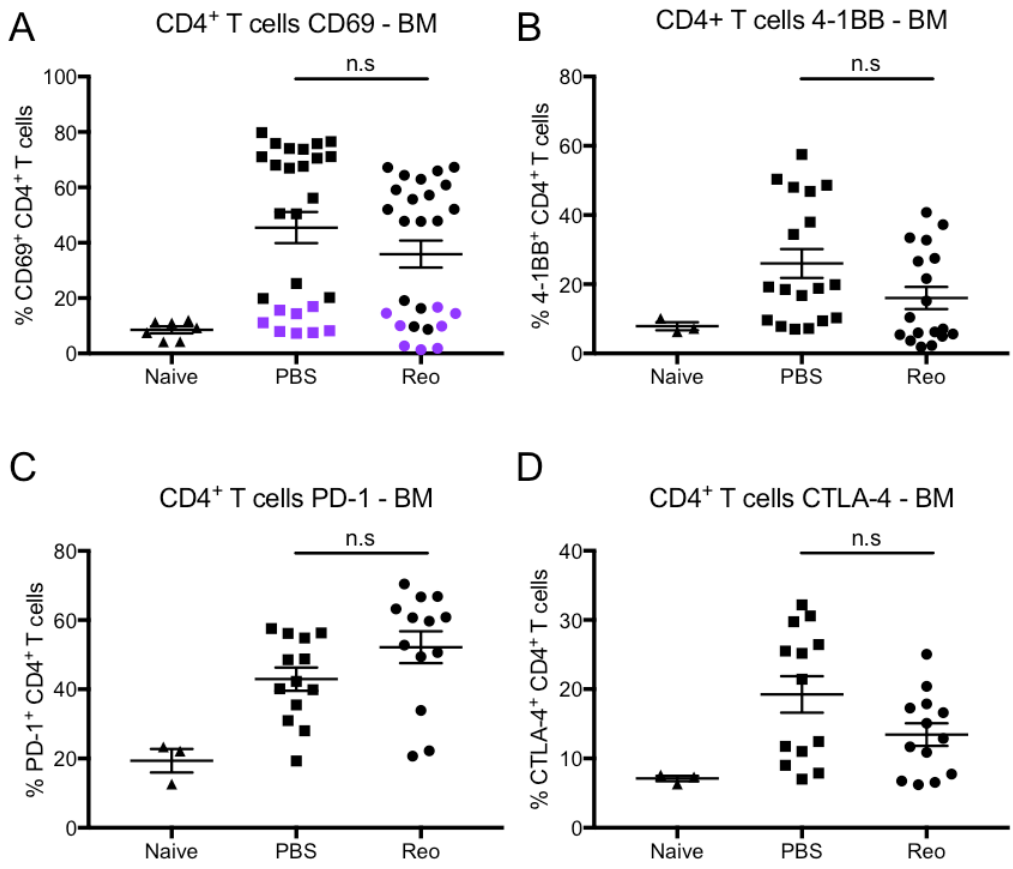

Figure 4-9: Phenotyping of CD4$^+$ T cells in the BM following reovirus treatment i.v.

Following repeated treatment with either PBS or reovirus, the BM was harvested and CD4$^+$ T cells (CD3$^+$CD4$^+$) were phenotyped for the expression of activation markers and immune checkpoint molecules by flow cytometry. Naïve control mice were non-tumour bearing and untreated. Results are shown as the percentage positive cells determined using a fluorescence minus one control. **A**: CD69 expression. Purple symbols indicate mice from Expt 2 (Table 4-2), n=26 per group, naïve=5. **B**: 4-1BB/CD137 expression (n=18 per group, naïve=3). **C**: PD-1/CD279 expression (n=13 per group, naïve=3). **D**: CTLA-4/CD152 expression (n=13 per group, naïve=3). Statistical significance was calculated using one-way ANOVA with Tukey's post-hoc test, n.s = not significant, error bars indicate s.e.m.

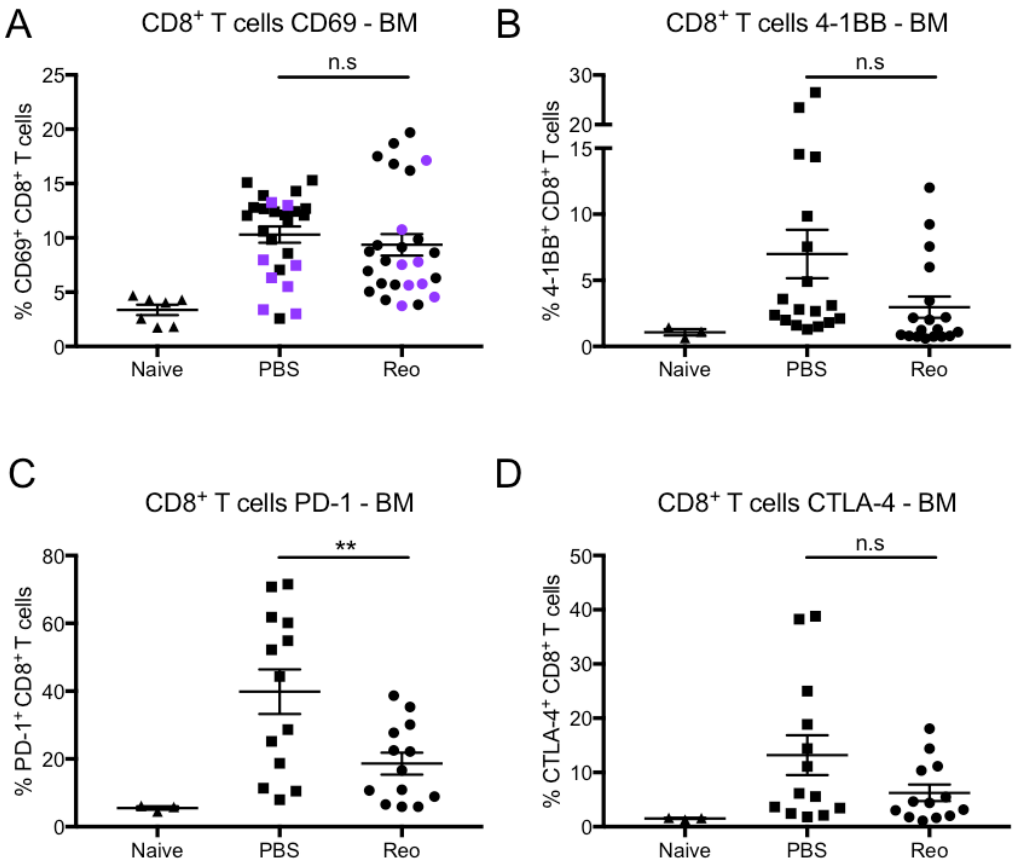

Figure 4-10: Phenotyping of CD8$^+$ T cells in the BM following reovirus treatment i.v.

Following repeated treatment with either PBS or reovirus, the BM was harvested and CD8$^+$ T cells (CD3$^+$CD8$^+$) were phenotyped for the expression of activation markers and immune checkpoint molecules by flow cytometry. Naïve control mice were non-tumour bearing and untreated. Results are shown as the percentage positive cells determined using a fluorescence minus one control. **A**: CD69 expression. Purple symbols indicate mice from Expt 2 (Table 4-2), n=26 per group, naïve=5. **B**: 4-1BB/CD137 expression (n=18 per group, naïve=3). **C**: PD-1/CD279 expression (n=13 per group, naïve=3). **D**: CTLA-4/CD152 expression (n=13 per group, naïve=3). Statistical significance was calculated using one-way ANOVA with Tukey's post-hoc test, * = p<0.05, n.s = not significant, error bars indicate s.e.m.

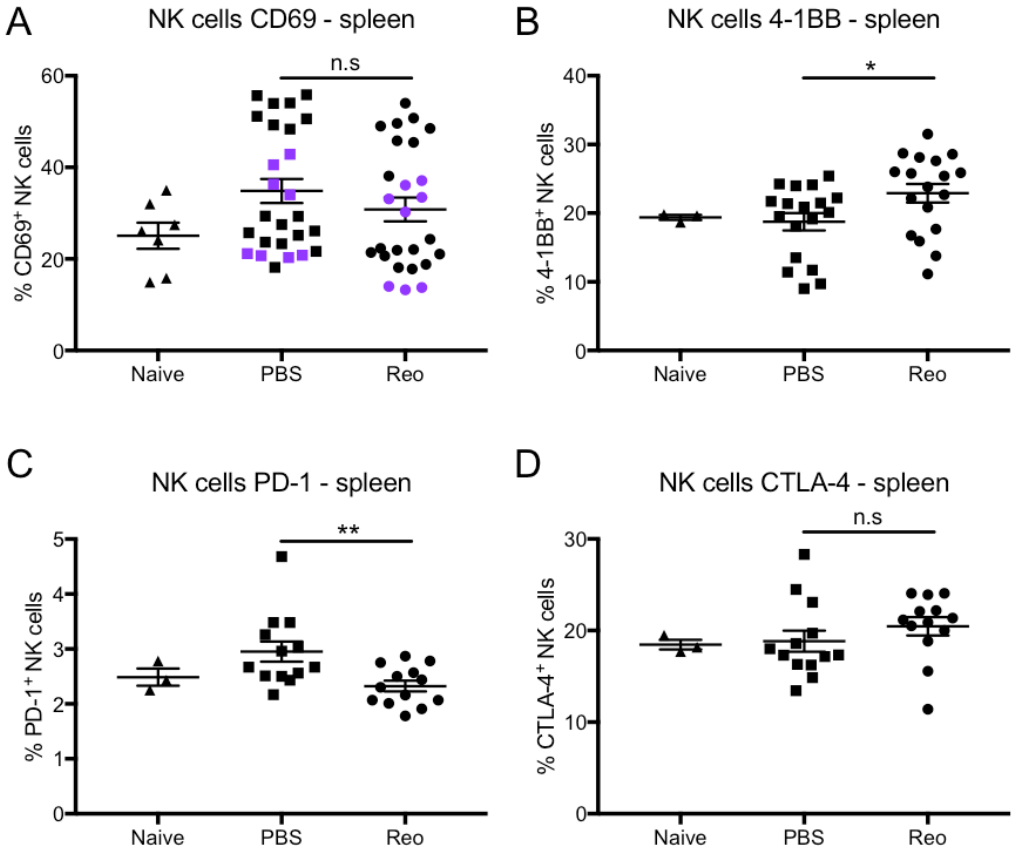

Figure 4-11: Phenotyping of NK cells in the spleen following reovirus treatment i.v.

5TGM1 tumour-bearing mice were repeatedly treated with either PBS or reovirus. The spleen was harvested and processed and NK cells ($CD3^{-}DX5^{+}$) were phenotyped for the expression of activation markers and immune checkpoint molecules by flow cytometry. Naïve control mice were non-tumour bearing and untreated. Results are shown as the percentage positive cells determined using a fluorescence minus one control. **A**: CD69 expression. Purple symbols indicate mice from Expt 2 (Table 4-2), n=26 per group, naïve=5. **B**: 4-1BB/CD137 expression (n=18 per group, naïve=3). **C**: PD-1/CD279 expression (n=13 per group, naïve=3). **D**: CTLA-4/CD152 expression (n=13 per group, naïve=3). Statistical significance was calculated using one-way ANOVA with Tukey's post-hoc test, * = $p<0.05$, ** = $p<0.01$, n.s = not significant, error bars indicate s.e.m.

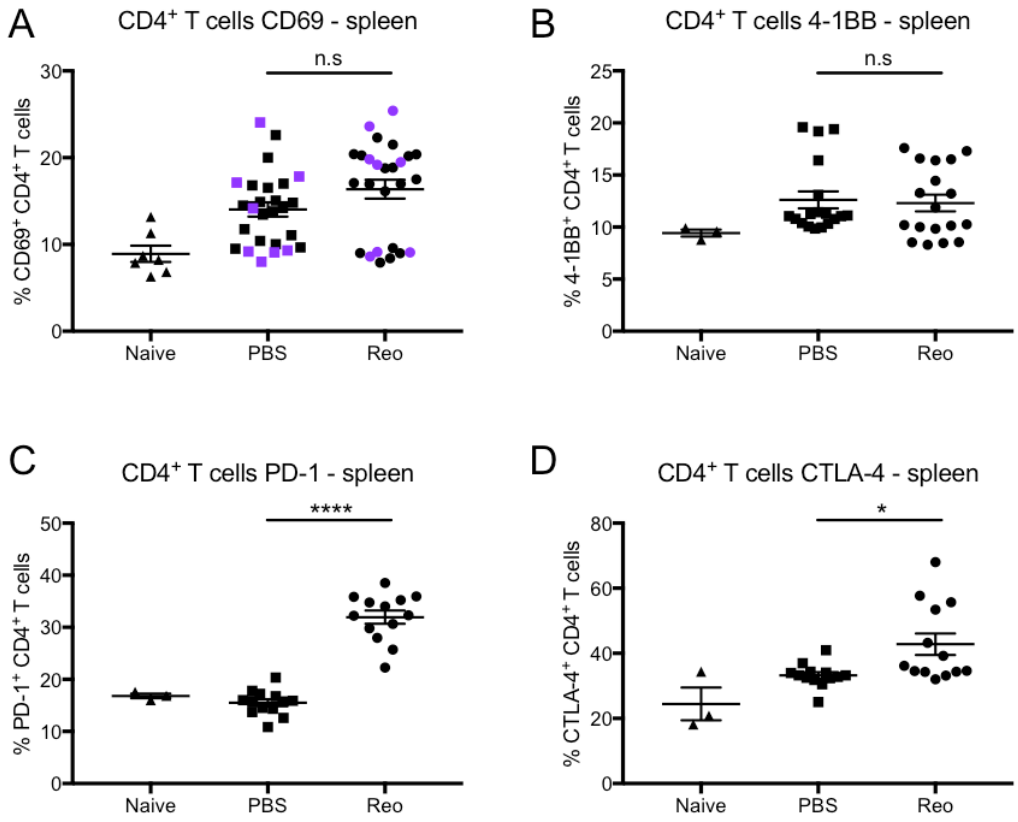

Figure 4-12: Phenotyping of CD4$^+$ T cells in the spleen following reovirus treatment i.v.

5TGM1 tumour-bearing mice were repeatedly treated with either PBS or reovirus. The spleen was harvested and processed and CD4$^+$ T cells (CD3$^+$CD4$^+$) were phenotyped for the expression of activation markers and immune checkpoint molecules by flow cytometry. Naïve control mice were non-tumour bearing and untreated. Results are shown as the percentage positive cells determined using a fluorescence minus one control. **A**: CD69 expression. Purple symbols indicate mice from Expt 2 (Table 4-2), n=26 per group, naïve=5. **B**: 4-1BB/CD137 expression (n=18 per group, naïve=3). **C**: PD-1/CD279 expression (n=13 per group, naïve=3). **D**: CTLA-4/CD152 expression (n=13 per group, naïve=3). Statistical significance was calculated using one-way ANOVA with Tukey's post-hoc test, * = p<0.05, **** = p<0.0001, n.s = not significant, error bars indicate s.e.m.

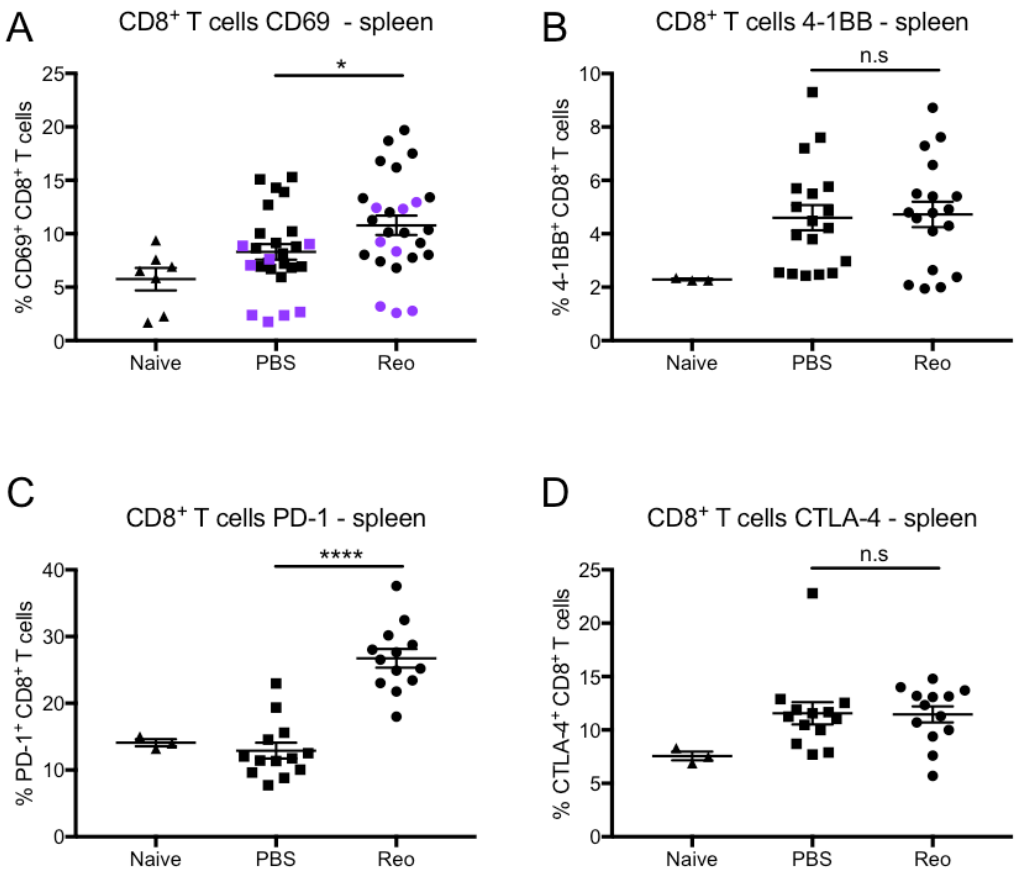

Figure 4-13: Phenotyping of CD8⁺ T cells in the spleen following reovirus treatment i.v.

5TGM1 tumour-bearing mice were repeatedly treated with either PBS or reovirus. The spleen was harvested and processed CD8⁺ T cells ($CD3^+CD8^+$) were phenotyped for the expression of activation markers and immune checkpoint molecules by flow cytometry. Naïve control mice were non-tumour bearing and untreated. Results are shown as the percentage positive cells determined using a fluorescence minus one control. **A**: CD69 expression. Purple symbols indicate mice from Expt 2 (Table 4-2), n=26 per group, naïve=5. **B**: 4-1BB/CD137 expression (n=18 per group, naïve=3). **C**: PD-1/CD279 expression (n=13 per group, naïve=3). **D**: CTLA-4/CD152 expression (n=13 per group, naïve=3). Statistical significance was calculated using one-way ANOVA with Tukey's post-hoc test, * = $p<0.05$, **** = $p<0.0001$, n.s = not significant, error bars indicate s.e.m.

Table 4-3: Overview of phenotypic changes in immune cells following i.v. treatment with reovirus.

NK cells, $CD4^+$, and $CD8^+$ T cells from the BM and spleen were phenotyped for the expression of CD69, 4-1BB, PD-1, and CTLA-4 using flow cytometry. Arrows indicate the overall change in expression with reovirus treatment, compared to PBS treatment.

BONE MARROW				
CELL TYPE	***CD69***	***4-1BB***	***PD-1***	***CTLA-4***
NK CELLS	X	X	↓	X
$CD4^+$ T CELLS	X	X	X	X
$CD8^+$ T CELLS	X	X	↓	X
SPLEEN				
NK CELLS	X	↑	↓	X
$CD4^+$ T CELLS	X	X	↑	↑
$CD8^+$ T CELLS	↑	X	↑	X

X = unchanged, ↑ = increased expression compared to PBS, ↓ = decreased expression compared to PBS.

4.2.2.5 Myeloid cell responses *in vivo* following i.v. treatment with reovirus

Lymphocytes are not the only immune cell population involved in an anti-tumour immune response and myeloid cells, including e.g. monocytes, macrophages, and MDSCs, are also pivotal in regulating anti-tumour immunity. Monocytes and macrophages are important regulators of the innate immune response, and act as APCs to facilitate the generation of adaptive immunity. By contrast, MDSCs (both monocytic and granulocytic) have immunosuppressive and tumour-promoting functions. To date, the effect of OV treatment on myeloid cells *in vivo*, in particular within the tumour microenvironment and sites of immune priming, such as the spleen, remain unclear (417). To examine the effect of reovirus on different myeloid cell subtypes, a flow cytometry phenotyping panel was developed to include myeloid cells in both the BM and the spleen, including monocytes, macrophage, and MDSC populations (Table 4-1 and Table 2-5). The treatment schedule and dosing remained the same as described in Figure 4-3A. As for previous experiments, the BM and spleen were harvested upon sacrifice of the animals at the end of the experiment and cells were examined by flow cytometry.

First, the percentage of monocytes (inflammatory), macrophages, and MDSCs in the BM and spleen, following reovirus treatment compared to PBS, was examined. Figure 4-14 shows that no significant changes were detected in the size of the myeloid populations in the BM in response to reovirus treatment, although there was suggestion of an enlargement, in particular for monocyte and macrophage populations. As observed for the lymphocyte populations, changes were again more pronounced in the spleen (Figure 4-15). For example, the monocyte population increased by 20.7% (Figure 4-15A), and the percentage of conventional ($CD11b^+$) macrophages increase by an average of 6.1% (Figure 4-15B) in response to reovirus treatment. By contrast, there was no change in the population size of red pulp macrophages (RPM) (Figure 4-15B). Interestingly, there was a significant reduction in the population of granulocytic MDSCs in the spleen from an average 27.6% to 17.2% (Figure 4-15C), whilst the monocytic MDSC population was unchanged.

Next, the expression of co-stimulatory molecules CD80 and CD86, and MHC Class II was assessed on monocytes and macrophages. As shown in Chapter 3, reovirus treatment of human monocyte-derived DCs *in vitro* significantly increased the expression of these markers with subsequent

efficient priming of tumour-specific CTLs (Section 3.2.2.3). CD80, CD86, and MHC Class II are markers of M1-polarized macrophages, as opposed to the M2 subtype and tumour-associated macrophages (TAM) (418). Unexpectedly, there was an indication of reduced expression of all three markers on monocytes in the BM, however; only the expression of MHC Class II was significantly reduced following reovirus treatment (Figure 4-16A). On BM macrophages, both CD80 and MHC Class II were significantly reduced (Figure 4-16B), indicating that macrophages might be polarised towards an M2 profile, but an extended phenotyping panel will be required to determine this. Despite the increase in the population sizes of both monocytes and conventional macrophages in the spleen (Figure 4-15), the expression of CD80, CD86, and MHC Class II remained unchanged on both cell types (Figure 4-17 A and B). However, on RPM in the spleen, all three markers were significantly upregulated (Figure 4-17C). Little is known about the function of RPM, and they are predominantly thought to be involved in the maintenance of red blood cell (RBC) homeostasis, however; a number of studies indicate that these macrophages might also be involved in antigen presentation. RPMs have been reported to phagocytose and display ovalbumin antigen on the cell surface *in vitro*, and importantly, they play a role in the priming of antiviral CTLs following VSV infection in mice (419, 420).

While many of the findings presented in this chapter are preliminary, not least those regarding myeloid cells, a number of interesting results were obtained. Immune activation induced by reovirus treatment demonstrated the potential of reovirus to modulate immune effector cells, but whether this plays a role in anti-tumour immunity or is mainly an antiviral response remains unknown. Overall, the reduction in tumour burden in an immunocompetent model strengthens the applicability of reovirus as a therapeutic option in MM. While a lot of work remains to fully confirm a role of anti-tumour immunity in an *in vivo* setting, the phenotyping data obtained through this work is particularly interesting in the context of combination treatments, such as checkpoint inhibitors, which could be employed to further enhance the anti-tumour effects of reovirus.

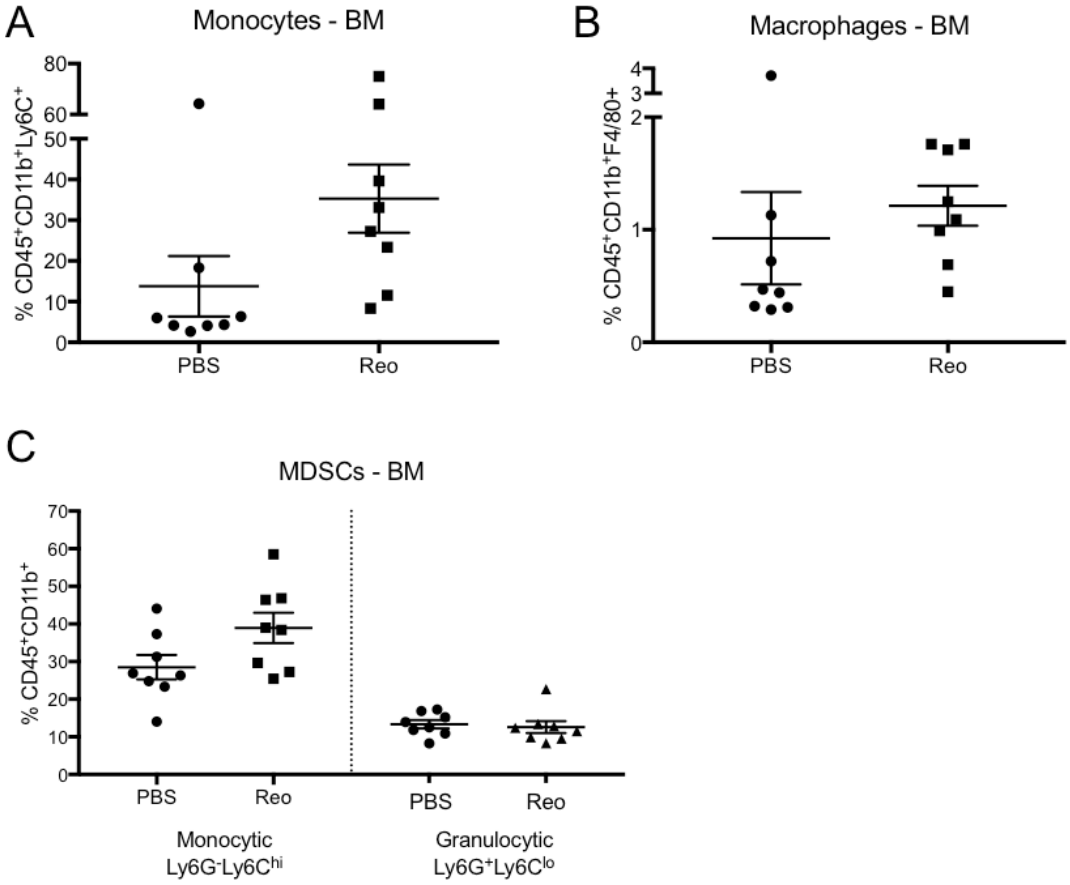

Figure 4-14: Myeloid cell populations in the BM following reovirus treatment i.v.

5TGM1 tumour-bearing mice were repeatedly treated with either PBS or reovirus. After sacrifice, the BM was harvested and the size of various myeloid cell populations was determined by flow cytometry (n=8 per group). **A**: Monocytes (inflammatory) were identified as $CD45^+CD11b^+Ly6C^+$ cells. **B**: Macrophages were identified as $CD45^+CD11b^+F4/80^+$ cells. **C**: MDSCs were identified as $CD45^+CD11b^+$ cells, with monocytic MDSCs being $Ly6G^-Ly6C^{hi}$ and granulocytic MDSCs being $Ly6G^+Ly6C^{lo}$. Statistical significance was calculated using two-tailed, unpaired *t*-tests, all determined to have $p>0.05$ (not significant), error bars indicate s.e.m.

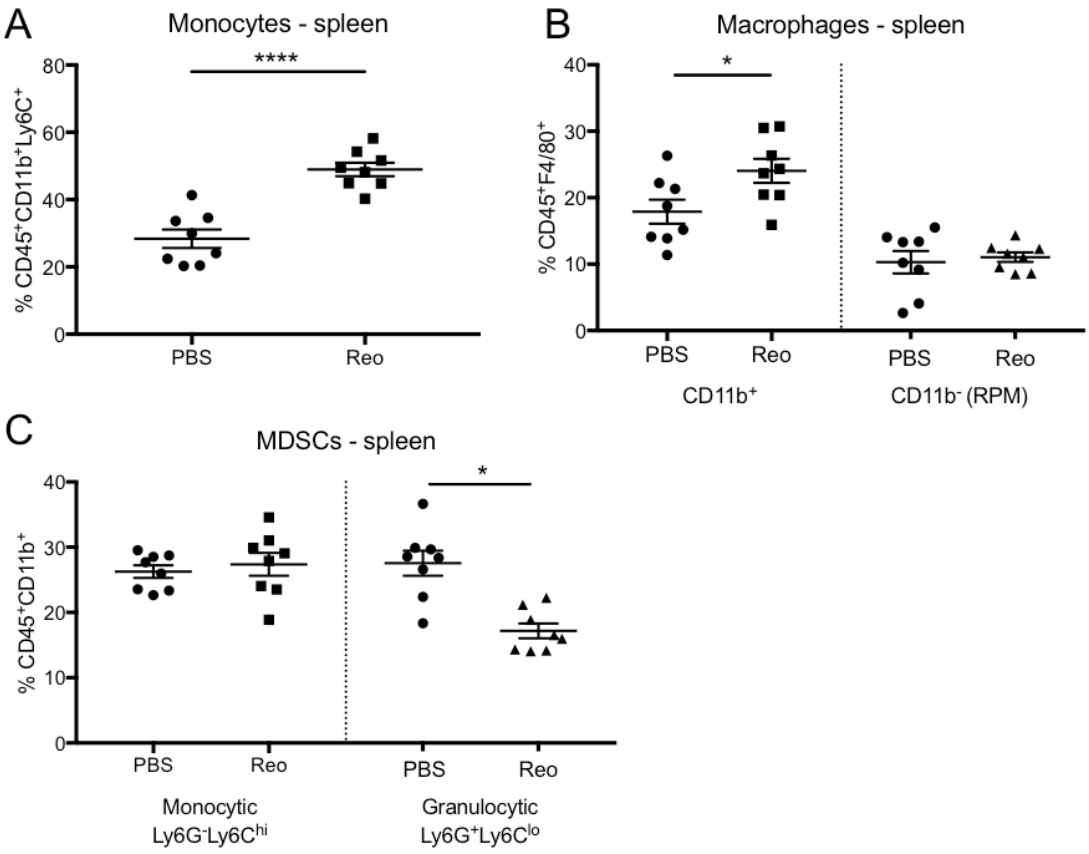

Figure 4-15: Myeloid cell populations in the spleen following reovirus treatment i.v.

5TGM1 tumour-bearing mice were repeatedly treated with either PBS or reovirus. After sacrifice, the spleen was harvested and processed and the size of various myeloid cell populations was determined by flow cytometry (n=8 per group). **A**: Monocytes (inflammatory) were identified as $CD45^+CD11b^+Ly6C^+$ cells. **B**: Conventional macrophages were identified as $CD45^+CD11b^+F4/80^+$ cells, and red pulp macrophages (RPM) as $CD45^+CD11b^-F4/80^+$ cells. **C**: MDSCs were identified as $CD45^+CD11b^+$ cells, with monocytic MDSCs being $Ly6G^-Ly6C^{hi}$ and granulocytic MDSCs being $Ly6G^+Ly6C^{lo}$. Statistical significance was calculated using two-tailed, unpaired *t*-tests, * = $p>0.05$, **** = $p<0.0001$, error bars indicate s.e.m.

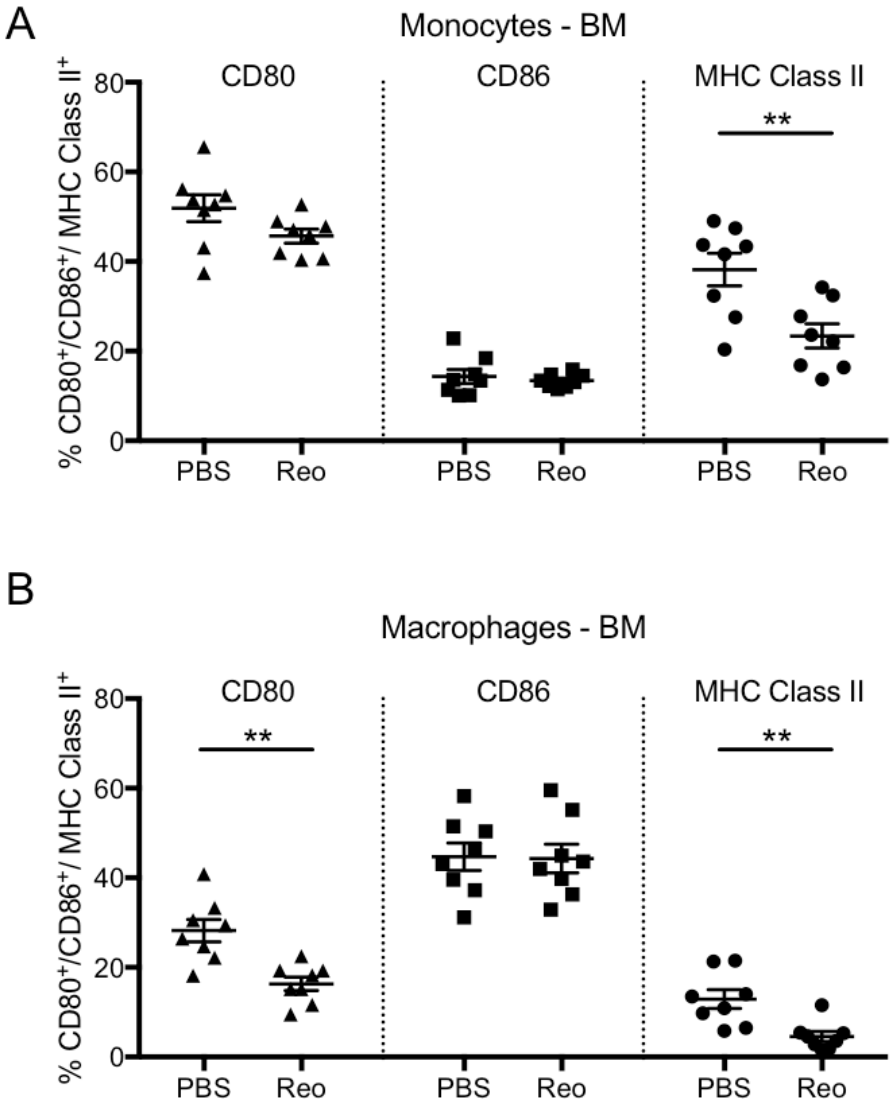

Figure 4-16: Phenotyping of monocytes and macrophages in the BM following reovirus treatment i.v.

Following repeated reovirus or PBS treatment i.v., the BM from 5TGM1 tumour-bearing mice was harvested and monocytes and macrophages were phenotyped for the expression of co-stimulatory markers CD80 and CD86, as well as MHC Class II by flow cytometry (n=8 per group). Results are shown as the percentage of positive cells, determined using a fluorescence minus one control. **A**: Expression of CD80, CD86, and MHC Class II on $CD45^+CD11b^+Ly6C^+$ monocytes. **B**: Expression of CD80, CD86, and MHC Class II on $CD45^+CD11b^+F4/80^+$ macrophages. Statistical significance was calculated using two-tailed, unpaired *t*-tests, ** = $p>0.01$, error bars indicate s.e.m.

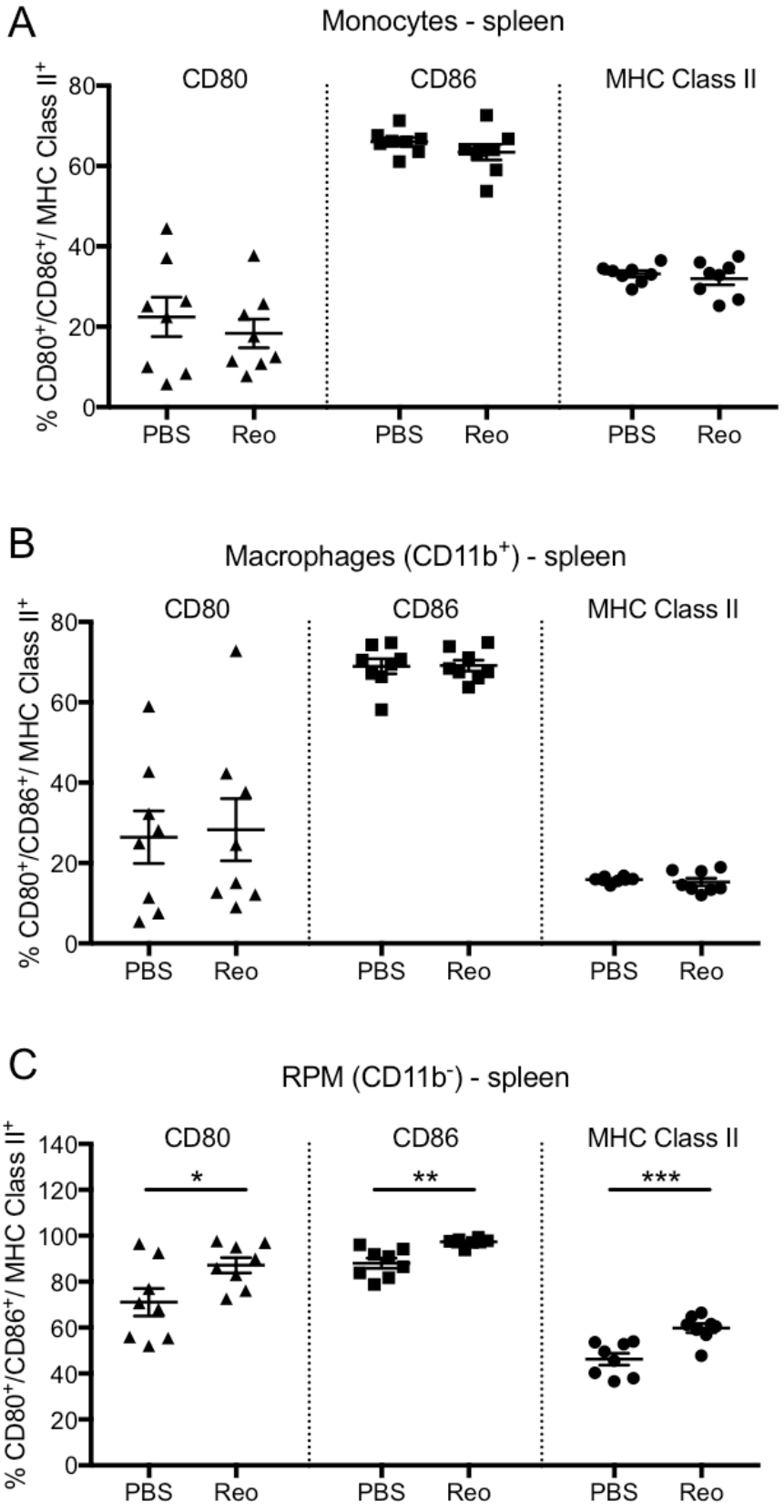
A
Monocytes - spleen
CD80
CD86
MHC Class II
% CD80+/CD86+/ MHC Class II+
0
20
40
60
80
PBS
Reo
PBS
Reo
PBS
Reo
B
Macrophages (CD11b+) - spleen
CD80
CD86
MHC Class II
% CD80+/CD86+/ MHC Class II+
0
20
40
60
80
PBS
Reo
PBS
Reo
PBS
Reo
C
RPM (CD11b-) - spleen
CD80
CD86
MHC Class II
*
**
***
% CD80+/CD86+/ MHC Class II+
0
20
40
60
80
100
120
140
PBS
Reo
PBS
Reo
PBS
Reo

Figure 4-17: Phenotyping of monocytes and macrophages in the spleen following reovirus treatment i.v.

Following repeated reovirus or PBS treatment i.v., the spleen from 5TGM1 tumour-bearing mice was harvested and processed and monocytes and macrophages were phenotyped for the expression of co-stimulatory markers CD80 and CD86, as well as MHC Class II by flow cytometry (n=8 per group). Results are shown as the percentage of positive cells, determined using a fluorescence minus one control. **A**: Expression of CD80, CD86, and MHC Class II on $CD45^+CD11b^+Ly6C^+$ monocytes. **B**: Expression of CD80, CD86, and MHC Class II on $CD45^+CD11b^+F4/80^+$ macrophages. **C**: Expression of CD80, CD86, and MHC Class II on $CD45^+CD11b^-F4/80^+$ red pulp macrophages (RPM). Statistical significance was calculated using two-tailed, unpaired *t*-tests, * = $p<0.05$, ** = $p>0.01$, *** = $p<0.001$, error bars indicate s.e.m.

4.3 Summary & Discussion

This chapter has examined the use of reovirus as a therapeutic option in an immunocompetent *in vivo* model of MM with a particular focus on the examination of immune responses induced by reovirus treatment. The experiments were performed using the syngeneic 5TGM1 model in C57Bl/KaLwRij mice. This model closely resembles human MM with features such as development of lytic bone lesions, decreased bone mineral density, hypercalcaemia, and paraprotein secretion (401, 402). The model has many benefits compared to other models, such as its high reproducibility, cost-effectiveness (due to short latency resulting from aggressiveness), pronounced osteolytic lesions, and the possibility to culture 5TGM1 cells *in vitro* (398, 400, 421, 422).

The *in vitro* susceptibility of 5TGM1 cells to reovirus was first established (Figure 4-1). This demonstrated significant susceptibility, with >95% of 5TGM1 cells eradicated at 72 hrs, even at low doses (0.01 pfu/cell). It is worth considering this high susceptibility in the context of developing an anti-tumour immune response as rapid elimination of tumour might not give sufficient time for the establishment of successful immunological memory. As expected, the results presented in Figure 4-1 also confirmed that 5TGM1 cells are completely resistant to CVA21, presumably due to the virus dependence on human ICAM-1 for its host cell entry rendering murine cells resistant (397). Genetically engineered models exist, which incorporate murine tumour cells transduced with human ICAM-1, however; the fact that CVA21 also does not activate murine immune cells (Section 4.2.1) makes it difficult to find a relevant immunocompetent *in vivo* model for studying immune responses induced by CVA21. The determinants of CVA21 immune activation are characterised in more detail in Chapter 5, which further demonstrated the dependence on human ICAM-1 for the induction of anti-tumour immunity.

Firstly, *in vivo* treatment with reovirus was tested using i.p. administration (Figure 4-2). With a treatment schedule based on repetitive reovirus administration, i.p. delivery was tested as a more accessible and less stressful route of administration for repeated dosing. Reovirus treatment was started on Day 13 after tumour cell injection and mice received four injections in total. Although not significant, some reduction in tumour burden in the BM was observed following reovirus treatment compared to PBS (Figure 4-2B), furthermore, there was suggestion of increased NK cell and $CD4^+$ T cell populations in the BM compartment (Figure 4-2D).

Disappointingly, the effect of reovirus treatment overall was limited with this therapeutic schedule. It is possible that the i.p. delivery protocol could generate an enhanced response with further optimisation, such as utilising an increased dose of reovirus, earlier treatment start, and additional injections. However, while systemic, substances delivered i.p. can be absorbed into mesenteric blood vessels which drain into the hepatic vein and pass through the liver before systemic distribution, resulting in a reduction in the final dose delivered to tissues. Drug absorption and distribution is also considerably slower than for i.v. administration (423). Successful i.p. administration of OVs has previously been documented for MV, oncolytic Semliki Forest virus, and Sindbis virus with significant tumour regression in different subcutaneous tumour models. Virus doses used were similar to the one used in the present study, ranging from 10^6 to 10^8 pfu per injection, but efficacy was seen already after a single injection of Semliki Forest virus and Sindbis virus (424-426).

In subsequent experiments, the administration route was changed to i.v. This administration route was proven successful in early pilot experiments with the 5TGM1 model and was also used by Kelly *et al.* in their reovirus and MM studies (318, 392, 406). Delivery i.v. is the preferred route of administration in human patients and thus, ultimately results in a more translational *in vivo* model. Successful distribution of virus to the BM following i.v. administration of both reovirus and measles virus in humans has previously been demonstrated in clinical trials (195, 198). In addition to switching administration routes, treatment was also started earlier in subsequent experiments and continued until development of HLP in control mice, resulting in varying numbers of injection repeats between experiments (Table 4-2). Treatment with reovirus i.v. resulted in a significant reduction of tumour burden in both the BM and the spleen (Figure 4-3 B and C). This was encouraging, and confirmed the observations made by Kelly *et al.*, who first successfully demonstrated tumour reduction using reovirus in an immunocompetent *in vivo* model (318, 392). The experiments performed by Kelly *et al.* used a treatment protocol with a higher dose of reovirus per injection ($5x10^8$ $TCID_{50}$, approximately 10-fold more than the dose used in this study), with one weekly injection over three weeks, starting from Day 7 after tumour cell administration. In the present study, the extent of tumour reduction in the BM was variable with an overall reduction in the percentage of $CD138^+$ cells in the BM from 47.9% to 23.9% (Figure 4-3B). As discussed, the effect was more pronounced in Expt. 2 (purple symbols), where mice received up to eight reovirus injections (seven for females), with an average

reduction in $CD138^+$ cells in the BM from 59.5% to 9.9%. Many variables can account for the enhanced response seen in this experiment. Mice were of similar age in the majority of experiments (Table 4-2), however, both the number of injections, and the viability and proliferative state of 5TGM1 cells at the time of injection may be responsible for the variation observed. Although not directly comparable, Kelly *et al.* observed similar reductions of 40-60% in 5TGM1 bioluminescence using reovirus as a monotherapy (318, 392). As discussed in more detail below, combination treatments might be required to potentiate the effect of reovirus and induce a complete, sustained response in the extended population. Kelly *et al.* demonstrated synergistic effects using reovirus in combination with bortezomib in the 5TGM1 model to improve the direct cytotoxic effect of reovirus treatment. As the bortezomib/reovirus combination treatment was also efficacious in an immunocompromised human xenograft model of MM, tumour reduction in response to this therapy was thought to be mediated mainly by direct oncolysis (318). However, in a subsequent study, Kelly *et al.* expanded their work with the 5TGM1 model to explore the involvement of immune-mediated mechanisms in reovirus treatment. This study demonstrated up-regulation of PD-L1 on 5TGM1 cells following reovirus treatment, with subsequent potentiation of anti-PD-L1 treatment (392). While this is encouraging, it remains unclear whether this response was due to an enhancement of ADCC induced by the anti-PD-L1 antibody or due to the potentiation of an existing OV-induced anti-tumour immune response.

The tumour eradication experiments performed in this chapter (Figure 4-3) were not sufficient to determine whether tumour eradication was due to direct oncolysis or the development of anti-tumour immune mechanisms. However, the absence of reovirus in the BM at termination of the experiment (Figure 4-3D) might indicate 1) early eradication of tumour by direct oncolysis and clearance of reovirus by antiviral mechanisms, or 2) the role for an anti-tumour immune response in tumour eradication (427). In light of the results presented in Chapter 3, it is encouraging that tumour reduction could be achieved in the context of a physiological BM microenvironment. BM stromal cells were shown in Chapter 3 to induce protection against reovirus direct oncolysis in MM, which might further suggest that anti-tumour immunity plays a role for tumour cell eradication at this site. Moreover, 5TGM1 interactions within the BM microenvironment can induce dormancy of 5TGM1 cells *in vivo*, with subsequent resistance to melphalan therapy and disease relapse (428). Thus, it would be particularly interesting to test whether the dormant, non-dividing cells are also resistant to reovirus

oncolysis, and to determine whether they could be eradicated by anti-tumour immune mechanisms induced by OVT. However, additional experiments are required to address these remaining questions.

Having confirmed efficacy in the immunocompetent model *in vivo*, the next sections in the chapter explored the immune response initiated following reovirus treatment, compared to PBS vehicle treatment. First, the composition of the BM (Figure 4-4) and spleen (Figure 4-5) in terms of lymphoid immune cell populations was examined. In the BM, both the NK cell, $CD4^+$ T cell, and $CD8^+$ T cell populations were significantly larger in mice treated with reovirus, compared to PBS. However, population sizes reached approximately that of naïve (non-tumour bearing, untreated) mice, which may suggest a normalisation and reconstitution of the BM composition due to tumour eradication, rather than an infiltration of immune cells as part of an ongoing immune response. In the spleen, the response was similar, however, only the $CD8^+$ T cell population was significantly increased with reovirus treatment compared to PBS (Figure 4-5C). Immune reconstitution of the BM in particular is encouraging and has similarly been demonstrated in MM patients with long-term disease control, who experienced an expansion of NK cells and $CD8^+$ T cells in the BM, along with a reduction in T regulatory (T_{reg}) cells, compared to patients with symptomatic MM (429). Upon examination of the ratio of $CD4^+$ and $CD8^+$ naïve T cells to T_{EM} in the BM and spleen, there were no significant changes in the populations of either $CD4^+$ or $CD8^+$ naïve T cells or T_{EM} in the BM following reovirus treatment (Figure 4-6). This suggests a normalisation of the BM composition in response to reovirus treatment, rather than the onset of a T cell-mediated immune response. In contrast, a significant increase in both $CD4^+$ and $CD8^+$ T_{EM} was confirmed in response to reovirus treatment in the spleen, concordant with a decrease in the naïve T cell populations. In light of the expanded population of $CD8^+$ T cells in the spleen, this is encouraging for the onset of an adaptive immune response however, the specificity of this response remains to be elucidated. The spleen and lymph nodes are the main sites for priming of an adaptive T cell response and an expansion of the T_{EM} population is characteristic following antigen recognition and generation of immunological memory (407). In particular $CD8^+$ T_{EM}, corresponding to CTLs, are important for the eradication of tumour cells and for generation of a long-term protective response against tumour recurrence (181-183). However, priming of reovirus-specific CTLs has also been confirmed as an important part of the host immune response to reovirus infection, with preferential priming against the viral protein, haemagglutinin

(430, 431). Further studies are required to characterise the specificity of the CTLs generated in 5TGM1 mice following reovirus treatment, in particular with regards to their antiviral vs. anti-TAA effects (173, 432). Similar to the experiments performed in Chapter 3, degranulation or intracellular flow cytometry for IFN-γ secretion in splenocytes following re-challenge with tumour cells (± reovirus infections), reovirus alone, or specific TAA could be used to further determine the antigen specificity of $CD8^+$ T cells generated in response to reovirus treatment.

To further examine the immune response following reovirus treatment, NK cells, $CD4^+$ T cells, and $CD8^+$ T cells were phenotyped for the expression of the activation marker CD69, the marker of T cell antigen recognition 4-1BB, and the immune checkpoint molecules, PD-1 and CTLA-4. An overview of the phenotypic changes in each cell type in the BM and the spleen was provided in Table 4-3. Again, the responses seen in the BM were limited, with the only significant change observed following reovirus treatment being a decrease in the expression of PD-1 on NK cells and $CD8^+$ T cells (Figure 4-8C and Figure 4-10C). In particular the reduction of PD-1 expression on NK cells is interesting in this context. Similar to the results obtained in this study, NK cells from MM patients have been shown to upregulate the expression of PD-1 on the cell surface, while expression on healthy NK cells is low. This has prompted evaluation of the effect of anti-PD-1 antibody treatment on NK cell cytotoxicity. As described by Benson Jr *et al.*, blockade of PD-1 enhanced both NK cell activation and cytotoxicity against MM cell targets, in particular in combination with lenalidomide which reduced the expression of PD-L1 on MM tumour cells (433). Accordingly, elevated PD-1 expression on NK cells has been associated with exhaustion and reduced cytotoxicity in several types of cancers (434, 435). Thus, a reduction in PD-1 expression following reovirus treatment could lead to improved function of NK cells in the BM.

The spleen again provided more interesting changes with an increase in the expression of 4-1BB on NK cells, an increase in both PD-1 and CTLA-4 on $CD4^+$ T cells, and an increase in CD69 as well as PD-1 expression on $CD8^+$ T cells. Increased CD69 expression on splenic $CD8^+$ T cells in response to i.v. reovirus administration has previously been demonstrated in WT, tumour-bearing C57Bl/6J mice, with a significant increase in expression two days after reovirus infusion. Splenic $CD8^+$ T cells also showed an increased expression of CD107 following reovirus treatment, however, it was not determined whether this formed part of an antiviral or anti-tumour immune

response (436). While OV treatment has predominantly been associated with increased expression of PD-L1 on tumour cells, VSV treatment has also been reported to increase the expression of PD-1 on T_{EM} cells in the peripheral circulation of mice. Similar to what was observed in this study, the proportion of $CD44^+CD62L^-CD8^+$ effector T cells increased in response to VSV treatment, moreover, a majority of the T cells also had increased expression of both the inhibitory receptors, TIM-3 (T cell immunoglobulin and mucin-domain containing-3) and PD-1. Interestingly, combination therapy with VSV and either anti-PD-1 or anti-TIM-3 antibodies did not provide a survival advantage compared to VSV alone in this study, highlighting the importance of understanding exactly which immune subsets, if any, are required for tumour eradication during different forms of OVT (437). Nonetheless, combination treatment with reovirus and checkpoint inhibitors remains an interesting avenue to explore and the phenotypic analysis presented in this chapter further confirms this. PD-1 expression was reduced on NK cells and $CD8^+$ T cells in both the BM and the spleen, although both PD-1 and CTLA-4 expression was increased in response to reovirus treatment on $CD4^+$ T cells in the spleen, (Figure 4-12 C and D). This might indicate scope for successful combinations with both anti-PD-1 and/or anti-CTLA-4 antibodies, to stimulate the $CD4^+$ T cell compartment.

Interestingly, the experiments performed here also allowed examination of the effect of MM itself on immune cells by comparing naïve mice with PBS-treated mice. For example, this demonstrated that in the BM, but not the spleen, both PD-1 and CTLA-4 expression was up-regulated on NK cells, $CD4^+$ and $CD8^+$ T cells in the presence of established MM, suggesting that the presence of tumour cells induced an immunosuppressive environment in the BM (Figure 4-8 - Figure 4-10). CD69 expression was also increased on T cells in both the BM and spleen, as well as NK cells in the spleen. This could be explained by the fact that CD69 expression on lymphocytes can be induced in hypoxic environments, such as the BM.

While these changes provide insight into the ongoing immune response, the activated state of $CD8^+$ T cells is particularly interesting in the light of the expanded $CD8^+$ T_{EM} population. As discussed in Chapter 3, priming of tumour-specific CTLs has been previously established as an important mechanism of action following reovirus treatment in several different studies, both human and murine (247, 379, 393, 438). In a syngeneic *in vivo* model of breast cancer, antibody-mediated depletion of $CD8^+$ T cells resulted in a loss of reovirus therapy efficacy, indicating the importance of $CD8^+$ T cells for

the treatment response (393). Priming of a tumour-specific T cell response has also been confirmed using *ex vivo* re-stimulation of splenocytes obtained from melanoma-bearing reovirus-treated mice. Following re-stimulation with either B16 tumour cell lysates or TAA, a Th_1 response with secretion of IFN-γ and IL-12 was elicited (246, 438). In a different approach, Prestwich *et al.* used non-antigen specific T cells as carriers for reovirus in the reovirus-resistant B16ova model of melanoma. Despite B16ova cells being non-permissive to reovirus replication both *in vitro* and *in vivo*, the metastatic burden in both lymph nodes and the spleen was reduced following reovirus treatment. In addition, splenocytes recovered from reovirus-treated animals showed specificity for TAA, and to further support a role for the immune system in generating this response, it was confirmed that the therapeutic efficacy against B16ova cells was lost in immunodeficient SCID mice (247). Similarly, using the reovirus-susceptible B16.F10 model of melanoma, treatment with UV-inactivated reovirus resulted in significant tumour regression (439). Furthermore, in an immunocompetent *in vivo* model of hepatocellular carcinoma, no significant difference in the anti-tumour effect of live and UV-inactivated reovirus was observed (394). Together, these results demonstrate that direct oncolysis is not strictly necessary for efficient reovirus therapy and that immune-mediated mechanisms can play a role in tumour eradication. Other RNA viruses, including poliovirus, VSV, and MV have also been reported to rely on $CD8^+$ T cell activation and anti-tumour immune priming, to some extent, for the induction of efficacious responses (362, 440-443). Notably, Bartee *et al.*, used an immunocompetent *in vivo* model (MOPC-315 cells in Balb/c mice) to study myxoma virus efficacy in MM, which confirmed that eradication of MRD was mediated by tumour-specific $CD8^+$ T cells (194). In line with previous studies which have confirmed a role for anti-tumour immunity and the priming of tumour-specific CTLs in response to reovirus treatment *in vivo*, $CD8^+$ T cell depletion experiments and splenocyte re-stimulation with tumour lysates or TAA will be required to clarify whether reovirus can induce an anti-tumour immune response in the 5TGM1 MM model.

Similar to the lymphoid populations, the reovirus treatment effect on myeloid cells was most pronounced in the spleen. When examining the composition of the BM with regards to myeloid cells, there was a tendency towards increased monocyte and macrophage populations in response to reovirus treatment, but the increase was not statistically significant (Figure 4-14). However, both the expression of CD80 and CD86 was down-regulated in

response to reovirus treatment, compared to PBS, on both cells types (Figure 4-16). As no naïve control mice were included in this experiment, it remains unknown whether the expression observed is truly a down-regulation or a normalisation as a result of reconstitution of the BM. Another reason for the lower expression of CD80/86 after reovirus treatment might be that myeloid cells have migrated away from the BM in response to treatment, e.g. to perform antigen presentation functions in the lymph nodes or spleen. Interestingly, the presence of malignant plasma cells can increase the expression of both CD80 and CD86 on myeloid-derived DC from MM patient BM samples (444, 445). However, increased expression of the CD80/86 receptor CD28 on plasma cells was also seen in response to progressing MM. The engagement of CD28 with CD80 or CD86 resulted in down-regulation of proteasome subunits in the malignant plasma cells, which has previously been associated with reduced susceptibility to CTL-mediated killing (444, 445). Thus, a reduced expression of CD80/86 in the BM might indicate that immune evasion strategies present in MM are reduced as a consequence of reovirus treatment. In addition, reduced CD80/86 expression could be an indication of a normalisation of the BM microenvironment following the eradication of plasma cells.

In the spleen on the other hand, both populations of monocytes and conventional ($CD11b^+$) macrophages were enlarged in response to reovirus treatment (Figure 4-15), but no significant change in the expression of costimulatory markers or MHC Class II were detected (Figure 4-17 A and B). RPM are spleen-resident CD11b-negative macrophages which are important for RBC haemostasis and iron metabolism (446). Much remains unknown with regards to the immunological function of RPM, but they may be involved in the differentiation of T_{regs}, and IFN-α secretion in response to parasitic infections (447, 448). Their antigen presentation ability appears low compared to conventional DC, but they are able to present antigenic peptides to T cells (419, 448). While there was no significant increase in the RPM population size with reovirus (Figure 4-15B), both the expression of CD80, CD86, and MHC Class II was up-regulated on these cells following reovirus treatment, compared to PBS, suggesting an improved ability for antigen presentation and T cell activation (Figure 4-17C).

Little is known about the role of myeloid cells in the generation of an anti-tumour immune response by reovirus. One study has demonstrated a role for peripheral blood monocytes in the protected carriage of reovirus to tumour sites (252). Moreover, myeloid cells can be important for the

clearance of reovirus, which coincides with a transition from an M1 to an M2 phenotype in macrophages (449). Overall, evidence for the importance of myeloid cells for successful OVT is sparse, and controversial. TAMs can enhance the oncolytic effects of both adenovirus, measles, and mumps virus (450-452). For example, both measles and mumps virus treatment induce a more anti-tumour or M1 like phenotype in macrophages, which contributes to tumour cell eradication (450). Macrophages as cell carriers can also protect adenovirus from neutralisation and improve local delivery to tumour sites (451, 452). On the contrary, several studies have demonstrated an impairment of OV efficiency caused by TAM-mediated immunosuppression, for example with the use of HSV-1 and VSV (453, 454), where TAMs increase viral clearance and induce a potent antiviral state in the local tumour microenvironment. The effect of OVT on MDSCs similarly remains unclear. Reovirus treatment has on one hand been shown to recruit MDSCs to the tumour microenvironment in an ovarian cancer model, something that was also indicated, although not significant, for the BM site in this study (325). On the other hand, reovirus has been shown to inhibit the immunosuppressive effect of MDSCs on T cells in the spleen, in a TLR3-dependent manner (436). While there was no significant change in the size of the monocytic MDSC population in the spleen in this study, the population of granulocytic MDSCs was significantly reduced in response to reovirus treatment. It is likely that reduction of the MDSC population will be important for successful OVT in MM as MDSCs mediate suppression of tumour-specific T cell responses through the induction of both T cell anergy and T_{reg} development in the MM microenvironment (58). While both monocytic and granulocytic MDSCs can have immunosuppressive functions, granulocytic MDSC also have a pro-angiogenic effect in MM (455). Moreover, MDSC populations are significantly increased in MM patients and correlate with disease stage and clinical outcome (58).

Successful generation of anti-tumour immunity in MM *in vivo* models using other therapeutic strategies has been previously documented. For example, the administration of IAP (inhibitor of apoptosis) agonists to transgenic MM mice resulted in long-term protection and cure of a subset of mice (456). The response was dependent on an initial type I IFN response with recruitment of macrophages and DC, followed by generation of an adaptive response with successful long-term protection which was potentiated in combination with anti-PD-1 checkpoint inhibitors (456). Also studies using the 5TGM1 model have demonstrated efficient mobilisation of anti-tumour immunity. Interestingly, as 5TGM1 cells are resistant to lenalidomide-induced

apoptosis, the model has been used to study the immunomodulatory effects of lenalidomide in isolation, confirming the crucial role of $CD4^+$ T cells for the establishment of an anti-tumour immune response with generation of cytotoxic CTL following lenalidomide treatment (457). The 5TGM1 model has also been used to study the generation of idiotype-specific T cells with high *ex vivo* cytotoxicity against MM target cells. Following adoptive transfer of either idiotype-specific CTLs or Th_1 cells, MM development was significantly impaired (458). The results from these previously published studies demonstrate that the 5TGM1 model is suitable for the study of anti-tumour immune responses and that anti-tumour immunity is an important factor in the eradication of MM.

Taken together, the results presented in this chapter demonstrate that while significant reduction in the BM tumour burden can be achieved with reovirus treatment, the most prominent immunological responses are seen in the spleen and it remains to be clarified whether this is an anti-tumour or antiviral response. As discussed, the 5TGM1 model has previously been used in combination with reovirus treatment in studies by Kelly *et al.* (318, 392), confirming reovirus-mediated up-regulation of PD-L1 on 5TGM1 cells with subsequent enhanced efficacy of anti-PD-L1 treatment, but no other immune functions were explored in this study. This reveals the limited research efforts which have been invested in studying the potential for reovirus treatment to induce an anti-tumour immune response in MM. As discussed, the majority of *in vivo* studies of reovirus as a treatment for MM have employed immunocompromised murine models. While these models have their purpose in the study of mechanisms for direct cytotoxicity in isolation, it is a major limitation that the contribution of anti-tumour immunity to therapy efficacy cannot be evaluated. As demonstrated by the early work performed in this chapter, the 5TGM1 model has potential for revealing mechanisms behind anti-tumour immunity in response to reovirus treatment, as well as the importance of direct cytotoxicity and anti-tumour immunity, respectively, required for a durable treatment response. Continuation of this work has the potential to identify the immune cell types involved in MM eradication, as well as reveal suitable areas for combination strategies to further enhance therapy efficacy. While the work performed by Kelly *et al*. confirmed up-regulation of PD-L1 on tumour cells in response to reovirus treatment, the results obtained here indicated that the phenotypic changes on immune cells in response to reovirus treatment are extensive and many more opportunities for innovative combinations might still be unknown. A significant amount of work still remains to fully establish the contribution of

anti-tumour immunity to reovirus efficacy in the 5TMG1 *in vivo* model. More specifically, some particularly important experiments are antibody-depletion of different immune cell population to confirm their individual contribution to therapy response, examination of antigen-specificity of $CD8^+$ T cells in the spleen (antiviral vs anti-tumour), and temporal distribution of reovirus following i.v. injection. Furthermore, it is important to distinguish between anti-tumour immune responses and host antiviral responses. Thus, virus neutralization by nAb, and the role of the immune system in clearing the virus after injection need to be investigated to obtain a complete understanding of reovirus mechanisms of action. Full clarification of the mechanisms by which reovirus induces its effect remains important and will allow for new combinational therapies to be developed, to harness the true potential of reovirus and generate complete eradication of MM.

Chapter 5

Anti-tumour immunity induced by coxsackievirus A21 in acute myeloid leukaemia

Chapter 5
Anti-tumour immunity induced by coxsackievirus A21 in acute myeloid leukaemia

5.1 Introduction

With its oncolytic potential first discovered in 2004 (146), CVA21 is a more novel oncolytic agent than reovirus, and has not yet been tested to the same extent in either pre-clinical or clinical studies. The results presented in Chapter 3 demonstrated that CVA21 has the potential to be a viable therapeutic option in MM, and that an efficient anti-tumour immune response could be generated with induction of both innate and adaptive anti-tumour functions. However, very little is currently known about the immunobiology of CVA21, including how it is detected by the immune system and how an immune response towards the virus is initiated.

Thus, the main aim of this chapter was to examine the anti-tumour immune response induced by CVA21 in more detail, with a particular focus on cellular mechanisms and elucidating the critical mediators of the immune response. In order to examine the anti-tumour immune response in isolation, the disease model was switched from MM to AML, which had been shown in preliminary experiments to be resistant to the direct oncolytic effect of CVA21.

The secondary aim of the work performed in this chapter was to evaluate CVA21 as a treatment option in AML. As previously discussed, new treatments which are more tolerable and have better specificity, and efficacy, are urgently needed in AML. With a limited direct oncolytic effect on AML cell lines, efficient induction of anti-tumour immunity is particularly relevant in this disease setting. Thus, the onset of anti-tumour immunity induced by CVA21 in AML was first established, prior to examining the cellular mechanisms responsible. While CVA21 has not previously been investigated in a haematological context, other OVs, including myxoma virus, VSV, HSV-1, and reovirus, have been suggested as potential treatments in AML (205-208). However, rather disappointingly, only one OV so far (VSV genetically modified to express IFN-β and NIS genes), has been taken forward to clinical trials (196). In order to add clinical relevance to this study, a cohort of

primary samples from AML patients undertaking treatment at St. James's University Hospital, Leeds, was examined for their response to CVA21 *ex vivo* (Table 5-1), including their ability to initiate an anti-tumour immune response. Additionally, the clinical trial samples from the STORM Phase I clinical trial, which was introduced in Chapter 3, were further analysed in this context to provide "proof of principle" evidence for the *in vivo* onset of an anti-tumour immune response following CVA21 administration i.v. – an important step in paving the way for future clinical translation of CVA21 as an immunotherapeutic agent.

5.2 Results

5.2.1 CVA21-mediated direct oncolysis of AML cell lines and primary AML blast cells

As discussed previously, ICAM-1 expression has been hypothesised to be the determining factor of tumour cell susceptibility to CVA21 (279, 397). Thus, ICAM-1 expression was first evaluated on six different human AML cell lines using flow cytometry. ICAM-1 expression on all AML cell lines was found to be low compared to the myeloma control cell line U266B, previously confirmed to be CVA21-susceptible (Figure 3-2 E and F), with the highest expression seen in KG-1 and kasumi-1 cells (Figure 5-1A). For these cell lines, the average ICAM-1 expression was three-fold higher than isotype control expression, compared to 13-fold for U266B cells. Next, direct susceptibility to the oncolytic effect of CVA21 was evaluated. As expected following confirmation of low ICAM-1 expression, direct oncolysis of AML cell lines after 72 hrs of treatment (up to 1 pfu/cell) was very limited compared to the control cell line U266B, with no significant oncolysis observed for any of the AML cell lines (Figure 5-1B).

As a tool to further study the importance of ICAM-1 in AML oncolysis and anti-tumour immunity, ICAM-1-expressing KG-1 cells were generated using lentiviral transduction (described in Section 2.1.4). Using flow cytometry, ICAM-1-transduced cells were confirmed to express more ICAM-1 than parental KG-1 cells (Figure 5-1C), up to 15-fold more than the isotype control, which is comparable to the CVA21-susceptible U266B cells. Accordingly, transduced cells were susceptible to CVA21-mediated direct oncolysis (Figure 5-1D). Treatment of ICAM-1-expressing KG-1 with 1 pfu/cell CVA21 for 72 hrs resulted in an average 61.9% cell death, compared to 15.7% for parental KG-1 cells. To determine whether ICAM-1 expression and susceptibility observed correlated with viral replication the ability of CVA21 to enter and replicate in AML cell lines and ICAM-1-transduced KG-1 cells was examined. Using $TCID_{50}$ assays (Section 2.7.1), low level replication was detected in one out of the six parental cell lines (KG-1) and, as expected, in ICAM-1-transduced KG-1 cells (Figure 5-1E). A 133-fold increase in the viral titre was detected following 72 hrs treatment of parental KG-1 cells, which is negligible in comparison to cell lines previously demonstrated to be susceptible to CVA21-mediated oncolysis (202, 459). Replication in ICAM-1-transduced KG-1 cells was lower than in parental KG-1 cells, which might be due to the high susceptibility of ICAM-1-transduced cells which does not allow extended replication. Interestingly, this suggests

that most AML cell lines are resistant to CVA21-mediated oncolysis due to the absence of ICAM-1, while CVA21 is able to enter, and replicate in, KG-1 cells indicating that another intrinsic mechanism of resistance might also be involved. However, as ICAM-1-transduced KG-1 cells with a higher expression of ICAM-1 were rendered susceptible, the absolute level of surface ICAM-1 also appeared to play a role in CVA21 susceptibility.

It is commonly known that, with extensive propagation, cell lines can develop characteristics that are not true of the original primary cells. To ensure clinically relevant results, the direct oncolytic effect of CVA21 was next evaluated in primary AML patient samples. The cohort of primary samples consisted of peripheral blood taken from 31 patients undertaking treatment for various subtypes and stages of AML at St. James's University Hospital, Leeds, between January 2016 and June 2017 (Table 5-1). Both males and females were included in the study, with an age range from 29 to 88 years (median 66 years). Mirroring the wide disease spectrum of AML, the diagnoses within the cohort were heterogeneous with a range of subtypes, mutations and cytogenetics identified. Most patients were on a designated treatment schedule before blood samples for this study were taken. As described in Section 2.2.1, blood samples were processed using density gradient centrifugation to obtain AML blasts as part of the PBMC fraction and thus, AML blasts were treated together with any recoverable immune cells within the PBMC fraction, depending on the clinical status of the patient.

First, ICAM-1 expression on blast cells at the time of isolation was measured using flow cytometry. Blast cells were identified within the PBMC fraction using a combination of anti-CD45, anti-CD34, and anti-CD117 antibodies (Section 2.3). All AML blasts were considered $CD45^{lo}$, with CD34 and CD117 expression varying depending on clinical diagnosis (460). An overview of the blast cell gating strategy is provided in Figure 2-2. Similar to the cell lines, ICAM-1 expression was low on AML blasts with an average 4.5-fold increase in expression compared to the isotype control (Figure 5-2A). However, there was significant variation within the cohort, from ICAM-1 expression too low to detect, up to a 16-fold increase in expression over the isotype control in sample AML-31. Next, susceptibility to CVA21 was examined by treating AML blasts as part of the PBMC fraction with 0.1 or 1 pfu/cell CVA21 for 72 hrs. Following staining with a Live/Dead® discrimination stain, blast cell death was measured using the gating strategy described above (Figure 2-2). Interestingly, in contrast to the AML cell lines,

a number of samples were identified as being susceptible to CVA21 after 72 hrs of treatment (Figure 5-2B). Using a 10% increase in cell death as a cut-off limit, eight out of 16 samples tested were identified as CVA21 responsive (black solid lines). However, surprisingly, as shown in Figure 5-2C, CVA21 susceptibility did not correlate significantly with the level of ICAM-1 expression on AML blasts (p=0.65, Pearson's r=0.122). Furthermore, low level CVA21 replication was only detected in one out of ten samples tested (data not shown), suggesting that cell death was not due to direct oncolysis and thus bringing into question the relevance of ICAM-1 on tumour cells as an independent cellular determinant of CVA21 susceptibility.

As these findings were conflicting with present evidence, the role of ICAM-1 in CVA21 susceptibility was further explored. To test the hypothesis that ICAM-1 expression confers susceptibility to CVA21, TNF-α treatment was used to increase the expression of ICAM-1 on AML cell lines and primary blasts. Following TNF-α treatment with up to 10 000 U/ml for 24 hrs, ICAM-1 expression was elevated on all cell lines tested (Figure 5-3A), and on some AML primary samples (Figure 5-3B). After TNF-α treatment, ICAM-1 expression on THP-1 and kasumi-1 cells exceeded the levels on CVA21-susceptible U266B cells (17-fold and 22-fold increase at the high treatment dose, respectively). For the primary blast cells, the response was more variable, but in responsive samples similar increases in ICAM-1 expression were seen in response to TNF-α treatment (Figure 5-3B). Next, to determine whether cells with an elevated expression of ICAM-1 became susceptible to CVA21-mediated oncolysis, cells were pre-treated with TNF-α for 24 hrs, followed by CVA21 treatment for 72 hrs, and cell death was measured by flow cytometry using a Live/Dead® discrimination stain. Figure 5-3C shows that an increase in ICAM-1 expression only conferred susceptibility to the already replication-permissive KG-1 cells and not to the resistant THP-1 and kasumi-1 AML cell lines. There was an indication of a small increase in the cell death of THP-1 cells with the highest dose of TNF-α and CVA21, but this was not statistically significant. However, some cell death was observed in response to TNF-α alone, particularly in kasumi-1 cells. Primary samples were also highly susceptible to TNF-α treatment alone, but in one of the samples tested, susceptibility to CVA21 treatment was increased following pre-treatment with 1000 U/mL TNF-α (data not shown). These results also suggest that ICAM-1 expression is not the only factor involved in determining susceptibility to CVA21 infection and oncolysis.

Taken together, the results presented in this section have demonstrated that AML cell lines (KG-1, HL-60, THP-1, kasumi-1, ML-1, and OCI-M2) are resistant to CVA21-mediated direct oncolysis. However, in 50% of the tested AML patient samples, death of primary blasts was detected following CVA21 treatment. Interestingly, there was no correlation between CVA21-mediated death and ICAM-1 expression (or CVA21 replication) in primary samples. Considering that primary blasts, as opposed to cell lines, were treated as part of a PBMC fraction in the experiments performed, these results suggested that anti-tumour immune mechanisms may be involved in the elimination of blast cells in primary samples. This possibility was further explored in the following sections.

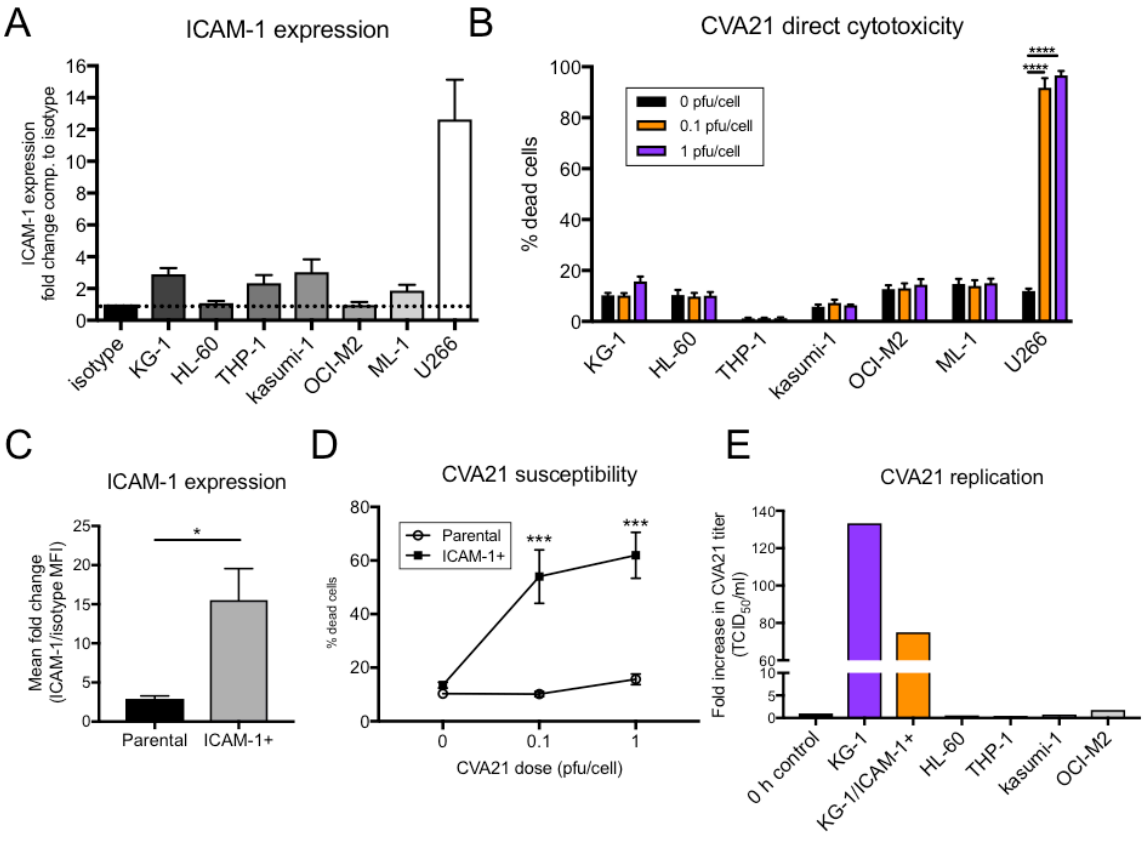

Figure 5-1: CVA21-mediated direct oncolysis of AML cell lines.

A: ICAM-1 expression on AML cell lines KG-1, HL-60, THP-1, kasumi-1, OCI-M2, and ML-1, and MM cell line U266B was measured using flow cytometry. Expression is presented as the fold increase in median fluorescence intensity (MFI) compared to an isotype control antibody (n=4). **B**: Direct oncolytic effect of CVA21. Six AML cell lines and the MM cell line U266B were either untreated or treated with 0.1 or 1 pfu/cell CVA21 for 72 hrs. Cell death was measured by flow cytometry using a Live/Dead® discrimination stain (n=3). Statistical significance was calculated using a two-way ANOVA with Tukey's post-hoc test. **C**: ICAM-1 expression on parental KG-1 cells, compared to KG-1 cells transduced with ICAM-1. ICAM-1 expression was measured by flow cytometry and is presented as the fold increase in MFI compared to an isotype control antibody (n=3). Statistical significance was calculated using an unpaired, two-tailed *t*-test. **D**: Susceptibility to CVA21 of parental KG-1 cells and KG-1 cells transduced with ICAM-1 following treatment with CVA21 for 72 hrs. (0, 0.1, or 1 pfu/cell). Cell death was measured by flow cytometry using a Live/Dead® discrimination stain (n=3). Statistical significance was calculated using a two-way ANOVA with Šídák's post-hoc test. **E**: CVA21 replication in AML cell lines was measured using a $TCID_{50}$ assay. Cells and supernatants were harvested at 0 hr and 72 hrs after CVA21 treatment and cells were lysed using repeated freeze-thaw cycles. The supernatants were serially diluted and added to SK-Mel-28 cells. After six days, SK-Mel-28 cells were stained with methylene blue and the cytopathic effect was counted for each dilution. The titre is presented as the fold increase in $TCID_{50}$/ml 72 hrs after treatment (n=1). Error bars indicate s.e.m, * = $p<0.05$, *** = $p<0.001$, **** = $p<0.0001$.

Table 5-1: Demographics of AML patients included in the study.

Diagnosis was confirmed by the Haematological Malignancy Diagnostic Service (HMDS) at St. James's University Hospital (Leeds) using fluorescence *in situ* hybridisation and next generation sequencing.

Sample	Symbol	Age	Sex	AML subtype (WHO)	Known mutations	Cytogenetics
AML-1	●	37	F	NOS	None detected	5q del.
AML-2	■	30	M	inv(16)(p13;q22)	*CFS3R, WT-1, c-Kit*	16 inv.
AML-3	▼	74	M	RAEB	*STAG2*	Normal
AML-4	▲	74	F	NOS	Not done	Not done
AML-5	◆	43	F	NOS	*CFS3R*	16q del?
AML-6	★	78	F	MDS → AML	Not done	Not done
AML-7	✚	61	F	AML relapse (monoblastic)	*FLT3-ITD*	Trisomy 8, Trisomy 11
AML-8	✕	72	M	t(8;21)(q22;q22)	*FLT3-ITD, RUNX1-RUNX1T1* fusion	t(8;21)(q22;q22)
AML-9	●	88	M	NOS	*FLT3-ITD, NPM1, DNMT3A*	Normal
AML-10	■	70	F	NOS	*DNMT3A, IDH2*	Normal
AML-11	▼	61	M	NOS	*SRSF2, IDH1, TET2*	Trisomy 8
AML-12	▲	60	M	NOS	*NRAS, TET2*	t(2;3), -7
AML-13	◆	58	M	NOS	IDH2, NPM1	Normal
AML-14	★	75	M	AML with adverse cellular features	*FLT3-ITD, DNMT3A*	Normal
AML-15	✚	61	F	t(8;21)(q22;q22)	*RUNX1-RUNX1T1* fusion	t(8;21)
AML-16	✕	35	M	inv(16)(p13;q22)	*FLT3-TKD, c-Kit, TET2, EZH2*	16 inv.
AML-17	●	68	M	t(8;21)(q22;q22)	*RUNX1-RUNX1T1* fusion, *WT-1*	t(8;21)
AML-18	■	47	F	AML with MLL (KMT2A) (11q23) rearrangement	*WT-1*	t(9;11)(p21.3;q23.3)
AML-19	▼	53	F	NOS	*NPM1, DNMT3A*	Normal
AML-20	▲	47	F	inv(16)(p13;q22)	*CBFB-MYH11* fusion	16 inv.
AML-21	◆	73	F	t(8;21)(q22;q22)	*FLT3-ITD, RUNX1-RUNX1T1* fusion	t(8;21)(q22;q22)
AML-22	★	73	M	MDS with excess blasts	None detected	Normal
AML-23	✚	55	M	NOS	Not done	Incomplete
AML-24	✕	69	M	AML:lymphoma mixed	None detected	Complex
AML-25	●	71	F	inv(16)(p13;q22)	*CBFB-MYH11* fusion	16 inv.
AML-26	■	58	M	NOS	*CSF3R, TP53*	Complex
AML-27	▼	70	M	AML with mutated NPM1	*NPM1, TET2, FLT3-ITD*	Normal
AML-28	▲	66	M	NOS	*CSF3R, DNMT3A*	Normal
AML-29	◆	61	M	AML with mutated NPM1	*NPM1, TET2*	Normal
AML-30	★	67	M	AML with mutated NPM1	*NPM1, TET2*	Normal
AML-31	✚	29	M	inv(16)(p13;q22)	*CBFB-MYH11* fusion	16 inv.

NOS: not otherwise specified, RAEB: refractory anemia with excess blasts, MDS: myelodysplastic syndrome, MLL: mixed lineage leukemia, ITD: internal tandem duplication, del: deletion, inv: inversion, t: translocation, TKD: tyrosine kinase domain.

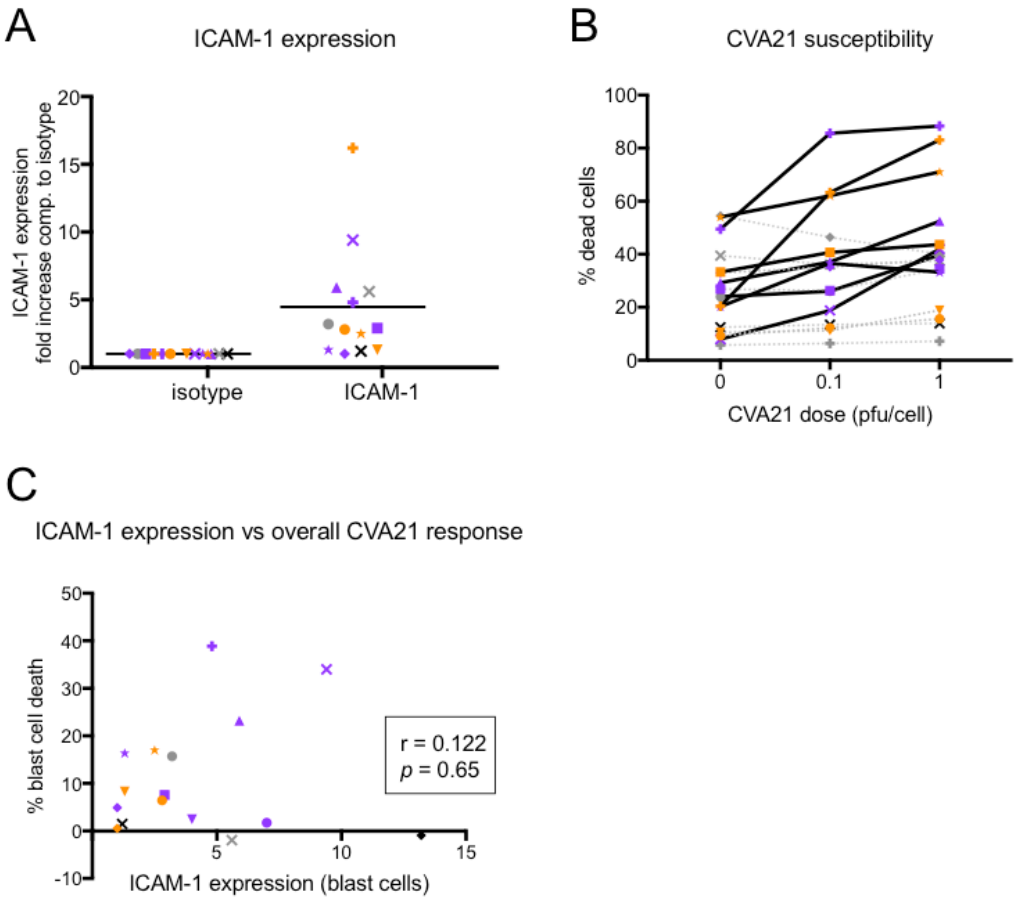

Figure 5-2: Primary AML sample ICAM-1 expression and susceptibility to CVA21.

AML blast cells were isolated from peripheral blood samples as part of the PBMC fraction using density gradient centrifugation. Blast cells were identified within the PBMC fraction using flow cytometry and a panel of anti-CD45, anti-CD34, and anti-CD117 antibodies. Symbols indicate individual samples and are detailed in Table 5-1. **A**: ICAM-1 expression on primary blast cells at the time of isolation was measured using flow cytometry. Expression is presented as the fold increase in MFI compared to an isotype control antibody (n=13). **B**: Death of primary blast cells following CVA21 treatment (0, 0.1, or 1 pfu/cell) for 72 hrs as measured by flow cytometry using a Live/Dead® discrimination stain (n=21). Solid black lines indicate samples with an increase in cell death >10%, compared to unresponsive samples (grey lines). **C**: Correlation of ICAM-1 expression on primary blast cells and the percentage of dead blast cells following CVA21 treatment for 72 hrs (n=15).

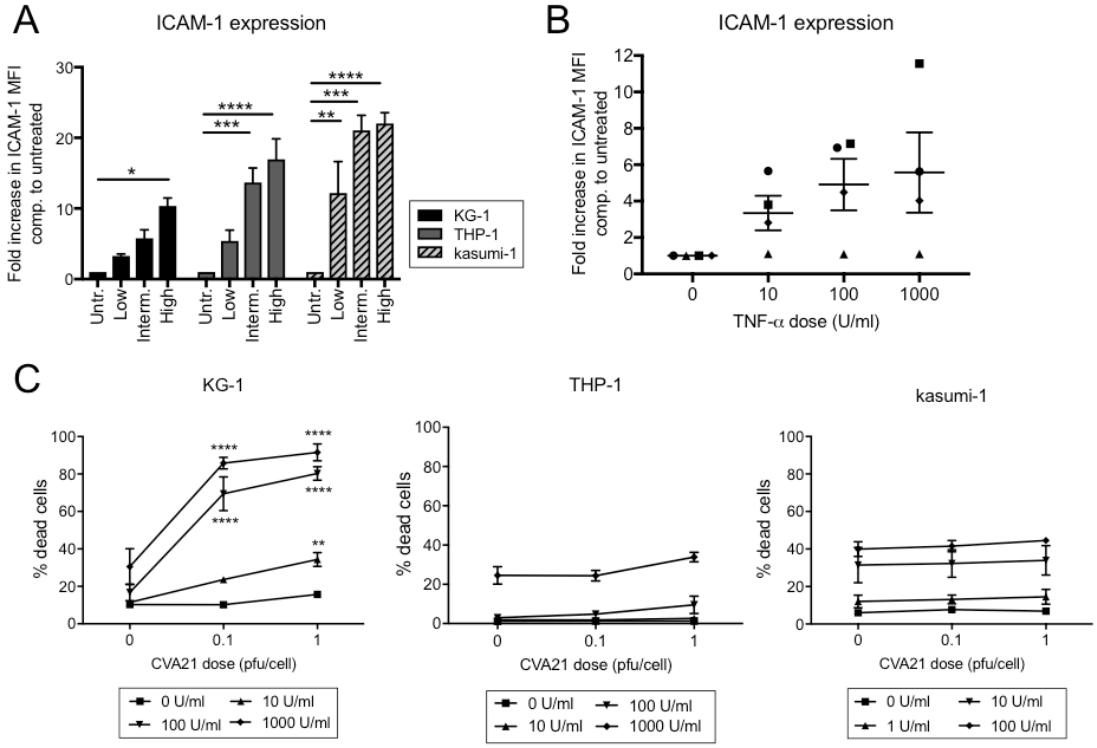

Figure 5-3: Increased ICAM-1 expression only sensitizes KG-1 cells to direct CVA21 oncolysis.

A: AML cell lines KG-1, THP-1, and kasumi-1 were treated with TNF-α for 24 hrs, then ICAM-1 expression on the cell surface was measured by flow cytometry. TNF-α doses were adjusted based on toxicity, for KG-1 and THP-1; Low=10 U/mL, Interm.=100 U/mL, High=1000 U/mL. For kasumi-1; Low=1 U/mL, Interm.=10 U/mL, High=100 U/mL. ICAM-1 expression is presented as the fold increase in MFI compared to untreated cells. Statistical significance was calculated using a two-way ANOVA with Tukey's post-hoc test (n=3). **B**: Primary blast cells were treated with TNF-α (0/10/100/1000 U/mL) for 24 hrs, then ICAM-1 expression was measured by flow cytometry on $CD45^{-}CD34^{+}$ and/or $CD117^{+}$ cells. ICAM-1 expression is presented as the fold increase in MFI compared to untreated cells, n=4. **C**: Susceptibility to CVA21 after up-regulation of ICAM-1 using TNF-α pre-treatment. KG-1, THP-1, and kasumi-1 cells were pre-treated with TNF-α as indicated for 24 hrs, then treated with CVA21 (0, 0.1, or 1 pfu/cell) for 72 hrs. Cell death was measured by flow cytometry using a Live/Dead® discrimination stain. Statistical significance was calculated using a two-way ANOVA with Tukey's post-hoc test (n=3). Error bars indicate s.e.m, * = p<0.05, ** = p<0.01, *** = p<0.001, **** = p<0.0001.

5.2.2 Interferon-mediated antiviral response to CVA21 treatment

As confirmed in Chapter 3, PBMCs from healthy donors secrete large amounts of both IFN-α and IFN-γ in response to 48 hrs of CVA21 treatment (Figure 3-4). To confirm a similar response in AML patient samples, the IFN-α secretion from patient PBMCs treated with CVA21 was first examined using an ELISA. As expected, the response was largely variable between patients, but overall a significant secretion of IFN-α in response to 48 hrs CVA21 treatment (1 pfu/cell) was confirmed (Figure 5-5A). However, the levels were lower than those observed for healthy donors, with a maximum secretion of 2390 pg/mL in sample AML-65 at the 1 pfu/cell treatment dose, and an overall average of 540 pg/mL.

Although cytokine secretion from immune cells in response to CVA21 can have a cytotoxic effect on tumour cells, as demonstrated in Chapter 3 (Section 3.2.2.1), type I IFN secretion is also one of the first protective cellular responses initiated following viral infection (461). IFN-α acts both to activate NK cells which are important for the eradication of virally infected cells, and to induce a virus hostile environment in healthy cells through the transcription of multiple interferon-stimulated genes (ISG) via the Jak-STAT signalling pathway (179, 461, 462). To evaluate the antiviral potential of IFN-α secreted in response to CVA21 treatment, the ICAM-1-transduced KG-1 cells, confirmed to be susceptible to direct oncolysis, were utilised. Cells were treated with IFN-α in combination with CVA21 and cell death was evaluated by flow cytometry using a Live/Dead® discrimination stain (Figure 5-4B). A set standard 1 pfu/cell dose of CVA21 was used, which induced an average of 44.1% cell death (grey line). In the presence of IFN-α (purple line), as little as 500 pg/mL (comparable to the amount secreted by AML patient samples) significantly reduced CVA21-mediated oncolysis. Furthermore, at the 5000 pg/mL IFN-α dose, there was no significant difference in the level of cell death between IFN-α treatment alone and IFN-α + CVA21 treatment, indicating that cell death observed was due to IFN-α toxicity and not mediated by CVA21 oncolysis. Therefore, this data suggests that the presence of IFN-α following CVA21 treatment may impede the direct oncolytic effect of CVA21. A time course of IFN-α secretion in response to CVA21 was generated by treating PBMC from healthy donors with 1 pfu/PBMC CVA21 and harvesting cell-free supernatants for ELISA at various time points. Analysis of the supernatants obtained indicated that IFN-α secretion in response to CVA21 was detectable between 8 and 16 hrs after CVA21 treatment (Figure 5-4B). These findings are interesting, in particular

for the kinetics of direct oncolysis, and indicate that in a physiological system, efficient oncolysis might not take place before the virus has been effectively neutralised by IFN-α secreted as part of the innate antiviral immune response.

In conclusion, this demonstrates that in addition to ICAM-1 expression, the levels of IFN-α secretion in response to CVA21 treatment may also be important for the generation of direct oncolysis. This indicates that the direct lytic effect of CVA21 may be inhibited in AML blasts which have the ability to produce IFN-α (Figure 5-4). Nonetheless, AML blast cells were killed in response to CVA21 treatment (Figure 5-2), which further suggested a potential role for anti-tumour immunity in the AML setting. Thus, anti-tumour immunity was next explored as the preferential mechanism of action of CVA21 in AML.

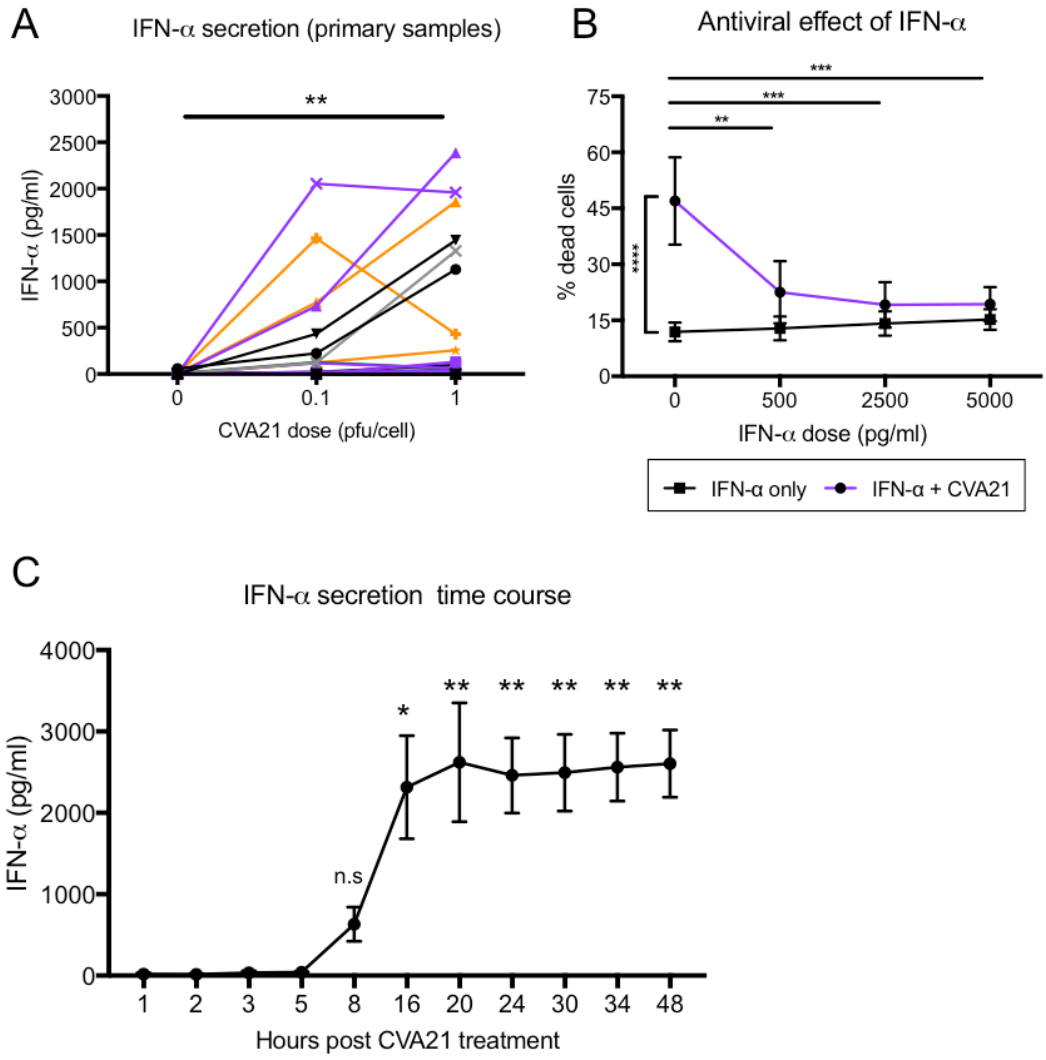

Figure 5-4: IFN-α secretion in response to CVA21 is detrimental for direct oncolytic killing of AML cells.

A: PBMC were isolated from peripheral blood samples from AML patients and treated with CVA21 for 48 hrs. Cell-free supernatants were harvested and IFN-α secretion was measured using an ELISA assay with matched paired antibodies, n=21. **B:** KG-1 cells transduced with ICAM-1, confirmed to be susceptible to CVA21-mediated oncolysis, were used to measure the antiviral effect of IFN-α. Cells were treated either with IFN-α alone (0, 500, 2500, or 5000 pg/mL, black line), CVA21 alone (1 pfu/cell, grey line), or a combination of both (purple line). After 72 hrs, cell death was measured by flow cytometry using a Live/Dead® discrimination stain (n=3). Statistical significance was calculated using a two-way ANOVA with Šídák's post-hoc test and refers to comparison between black and purple curves. **C**: PBMCs were isolated from healthy donors (n=4) and treated with 1 pfu/cell CVA21, cell-free supernatants were harvested at the indicated time points for use in an IFN-α ELISA assay. Statistical significance was calculated using a one-way ANOVA with Tukey's post-hoc test and refers to comparison with the 1 hr time point. Error bars indicate s.e.m, * = $p<0.05$, ** = $p<0.01$, *** = $p<0.001$, **** = $p<0.0001$, n.s = not significant.

5.2.3 CVA21-mediated potentiation of innate and adaptive anti-tumour immunity

Using a strategy similar to that demonstrated in Chapter 3, the ability of CVA21 to induce an anti-tumour immune response in AML was evaluated by examining both innate (cytokine-mediated bystander killing, and NK cell-mediated cytotoxicity), and adaptive (priming of tumour-specific cytotoxic CTLs) immune mechanisms.

5.2.3.1 Pro-inflammatory cytokines secreted in response to CVA21 induce bystander killing of AML cells

In Chapter 3, it was shown that CM generated from PBMC treated with CVA21 had a significant cytotoxic effect on oncolysis-resistant OPM2 cells (Figure 3-6). Accordingly, a similar strategy was applied for inducing a bystander killing effect in AML cells. Like in MM, IFN-α has also been tested as a therapeutic agent in AML due to its toxic effect on AML blasts (112, 463, 464). Thus, the toxicity of IFN-α alone was first examined using KG-1 and HL-60 cells. Surprisingly, following treatment with up to 5000 pg/mL recombinant IFN-α for 96 hrs, very little toxicity was observed in either cell line (Figure 5-5A). Although there was a significant increase in the death of KG-1 cells, this was only an average 9% increase at the highest treatment dose. However, when combining IFN-α treatment with recombinant IFN-γ treatment, more extensive cytotoxicity was seen, with up to 59% of KG-1 cells killed (Figure 5-5B). This was a promising indication for the cytotoxic potential of combined cytokines present in CVA21-CM on AML cells.

As described in Section 2.12.2, the cytokine and chemokine content of CVA21-CM was measured using a 48-plex Luminex assay (Figure 3-4E). As for MM, several of the identified cytokines (e.g. IL-2, IL-6, and IL-1β) have previously been reported as having a cytotoxic effect in AML, either alone or in various combination treatments (465-467). To assess the cytotoxic potential of this pro-inflammatory cytokine cocktail, PBMC-conditioned medium was generated by treating PBMC (from either healthy donors or primary AML samples) with CVA21 for 48 hrs with subsequent harvest of cell-free culture medium by centrifugation. AML cell lines were cultured in PBMC-conditioned medium for 96 hrs and cell viability was evaluated using an MTS assay (Figure 3-5A). As all cell lines were resistant to the direct oncolytic effect of CVA21, no UV treatment of CM was necessary; 96 hrs

culture in CVA21-CM significantly reduced the viability of all three cell lines tested (KG-1, HL-60, and kasumi-1). KG-1 cells were the most susceptible, with a 48.8% reduction in viability using the 1 pfu/PBMC CM (Figure 5-6A). This confirmed the induction of a bystander killing effect in response to CVA21 treatment, similar to that induced in the MM setting. Next, it was tested whether CM generated from primary AML sample PBMCs could induce a similar bystander killing effect on AML cell lines. CM from up to 20 patients was tested and encouragingly, patient CM also induced significant cell death in KG-1, HL-60, and kasumi-1 cells (Figure 5-6B). KG-1 cells were consistently the most susceptible to the cytokine-induced death with a 21.5% reduction in viability being achieved using the 1 pfu/PBMC patient-derived CM. It is not surprising that the cytotoxic potential of patient CM was lower than that observed for healthy donors, considering that many patients had a reduced number of immune cells in the PBMC fraction, compared to healthy donors, and thereby lower potential for CVA21-induced cytokine secretion.

These results demonstrate that, while cytokine secretion in response to CVA21 treatment might be detrimental to direct oncolysis, it also has the potential to induce a bystander killing effect on AML cells. Despite the potential for neutralisation of direct oncolysis, bystander killing contributed to a significant reduction in AML cell viability as part of an anti-tumour immune response. Cytokine secretion is also crucial for initiating downstream anti-tumour immune mechanisms which will be examined in the following sections (468).

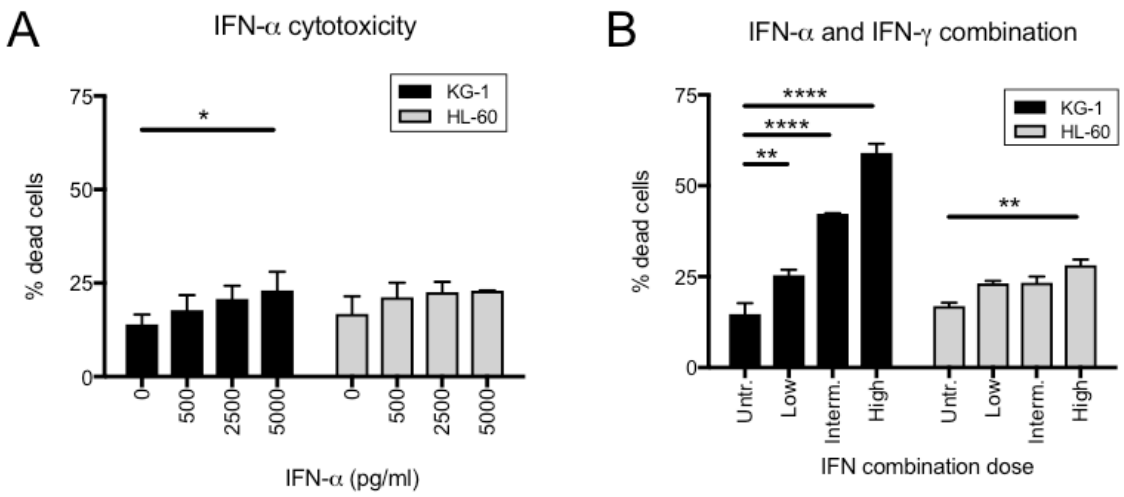

Figure 5-5: AML cell line toxicity of type I and type II IFNs.

A: KG-1 and HL-60 cells were treated with human recombinant IFN-α (0, 500, 2500, 5000 pg/mL) for 96 hrs, then cell death was measured by flow cytometry using a Live/Dead® discrimination stain. **B**: Combination treatment of KG-1 and HL-60 cells with human recombinant IFN-α and IFN-γ. Low = 500 pg/mL IFN-α + 500 pg/mL IFN-γ, Interm. = 2500 pg/mL IFN-α + 1500 pg/mL IFN-γ, High = 5000 pg/mL IFN-α + 3000 pg/mL IFN-γ. Cells were treated for 96 hrs, then cell death was measured by flow cytometry using a Live/Dead® discrimination stain (n=3). Statistical significance was calculated using one-way ANOVA with Tukey's post-hoc test, * = $p<0.05$, ** = $p<0.01$, **** = $p<0.0001$. Error bars indicate s.e.m.

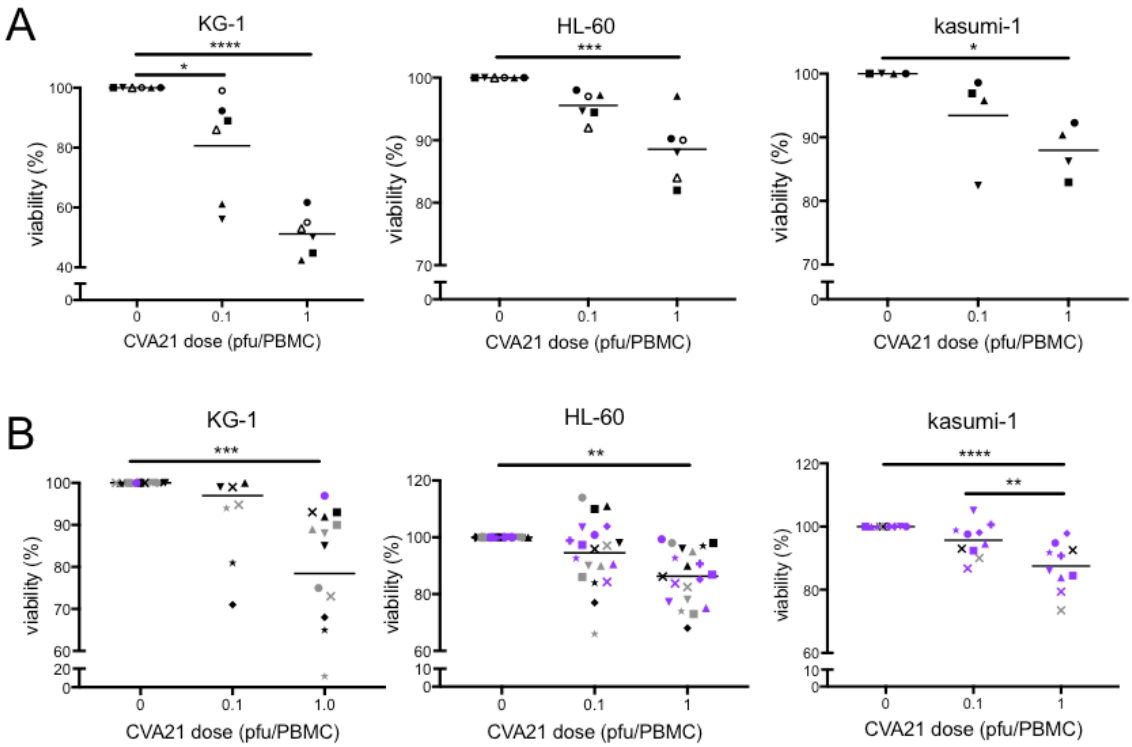

Figure 5-6: Conditioned medium from PBMCs treated with CVA21 induced a bystander killing effect on AML cell lines.

PBMCs from healthy donors (**A**) and primary AML patient samples (**B**) were harvested and treated with CVA21 (0, 0.1, or 1 pfu/cell) for 48 hrs. The conditioned culture medium (CM) was harvested and KG-1, HL-60, and kasumi-1 cells were cultured in CM (diluted 1:1 in fresh medium) for 96 hrs. Cell viability was measured using an MTS assay, each CM was tested in triplicate. Cell viability was normalised to CM from PBMCs without CVA21 treatment. **A**: CM from healthy donors, KG-1 and HL-60; n=6, kasumi-1; n=4. **B**: CM from patient samples PBMCs, KG-1; n=13, HL-60; n=20, kasumi-1; n=10. Statistical significance was calculated using one-way ANOVA with Dunnett's post-hoc test, * = p<0.05, ** = p<0.01, *** = p<0.001, **** = p<0.0001. Bars indicate the mean.

5.2.3.2 CVA21-mediated activation of NK cells enhances cellular cytotoxicity against AML cells

To further investigate the ability of CVA21 to induce innate anti-tumour immune mechanisms in AML, its effect on NK cells was next examined. The results presented in Chapter 3 demonstrated that CVA21 significantly activated NK cells from healthy donors with an upregulation in the expression of CD69 after 48 hrs of treatment (Figure 3-8C). Moreover, CVA21-activated NK cells degranulated to an enhanced extent against MM target cells and were significantly better at killing MM target cells compared to NK cells without prior CVA21 treatment (Figure 3-9E). To examine if this response could also be induced in the AML setting, NK cells from healthy donors were similarly treated with CVA21 for 48 hrs as part of the total PBMC population and were then identified as the $CD3^{-}CD56^{+}$ population by flow cytometry (Figure 3-8A). First, NK cell degranulation against AML target cells (KG-1, HL-60, THP-1, kasumi-1, and OCI-M2) following activation with CVA21 was measured as the percentage of CD107-positive NK cells following five hours of co-culture with target cells. As shown in Figure 5-7A, NK cells that were pre-treated with CVA21 degranulated significantly more against all target cells except HL-60, compared to untreated NK cells; an increase in degranulation was observed when using HL-60 cells but was not statistically significant. Overall, NK cell degranulation against AML cell targets was higher than observed in MM. OCI-M2 cells were the most susceptible target cell line with an average 55.7% of NK cells degranulating against OCI-M2 cells at the 0.1 pfu/PBMC treatment dose. Next, CVA21-treated PBMCs were included in a chromium release killing assay (Section 2.15) to evaluate whether NK cell degranulation was associated with increased killing of target cells. Pre-treating PBMCs with CVA21 caused increased lysis of all target cell lines tested, compared to untreated PBMCs, although the increase was not statistically significant for kasumi-1 cells (Figure 5-7B). The potentiation of killing was most pronounced against THP-1 cells with an average increase in lysis of 43.0% compared to using untreated PBMCs, resulting in an average of 51.5% of target cells killed. Although the increase in killing of OCI-M2 cells was smaller than for THP-1 cells, due to a higher baseline killing from untreated PBMC, the overall cell lysis remained the highest of all cell lines tested, with an average of 54.1% OCI-M2 cells lysed. The balance between engagement of activating and inhibitory receptors by target cells determines the cytotoxic response in NK cells (469), thus all cell lines were subsequently phenotyped for their expression of activating NK cell ligands using flow cytometry. The

phenotyping panel consisted of both NKG2D ligands (MIC A/B, ULBP-1, and ULBP-2/5/6), and DNAM-1 ligands (PVR and Nectin-2). As expected from the favourable response in the NK cell experiments, THP-1 (purple) and OCI-M2 cells (orange) displayed the highest expression of activating NK cell ligands overall (Figure 5-7C). Both cell lines had higher expression of MIC A/B, ULBP-1, ULBP-2/5/6, and Nectin-2, but not PVR, than KG-1, HL-60, and kasumi-1 cell lines. In addition to NK cell activation, PVR is also involved in cell motility during metastasis and invasion, and is thought to promote tumorigenesis (470, 471). As OCI-M2 cells proved to be the overall best target in the NK cell-mediated cytotoxicity experiments, these cells were chosen as the preferred target cells in subsequent NK cell experiments.

As all experiments so far were performed using PBMCs from healthy donors, the next step was to evaluate the NK cell response in the primary AML sample cohort. As expected, the percentage of NK cells in the PBMC fraction in most patient samples was much lower than in healthy donors (data not shown). Following CVA21 treatment for 48 hrs, NK cell activation and degranulation against OCI-M2 target cells was examined and, as expected, the results within the cohort were variable. Figure 5-8A shows the NK cell activation in response to CVA21 treatment. Overall, a significant increase in CD69 expression on NK cells was observed. Using a 15% increase in CD69 expression as a cut-off point, 12 out of 27 patients were classed as being able to mount an NK cell response following CVA21 treatment. The best responses were seen in samples AML-42 and AML-70, with an average increase in CD69-positive NK cells of 65.5% and 79.8%, respectively. Having identified that AML patient NK cells are activated in response to CVA21, the ability of CVA21-activated patient NK cells to degranulate against OCI-M2 targets was tested. Encouragingly, NK cells treated with CVA21 for 48 hrs degranulated significantly more against OCI-M2 target cells than untreated NK cells (Figure 5-8B). For some patients the 0.1 pfu/PBMC dose generated the best response, while for others, 1 pfu/PBMC was required to generate a more pronounced response. Both samples AML-42 and AML-70, which showed the largest increase in NK cell activation, also generated some of the best degranulation responses with a 22.2% and 25.0% increase in the number of CD107-positive NK cells following CVA21 treatment, respectively.

In an attempt to further enhance the clinical relevance of the study, autologous blast cells were next examined as NK cell targets. First, the expression of activating NK cell ligands on autologous blast cells was

examined by flow cytometry. Blast cells were identified as described in Section 5.2.1, and representative flow cytometry plots from patient sample AML-2 are shown in Figure 5-8C, demonstrating that the expression of both NKG2D and DNAM-1 ligands was low to non-existent, which was true for the majority of the samples obtained. Additionally, most samples expressed high levels of MHC Class I (HLA-ABC), which acts as an inhibitory ligand when binding to cognate NK cell receptors (469). To include autologous blast cells in the flow cytometry-based degranulation assay, untreated PBMC (including AML blasts) were kept in culture and stained with a Cell Tracker dye before inclusion in the degranulation assay together with CVA21-treated PBMCs. CD107 expression was then evaluated on unstained, CVA21-treated or untreated, NK cells. In line with the NK ligand expression profile, CVA21-activated NK cells demonstrated a limited ability to degranulate against autologous AML blasts and no significant increase in the percentage of CD107-positive cells was identified (Figure 5-8D). The most prominent response was seen in AML-49 (black X symbol) with a 9.6% increase in the percentage of CD107-positive NK cells following CVA21 treatment, compared to untreated NK cells, however; on average the increase across all samples was negligible (~1.4%). As discussed later, several options for combination treatments exist with the potential to make AML blast cells more attractive targets for NK cells and thereby improve the efficacy of CVA21 treated NK cells against AML.

In summary, the results presented in this section confirm the data previously presented in Chapter 3 in a second malignancy; AML. Similar to the MM setting, NK cells pre-treated with CVA21 degranulated against AML target cells to a significantly enhanced extent and NK cell degranulation was associated with an increase in target cell killing. Importantly, enhanced NK cell degranulation was also observed in NK cells from primary patient samples. Despite limited efficacy against autologous blast cell targets, it was encouraging that NK cells from primary samples were able to degranulate against OCI-M2 cells which have high expression of activating NK ligands. This indicated that CVA21 has the ability to potentiate the function of NK cells against AML, and that innate anti-tumour immunity may contribute to achieving treatment efficacy in this setting.

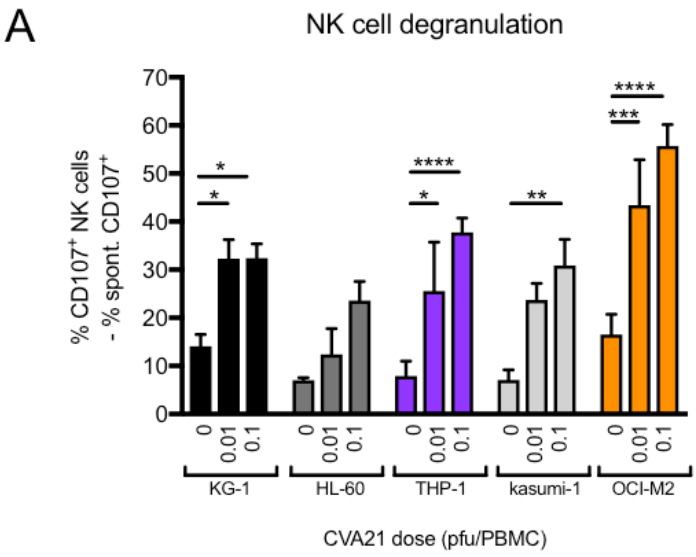
A
NK cell degranulation
% CD107+ NK cells
- % spont. CD107+
70
60
50
40
30
20
10
0
*
*
****
*
**
****
***
0
0.01
0.1
KG-1
HL-60
THP-1
kasumi-1
OCI-M2
CVA21 dose (pfu/PBMC)

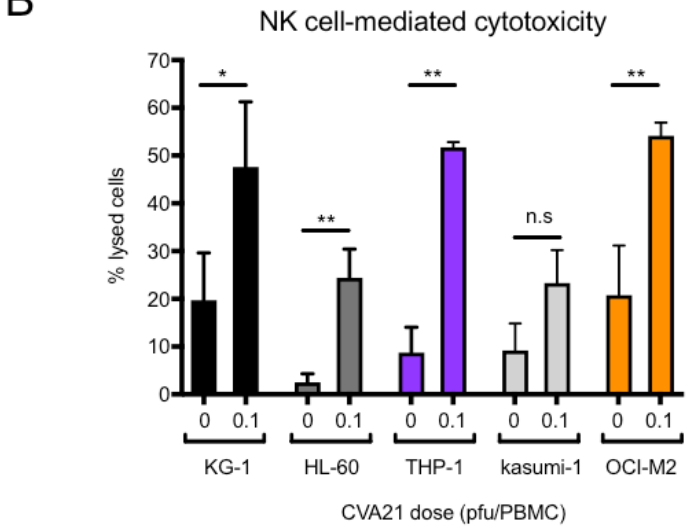
B
NK cell-mediated cytotoxicity
% lysed cells
70
60
50
40
30
20
10
0
*
**
**
**
n.s
0
0.1
KG-1
HL-60
THP-1
kasumi-1
OCI-M2
CVA21 dose (pfu/PBMC)

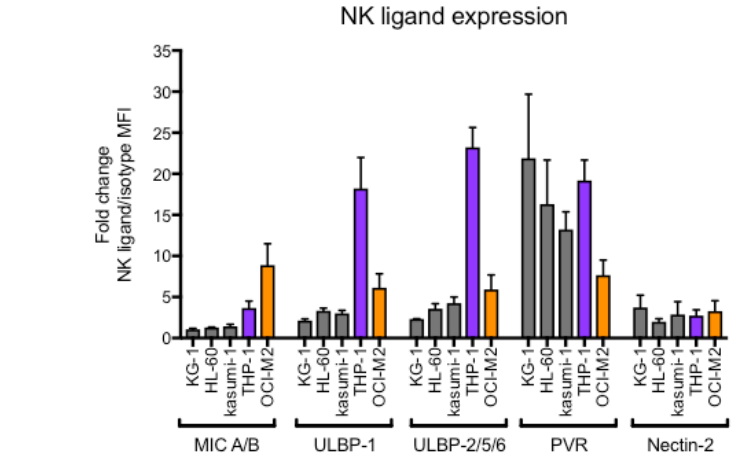
C
NK ligand expression
Fold change
NK ligand/isotype MFI
35
30
25
20
15
10
5
0
KG-1
HL-60
kasumi-1
THP-1
OCI-M2
MIC A/B
ULBP-1
ULBP-2/5/6
PVR
Nectin-2

Figure 5-7: Potentiation of NK cell-mediated cytotoxicity in healthy donors following CVA21 treatment.

A and **B**: PBMCs from healthy donors were either untreated or treated with CVA21 at the indicated doses for 48 hrs. **A**: Flow cytometry-based NK cell degranulation assay. PBMCs were co-cultured with AML target cells for 1 hr before addition of Brefeldin A, followed by another 4 hrs co-culture. Degranulation was measured as the CD107 expression on $CD3^{-}CD56^{+}$ cells (n=4). Statistical significance was calculated using one-way ANOVA and Tukey's post-hoc test. **B**: Chromium release assay. AML target cells were labelled with ^{51}Cr, then co-cultured with PBMCs at a 25:1 E:T ratio for 4 hrs. Target cell lysis was estimated using a scintillation counter, and maximum and spontaneous release controls, n=3. Statistical significance was calculated using paired, two-tailed *t*-tests. **C**: Phenotypic analysis of KG-1, HL-60, kasumi-1, THP-1, and OCI-M2 cells. The expression of activating NK ligands MIC A/B, ULBP-1, ULBP-2/5/6, PVR, and Nectin-2 was measured using flow cytometry. Expression is presented as the fold increase in MFI over an isotype control antibody (n=3). Error bars indicate s.e.m, * = $p<0.05$, ** = $p<0.01$, *** = $p<0.001$, **** = $p<0.0001$, n.s = not significant.

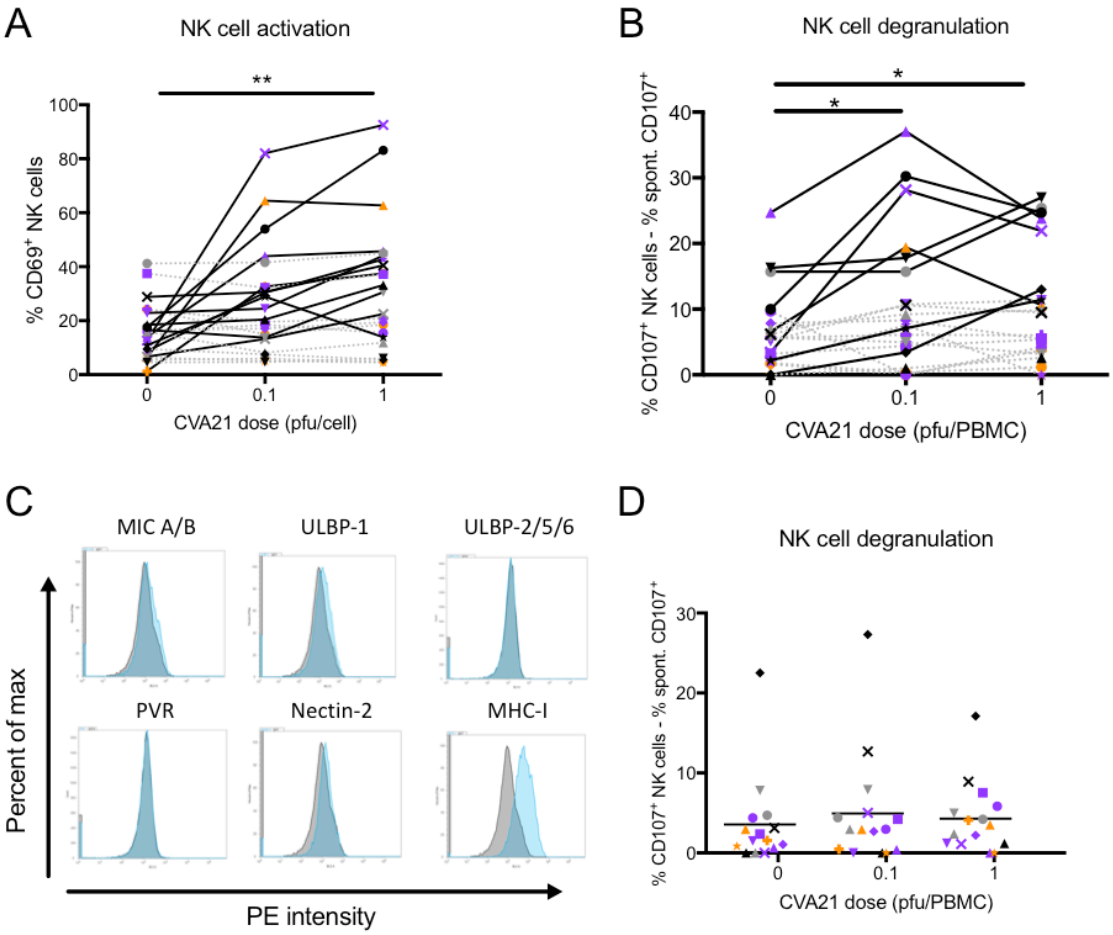

Figure 5-8: Potentiation of NK cell-mediated cytotoxicity in AML patient samples following CVA21 treatment.

A, **B**, and **D**: PBMCs isolated from peripheral blood samples from AML patients were untreated or treated with CVA21 at the indicated doses for 48 hrs. **A**: NK cell activation after 48 hrs of CVA21 treatment was estimated by measuring CD69 expression on $CD3^{-}CD56^{+}$ cells by flow cytometry (n=23). **B**: Flow cytometry-based NK cell degranulation assay. PBMCs were co-cultured with OCI-M2 target cells for 1 hr before addition of Brefeldin A, followed by another 4 hrs co-culture. Degranulation was measured as the CD107 expression on $CD3^{-}CD56^{+}$ cells (n=21). **C**: Representative flow cytometry histograms from a phenotypic analysis of AML blast cells at the time of isolation. The expression of activating NK ligands MIC A/B, ULBP-1, ULBP-2/5/6, PVR, and Nectin-2 was measured using flow cytometry. **D**: A flow cytometry-based NK cell degranulation assay was performed as described in **B**, using autologous blast cells stained with Cell Tracker Violet as target cells (n=15). Statistical significance was calculated using one-way ANOVA with Tukey's post-hoc test, * = $p<0.05$, ** = $p<0.01$.

5.2.3.3 Priming of AML-specific cytotoxic T cells using CVA21

Innate anti-tumour immune mechanisms are important for the immediate eradication of tumour cells (472, 473), but as discussed previously, an adaptive response is thought to be necessary for long-term protection against tumour recurrence (181-183). Results presented in Chapter 3 demonstrated that pre-treatment of MM cells with CVA21 resulted in priming of myeloma-specific CTLs with reactivity towards TAA commonly expressed in MM (Figure 3-17B). To examine if CVA21 could also induce the priming of AML-specific CTLs, the T cell priming protocol described in Chapter 3 was used, switching target cells to AML cell lines (Appendix, Figure A-1). Based on the results obtained in Chapter 3, which indicated that more efficient priming could be generated with oncolysis-susceptible target cells, ICAM-1-expressing KG-1 cells were first explored as target cells for the AML priming. Briefly, the protocol involved long-term culture of CVA21-treated ICAM-1-expressing KG-1 cells with conventional myeloid-derived dendritic cells (cDC) and autologous PBMC containing naïve T cells (Section 2.14.2).

First, CTLs primed using either untreated ICAM-1^+ KG-1 cells, or cells treated with 0.1 pfu/cell CVA21 for 24 hrs were included in a chromium release killing assay to examine the ability of primed CTLs to kill relevant target cells. As shown in Figure 5-9A, the CTLs generated in the presence of CVA21 were significantly better at killing KG-1 target cells than CTLs generated without prior CVA21 treatment of tumour cells. Using a 25:1 E:T ratio, an average 65.0% of target cells were lysed using CTLs primed in the presence of CVA21, compared to only 11.2% without CVA21 treatment. As a first step to examine the antigen-specificity of the primed CTLs, the degranulation of $CD8^+$ T cells in response to relevant (ICAM-1^+ KG-1) and irrelevant (Raji, non-Hodgkin lymphoma cell line) target cells was examined by flow cytometry after five hrs of co-culture at a 2:1 E:T ratio. Following co-culture, CTLs primed in the presence of CVA21 degranulated specifically against ICAM-1^+ KG-1 cells, while no potentiation of degranulation was observed against irrelevant Raji targets (Figure 5-9B). Using CTLs primed in the presence of CVA21, an average 28.4% of CTLs expressed CD107 when challenged with relevant targets, compared to only 6.2% using irrelevant target cells. Interestingly, this response was much more pronounced than in the MM setting, where only low levels of CTL degranulation could be detected when using CVA21 as the immunological agent (Figure 3-15B). To further characterise the generated CTLs, degranulation experiments were performed in the presence of an MHC Class I-blocking antibody, or an

isotype control antibody, to interrupt the interaction between the antigen-presentation molecule, MHC Class I, and the CD8 co-stimulatory molecule, necessary for CTL degranulation. While the isotype antibody control had no significant effect, blocking MHC Class I (orange) completely abrogated CTL degranulation against relevant target cells with a reduction in CD107-positive CTLs from 19.3% to 7.0% (Figure 5-9C). Taken together, these results indicated antigen-specificity of the primed CTLs and confirmed that the generated CTLs were dependent on MHC Class I recognition of antigen, characteristic of antigen-primed $CD8^+$ CTLs.

As discussed in Chapter 3, IFN-γ is a particularly important cytokine in the priming of a Th_1 response with efficient CTLs. Thus, the IFN-γ response in the priming cultures was examined. Initially, IFN-γ secretion, during the CTL priming experiments, was examined by ELISA (Section 2.12.1). As described for the MM priming cultures (Figure 3-16B), enhanced IFN-γ (average 21 600 pg/mL) secretion was observed in cultures primed in the presence of CVA21, compared to those primed without CVA21 (average 7600 pg/mL) (Figure 5-10A). However, as the difference was not statistically significant, and to confirm that IFN-γ was secreted from $CD8^+$ T cells, and not as part of an innate antiviral immune response, intracellular flow cytometry was used. Following five hours co-culture of primed CTLs with either relevant (KG-1) or irrelevant (Raji) target cells, cells were permeabilised and stained with an anti-IFN-γ antibody prior to flow cytometry analysis (Section 2.13.4). These data confirmed a significant increase in IFN-γ production following co-culture with relevant, but not irrelevant, target cells (Figure 5-10B). Using CTLs primed in the presence of CVA21, an average 7.6% of CTLs stained positive for IFN-γ after co-culture with relevant target cells, compared to only 2.1% using CTLs primed in the absence of virus. Co-culture of CVA21-primed CTLs with irrelevant targets only generated 0.2% IFN-γ-positive CTLs, further confirming the AML-specificity of *in vitro* generated CTLs.

Next, the antigen-specificity of CTLs was further explored using a peptide library generated from the PRAME protein – a TAA commonly expressed in AML. As discussed in Chapter 3, PRAME is also a commonly expressed TAA in MM, but is also expressed at high frequency in AML, and importantly on KG-1 cells (26, 474). Autologous $CD14^+$ cells were loaded with a PRAME peptide pool and subsequently co-cultured with KG-1-primed CTL at a 2:1 E:T ratio for five hours. As described above, cells were then permeabilised and stained with an anti-IFN-γ antibody for intracellular flow cytometry

analysis. Encouragingly, IFN-γ, was detected in CVA21-primed CTL when they were presented with PRAME antigen (Figure 5-10C). These data suggest that CVA21 can induce priming of CTLs against known TAA in the AML setting.

Two interesting questions related to CTL priming using CVA21 where highlighted in Chapter 3; the ability to efficiently prime CTLs despite very little maturation of DC induced by CVA21 (Figure 3-12B), and whether direct oncolysis is required for efficient priming (Figure 3-18). To further explore these questions, CTL priming was first performed without inclusion of autologous iDCs. As CVA21 treatment did not induce maturation of DCs, it was hypothesised that DCs might be dispensable for CVA21 priming. ICAM-1-expressing KG-1 target cells were treated with 0.1 pfu/cell CVA21 for 24 hrs as previously described, free virus was then removed and target cells were cultured for a further 48 hrs before addition to PBMCs containing naïve T cells. Subsequently, primed CTLs were included in chromium release killing assays and CTL degranulation assays, as previously described. Interestingly, as shown in Figure 5-11A, exclusion of DCs from the priming assay had no effect on the ability of primed CTLs to kill relevant target cells. At the 25:1 E:T ratio, the average target cell lysis achieved with CTLs primed using autologous DCs was 62.1%, compared to 54.1% without DCs. Furthermore, upon assessment of CTL degranulation CTLs primed without DCs, using CVA21-treated ICAM-1$^+$ KG-1 cells, degranulated significantly more against relevant targets than CTLs primed with untreated targets cells (19.2% CD107-positive CTLs, compared to 4.9%), and levels were comparable to those obtained using CTLs primed using DCs (Figure 5-11B). Importantly, no significant degranulation against irrelevant Raji cells was observed, confirming the antigen-specificity of CTLs primed without addition of autologous *in vitro* generated DCs.

As ICAM-1-transduced KG-1 cells susceptible to CVA21 oncolysis were used in CTL experiments presented so far, CTLs were next generated using parental KG-1 and THP-1 cells, both resistant to CVA21-mediated oncolysis, to explore the requirement for OV susceptibility. In Chapter 3, priming against CVA21-resistant OPM2 cells was unsuccessful as primed CTLs were unable to recognise and kill relevant OPM2 targets (Figure 3-18D). As shown in Figure 5-1D, CVA21 was able to enter and replicate at low levels in KG-1 cells, but not in THP-1 cells, which is similar to the OPM2 response to CVA21 (225). Initially, the priming protocol was used as originally described, including autologous DCs (Appendix, Figure A-1), and the primed CTLs

were examined using CTL degranulation assays. Encouragingly, CTLs with the ability to degranulate specifically against relevant (KG-1 or THP-1, respectively), but not irrelevant (Raji), target cells were successfully generated with both parental KG-1 cells (Figure 5-11C), and THP-1 cells (Figure 5-11D). Interestingly, using CTLs primed against parental KG-1 cells in the presence of CVA21, the average percentage of CD107-positive CTLs following co-culture with relevant targets was 13.7%, which was lower than the degranulation achieved using the CVA21 susceptible ICAM-1$^+$ KG-1 (28.4% CD107-positive CTLs). Moreover, with CTLs primed against THP-1 cells, in the presence of CVA21, a total of 17.2% of CTLs degranulated against relevant target cells (Figure 5-11D). Although degranulation levels were reduced, these data suggest that efficient priming of tumour-specific CTLs is possible in cells which are less permissive to CVA21 infection and oncolysis.

In summary, the results presented in this section have demonstrated that CVA21 can induce the priming of AML-specific CTLs. These CTLs display pronounced cytotoxicity against relevant target cells in an antigen-dependent manner, with CTL degranulation and specific secretion of IFN-γ. Moreover, primed CTLs recognised a commonly expressed TAA in AML when presented as a peptide pool on autologous CD14$^+$ cells. These results confirm and strengthen those obtained in Chapter 3, which also demonstrated successful priming of tumour-specific CTLs in the MM model. Furthermore, questions raised in Chapter 3 were explored by priming CTLs in the absence of autologous DC, as well as using oncolysis-resistant target cells. Both methods generated efficient antigen-specific CTLs, suggesting that conventional DCs may be of little importance for successful priming using CVA21, and that oncolysis may not be absolutely necessary for the induction of anti-tumour immunity. Given that conventional DC were not necessary for priming of anti-tumour specific CTLs, and little is known about CVA21 interaction with the human immune system, the cellular mechanisms responsible for the anti-tumour immunity induced by CVA21 were explored.

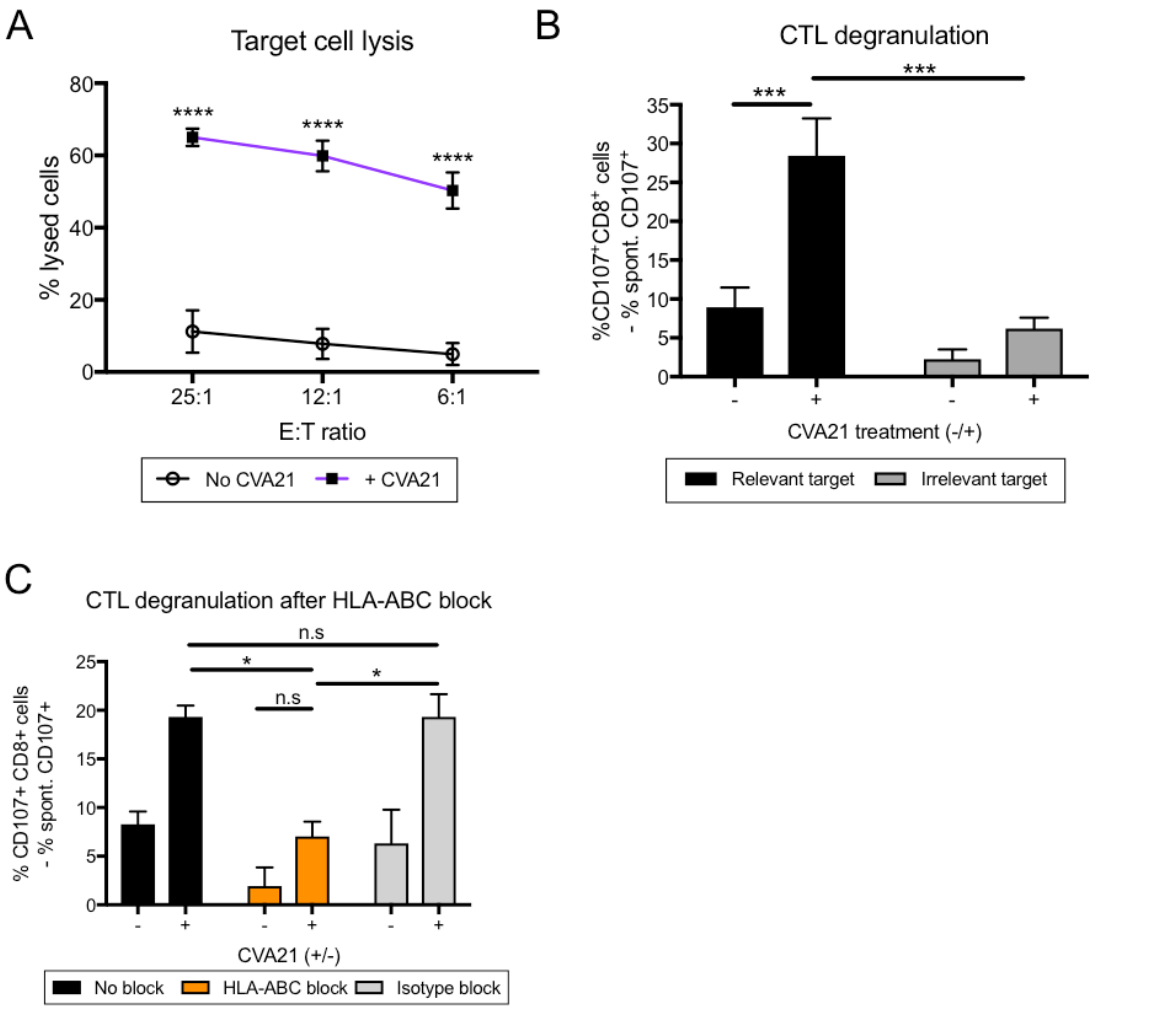

Figure 5-9: Priming of AML-specific CTLs using CVA21.

Primed CTLs were generated after co-culturing PBMC with autologous DC, pre-loaded with ICAM-1$^+$ KG-1 cells treated with 0.1 pfu/cell CVA21 for 24 hrs. Following one re-stimulation with CVA21/ICAM-1$^+$ KG-1-loaded DC, primed CTLs were examined in a chromium release assay (**A**) and CTL degranulation assays (**B** and **C**). **A**: CTLs generated with (purple) or without (black) CVA21 were co-cultured with ^{51}Cr-labelled relevant (ICAM-1$^+$ KG-1) target cells for 4 hours at different effector:target ratios. The percentage of cell lysis was determined after 4 hours (n=6). Statistical significance was calculated using two-way ANOVA with Tukey's post-hoc test. **B**: PBMCs primed in the presence (+) or absence (-) of CVA21 were co-cultured with relevant (ICAM-1$^+$ KG-1) or irrelevant (Raji) target cells at a 2:1 effector:target ratio for 1 h, followed by another 4 hrs incubation in the presence of Brefeldin A. Surface expression of CD107a/b was measured by flow cytometry on CD3$^+$CD8$^+$ CTL (n=6). **C**: CTL degranulation assay as performed in **B** following pre-incubation of relevant target cells with either HLA-ABC-blocking antibodies (orange) or an isotype control (n=3). Statistical significance in **B** and **C** was calculated using one-way ANOVA with Tukey's post-hoc test, * = p<0.05, *** = p<0.001, **** = p<0.0001, n.s = not significant. Error bars indicate s.e.m.

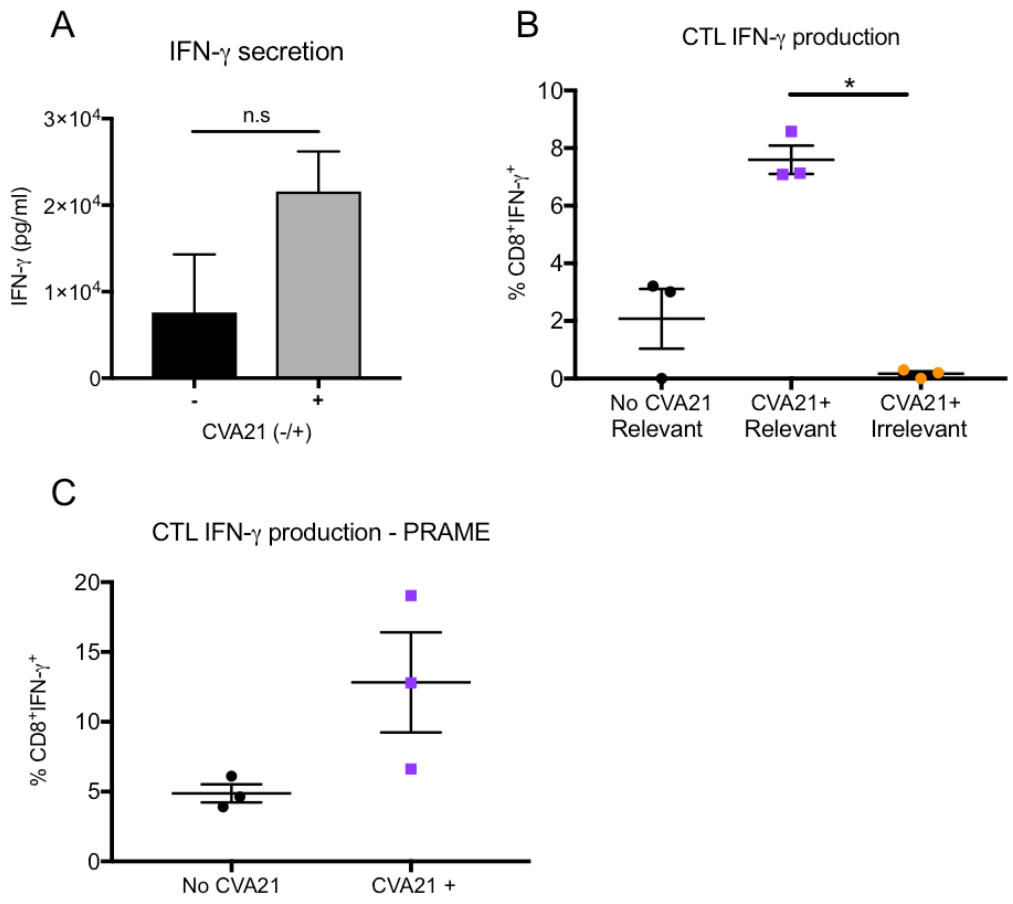

Figure 5-10: IFN-γ secretion from AML-specific CTLs following antigen recognition.

A: IFN-γ secretion into culture medium was measured at the end of the priming protocol using an ELISA with matched paired antibodies (n=4). **B** and **C**: Intracellular IFN-γ in CTLs ($CD3^+CD8^+$) generated using CVA21-treated ICAM-1^+ KG-1 cells was measured by flow cytometry after permeabilization of cells with saponin and staining with an anti-IFN-γ antibody. **B**: PBMCs primed in the presence of CVA21 (n=3) were co-cultured with relevant (ICAM-1^+ KG-1) or irrelevant (Raji) target cells at a 2:1 effector:target ratio for 1 h, followed by another 4 hrs incubation in the presence of Brefeldin A. **C**: Autologous $CD14^+$ cells were loaded with a PRAME peptide pool (1 hr at 37°C) and co-cultured with PBMC primed using ICAM-1^+ KG-1 in the presence or absence of CVA21. Statistical significance was calculated using paired, two-tailed *t*-tests, * = $p<0.05$, n.s = not significant. Error bars indicate s.e.m.

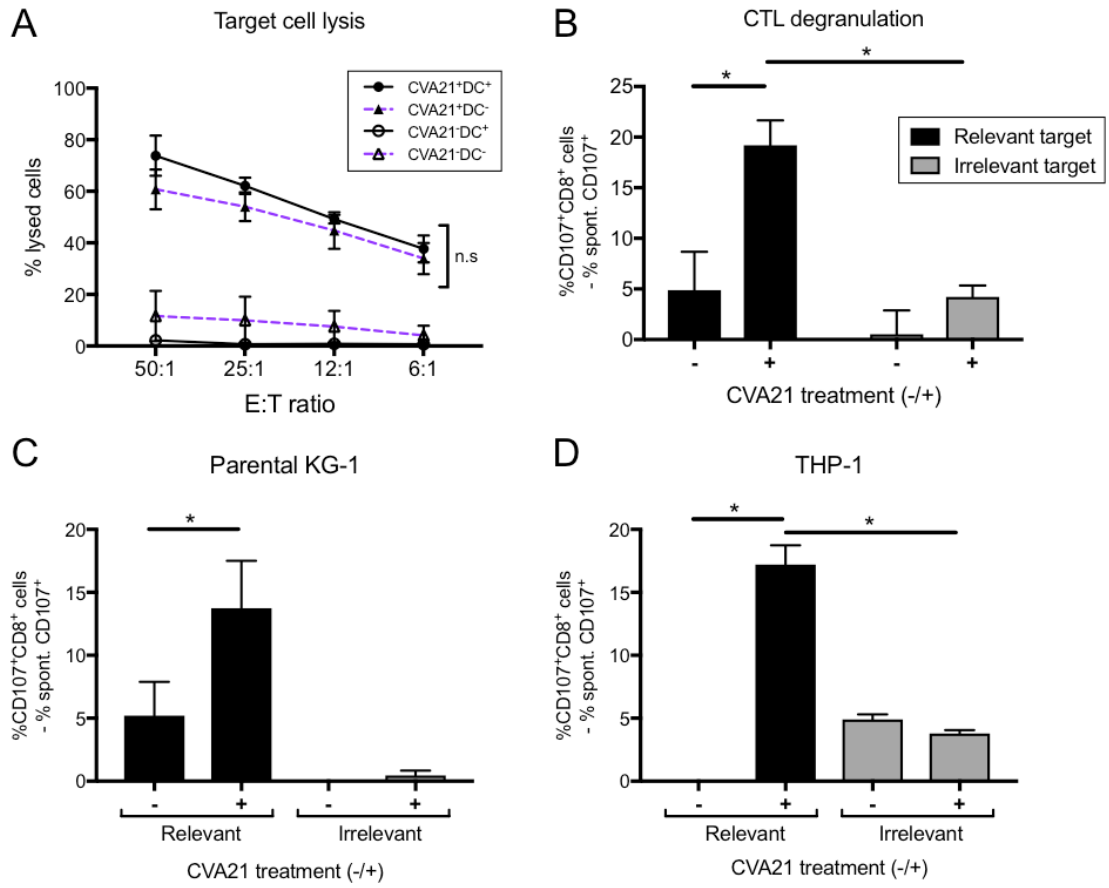

Figure 5-11: Priming of AML-specific CTLs without addition of DC, or using target cells not susceptible to CVA21-mediated oncolysis.

A and **B**: ICAM-1$^+$ KG-1 were treated with 0.1 pfu/cell CVA21 for 24 hrs, then virus was washed off and cells were incubated for another 48 hrs. Primed CTLs were generated after co-culturing PBMCs with untreated or CVA21-treated ICAM-1$^+$ KG-1 cells. Following one re-stimulation with ICAM-1$^+$ KG-1 (with or without prior CVA21 treatment), primed CTLs were examined in a chromium release assay (**A**) and a CTL degranulation assay (**B**). **A**: CTLs generated with (black) or without (purple) autologous DC were co-cultured with ^{51}Cr-labelled relevant (ICAM-1$^+$ KG-1) target cells for 4 hours at different effector:target ratios. The percentage of cell lysis was determined after 4 hours (n=3). *p*-value >0.05 for comparison of DC$^+$ and DC$^-$ at each E:T ratio was calculated using two-way ANOVA with Tukey's post-hoc test. **B**: PBMCs primed without addition of autologous DC in the presence (+) or absence (-) of CVA21 were co-cultured with relevant (ICAM-1$^+$ KG-1) or irrelevant (Raji) target cells at a 2:1 effector:target ratio for 1 h, followed by another 4 hrs incubation in the presence of Brefeldin A. Surface expression of CD107a/b was measured by flow cytometry on CD3$^+$CD8$^+$ CTL (n=3). **C** and **D**: Primed CTLs were generated after co-culturing PBMC with autologous DC, pre-loaded with parental KG-1 cells (**C**) or THP-1 cells (**D**) treated with 0.1 pfu/cell CVA21 for 24 hrs. Following one re-stimulation with CVA21/target cell-loaded DC, primed CTLs were examined using CTL degranulation assays as described in **B**. Statistical significance in **B**-**D** was calculated using one-way ANOVA with Tukey's post-hoc test, * = p<0.05, n.s = not significant. Error bars indicate s.e.m.

5.2.4 Cellular mechanisms of CVA21-mediated induction of anti-tumour immunity

The results presented so far have demonstrated that an anti-tumour immune response can be initiated by CVA21 in both MM and AML. As very little is known about the immunobiology of CVA21 and the mechanisms behind activation of the anti-tumour immune response, this was explored using the AML model to exclude the effect of direct oncolysis during the experiments. The first step in elucidating the mechanisms behind induction of anti-tumour immunity was to examine the ability of CVA21 to directly activate NK cells in isolation. $CD56^+$ cells were isolated from healthy donor PBMCs using magnetic cell separation, and then treated with 0.1 or 1 pfu/cell CVA21 for 48 hrs as previously described for PBMCs. CD69 expression was measured using flow cytometry, which confirmed that CVA21 was inefficient at directly activating NK cells (Figure 5-12A). Thus, it was hypothesized that the CVA21-mediated anti-tumour immune mechanisms are initiated by cross-talk with another cell type in the PBMC population. The most likely candidate for immune activation in the scenario of a viral infection is type I IFN, but the lack of activation of isolated NK cells suggested another cell type was responsible for the production of this cytokine. To further investigate this, the importance of type I IFNs for the induction of anti-tumour immunity was explored.

5.2.4.1 The importance of IFN-α for CVA21-mediated anti-tumour immunity

While experiments in both this chapter and in Chapter 3 confirmed the direct toxic effect of IFN-α on tumour cells, the main role of type I IFNs is to initiate an antiviral response by recruiting immune cells and inducing a protective antiviral state in healthy cells (179, 461). To confirm the importance of type I IFNs for the CVA21-mediated NK cell response, NK cell activation and degranulation was examined in the presence or absence of a type I IFN-blocking antibody cocktail (Section 2.9). Briefly, PBMCs were pre-treated with blocking antibodies against both the IFNA2 receptor, soluble IFN-α, and soluble IFN-β (or an isotype control mix) before treatment with CVA21 for 24 hrs. Figure 5-12B shows NK cell activation as measured by CD69 expression. When both the IFNA2 receptor and soluble IFN-α and IFN-β were inhibited, CVA21 treatment did not induce significant activation of NK cells (purple bars). At the 1 pfu/PBMC CVA21 dose, 84.4% of NK cells expressed CD69 in the absence of blocking antibody treatment while CD69

expression was reduced to just 20.2% in the presence of type I IFN-blocking antibodies. By contrast, when PBMCs were pre-treated with the isotype control antibody mix, NK cell activation was similar to levels observed for PBMCs without pre-treatment.

To further confirm the role for type I IFNs, NK cell degranulation against OCI-M2 cells was examined following pre-treatment of PBMCs with the blocking antibody mix, isotype control mix, or culture medium alone, prior to treatment with 0.1 pfu/cell CVA21 for 24 hrs. Consistent with the previous data, NK cells treated with CVA21 degranulated to a significant extent against OCI-M2 target cells, with an average 32.1% CD107-positive NK cells (Figure 5-12C). Furthermore, the potentiation in NK cell degranulation was completely lost in the presence of type I IFN-blocking antibodies, with a reduction in CD107-positive NK cells to just 9.5%. As expected, the degranulation response was not affected by pre-treatment with the isotype control antibody mix. Interestingly, a correlation calculation (Figure 5-12C) confirmed that enhanced NK cell degranulation of primary patient NK cells following CVA21 treatment (Figure 5-8B) significantly correlated with IFN-α secretion in these samples (Figure 5-5A, p=0.0009, Pearson's r=0.74), further indicating IFN-α secretion as a crucial factor for NK cell activation in response to CVA21.

In summary, these experiments confirmed the importance of type I IFNs for the initiation of CVA21-mediated NK cell anti-tumour immunity in healthy donors, with indication that this might also be true in primary AML samples. The next step in identifying the cell type responsible for initiating the anti-tumour immune response was to examine the importance of ICAM-1 expression for the onset of anti-tumour immunity.

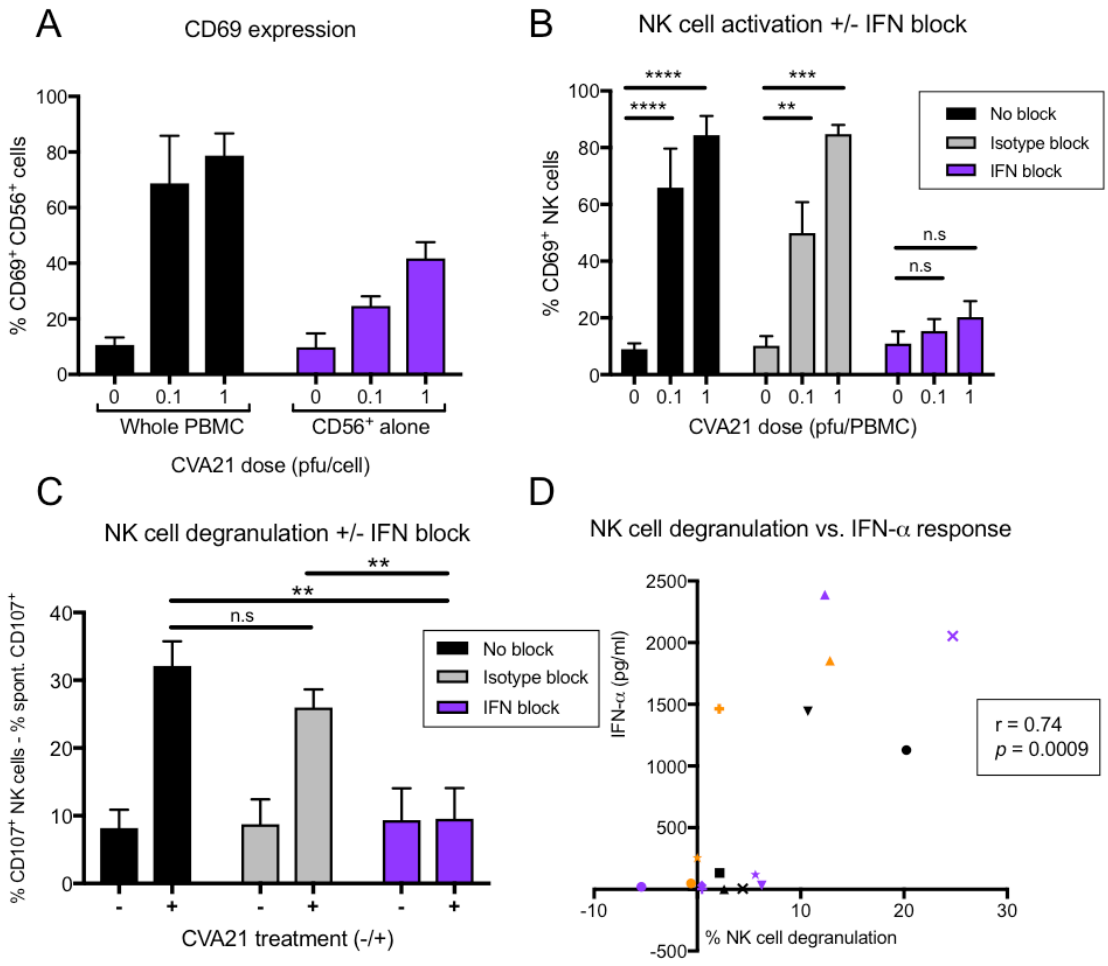

Figure 5-12: Secretion of type I IFNs is crucial for CVA21-mediated potentiation of NK cell-mediated cytotoxicity.

A: Whole PBMC or $CD56^+$ cells alone (purple), isolated using magnetic cell separation, were treated with CVA21 (0, 0.1, or 1 pfu/cell) for 48 hrs. NK cell activation was estimated by measuring CD69 expression on $CD3^-CD56^+$ cells using flow cytometry (n=2). **B** and **C**: PBMC were either untreated, pre-treated with a type I IFN-blocking antibody cocktail (purple), or corresponding isotype control antibodies (grey) for 30 min. All PBMCs were treated with CVA21 as indicated (+ = 0.1 pfu/cell) for 24 hrs, then NK cell activation (**B**) and degranulation (**C**) was measured. Statistical significance was measured using one-way ANOVA with Tukey's post-hoc test. **B**: CD69 expression measured on $CD3^-CD56^+$ cells using flow cytometry (n=4). **C**: Expression of CD107a/b on NK cells following co-culture with OCI-M2 target cells (2:1 E:T ratio) for 1 h, then in the presence of Brefeldin A for 4 hrs, was measured by flow cytometry (n=3). **D**: Correlation of IFN-α secretion in response to CVA21 from PBMCs isolated from AML patient samples and the percentage of NK cell degranulation against OCI-M2 target cells following CVA21 treatment (n=16). Error bars indicate s.e.m, ** = $p<0.01$, *** = $p<0.001$, **** = $p<0.0001$, n.s = not significant.

5.2.4.1 The importance of ICAM-1 for CVA21-mediated anti-tumour immunity

As discussed, ICAM-1 has been confirmed as the entry receptor required for CVA21 entry into host tumour cells (279, 397), but its importance for immune detection of CVA21 has not been examined to date. Thus, similar to the experiments performed in the previous section, the NK cell response to CVA21 treatment was evaluated in the presence or absence of an ICAM-1-blocking antibody (Section 2.10). PBMCs were pre-treated with the ICAM-1-blocking antibody or an isotype control antibody, and then treated with 0.1 or 1 pfu/PBMC CVA21 for 24 hrs. Without pre-treatment, or with pre-treatment using the isotype control antibody, the percentage of CD69-positive NK cells reached similar levels as observed in previous experiments (69.2% and 67.9%, respectively). However, when PBMCs were pre-treated with the ICAM-1-blocking antibody, CVA21 was unable to induce CD69 expression on NK cells (Figure 5-13A).

Next, the secretion of IFN-α from PBMCs in response to CVA21 was measured, with or without pre-treatment with the ICAM-1-blocking antibody. Cell-free supernatants were harvested from cell cultures and examined by ELISA (Section 2.12.1). In the absence of ICAM-1 blockade, PBMCs secreted an abundance of IFN-α (Figure 5-13B), which was also demonstrated in Chapter 3 (Figure 3-4B). However, when CVA21 was not able to interact with ICAM-1 following pre-treatment of PBMCs with the ICAM-1-blocking antibody, IFN-α secretion was completely abrogated (Figure 5-13B). Taken together, these findings suggested that ICAM-1 expression is not only necessary for tumour cell entry of CVA21, but also for entry into immune cells and initiation of the IFN-α antiviral response.

The importance of ICAM-1 for CVA21 efficacy was further confirmed by analysing the ICAM-1 expression on mature haematopoietic cells ($CD45^+$) in the AML primary sample cohort using flow cytometry. Figure 5-14A shows that mature immune cells in the primary samples expressed ICAM-1, with some variability between samples (mean 2.6-fold higher expression than isotype control). Interestingly, the level of ICAM-1 expression on mature immune cells significantly correlated with the overall death of AML blasts in the primary samples (Figure 5-14B, p=0.009, Pearson's r=0.67). This suggested that patients with higher ICAM-1 expression on functional immune cells, and therefore increased ability to detect CVA21 and initiate an antiviral immune response, have a better response to CVA21 treatment.

Lastly, to more specifically determine the cell types that might be responsible for the induction of an antiviral, and subsequent anti-tumour immune response following CVA21 treatment, ICAM-1 expression on different immune cell populations was examined by flow cytometry. Before ICAM-1 phenotyping, the pDC population was enriched using magnetic cell separation (Section 2.11.2), the other, more common cell types were identified using antibodies described in Table 2-4. As shown in Figure 5-14C, this experiment demonstrated that $CD14^+$ monocytes and pDC express significantly more ICAM-1 than NK cells, $CD4^+$ T cells and $CD8^+$ T cells. Over 97.0% of both $CD14^+$ monocytes and pDC expressed ICAM-1, compared to 25.6% of NK cells, 49.7% of $CD4^+$ T cells, and 44.4% of $CD8^+$ T cells, highlighting monocytes and pDC as the most interesting candidates to explore further.

Collectively, the data presented have demonstrated the requirement for IFN-α secretion and ICAM-1 expression on PBMCs for the generation of an NK cell-mediated anti-tumour immune response by CVA21. Moreover, ICAM-1 phenotyping implicated $CD14^+$ monocytes and pDC as the cell populations with the highest expression of ICAM-1. Both these cells types are known to be avid secretors of IFN-α (138, 475-477) and thus, $CD14^+$ monocytes and pDC were examined for their role in coordinating the anti-tumour immune response induced by CVA21.

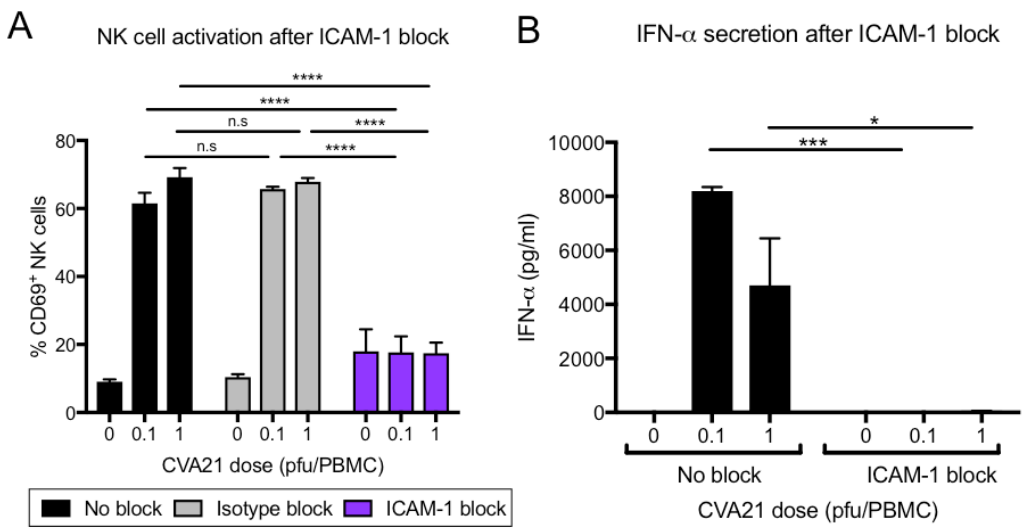

Figure 5-13: ICAM-1 expression is crucial for CVA21-mediated potentiation of NK cell-mediated cytotoxicity.

PBMC were either untreated, pre-treated with an ICAM-1-blocking antibody (purple), or an isotype control antibody (grey) for 30 min. Subsequently, PBMCs were treated with CVA21 (0, 0.1, or 1 pfu/cell) for 24 hrs, then NK cell activation (**A**) and IFN-α secretion (**B**) was measured. **A**: CD69 expression measured on $CD3^-$ $CD56^+$ cells using flow cytometry (n=3). **B**: Cell-free supernatants were harvested from PBMCs following CVA21 treatment for 24 hrs and IFN-α secretion was measured by ELISA using matched paired antibodies. Statistical significance was calculated using one-way ANOVA with Tukey's post-hoc test, * = $p<0.05$, *** = $p<0.001$, **** = $p<0.0001$, n.s = not significant. Error bars indicate s.e.m.

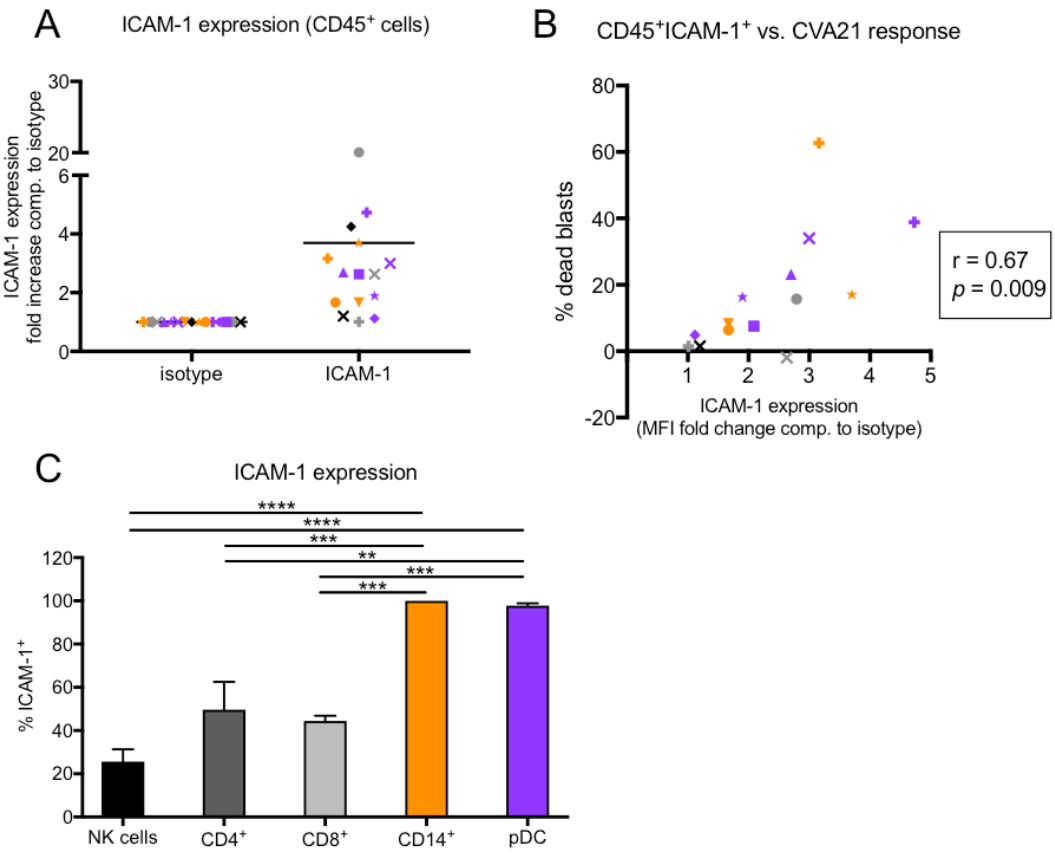

Figure 5-14: ICAM-1 expression on immune cells from healthy donors and primary AML samples.

A: PBMCs were isolated from peripheral blood samples obtained from AML patients and ICAM-1 expression on mature haematopoietic cells ($CD45^+$) was measured at the time of isolation using flow cytometry (n=15). ICAM-1 expression is presented as the fold increase in MFI compared to an isotype control antibody. **B**: Correlation of ICAM-1 expression on $CD45^+$ cells in primary patient samples and the percentage of dead blast cells following CVA21 treatment (n=14). **C**: PBMC were isolated from peripheral blood samples obtained from healthy donors and ICAM-1 expression was measured on NK cells ($CD3^-CD56^+$), $CD4^+$ T cells ($CD3^+CD4^+$), $CD8^+$ T cells ($CD3^+CD8^+$), $CD14^+$ monocytes, and pDC ($CD123^+CD303^+$) using flow cytometry (n=4). pDC were enriched using magnetic cell separation before flow cytometry staining. ICAM-1 expression is presented as the percentage of $ICAM\text{-}1^+$ cells. Statistical significance was calculated using a one-way ANOVA with Tukey's post-hoc test, ** = $p<0.01$, *** = $p<0.001$, **** = $p<0.0001$. Error bars indicate s.e.m.

5.2.4.2 Plasmacytoid dendritic cells orchestrate innate and adaptive anti-tumour immunity induced by CVA21

As discussed, both monocytes and pDC are important components in the innate immune response and avid secretors of IFN-α, which often kick-starts the innate immune response (138, 342, 461, 475, 477). The main roles of monocytes in the innate immune response are phagocytosis of antigens and ADCC (478-480). pDC can be developed via both lymphoid and myeloid differentiation routes and are innate sensors of viral infection by employment of TLR7 and -9, resulting in the secretion of IFN-α (481, 482). Both monocytes and pDC are able to activate NK cells in response to viral infection (483). To elucidate the role of $CD14^+$ monocytes and pDC, respectively, for the induction of anti-tumour immunity by CVA21, whole PBMCs were depleted of either $CD14^+$ monocytes, pDC, or both, using magnetic cell separation (Figure 5-15 and Section 2.11). Both whole and depleted PBMCs were then used in the experiments to evaluate the effect on both innate and adaptive anti-tumour immunity.

First, IFN-α secretion in response to CVA21 treatment was examined under the different conditions. PBMCs from healthy donors were either depleted of $CD14^+$ cells, pDC, or both, and were then treated with CVA21 for 48 hrs as previously described. Cell-free supernatants were harvested and the amount of IFN-α secreted in each culture was measured by ELISA (Section 2.12.1). This indicated that depletion of pDC significantly reduced the amount of IFN-α secreted, while depletion of $CD14^+$ monocytes had no significant effect on IFN-α levels (Figure 5-16A). Using whole PBMC, an average 6530 pg/mL IFN-α was secreted in response to 0.1 pfu/PBMC CVA21. Without $CD14^+$ monocytes the amount of secreted IFN-α remained at an average 7120 pg/mL. However, without pDC present, IFN-α levels were reduced to 1080 pg/mL, and similarly using double-depleted PBMCs to 1270 pg/mL. Accordingly, pDC in isolation (orange bars) secreted large amounts of IFN-α in response to 1 pfu/cell CVA21 (average 5990 pg/mL) while $CD14^+$ cells in isolation only secreted minimal amounts (average 310 pg/mL). This strongly implied pDC as the source of IFN-α in response to CVA21 treatment.

To further evaluate the importance of pDC in anti-tumour immunity, the various depleted PBMC populations were included in CM, NK cell, and CTL priming experiments, respectively. First, the toxicity of CM generated using whole, or depleted, PBMC populations was examined. Cell free-CM was collected from various PBMC populations following CVA21 treatment for 48 hrs, and HL-60 and kasumi-1 cells were cultured in CM diluted 1:1 in fresh

medium for 96 hrs (Figure 3-5A). Cell viability was estimated using an MTS assay (Section 2.8). As demonstrated in Figure 5-16, and consistent with the data presented in Section 5.2.3.1, CM from whole PBMC treated with CVA21 was toxic to both HL-60 (Figure 5-16B) and kasumi-1 (Figure 5-16C) cells, with a significant reduction in viability (W.PBMC + CVA21). Despite some variability, depletion of $CD14^+$ cells had no significant effect on CM toxicity on either cell line. However, CM generated in the absence of pDC (purple bars), or the absence of both pDC and $CD14^+$ cells, lost its cytotoxic potential against both HL-60 and kasumi-1 cells. For example, the viability of HL-60 and kasumi-1 cells was similar to levels observed following treatment with CM generated in the absence of CVA21 treatment (W.PBMC). These results suggested that pDC were crucial for the induction of the innate anti-tumour immune response mediated by CVA21-CM, with $CD14^+$ monocytes being dispensable in this context.

Next, the role of monocytes and pDC, respectively, in NK cell-mediated anti-tumour immunity was examined. NK cell experiments, including NK cell activation and degranulation, were repeated using whole PBMC and PBMC depleted of $CD14^+$ monocytes, pDC, or both. PBMCs were treated with CVA21 for 48 hrs and NK cell activation was estimated by measuring CD69 expression on NK cells using flow cytometry. As outlined in Figure 5-17A, a significant increase in CD69 expression on NK cells was confirmed in response to CVA21 treatment of whole PBMC. Depleting PBMC of $CD14^+$ cells again had no effect and the increase in CD69 expression remained similar to that observed for whole PBMC (11-fold increase compared to untreated NK cells). However, as depicted in the purple bars, depletion of pDC from the PBMC population resulted in a significant reduction in NK cell activation in response to CVA21 treatment. For example, at the 0.1 pfu/PBMC dose of CVA21, the fold increase in CD69 expression over untreated PBMCs was just 2.4 in the absence of pDC. Using double-depleted PBMC, the results were similar, with a complete loss of NK cell activation in response to CVA21 treatment. Additionally, NK cell degranulation assays were also performed using OCI-M2 cells as target cells (Section 2.13.3). Using whole PBMCs treated with CVA21, the percentage of CD107-positive NK cells following co-culture with OCI-M2 cells was an average 35.2% (Figure 5-17B) and depletion of $CD14^+$ monocytes had no effect on NK cell degranulation, with an average 40.4% CD107-positive cells. By contrast, depletion of pDC, or double-depleted cultures, had more dramatic consequences with a significant reduction in NK cell degranulation to 21.8% and 19.0%, respectively. These experiments

again unanimously indicated the importance of pDC for successful induction of anti-tumour immunity and were consistent with the importance of both IFN-α and ICAM-1 for both NK cell activation and degranulation (Figure 5-12 and Figure 5-13), as pDC were confirmed as the main producers of IFN-α in response to CVA21 treatment.

Lastly, the importance of pDC for adaptive anti-tumour immunity was evaluated by repeating T cell priming experiments using whole PBMCs, and PBMCs depleted of either $CD14^+$ cells or pDC. The CTL priming protocol with ICAM-1-expressing KG-1 cells was used, excluding autologous DCs (Appendix, Figure A-1), but before addition of autologous PBMCs containing the naïve T cells, $CD14^+$ monocytes or pDC were depleted from the PBMCs. As demonstrated previously (Figure 5-9B), CTLs primed in the presence of CVA21 were significantly better at recognising, and degranulating against, relevant ($ICAM\text{-}1^+$ KG-1) target cells than CTLs primed without CVA21 (Figure 5-18). An average 17.0% of $CD8^+$ T cells, primed in the presence of CVA21, expressed CD107 following co-culture with relevant targets, compared to only 3.7% of $CD8^+$ T cells primed in the absence of CVA21 treatment. When PBMCs without $CD14^+$ cells were used, CTLs responsive to relevant targets were generated at a similar frequency with 13.7% of CVA21-primed $CD8^+$ T cells degranulating against relevant targets. However, depletion of pDC during the course of the CTL priming assays significantly reduced the efficiency of CTL priming (purple bar), for example, following pDC depletion only 7.0% of CVA21-primed $CD8^+$ T cells degranulated against relevant targets, a percentage similar to that observed for CTLs primed in the absence of CVA21. While this, in accordance with published literature (484, 485), suggests an important role for IFN-α for cross-priming of $CD8^+$ T cells, the exact role of the pDC in the CTL priming system has not been established in this study. However, the fact that exclusion of conventional DCs from priming cultures had no effect on priming efficiency (Figure 5-11 A and B) indicates that another cell type, such as pDC, may be acting as the APC in this system.

In summary, this section has introduced pDC as the predominant cell type for inducing anti-tumour immunity in response to CVA21 treatment. When pDC were depleted from PBMCs, CM toxicity, NK cell-mediated killing, and priming of tumour-specific CTLs were abrogated. Likely, CVA21 utilises ICAM-1 on the surface of pDC, and following cell entry CVA21 ssRNA is recognised by TLR7 in the endosomes of pDC (486, 487). This initiates a signalling cascade resulting in the secretion of large amounts of IFN-α

which, through its downstream effects, mediates anti-tumour immunity mechanisms including CM-mediated bystander killing, NK cell-mediated killing, and priming of tumour-specific CTLs.

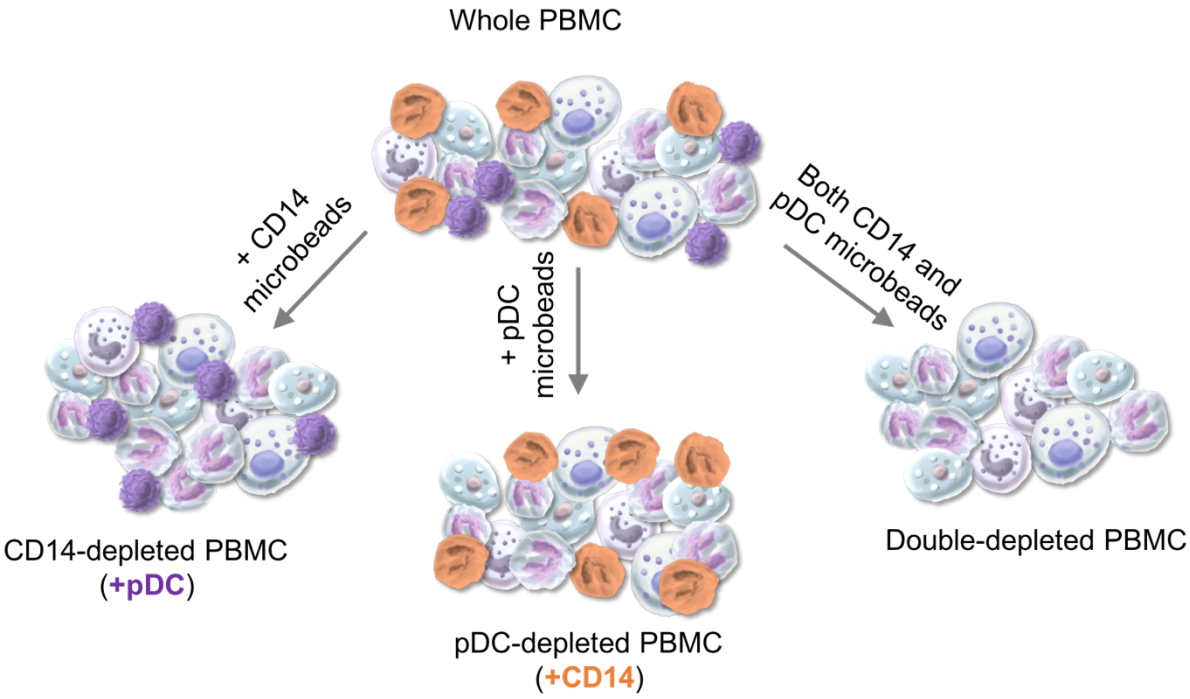

Figure 5-15: Schematic showing depletion of $CD14^+$ cells, pDC, or both from whole PBMC.

Using magnetic cell sorting, whole PBMC were depleted of either $CD14^+$ cells (orange), pDC (purple), or both. $CD14^+$-depleted PBMC contained pDC but not $CD14^+$ cells (left), pDC-depleted cells contained $CD14^+$ cells but no pDC (middle), and double-depleted PBMC were depleted of both $CD14^+$ cells and pDC (right). $CD14^+$ cells were removed using a positive selection with $CD14^+$-specific microbeads, pDC were removed by negative selection using a non-pDC biotin-conjugated antibody and biotin-specific microbeads (Section 2.11).

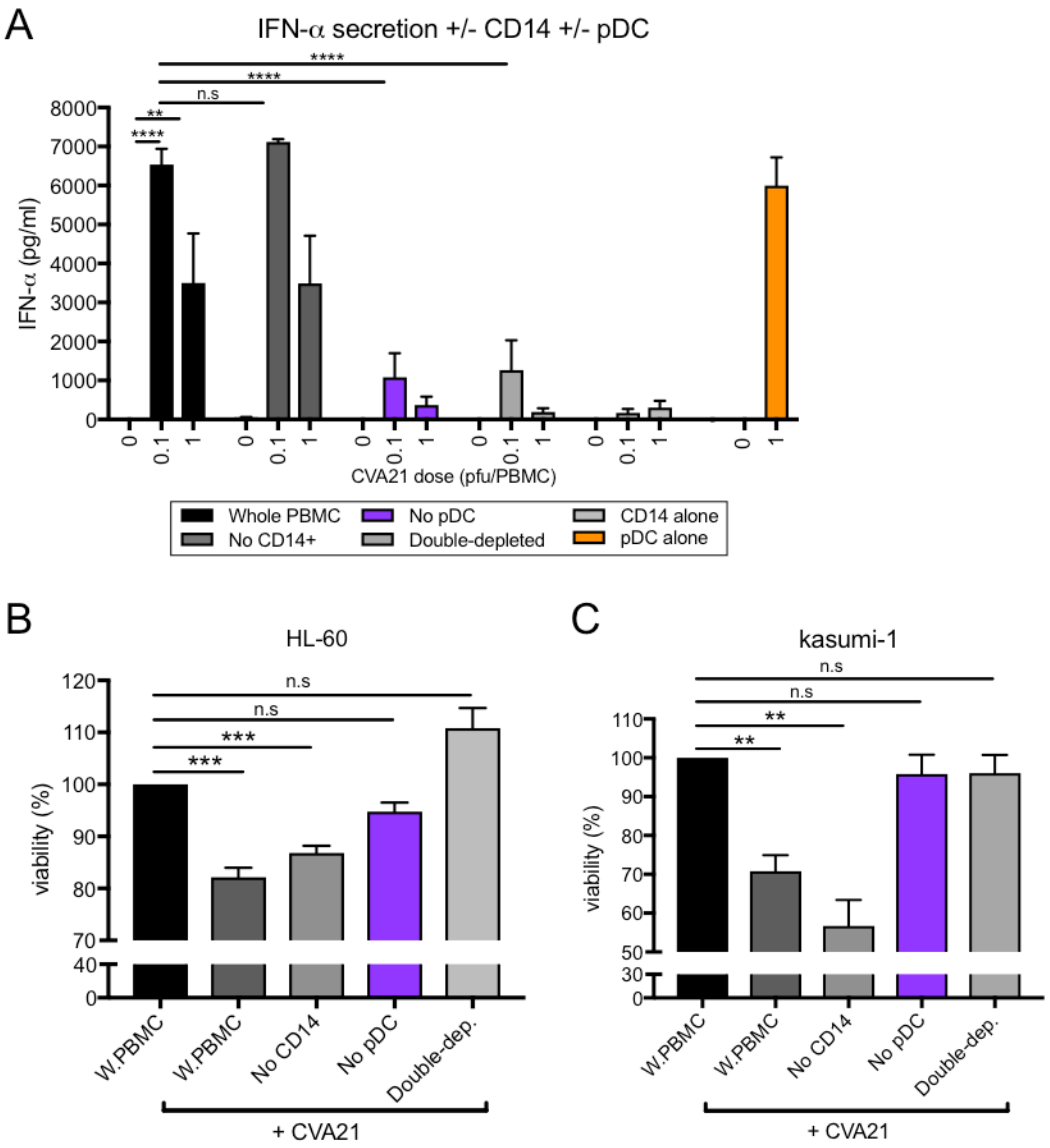

Figure 5-16: The importance of CD14⁺ monocytes and pDC for IFN-α secretion and CVA21-mediated bystander killing.

Whole PBMC were depleted of either CD14⁺ monocytes, pDC, or both using magnetic cell separation as described in Figure 5-15. PBMCs (whole and depleted), CD14⁺ cells alone, and pDC alone were then treated with CVA21 as indicated for 48 hrs. **A**: Cell-free supernatants were harvested and IFN-α secretion was measured by ELISA using matched paired antibodies (n=4). Statistical significance was calculated using a one-way ANOVA with Tukey's post-hoc test. **B** and **C**: Following treatment with 1 pfu/cell CVA21, conditioned medium (CM) from the various whole and depleted PBMC populations was harvested. HL-60 (**B**) and kasumi-1 (**C**) were cultured in CM for 96 hrs in triplicate and cell viability was measured using an MTS assay (n=6). Viability was normalised to CM from whole PBMC without CVA21 treatment. Statistical significance was calculated using one-way ANOVA with Dunnett's post-hoc test, ** = p<0.01, *** = p<0.001, **** = p<0.0001, n.s = not significant. Error bars indicate s.e.m.

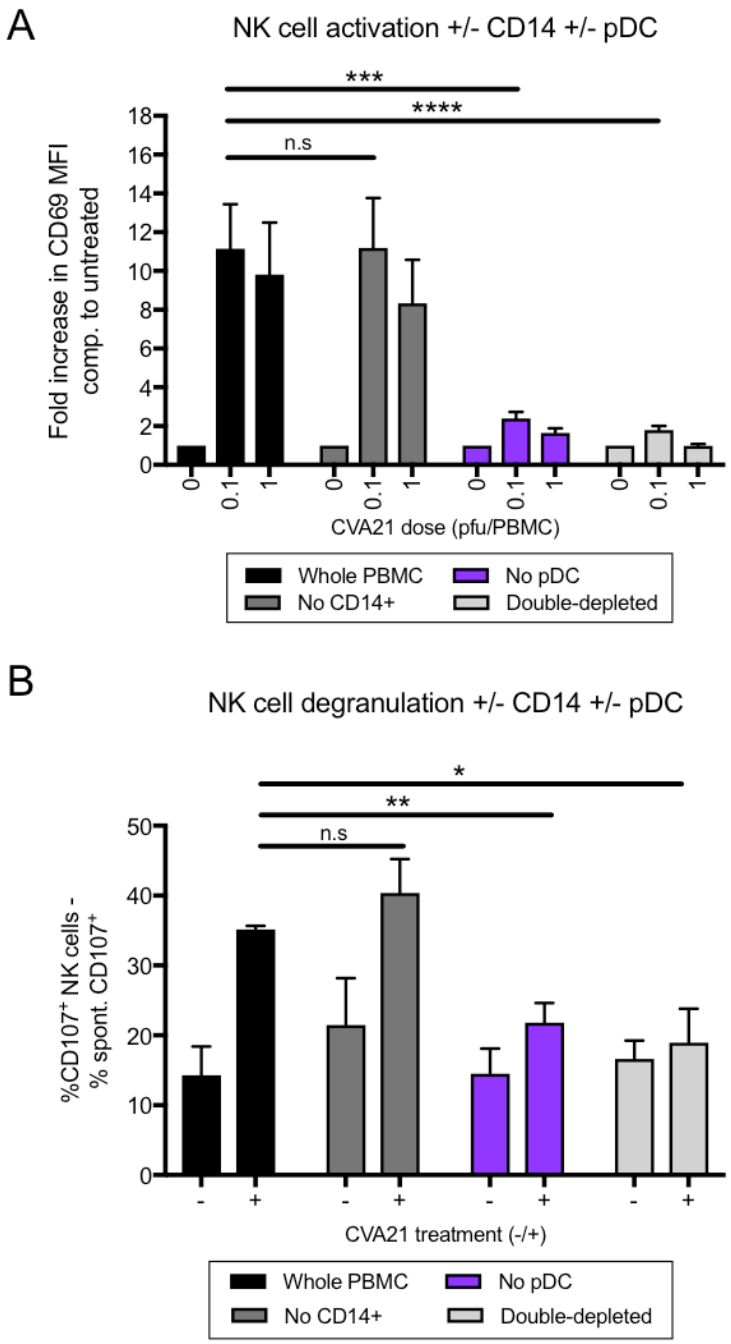

Figure 5-17: The importance of CD14$^+$ monocytes and pDC for CVA21-induced potentiation of NK cell-mediated cytotoxicity.

Whole PBMC from healthy donors were depleted of either CD14$^+$ cells (dark grey), pDC (purple), or both, using magnetic cell separation as described in Figure 5-15. Whole and depleted PBMCs were then treated with CVA21 as indicated for 48 hrs (0, 0.1, or 1 pfu/cell, + = 0.1 pfu/cell). **A**: NK cell activation was estimated by the expression of CD69 on CD3$^-$CD56$^+$ following CVA21 treatment and was measured by flow cytometry (n=7). Expression is presented as the fold increase in MFI compared to untreated NK cells. **B**: PBMCs pre-treated with CVA21 were co-cultured with OCI-M2 target cells at a 2:1 E:T ratio for 1 h, then for another 4 hrs in the presence of Brefeldin A. NK cell degranulation was estimated by CD107a/b expression on CD3$^-$CD56$^+$ cells (n=3). Statistical significance was calculated using one-way ANOVA with Tukey's post-hoc test, * = p<0.05, ** = p<0.01, *** = p<0.001, **** = p<0.0001, n.s = not significant. Error bars indicate s.e.m.

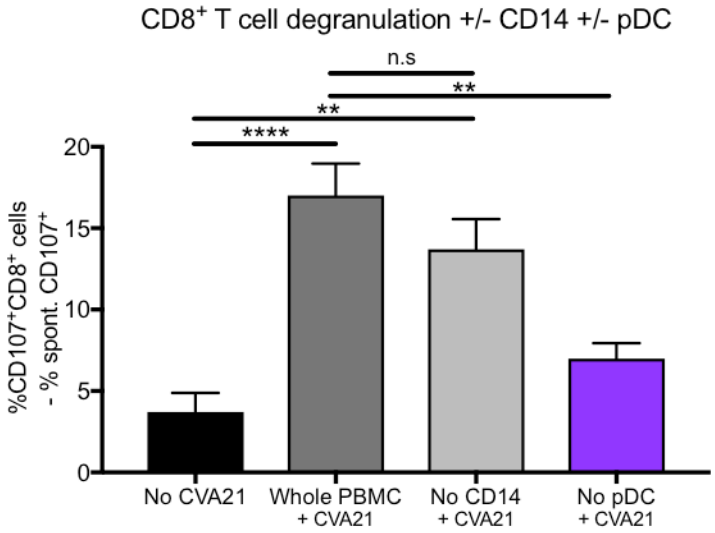

Figure 5-18: The importance of CD14+ monocytes and pDC for efficient priming of AML-specific CTLs using CVA21.

To generate primed CTLs, ICAM-1$^+$ KG-1 cells pre-treated with 0.1 pfu/cell CVA21 for 24 hrs. Autologous PBMCs were depleted of either CD14$^+$ cells or pDC (purple) using magnetic cell separation, and ICAM-1$^+$ KG-1 cells were then co-cultured with either whole or depleted PBMCs. Following one re-stimulation with CVA21-treated ICAM-1$^+$ KG-1 cells, primed CTLs were examined in a CTL degranulation assay. Primed CTLs were co-cultured with relevant target cells (ICAM-1$^+$ KG-1) at a 2:1 E:T ratio for 1 h, and then for a further 4 hrs in the presence of Brefeldin A. CTL degranulation was estimated by CD107a/b expression on CD3$^+$CD8$^+$ cells (n=5). Statistical significance was calculated using a one-way ANOVA with Tukey's post-hoc test, ** = p<0.01, **** = p<0.0001, n.s = not significant. Error bars indicate s.e.m.

5.2.5 Intravenous infusion of CVA21 activates immune responses necessary for the onset of anti-tumour immunity

Lastly, with the ultimate aim to evaluate the potential for translating CVA21 into the clinic with a focus on exploiting anti-tumour immunity, samples from the STORM Phase I clinical trial introduced in Chapter 3 were further examined with regards to the onset of an IFN response. Additionally, the cytotoxicity of CVA21 against healthy, mature immune cells was evaluated.

5.2.5.1 Initiation of an IFN response following i.v. administration of CVA21

As described in Chapter 3, blood samples from the STORM Phase I clinical trial were obtained and used as a proof of principle for the induction of an immune response following i.v. infusion of CVA21. The STORM trial was a Phase I, non-randomised, dose escalation trial, recruiting patients with various solid malignancies (Figure 3-1B and Table 3-1). As discussed in Chapter 3, none of the patients recruited in the trial had a haematological malignancy, but the samples still serve as a useful indicator of whether an anti-tumour immune response could be induced following i.v. infusion of CVA21 in immunocompromised patients. As shown in Table 3-1, patients received a dose of either $1x10^8$ $TCID_{50}$ (orange symbols) or $1x10^9$ $TCID_{50}$ (black symbols) of clinical grade CVA21 on Day 1, Day 3 and Day 5, and peripheral blood samples were collected prior to first infusion (Sample A), one hour post first infusion (Sample B), and on Day 3 (Sample C), prior to second CVA21 infusion (Figure 3-1B). The results presented from the STORM trial in Chapter 3 confirmed that by Day 3, patients experienced an activation of both NK cells, $CD4^+$ T cells, and $CD8^+$ T cells in response to CVA21 administration (Figure 3-8E and Figure 3-11).

Initially, a Luminex screen was performed on the serum obtained from patients before CVA21 treatment (Sample A) and three days post CVA21 treatment (Sample C) to examine the cytokine secretion in response to virus. Disappointingly, very few cytokines changed consistently between the patients, and no patient displayed a significant increase in the secretion of IFN-α at this time point (personal communication; data not shown). As IFN-α secretion can be detected 8-16 hrs following CVA21 treatment *in vitro* (Figure 5-4), and all data previously obtained on IFN-α secretion in this study was obtained 24 or 48 hrs after CVA21 treatment, it is possible that by Day 3 after CVA21 infusion, soluble IFN-α in the circulation may have been

degraded or sequestered. Following immediate secretion of IFNs in response to virus treatment, downstream signalling cascades would be initiated with a subsequent increase in the transcription of ISGs, such as *IFIT1*, *IFI44L*, and *OAS1* (388). Thus, in a further attempt to examine the onset of an IFN response in STORM trial samples, cDNA was generated from cryopreserved PBMCs (Samples A and C). Using qPCR, the expression of ISGs *IFIT1*, *IFI44L,* and *OAS1* in the total PBMC population was measured at each time point. Encouragingly, an upregulation of both *IFIT1*, *IFI44L,* and *OAS1* on Day 3 after CVA21 infusion was confirmed, indicating the onset of a type I IFN response (Figure 5-19A). Moreover, the effect was more pronounced in patients who received a higher dose of CVA21 (black symbols), with an overall higher fold increase in ISG expression. Sample C from patient STORM-4 and STORM-6 (both high dose CVA21) showed a 46- and 77-fold increase in *IFIT1* expression, respectively, compared to Sample A, while the low dose samples from STORM-1 and STORM-2 displayed a 14- and 17-fold increase, respectively. The results were similar for *IFI44L* expression. Disappointingly, Patient STORM-5, who received high dose CVA21 showed very little expression of both *IFIT1* and *IFI44L*. Interestingly, when analysing *OAS1* expression, patient STORM-5 showed a high expression (23-fold increase compared to Sample A), while the expression in STORM-4 samples was similar to that of the low dose CVA21 samples (5-fold increase compared to Sample A).

As activation of NK cells following CVA21 treatment was confirmed (Figure 3-8E), an attempt was made to evaluate the ability of NK cells from STORM patients to degranulate against the well-known NK cell target cell line, K562*, in vitro*. Unfortunately, cryopreserved PBMCs only recovered well enough to perform the NK cell degranulation assay in one patient sample (STORM-6). Figure 5-19B shows the flow cytometry histograms from the degranulation assay after five hours co-culture of STORM PBMCs and K562 target cells, with CD107 expression presented on the x-axis. Albeit anecdotal, this assay showed a promising increase in the ability of NK cells to degranulate against target cells on Day 3 post CVA21 infusion (right panel, 40.1% CD107-positive NK cells), compared to pre-infusion samples (left panel, 31.3% CD107-positive NK cells).

Together with the data presented in Chapter 3, these results demonstrate the potential onset of an immune response mediated by type I IFN in the peripheral circulation of immunocompromised patients, a prerequisite for the induction of CVA21-mediated anti-tumour immunity. In particular, a response

observed following i.v. administration is encouraging, as this would be the preferred route of administration for both MM and AML.

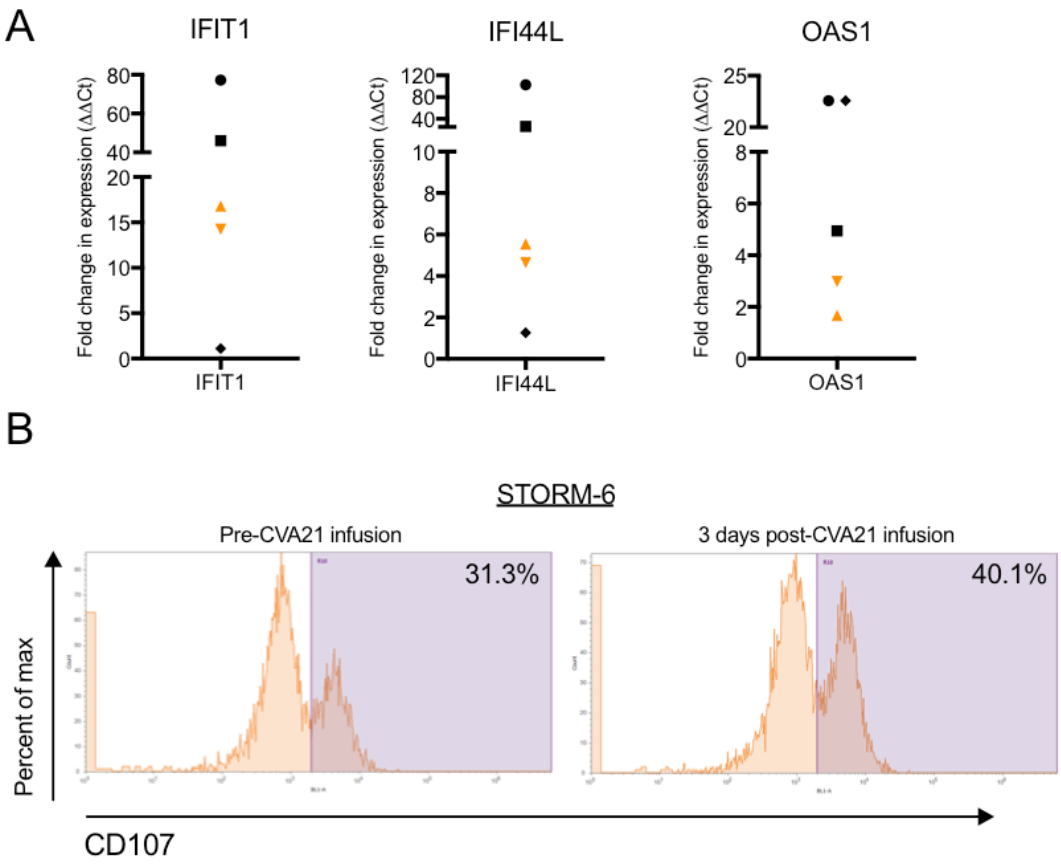

Figure 5-19: Type I IFN response following i.v. infusion of CVA21.

A: Cryopreserved PBMCs from patients taking part in the STORM clinical trial were thawed (Sample A and C) and RNA was isolated using an RNEasy Mini Kit. cDNA was generated by reverse transcription and the expression of *IFIT1, IFI44L*, and *OAS1* was measured by qPCR. Results were normalized to *18S* RNA expression and the fold increase in expression at Day 3 (calculated as ΔΔCt) compared to pre-infusion is presented. Black symbols = 10^9 $TCID_{50}$ CVA21 dose, orange symbols = 10^8 $TCID_{50}$ CVA21 dose, n=5. **B**: PBMCs from patient STORM-6 were recovered from cryopreservation and included in an NK cell degranulation assay using K562 cells as target cells. Following effector and target cell co-culture for 5 hrs, the expression of CD107a/b on $CD3^-CD56^+$ cells was measured using flow cytometry. The percentage of CD107-positive cells Pre-CVA21 infusion (left panel) and at Day 3 (right panel) is indicated in the purple gate.

5.2.5.2 CVA21 shows no oncolytic effect on normal haematopoietic cells

A further prerequisite for the onset of anti-tumour immunity in the peripheral circulation, and for patient safety, is that any normal, mature immune cells are not killed by CVA21 treatment. To confirm this, both resting and activated PBMCs from healthy volunteers were treated with CVA21 for 120 hrs and the death of NK cells, $CD4^+$ T cells, $CD8^+$ T cells, and monocytes was determined by flow cytometry using a Live/Dead® discrimination stain in combination with antibodies detailed in Table 2-4. To more closely model the proliferative intracellular milieu of a tumour cell NK cells, $CD4^+$ T cells, and $CD8^+$ T cells were activated with 10 μg/mL phytohaemagglutinin (PHA) for 36 hrs before CVA21 treatment. Encouragingly, as shown in Figure 5-20A, no death of immune cell populations was detected, and activation prior to treatment did not affect survival of the lymphocytes. Additionally, the viability of the population of mature, $CD45^+$ haematopoietic cells in the primary AML sample cohort was examined following CVA21 treatment *in vitro* for up to 6 days. Importantly, this confirmed that CVA21 did not induce cell death in this population of healthy cells and hence, only displayed a cytotoxic effect on malignant cells, consistent with the current dogma of OVT (Figure 5-20B).

In conclusion, the results presented in this chapter have demonstrated that despite CVA21 being unable to induce direct oncolysis in AML, it could still be a viable treatment option through the induction of anti-tumour immunity. As in MM, CVA21-mediated anti-tumour immunity consisted of both cytokine-induced bystander killing, NK cell-mediated cytotoxicity, and the priming of AML-specific cytotoxic CTLs. It is the first time that CVA21-mediated anti-tumour immunity has been demonstrated in HM. Furthermore, using the oncolysis-resistant AML model, the cellular mechanisms responsible for induction of CVA21-mediated anti-tumour immunity were elucidated. The response was confirmed to rely on IFN-α secretion from pDC, which are dependent on ICAM-1 expression for the detection of CVA21. Thus, this is the first study to implicate ICAM-1 expression as the overall determinant of susceptibility to CVA21 therapy, including anti-tumour immunity, and not only to CVA21-mediated direct oncolysis.

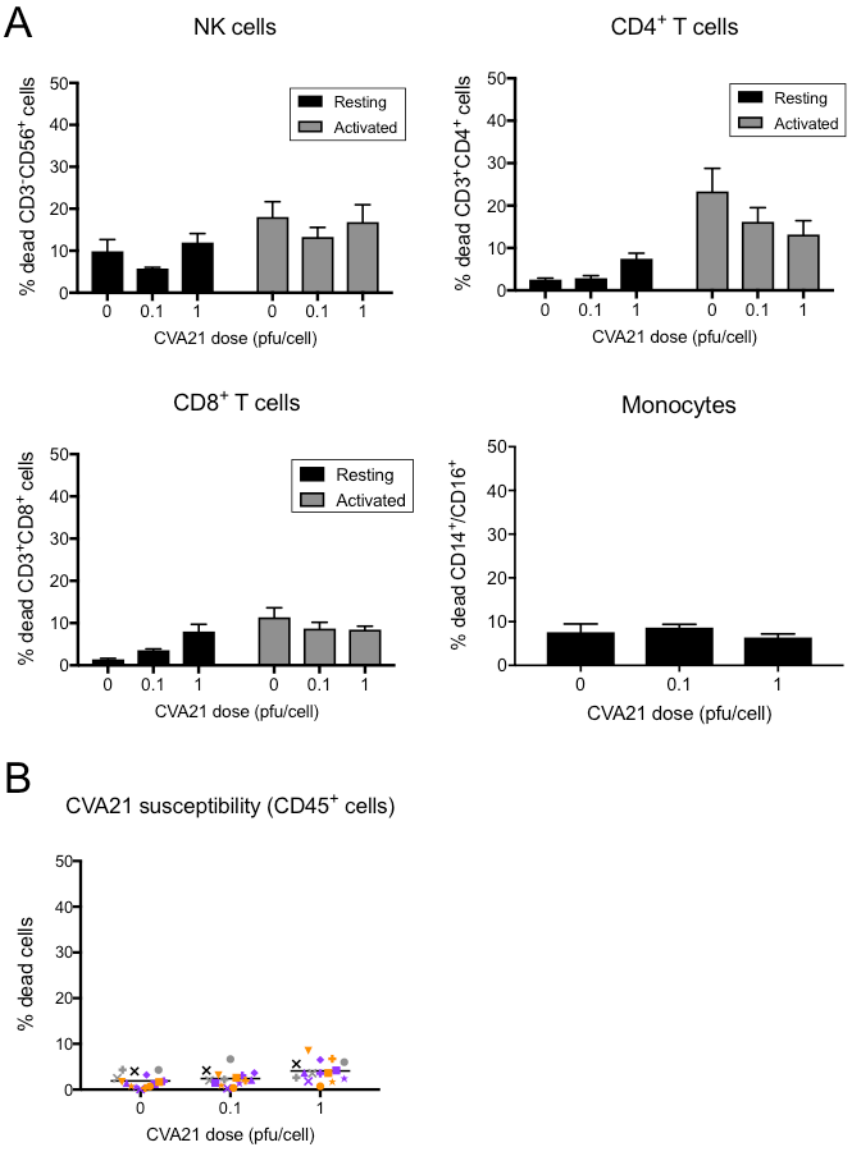

Figure 5-20: CVA21 has no direct oncolytic effect on normal haematopoietic cells.

A: CVA21 direct cytotoxicity on immune cells from healthy donors. PBMCs were isolated from healthy donors and were either left resting or activated with PHA for 36 hrs before CVA21 treatment for 120 hrs (0, 0.1, or 1 pfu/cell). Cell death was measured on NK cells ($CD3^-CD56^+$), $CD4^+$ T cells ($CD3^+CD4^+$), $CD8^+$ T cells ($CD3^+CD8^+$), $CD14^+$ monocytes using flow cytometry and a Live/Dead® discrimination stain (n=3). **B**: PBMCs were harvested from primary AML patient samples and treated with CVA21 for 72 hrs as indicated. Cell death of $CD45^+$ mature haematopoietic cells was measured by flow cytometry as described in **A** (n=15). *p*-values >0.05 were calculated for all conditions using one-way ANOVA with Tukey's post-hoc test.

5.3 Summary & Discussion

Expanding on the findings from Chapter 3, anti-tumour immunity induced by CVA21 was further explored in this chapter, using AML as a model to dissect mechanisms of anti-tumour immunity. Additionally, the results presented in this chapter demonstrated that CVA21 could have a role in the treatment of oncolysis-resistant AML due to the efficient onset of anti-tumour immunity.

The data presented in Figure 5-1 confirmed that all six AML cell lines tested were resistant to CVA21-induced oncolysis, presumably due to the low expression of ICAM-1 on the cell surface (Figure 5-1 A and B). Interestingly, for KG-1 cells, replication of CVA21 was detected using a $TCID_{50}$ assay (Figure 5-1E), which confirmed that the virus was able to enter these cells but remained incapable of inducing efficient oncolysis. However, replication was very limited (130-fold increase in $TCID_{50}$/mL) compared to what has previously been reported for CVA21-susceptible cell lines (up to 4-log increase for breast cancer cell lines and 5-log increase for MM cell lines); experimental repetition is required to confirm this result as well as measuring replication at earlier time points (202, 459). Mechanisms which specifically make malignantly transformed cells susceptible to OV infection, including a dysfunctional IFN response, were discussed in the introduction (Section 1.4.2.1). The fact that KG-1 cells were responsive to IFN-α, which protected them against CVA21 oncolysis (Figure 5-4B), suggests that the IFN response in this cell line may be functional and prevent successful oncolysis.

In Figure 5-2, the primary AML sample cohort was introduced, which demonstrated that blast cells isolated from the peripheral blood of AML patients express low levels of ICAM-1 (Figure 5-2A), but following treatment with CVA21, some cell death was still observed in 50% of the samples tested (Figure 5-2B). The absence of correlation between the level of ICAM-1 expression and the level of cell death observed (Figure 5-2C) indicated that ICAM-1 expression on tumour cells might not be the sole determining factor for CVA21 susceptibility. Moreover, primary blast cells were treated as a part of the entire PBMC fraction, which suggested that anti-tumour immunity could be responsible for death of the AML blasts. While it is the first time that CVA21 has been explored in AML, a number of other OVs have previously been examined for their direct oncolytic potential in this setting (Table 1-5), including myxoma virus (208), VSV (205), reovirus (206), and engineered adenoviruses (209, 488). The trend among these studies was to use cell line data and murine xenograft *in vivo* studies rather than primary AML patient samples *ex vivo*. VSV was tested in a small cohort of

primary AML samples, which confirmed large variability in susceptibility, but identified approximately 50% of samples as susceptible to VSV infection (205). Disappointingly, only one OV, VSV genetically modified to express IFN-β and NIS, has progressed to early clinical trials dedicated to AML (196).

ICAM-1 has been described as being crucial for oncolysis mediated by the *Kuykendall* prototype strain of CVA21 (489). As previously discussed, ICAM-1 mediates cell entry, in collaboration with the DAF protein which acts as a co-receptor and facilitates virion adherence to the cell surface (279, 490). The exact mechanism by which cellular entry is processed via ICAM-1 has not been clarified. In accordance with this theory, both transduction of KG-1 cells with the ICAM-1 protein (Figure 5-1 C and D), and upregulation of ICAM-1 expression using TNF-α, increased their susceptibility to CVA21-mediated oncolysis (Figure 5-3C, left panel). Additionally, one primary AML sample pre-treated with TNF-α also showed increased susceptibility to CVA21 (data not shown). However, in THP-1 and kasumi-1 cells, which did not show any signs of CVA21 replication, increasing ICAM-1 expression with TNF-α pre-treatment had no effect on susceptibility to CVA21 oncolysis (Figure 5-3, middle and right panels). While TNF-α treatment did increase ICAM-1 expression, it also had a significant toxic effect in itself, in particular on kasumi-1 cells and primary samples. However, TNF-α would have multiple downstream consequences, in addition to modulating ICAM-1 expression, e.g. induction of apoptosis and antiviral responses, which could ultimately synergise or abrogate OV treatment in a cell-type dependent manner (491). The role of DAF in infectivity has been thoroughly investigated and, in some circumstances, DAF has mediated cell entry of bioselected variants of CVA21 independent of ICAM-1 (152, 489). Preliminary data obtained in the lab demonstrated that all AML cell lines tested expressed DAF (data not shown) and hence, DAF expression was thought not to be a determining factor for susceptibility and resistance in this model. In contrast to this, the oncolysis results obtained in Chapter 3 confirmed the importance of ICAM-1 as the MM cell lines that expressed high levels of ICAM-1 showed significant susceptibility to CVA21-induced death, while OPM2 cells expressed no ICAM-1 and were completely resistant to CVA21-mediated oncolysis (Section 3.2.1).

In addition to ICAM-1 expression, the secretion of IFN-α in response to CVA21 treatment had a significant impact on the induction of direct oncolysis. As discussed in Chapter 3, CVA21 treatment of healthy donor

PBMCs induced secretion of a range of cytokines, including IFN-α. Moreover, in this chapter it was confirmed that PBMCs from primary AML samples also have the ability to secrete IFN-α in response to CVA21 treatment (Figure 5-4A), which could have a detrimental effect on CVA21-mediated oncolysis, as demonstrated using ICAM-1-transduced KG-1 cells (Figure 5-4B). It is possible the IFN secreted from primary samples could inhibit CVA21-mediated oncolysis, which suggests that the IFN response plays an important role for CVA21 efficacy. These findings were also in line with the absence of any correlation between ICAM-1 expression on AML blast and CVA21-mediated death in primary samples (Figure 5-2C) and highlights the importance of other mechanisms of action, such as anti-tumour immunity, for the efficacy of CVA21 in AML. Susceptibility to IFN responses is not an uncommon feature in OVs and has been demonstrated for recombinant Newcastle disease virus and Maraba virus (492, 493). Moreover, this study provides further evidence that an antiviral response might be insignificant for the efficacy of OVT as it still permits, and indeed may mediate, the onset of anti-tumour immunity regardless of efficient direct oncolysis.

Interestingly, IFN-α has previously been shown to have a direct cytotoxic effect on AML blast cells and has been evaluated as a treatment option in multiple clinical trials in AML (112, 463, 464). Despite promising results *in vitro*, the trial outcomes were very variable and no clear benefit from IFN-α was confirmed. Several patients experienced acute GVHD when IFN-α was administered in connection with HSCT. While IFN-α alone showed very little toxicity against AML cell lines in this study, a mixture of cytokines (either a combination of IFN-α and IFN-γ, or the CVA21-CM) significantly enhanced the toxic effect (Figure 5-5 and Figure 5-6). Encouragingly, a similar bystander killing effect was achieved using CM generated from patient PBMCs (Figure 5-6B). The Luminex assay performed on CVA21-CM in Chapter 3 outlined the changes in secretion levels of 48 different cytokines and chemokines following CVA21 treatment of PBMC (Figure 3-4E). Several cytokines showed an enhanced secretion following CVA21 treatment, for example IL-2, IL-6, and IL-1β, which have all been implicated as therapeutics in AML due to their direct toxic effect on AML cells (465-467). As discussed in Chapter 3, the toxicity of OV-CM has not previously been examined in a haematological setting. However, a number of studies have examined the toxicity of tumour-CM following OV treatment in solid malignancies. In a study examining VSV in combination with Smac mimetics, VSV was shown to induce the secretion of IFN-β, TNF-α, and TRAIL from

glioblastoma cells. The CM from VSV-treated cells was cytotoxic to fresh glioblastoma cells after 48 hrs, which was further potentiated by combination with the pro-apoptotic Smac mimetics (494). A similar approach was used by Cai *et al.*, who demonstrated bystander killing induced by a toga virus (M1) which was mediated by IL-8, IL-1A, and TRAIL (495). Reovirus-treatment of melanoma cells also generates CM with a bystander toxicity against uninfected melanoma cells (496). It is interesting to note that several studies highlighted TRAIL secretion as important for bystander killing, as TRAIL was one of the most abundantly secreted cytokines in CVA21-CM besides IFN-α (Figure 3-4E). Moreover, TRAIL has been proven well-tolerated as a monotherapy for relapsed and refractory MM in clinical trials, and has also shown efficient toxicity in AML in combination with additional sensitizing agents such as pro-apoptotic XIAP inhibitors and bortezomib (497-499).

In Chapter 3, it was confirmed that NK cells from healthy volunteers become activated in response to CVA21 treatment as measured by an upregulation of CD69 expression. In accordance with the results presented in Chapter 3, CVA21 treatment of NK cells also significantly enhanced their ability to degranulate against AML target cells, and degranulation was associated with an increase in NK cell-mediated killing of target cells (Figure 5-7 A and B). THP-1 and OCI-M2 cells were most susceptible to the NK cell-mediated killing, and this correlated with their high expression of activating NK cell ligands (Figure 5-7C). This was encouraging, as levels of cell death up to 54.1% were observed for OCI-M2 cells, which clearly indicated a role for CVA21 in targeting AML despite the absence of direct oncolysis. In addition, NK cell activation in response to CVA21 treatment was confirmed also in primary AML patient samples, and although there was extensive variation between samples, a significant increase in NK cell degranulation against OCI-M2 targets was observed (Figure 5-8 A and B). However, unfortunately due to the overall low expression of activating NK cell ligands on primary blast cells, NK cell degranulation against autologous blasts was very limited (Figure 5-8D). Both HSV-1 and reovirus treatment have previously been shown to induce NK cell-mediated anti-tumour immunity in AML, resulting in significant eradication of AML cells (206, 207). Interestingly, in the study on reovirus, healthy virus-activated NK cells were able to recognise and degranulate against primary AML blast cells, indicating that with full functionality of NK cells, and allogeneic mismatch, eradication of AML blasts is possible (206). However, it would also be interesting to examine whether the different cytokine profiles induced by reovirus and CVA21, respectively, can lead to the activation of NK cells with different cytotoxicity profiles.

In Chapter 3, two main strategies for improving the recognition of MM cells by NK cell targets were discussed, which would also be relevant in the AML setting considering the very low expression of activating NK ligands on primary AML blast cells, and lack of killing in an autologous setting. First, based on the fact that rituximab treatment was able to potentiate NK cell-mediated ADCC of blast cells in CLL (138), a combination treatment with a monoclonal antibody would be attractive. Anti-CD33 antibodies have been extensively studied in AML, but limited efficacy and safety issues in clinical trials have reduced interest in this strategy (500). Thus, the more novel anti-CD123 antibodies could be a more interesting option for this combination approach. Encouragingly, a second generation anti-CD123 antibody was recently shown to enhance ADCC in a large cohort of AML patients in remission (136). Second, the HDAC inhibitor VPA, which is occasionally used in the treatment of AML, can increase the expression of NKG2D ligands on primary blast cells, similar to its effect in MM (501, 502). In addition, 5-azacitidine, a first-line treatment for patients with high-risk MDS and AML can boost NK cell recognition of malignant blasts both by increasing the expression of activating NK ligands on AML blasts, and through the alteration of KIR receptors on NK cells (503, 504). Similarly, a derivative of 5-azacitidine, the hypomethylating agent decitabine, has also been shown to increase NK ligand expression, and anti-CD33-mediated ADCC in AML patient samples (505). All these agents would be interesting options to explore in combination with CVA21 to improve NK cell targeting of primary blast cells.

The ability of CVA21 to induce priming of AML-specific CTLs was examined in Section 5.2.3.3. Using CVA21-treated ICAM-1^{+} KG-1 cells, CTLs with specificity and high cytotoxicity against relevant, and not irrelevant, target cells were generated (Figure 5-9 and Figure 5-10). Importantly, CTLs were also able to recognise PRAME, one of the most frequent TAA in AML (26), when presented as a peptide pool on autologous PBMCs. PRAME has previously been implicated for the priming of AML-specific CTLs (506, 507), and interestingly, decitabine has been shown to increase the expression of PRAME on AML cells, further strengthening its relevance for combination treatment with CVA21 (506).

Results generated in Chapter 3 indicated that CTL priming was ineffective against CVA21-resistant OPM2 cells (Figure 3-18D). This finding was further explored in the present chapter by investigating priming against parental KG-1 and THP-1 cells, which were both resistant to direct oncolysis.

Interestingly, tumour specific CTLs were generated using both cell lines, suggesting that oncolysis was not a strict requirement for successful CTL priming (Figure 5-11 C and D). In line with this, UV-inactivated, non-replicative rhabdoviruses (VSV and Maraba virus) have extensive toxicity against primary AML samples mediated by a strong T cell response, which resulted in long-term immunological protection (508). However, as opposed to THP-1 cells, KG-1 cells were permissive to CVA21 infection which resulted in a small amount of CVA21 replication (Figure 5-1E). This did not seem to affect the generation of tumour-specific CTLs as a higher number of degranulating CTLs were detected in priming cultures where THP-1 cells were used as targets, compared to parental KG-1 cells.

The experiments described in Chapter 3 demonstrated that iDCs had a very weak response to CVA21 treatment with a limited change in the expression of the maturation markers CD80, CD86, and MHC Class II, which are essential for efficient activation and antigen presentation to T cells (509). Despite this, CVA21 was able to induce priming of tumour-specific CTLs in both MM and AML. Upon further exploration, these studies demonstrated that addition of autologous DCs was not required to generate CTLs (Figure 5-11 A and B) and suggested that another cell type, such as pDC, might act as the APC in this system (510). While DCs are considered the prototype APC, several other cell types, including pDC, $CD169^{+}$ macrophages, and neutrophils, have previously been used to successfully cross-prime CTLs (511-514).

To date, only one study has previously examined the onset of adaptive anti-tumour immunity in AML using a replication-competent OV (205). This *in vivo* study used a syngeneic murine model of AML (C1498 cells in C57Bl/6 mice) which was treated with VSV engineered to express IFN-β and the NIS reporter. OV treatment generated CTLs with high specificity against a tumour-expressed GFP antigen, and treatment efficacy following VSV treatment was potentiated by combination treatment with an anti-PD-L1 antibody. Batenchuk *et al*. performed a study examining non-replicative rhabdovirus-derived particles where DBA/2 mice with syngeneic L1210 cells were used as a model of blast crisis in AML (508). DBA/2 mice are considered immunocompetent, comparable to C57Bl/6 mice, but do have some immunocompromising traits such as a lack for NKG2A expression on NK cells which might be important for recognition of cells with low expression of MHC Class I (515). Nonetheless, Batenchuk *et al*. demonstrated the onset of a strong T cell-activating cytokine response and T

cell-mediated protection against tumour challenge following a vaccination strategy in combination with non-replicative viral particles (508). In general, studies of anti-tumour immunity using *in vivo* models of AML are sparse. The C1498 syngeneic model of murine orthotopic AML has been used to study the PD-1/PD-L1 axis in AML with successful generation of tumour-specific CTLs following treatment with an anti-PD-L1 antibody (516). Similarly, it has been used in various DC vaccine and adoptive transfer strategies, including a WT1 peptide vaccine and *ex vivo* tumour lysate stimulation of T cells, resulting in high frequency generation of tumour-specific CTLs (517, 518). However, as discussed previously and enforced in this chapter, using murine models for the study of CVA21-induced anti-tumour immunity is complicated due to the requirement for human ICAM-1 expression. The introduction outlined several types of immunotherapies which are currently being explored for the treatment of AML (Section 1.3), with adoptive transfer of DCs and genetically engineered NK cells particularly showing encouraging results in clinical trials. However, both immune checkpoint and CAR-T cells therapies have not yet produced the encouraging results of other malignancies in the context AML, which demonstrates the importance of continued exploration of immunotherapy treatments and novel combination strategies in AML. Taken together, the results presented throughout this section confirmed the potential for an anti-tumour immune response in AML following CVA21 treatment, and like in MM, this response consisted of both innate and adaptive tumour-clearing immune mechanisms. The fact that the observed responses were reduced in primary AML samples compared to healthy donors indicates that future studies should focus on potentiating this response, e.g. by exploiting other types of immunotherapies which might result in a synergistic response, such as CAR-T cells (106).

Next, the mechanisms behind the onset of anti-tumour immunity in response to CVA21 treatment were explored in more detail. It was confirmed that NK cell-mediated cytotoxicity was dependent on type I IFN secretion from PBMCs (Figure 5-12 B and C), which is in accordance with previously published literature and an intrinsic part of the antiviral immune response with the aim to rapidly remove virally infected cells from the circulation to limit viral infections (179). Moreover, NK cell-mediated cytotoxicity was shown to also rely on ICAM-1 expression on PBMCs. This function of ICAM-1 has previously not been documented in the context of CVA21. However, ICAM-1 is an adhesion molecule with several functions throughout the

immune system, with particular importance for lymphocyte migration, formation of the immunological synapse, and the generation of $CD8^+$ T cell responses (519, 520). It is likely that CVA21 employs ICAM-1 also to enter immune cells, which can then recognise the virus via TLRs and initiate a downstream immune response (521, 522). TLR7 and -8 are the main PRRs recognising ssRNA (523). TLR7 is predominately expressed in pDC and B cells while TLR8 is known to be primarily expressed in monocytes/macrophages, myeloid DC, and neutrophils (524). However, both TLR7 and -8 are endosomal, which requires phagocytosis of virus or virally infected cells for successful recognition. There are also other cytosolic sensors of ssRNA, such as RIG-I and MDA5, which could be important in the immune detection of CVA21 and the subsequent IFN response (293).

Due to their high expression of ICAM-1 on the cell surface and prominent roles in type I IFN secretion, monocytes and pDC were next examined for their importance in the onset of CVA21-mediated anti-tumour immunity. The results demonstrated that pDC were responsible for the majority of IFN-α secreted in response to CVA21 (Figure 5-16 A) and the toxic effect of CM on both HL-60 and kasumi-1 cells. No loss of CM efficacy was seen following depletion of $CD14^+$ monocytes. Interestingly, recent studies have demonstrated that monocytes might only be able to produce pro-inflammatory cytokines and type I IFN in response to TLR8, but not TLR7, stimulation (524). This suggests that TLR7 might be the key mediator of the CVA21 response and cytokine secretion in response to CVA21 in particular. Accordingly, TLR7 has previously been shown to be the main sensor of CVB3 infection in pDC, although IFN-α secretion required concurrent nAb opsonisation and engagement with Fc receptors (291). Moreover, this might also indicate that IFN-α is one of the main toxic components of CM in the AML model, which is consistent with the literature documenting IFN-α as a treatment modality in AML (112, 463, 464). However, CM generated with PBMC depleted of pDC was only examined for its IFN-α content in this study and it is not known whether pDC depletion affects other cytokines in the CM with potential toxicity against AML cells, such as TRAIL. Interestingly, in a study of melanoma and HSV-1, pDC were shown to be responsible for secretion of both IFN-α and TRAIL into CM, which induced a bystander killing effect on melanoma cells and synergised with the direct oncolytic effect of HSV-1 (525). Clarification of the exact cytokines involved in the CM toxic effect on AML cells would require future experiments to employ individual antibody-mediated neutralisation of relevant candidate cytokines.

The findings that both NK cell activation and degranulation, as well as the generation of efficient anti-tumour specific CTLs, was abrogated in the absence of pDC, but not $CD14^+$ cells, further implicated pDC as crucial for induction of CVA21-mediated anti-tumour immunity. While it is not unexpected that pDC are the main sensors of CVA21 infection, this is the first study to confirm the importance of pDC for CVA21-mediated anti-tumour immunity and their role in orchestrating the anti-tumour immune response via IFN-α secretion. As discussed, pDC are important for the detection of viral infections and for initiation of antiviral immune responses. pDC have been shown to be important for the IFN-α response also following infection with the closely related CVB, with recognition of CVB ssRNA on TLR7 (291, 526). However, CVB uptake into pDC was mediated by antibody opsonisation and Fc receptors, rather than the ICAM-1 dependent mechanism of CVA21 which is proposed here (291). For OVs specifically, pDC are responsible for the recognition of both MV and myxoma virus as well, with ssRNA binding to TLR7 and generation of an antiviral response with IFN-α secretion being reported (527, 528). For MV, pDC engagement generated an anti-tumour response concordant with pDC phagocytosis of TAA and subsequent cross-presentation of antigen to $CD8^+$ T cells (527). By contrast, monocytes are important for the detection of the dsRNA reovirus (138) and membrane-expressed TLR2 can mediate HSV-1 (dsDNA) detection in NK cells (207). The identification of pDC as crucial for CVA21-mediated anti-tumour immunity provides an important contribution to CVA21 immunobiology and indicates that the level of pDC could act as a key cellular determinant to inform patient stratification and CVA21 responsiveness. Moreover, several novel immunotherapy methods utilising adoptive transfer of pDC are currently being explored, which opens up interesting possibilities for combination treatments with CVA21. One study in ALL used patient-derived $CD34^+$ progenitor cells which were differentiated into pDC *ex vivo*. These cells were then activated with either TLR7 or -9 agonists and following adoptive transfer, pDC significantly enhanced the anti-tumour toxicity of NK cells (529).

In addition to the data presented in Chapter 3, further analysis of STORM clinical trial samples in this chapter indicated the onset of an IFN response with increased expression of several ISGs and potential for enhanced NK cell cytotoxicity (Figure 5-19). The STORM trial is the only trial initiated to date with i.v. administration of CVA21. As discussed in Chapter 3,

unfortunately none of the patients included in the STORM clinical trial had a haematological malignancy diagnosis, however, the general ability of CVA21 to induce a type I IFN response and activate immune cells *in vivo* in a state of malignancy following i.v. administration is encouraging and acts as a proof of principle for future studies. Early reports from the STORM trial confirmed that repeated dosing of CVA21 i.v. was well tolerated with no Grade 3 or 4 adverse effects. Significant increases in nAb levels were not seen until Day 7, which seemed to allow successful replication of CVA21 in tumours (305). This clinical trial has now been extended to include combination treatment with the checkpoint inhibitor pembrolizumab in both bladder and lung cancer (309). Importantly, in the present study it was also confirmed that CVA21 was non-toxic to healthy immune cells (both resting and activated), both from healthy donors (NK cells, $CD4^+$ T cells, $CD8^+$ T cells, and monocytes) and AML patient samples ($CD45^+$ cells), which is crucial for clinical safety in HM (Figure 5-20). This is in line with the data previously presented by *Au et al.*, which confirmed that CVA21 treatment for 48 hrs (1 $TCID_{50}$/cell) induced no cytopathic effect in PBMCs, and PBMCs were unable to support productive CVA21 replication (202).

The patient samples included in this study is one of the largest cohorts used for *ex vivo* studies of OV in AML. Extensive variation existed in the cohort both with regards to demographics, diagnoses, and responses to CVA21 treatment. Taken together, the experiments performed throughout this chapter confirmed that CVA21 can have a toxic effect on primary AML blast cells, which did not seem to be determined by ICAM-1 expression. Overall, the evidence pointed to the onset of anti-tumour immunity with secretion of IFN-α in response to CVA21 treatment, and subsequent activation and degranulation of NK cells in a subset of samples. As discussed above, degranulation against autologous blast cells was disappointing, but several interesting dual treatment options for making blast cells more attractive targets for NK cells exist. With the extensive variation within the cohort, it was not possible to stratify a successful CVA21 response to a particular AML subtype, mutation, cytogenetic profile, or other variable. However, the FLT3-ITD subtype has been associated with a higher frequency of pDC (530) in AML therefore, patients with the FLT3-ITD mutation may show an enhanced benefit from CVA21 treatment. However, pDC from patients with this ITD could only be partially activated to secrete cytokines, which might explain the limited response to CVA21 observed in some of the primary samples used in this study, but could also again indicate the possibility for a treatment strategy with *ex vivo* expansion and activation of pDC in

combination with CVA21. Five patients in the cohort used in this study had confirmed FLT3-ITD (Table 5-1), and this group included both patients which produced IFN-α and displayed enhanced NK cell function (CD69/CD107 expression) in response to CVA21, and those who did not. Thus, a larger cohort of patients would be required to fully elucidate the efficacy of CVA21 against FLT3-ITD-mutated patients as well as those with other genotypes. Additionally, the majority of AML patient samples utilized for this study had limited numbers of immune effector cells. Hence, CVA21 treatment would likely be more beneficial for targeting MRD in patients nearing remission, or patients at early relapse, when disease burden may be low. Importantly, patients in remission have a reconstituted immune response with functional NK and T cells (531-533). CVA21 could potentially be used clinically as a mono-immunotherapy to target MRD, or as a maintenance treatment following completion of intensive chemotherapy. Personalised medicine approaches with CVA21 could also be considered, specifically targeting patients with normal to high pDC levels, or patients expressing high ICAM-1 on immune cell subsets but not malignant blasts. As discussed, the progress in immunotherapy for AML is encouraging and the results presented in this chapter show that OVs may be a viable option for the treatment of AML which warrants further investigation both as a single modality and in combination with other promising treatments, to ultimately prolong and improve the life of AML patients.

In conclusion, this chapter has demonstrated two major points using an AML model *in vitro*, 1) that pDC orchestrate the anti-tumour immune response induced by CVA21, and 2) that CVA21 could have a role in the treatment of AML despite low ICAM-1 expression on AML blasts. Furthermore, this work has also demonstrated that ICAM-1 expression is not only the determining factor of susceptibility to CVA21-mediated oncolysis, but overall susceptibility to CVA21 treatment, including anti-tumour immunity.

Conclusions and Future Work

Overall conclusions and implications of the study

The results presented within this study have demonstrated a role for OV-induced anti-tumour immunity in two different HM; MM and AML. Both reovirus and CVA21 induced an anti-tumour immune response in MM *in vitro*, comprising innate and adaptive immune mechanisms. This is the first time that the contribution of anti-tumour immunity for reovirus and CVA21 efficacy in MM has been examined. While CVA21 is a more novel OV, reovirus has been taken forward to clinical trials in MM and thus, it is important to fully clarify its mechanisms of action to optimise its therapeutic efficacy. To date, CVA21 had only been pre-clinically examined for its direct oncolytic effect in MM and the results presented here indicate that CVA21 should be tested further in the context of MM, as it has the potential to induce both direct oncolysis and a potent anti-tumour immune response, which is a good foundation for successful OVT.

Moreover, this study demonstrated that reovirus also has efficacy against MM in an immunocompetent *in vivo* model with successful onset of an immune response. While this response requires further characterisation, the use of this model will allow for future exploration of reovirus-induced anti-tumour immunity in an *in vivo* setting. Due to the complex nature of the immune system, development of this model will be important to confirm the onset of anti-tumour immunity in a complete physiological system.

This is the first study to examine CVA21 for the treatment of AML. Encouragingly, CVA21 was also able to induce an anti-tumour immune response with both innate and adaptive components in AML, and importantly, anti-tumour immunity was established in the absence of direct oncolysis. This indicates that OVT might have potential in malignancies which are not directly susceptible to viral infection. Furthermore, the results presented in this study demonstrated that ICAM-1 expression is not only the determinant of susceptibility to CVA21-mediated direct oncolysis, but the overall determinant of a successful response to CVA21 therapy, including anti-tumour immunity. Taken together, these findings might have implications for future stratification of CVA21 treatment and for the development of personalised treatment regimes, in both HM and solid malignancies.

pDC were identified as the immune cell type with the overall highest expression of ICAM-1 on the cell surface, and accordingly pDC were confirmed to orchestrate the anti-tumour immune response generated following CVA21 treatment. In the absence of pDC, cytokine-induced toxicity, NK cell-mediated cytotoxicity, and the priming of tumour-specific CTLs were abrogated. Thus, this study contributes new knowledge to the mechanisms of action of CVA21. While it was not surprising that pDC are the main sensors of CVA21 infection, the critical role of pDC for induction of both innate and adaptive anti-tumour immunity is important information for future optimal development of CVA21 treatment strategies. Interestingly, these results also highlight the differences between OVs in their induction of anti-tumour immune responses, as monocytes have previously been shown to be the main sensors of reovirus infection. Thus, these data have implications for selection of the most appropriate OV in a given patient, as well as providing further options for personalised medicine strategies.

The use of OVT in the context of HM is an under-investigated field, in particular in terms of anti-tumour immunity. The findings presented here demonstrate that OVT can be efficient in HM and provide a foundation for continued research in this area, with the ultimate aim to identify new treatment options and improve the outlook for HM patients.

Suggested future work

The results obtained in this study have predominantly been generated using *in vitro* experimentation with established cell lines and PBMC from healthy individuals. While this provides proof of principle, future studies would require inclusion of more patient-derived samples, murine *in vivo* studies, and eventually clinical testing to fully clarify the role of OVT in HM.

CVA21 has only been examined in one previous study in MM (202). The work presented here has highlighted the potential of CVA21 as a treatment option in MM, confirming the possibility for direct oncolysis, anti-tumour immunity, and the targeting of tumour cells in the BM microenvironment. This warrants further exploration and future studies should aim to fully establish if CVA21 is suited for development as a clinical tool in the treatment of MM. Preclinical work should initially include examination of CVA21 efficacy in primary MM samples to ensure the results can be reproduced in primary cells. However, as discussed, the *in vivo* testing of CVA21-induced anti-tumour immunity is difficult. While it is possible to transfect murine tumour cell lines with human ICAM-1 for the use in immunocompetent models, the results presented here have demonstrated that expression of human ICAM-1 on immune cells is required for the successful generation of anti-tumour immunity. It is possible that a transgenic system could be developed, however, it might be more relevant to establish a primary sample cohort, as well as advanced *in vitro* models of the BM microenvironment, to thoroughly test CVA21 efficacy (direct oncolysis and anti-tumour immunity) in MM ahead of clinical testing. A representative cohort would allow for stratification of treatment response to patient characteristics and identify any particular disease subtypes likely to gain benefit from CVA21 treatment. Several methods exist for advanced modelling of the BM *in vitro*, such as using various types of 3D scaffolds and microfluidic chips in combination with primary cells from BM aspirates (534, 535).

While efficient in experiments with established cell lines, the use of CVA21 in AML proved more difficult when expanding the work to primary samples. This demonstrates the importance of establishing efficacy in patient-derived samples and has highlighted the need for future work to focus on identifying combination strategies to enhance CVA21 efficacy in AML. As discussed, this could e.g. include methods to improve primary blasts as NK cell targets through pre-treatment with HDAC inhibitors or mAb. Additionally, the optimal timing of CVA21 administration in the treatment course needs to be

deciphered. Patients in remission have a reconstituted immune system with functional NK and T cells, hence patients nearing remission might benefit from the anti-tumour immune effects of CVA21 in the control of MRD (532, 533), but additional work is required to fully clarify this.

Furthermore, future work is required to establish in detail how pDC orchestrate anti-tumour immunity in response to CVA21. This work could be expanded by closer examination of the role of pDC in bystander killing and clarification of which cytokines are responsible for the cytotoxicity of virus-CM. Clarification of the exact role of pDC in CTL priming also requires further work. The results presented indicated that conventional DCs are not required for the CVA21-induced priming of tumour-specific CTLs and thus, the role of pDC as APCs in the CTL priming system would be interesting to explore, along with the importance of IFN-α for successful priming. In addition, molecular mechanisms relating to pDC uptake and recognition of CVA21 still remain to be revealed.

The identification of pDC as important for CVA21-mediated efficacy opens many questions regarding the optimal use of CVA21. It will be important for future studies to consider the impact of a low ICAM-1 expression or dysfunctional pDC on treatment outcomes. For example, it could become relevant to develop combination treatments designed to increase ICAM-1 expression on immune cells prior to OV administration. Interestingly, preliminary data generated as part of this study indicated that virus-CM can increase the expression of ICAM-1 on AML cells (data not shown). While this did not confer susceptibility to CVA21-mediated oncolysis, it demonstrated that the inflammatory environment generated in response to CVA21 could potentially directly manipulate ICAM-1 expression also on immune cells. However, even though healthy cells should be protected by a functional IFN response, care should be taken not to cause off-target effects through a generalised induction of ICAM-1 expression. Several strategies for exploiting the dependence of CVA21 on pDC are possible. The development of pDC for adoptive transfer is interesting to consider in the context of OV. *Ex vivo* expansion and adoptive transfer of pDC could help those patients with low numbers of circulating pDC and improve the response to CVA21 treatment (529). In this context, CVA21 could be considered as an activating agent for *ex vivo* expanded pDC, similar to common TLR7 and -9 agonists, such as imiquimod and oligodeoxynucleotides (CpG). Another way of boosting the number of circulating pDC is FLT3 ligand treatment. FLT3 ligand is an important differentiation factor for pDC and significantly increases the

number of pDC in the blood (536, 537). In addition, pDC could potentially be harnessed to improve the adaptive anti-tumour immune responses of CVA21. Interestingly, pDC can cross-present antigen to $CD8^+$ T cells and strategies of directing nanoparticles containing TAA to pDC, as well as vaccine regimens utilising *ex vivo* loading of pDC with TAA have been explored (538, 539).

To further develop the reovirus work, the *in vivo* model of reovirus treatment in MM in particular requires more work to fully establish the contribution of anti-tumour immunity to treatment efficacy. Based on the experiments performed in this study, reovirus has the potential to induce an immune response, predominantly in the spleen, but the nature of this response remains to be determined with regards to its antiviral or anti-tumour specificity. In particular, experiments to identify the immune cells that are critical for reovirus efficacy using antibody depletion should be performed, as well as *ex vivo* characterisation of the antigen specificity of $CD8^+$ T cells following reovirus treatment. In addition, experimental groups will need to be maintained at a minimum of 8-10 animals per group to ensure reliable results due to experimental variability. Although reovirus is already being tested in clinical trials for MM, it is important to fully establish its mechanism of action to allow for the identification of optimal combination therapies.

A number of methods could be considered to further enhance the anti-tumour immune responses described in this study. As discussed, Smac mimetics have been used in combination with OVs to potentiate bystander killing (494). This is an interesting avenue to explore in terms of cytokine-mediated tumour cell killing, but also for the potential of Smac mimetics to activate immune cells, such as NK cells (540). Moreover, it would be interesting to examine the consequential use of two or more OVs working through different immune mechanisms in a prime-boost strategy to further enhance adaptive anti-tumour immune responses. Reovirus has previously been used in prime-boost experiments in combination with a TAA-expressing VSV, which resulted in T cell-mediated long-term cures *in vivo* (438). Furthermore, it is worth considering options for genetic modification of both reovirus and CVA21 to enhance their immunogenicity. Identification of the cytokines specifically responsible for the cytotoxicity of virus-CM could provide cytokine candidates for conjugation to OVs. Similarly, OVs armed with TAA could potentially be used to improve the priming of tumour-specific CTLs. Another strategy would be to incorporate OV into current DC vaccine

regimens to harness both the enhanced antigen presentation of *ex vivo* manipulated DC and the T cell-stimulating effect of OV.

It will also be important to consider the onset of anti-tumour immunity in the context of tumour immune evasion and the suppressive TME. Various armed viruses have been designed with the purpose of interfering with immune evasion, e.g. viruses expressing checkpoint inhibitors or the PGE_2 inactivating enzyme hydroxyprostaglandin dehydrogenase (541). Other strategies use standard chemotherapeutic drugs in combination with OV to modulate the TME, for example paclitaxel, which can increase the expression of MHC Class I and promote CTL responses, synergises with MG-1 OVT, and therapeutics such as gemcitabine and temozolomide can deplete the TME of MDSCs and T_{regs}, respectively, in advance of OV administration (542-544). Although the modest size of both reovirus and CVA21 genomes is a limiting factor, several of these strategies could be considered to promote the induction of anti-tumour immunity by both viruses, in particular in the context of the BM microenvironment.

This work has demonstrated that reovirus and CVA21 could play a role in the treatment of HM, both MM and AML, in particular through the potentiation of anti-tumour immune responses. The results presented provide a solid foundation for development of these agents either alone or in combination with complementary therapeutics for translation to clinical trials and patient benefit.

References

References

1. Hoption Cann SA, van Netten JP, van Netten C. Dr William Coley and tumour regression: a place in history or in the future. Postgraduate Medical Journal. 2003;79(938):672-80.

2. Elliott RL. Combination cancer immunotherapy "Expanding Paul Ehrlich's Magic Bullet Concept". Surgical oncology. 2012;21(1):53-5.

3. Dunn GP, Old LJ, Schreiber RD. The three Es of cancer immunoediting. Annual review of immunology. 2004;22:329-60.

4. Kaplan DH, Shankaran V, Dighe AS, Stockert E, Aguet M, Old LJ, et al. Demonstration of an interferon gamma-dependent tumor surveillance system in immunocompetent mice. Proceedings of the National Academy of Sciences of the United States of America. 1998;95(13):7556-61.

5. Shankaran V, Ikeda H, Bruce AT, White JM, Swanson PE, Old LJ, et al. IFNgamma and lymphocytes prevent primary tumour development and shape tumour immunogenicity. Nature. 2001;410(6832):1107-11.

6. Smyth MJ, Thia KY, Street SE, Cretney E, Trapani JA, Taniguchi M, et al. Differential tumor surveillance by natural killer (NK) and NKT cells. The Journal of experimental medicine. 2000;191(4):661-8.

7. Gao Y, Yang W, Pan M, Scully E, Girardi M, Augenlicht LH, et al. Gamma delta T cells provide an early source of interferon gamma in tumor immunity. The Journal of experimental medicine. 2003;198(3):433-42.

8. Mehta RS, Randolph B, Daher M, Rezvani K. NK cell therapy for hematologic malignancies. International journal of hematology. 2018;107(3):262-70.

9. Cerwenka A, Baron JL, Lanier LL. Ectopic expression of retinoic acid early inducible-1 gene (RAE-1) permits natural killer cell-mediated rejection of a MHC class I-bearing tumor in vivo. Proceedings of the National Academy of Sciences of the United States of America. 2001;98(20):11521-6.

10. Diefenbach A, Jensen ER, Jamieson AM, Raulet DH. Rae1 and H60 ligands of the NKG2D receptor stimulate tumour immunity. Nature. 2001;413(6852):165-71.

11. Osinska I, Popko K, Demkow U. Perforin: an important player in immune response. Central-European journal of immunology. 2014;39(1):109-15.

12. Lord SJ, Rajotte RV, Korbutt GS, Bleackley RC. Granzyme B: a natural born killer. Immunological reviews. 2003;193:31-8.

13. Mocikat R, Braumuller H, Gumy A, Egeter O, Ziegler H, Reusch U, et al. Natural killer cells activated by MHC class I(low) targets prime dendritic cells to induce protective CD8 T cell responses. Immunity. 2003;19(4):561-9.

14. Adam C, King S, Allgeier T, Braumuller H, Luking C, Mysliwietz J, et al. DC-NK cell cross talk as a novel CD4+ T-cell-independent pathway for antitumor CTL induction. Blood. 2005;106(1):338-44.

15. Lanier LL. NK Cell Receptors. Annual review of immunology. 1998;16(1):359-93.

16. Banchereau J, Steinman RM. Dendritic cells and the control of immunity. Nature. 1998;392(6673):245-52.

17. Steinman RM. The dendritic cell system and its role in immunogenicity. Annual review of immunology. 1991;9:271-96.

18. Corthay A. A three-cell model for activation of naive T helper cells. Scandinavian journal of immunology. 2006;64(2):93-6.

19. Joffre OP, Segura E, Savina A, Amigorena S. Cross-presentation by dendritic cells. Nature reviews Immunology. 2012;12(8):557-69.

20. Flinsenberg TW, Compeer EB, Boelens JJ, Boes M. Antigen cross-presentation: extending recent laboratory findings to therapeutic intervention. Clinical and experimental immunology. 2011;165(1):8-18.

21. Gao Y, Tao J, Li MO, Zhang D, Chi H, Henegariu O, et al. JNK1 is essential for CD8+ T cell-mediated tumor immune surveillance. Journal of immunology (Baltimore, Md : 1950). 2005;175(9):5783-9.

22. Boesen M, Svane IM, Engel AM, Rygaard J, Thomsen AR, Werdelin O. CD8+ T cells are crucial for the ability of congenic normal mice to reject highly immunogenic sarcomas induced in nude mice with 3-methylcholanthrene. Clinical and experimental immunology. 2000;121(2):210-5.

23. Romero I, Garrido C, Algarra I, Collado A, Garrido F, Garcia-Lora AM. T lymphocytes restrain spontaneous metastases in permanent dormancy. Cancer research. 2014;74(7):1958-68.

24. Zhu J, Paul WE. CD4 T cells: fates, functions, and faults. Blood. 2008;112(5):1557-69.

25. Janeway CA Jr TP, Walport M, et al. Antigen recognition by T cells. New York, NY: Garland Science; 2001. Available from: https://www.ncbi.nlm.nih.gov/books/NBK27098/.

26. Anguille S, Van Tendeloo VF, Berneman ZN. Leukemia-associated antigens and their relevance to the immunotherapy of acute myeloid leukemia. Leukemia. 2012;26(10):2186-96.

27. Kwak LW, Campbell MJ, Czerwinski DK, Hart S, Miller RA, Levy R. Induction of immune responses in patients with B-cell lymphoma against the surface-immunoglobulin idiotype expressed by their tumors. The New England journal of medicine. 1992;327(17):1209-15.

28. Pellat-Deceunynck C. Tumour-associated antigens in multiple myeloma. British journal of haematology. 2003;120(1):3-9.

29. Dunn GP, Bruce AT, Ikeda H, Old LJ, Schreiber RD. Cancer immunoediting: from immunosurveillance to tumor escape. Nature immunology. 2002;3(11):991-8.

30. Mittal D, Gubin MM, Schreiber RD, Smyth MJ. New insights into cancer immunoediting and its three component phases--elimination, equilibrium and escape. Current opinion in immunology. 2014;27:16-25.

31. Hanahan D, Weinberg RA. Hallmarks of cancer: the next generation. Cell. 2011;144(5):646-74.

32. Garrido F, Cabrera T, Concha A, Glew S, Ruiz-Cabello F, Stern PL. Natural history of HLA expression during tumour development. Immunology today. 1993;14(10):491-9.

33. Garrido F, Ruiz-Cabello F, Cabrera T, Perez-Villar JJ, Lopez-Botet M, Duggan-Keen M, et al. Implications for immunosurveillance of altered HLA class I phenotypes in human tumours. Immunology today. 1997;18(2):89-95.

34. Kochan G, Escors D, Breckpot K, Guerrero-Setas D. Role of non-classical MHC class I molecules in cancer immunosuppression. Oncoimmunology. 2013;2(11):e26491.

35. Strand S, Hofmann WJ, Hug H, Muller M, Otto G, Strand D, et al. Lymphocyte apoptosis induced by CD95 (APO-1/Fas) ligand-expressing tumor cells--a mechanism of immune evasion? Nature medicine. 1996;2(12):1361-6.

36. Owen-Schaub LB, van Golen KL, Hill LL, Price JE. Fas and Fas ligand interactions suppress melanoma lung metastasis. The Journal of experimental medicine. 1998;188(9):1717-23.

37. Jaganathan J, Petit JH, Lazio BE, Singh SK, Chin LS. Tumor necrosis factor-related apoptosis-inducing ligand-mediated apoptosis in established and primary glioma cell lines. Neurosurgical focus. 2002;13(3):ecp1.

38. Koyama S, Koike N, Adachi S. Expression of TNF-related apoptosis-inducing ligand (TRAIL) and its receptors in gastric carcinoma and tumor-infiltrating lymphocytes: a possible mechanism of immune evasion of the tumor. Journal of cancer research and clinical oncology. 2002;128(2):73-9.

39. de Charette M, Houot R. Hide or defend, the two strategies of lymphoma immune evasion: potential implications for immunotherapy. Haematologica. 2018;103(8):1256-68.

40. Carter L, Fouser LA, Jussif J, Fitz L, Deng B, Wood CR, et al. PD-1:PD-L inhibitory pathway affects both CD4(+) and CD8(+) T cells and is overcome by IL-2. European journal of immunology. 2002;32(3):634-43.

41. Freeman GJ, Long AJ, Iwai Y, Bourque K, Chernova T, Nishimura H, et al. Engagement of the PD-1 immunoinhibitory receptor by a novel B7 family member leads to negative regulation of lymphocyte activation. The Journal of experimental medicine. 2000;192(7):1027-34.

42. Mohme M, Riethdorf S, Pantel K. Circulating and disseminated tumour cells - mechanisms of immune surveillance and escape. Nature reviews Clinical oncology. 2017;14(3):155-67.

43. Chao MP, Majeti R, Weissman IL. Programmed cell removal: a new obstacle in the road to developing cancer. Nature reviews Cancer. 2011;12(1):58-67.

44. Jaiswal S, Jamieson CH, Pang WW, Park CY, Chao MP, Majeti R, et al. CD47 is upregulated on circulating hematopoietic stem cells and leukemia cells to avoid phagocytosis. Cell. 2009;138(2):271-85.

45. Seoane J. Escaping from the TGFbeta anti-proliferative control. Carcinogenesis. 2006;27(11):2148-56.

46. Chen W, Jin W, Hardegen N, Lei KJ, Li L, Marinos N, et al. Conversion of peripheral CD4+CD25- naive T cells to CD4+CD25+ regulatory T cells by TGF-beta induction of transcription factor Foxp3. The Journal of experimental medicine. 2003;198(12):1875-86.

47. Gabrilovich D, Ishida T, Oyama T, Ran S, Kravtsov V, Nadaf S, et al. Vascular endothelial growth factor inhibits the development of dendritic cells and dramatically affects the differentiation of multiple hematopoietic lineages in vivo. Blood. 1998;92(11):4150-66.

48. Kim R, Emi M, Tanabe K. Cancer immunosuppression and autoimmune disease: beyond immunosuppressive networks for tumour immunity. Immunology. 2006;119(2):254-64.

49. Jewett A, Tseng HC. Tumor induced inactivation of natural killer cell cytotoxic function; implication in growth, expansion and differentiation of cancer stem cells. Journal of Cancer. 2011;2:443-57.

50. Curiel TJ, Coukos G, Zou L, Alvarez X, Cheng P, Mottram P, et al. Specific recruitment of regulatory T cells in ovarian carcinoma fosters immune privilege and predicts reduced survival. Nature medicine. 2004;10(9):942-9.

51. Bates GJ, Fox SB, Han C, Leek RD, Garcia JF, Harris AL, et al. Quantification of regulatory T cells enables the identification of high-risk breast cancer patients and those at risk of late relapse. Journal of clinical oncology : official journal of the American Society of Clinical Oncology. 2006;24(34):5373-80.

52. Kobayashi N, Hiraoka N, Yamagami W, Ojima H, Kanai Y, Kosuge T, et al. FOXP3+ regulatory T cells affect the development and progression of hepatocarcinogenesis. Clinical cancer research : an official journal of the American Association for Cancer Research. 2007;13(3):902-11.

53. Kryczek I, Wei S, Zou L, Zhu G, Mottram P, Xu H, et al. Cutting edge: induction of B7-H4 on APCs through IL-10: novel suppressive mode for regulatory T cells. Journal of immunology (Baltimore, Md : 1950). 2006;177(1):40-4.

54. Grossman WJ, Verbsky JW, Barchet W, Colonna M, Atkinson JP, Ley TJ. Human T regulatory cells can use the perforin pathway to cause autologous target cell death. Immunity. 2004;21(4):589-601.

55. Mills CD, Lenz LL, Harris RA. A Breakthrough: Macrophage-Directed Cancer Immunotherapy. Cancer research. 2016;76(3):513-6.

56. Sica A, Schioppa T, Mantovani A, Allavena P. Tumour-associated macrophages are a distinct M2 polarised population promoting tumour progression: potential targets of anti-cancer therapy. European journal of cancer. 2006;42(6):717-27.

57. Noy R, Pollard JW. Tumor-associated macrophages: from mechanisms to therapy. Immunity. 2014;41(1):49-61.

58. Malek E, de Lima M, Letterio JJ, Kim BG, Finke JH, Driscoll JJ, et al. Myeloid-derived suppressor cells: The green light for myeloma immune escape. Blood reviews. 2016;30(5):341-8.

59. Bronte V, Serafini P, Mazzoni A, Segal DM, Zanovello P. L-arginine metabolism in myeloid cells controls T-lymphocyte functions. Trends in immunology. 2003;24(6):302-6.

60. Esteve FR, Roodman GD. Pathophysiology of myeloma bone disease. Best Practice & Research Clinical Haematology. 2007;20(4):613-24.

61. Cook L, Macdonald DHC. Management of paraproteinaemia. Postgraduate Medical Journal. 2007;83(978):217-23.

62. Kuehl WM, Bergsagel PL. Molecular pathogenesis of multiple myeloma and its premalignant precursor. The Journal of clinical investigation. 2012;122(10):3456-63.

63. Furukawa Y, Kikuchi J. Molecular pathogenesis of multiple myeloma. International journal of clinical oncology. 2015;20(3):413-22.

64. Cancer Research UK. Myeloma statistics. Available from: https://www.cancerresearchuk.org/health-professional/cancer-statistics/statistics-by-cancer-type/myeloma.

65. Rajkumar SV, Kumar S. Multiple Myeloma: Diagnosis and Treatment. Mayo Clinic proceedings. 2016;91(1):101-19.

66. Morgan GJ, Walker BA, Davies FE. The genetic architecture of multiple myeloma. Nature reviews Cancer. 2012;12(5):335-48.

67. Asosingh K, De Raeve H, de Ridder M, Storme GA, Willems A, Van Riet I, et al. Role of the hypoxic bone marrow microenvironment in 5T2MM murine myeloma tumor progression. Haematologica. 2005;90(6):810-7.

68. Reagan MR, Rosen CJ. Navigating the bone marrow niche: translational insights and cancer-driven dysfunction. Nature reviews Rheumatology. 2016;12(3):154-68.

69. Treon SP, Anderson KC. Interleukin-6 in multiple myeloma and related plasma cell dyscrasias. Current opinion in hematology. 1998;5(1):42-8.

70. Fairfield H, Falank C, Avery L, Reagan MR. Multiple myeloma in the marrow: pathogenesis and treatments. Annals of the New York Academy of Sciences. 2016;1364:32-51.

71. Gooding S, Edwards CM. New approaches to targeting the bone marrow microenvironment in multiple myeloma. Current opinion in pharmacology. 2016;28:43-9.

72. Estey E, Dohner H. Acute myeloid leukaemia. Lancet (London, England). 2006;368(9550):1894-907.

73. Rubnitz JE, Gibson B, Smith FO. Acute myeloid leukemia. Hematology/oncology clinics of North America. 2010;24(1):35-63.

74. Medinger M, Passweg JR. Acute myeloid leukaemia genomics. British journal of haematology. 2017;179(4):530-42.

75. Yohe S. Molecular Genetic Markers in Acute Myeloid Leukemia. Journal of clinical medicine. 2015;4(3):460-78.

76. Cancer Research UK. Acute myeloid leukaemia (AML) statistics. Available from: https://www.cancerresearchuk.org/health-professional/cancer-statistics/statistics-by-cancer-type/leukaemia-aml.

77. Walter RB, Estey EH. Management of older or unfit patients with acute myeloid leukemia. Leukemia. 2015;29(4):770-5.

78. Talati C, Sweet K. Recently approved therapies in acute myeloid leukemia: A complex treatment landscape. Leukemia research. 2018;73:58-66.

79. Burnett AK. Treatment of acute myeloid leukemia: are we making progress? Hematology American Society of Hematology Education Program. 2012;2012:1-6.

80. Buss EC, Ho AD. Leukemia stem cells. International journal of cancer. 2011;129(10):2328-36.

81. Arber DA, Orazi A, Hasserjian R, Thiele J, Borowitz MJ, Le Beau MM, et al. The 2016 revision to the World Health Organization classification of myeloid neoplasms and acute leukemia. Blood. 2016;127(20):2391-405.

82. Kitawaki T. DC-based immunotherapy for hematological malignancies. International journal of hematology. 2014;99(2):117-22.

83. Ruggeri L, Mancusi A, Capanni M, Urbani E, Carotti A, Aloisi T, et al. Donor natural killer cell allorecognition of missing self in haploidentical hematopoietic transplantation for acute myeloid leukemia: challenging its predictive value. Blood. 2007;110(1):433-40.

84. Ruggeri L, Capanni M, Urbani E, Perruccio K, Shlomchik WD, Tosti A, et al. Effectiveness of donor natural killer cell alloreactivity in mismatched hematopoietic transplants. Science (New York, NY). 2002;295(5562):2097-100.

85. Asai O, Longo DL, Tian ZG, Hornung RL, Taub DD, Ruscetti FW, et al. Suppression of graft-versus-host disease and amplification of graft-versus-tumor effects by activated natural killer cells after allogeneic bone marrow transplantation. The Journal of clinical investigation. 1998;101(9):1835-42.

86. Fehniger TA, Miller JS, Stuart RK, Cooley S, Salhotra A, Curtsinger J, et al. A Phase 1 Trial of CNDO-109-Activated Natural Killer Cells in Patients with High-Risk Acute Myeloid Leukemia. Biology of blood and marrow transplantation : journal of the American Society for Blood and Marrow Transplantation. 2018;24(8):1581-9.

87. Wiernik A, Foley B, Zhang B, Verneris MR, Warlick E, Gleason MK, et al. Targeting Natural Killer cells to Acute Myeloid Leukemia in vitro with a CD16x33 bispecific killer cell engager (BiKE) and ADAM17 inhibition. Clinical cancer research : an official journal of the American Association for Cancer Research. 2013;19(14):3844-55.

88. Vallera DA, Felices M, McElmurry R, McCullar V, Zhou X, Schmohl JU, et al. IL15 Trispecific Killer Engagers (TriKE) Make Natural Killer Cells Specific to CD33+ Targets While Also Inducing Persistence, In Vivo Expansion, and Enhanced Function. Clinical cancer research : an official journal of the American Association for Cancer Research. 2016;22(14):3440-50.

89. Chang SK, Hou J, Chen GG, Yu DD, Wu HQ, Xie YS, et al. Carfilzomib combined with ex vivo-expanded patient autologous natural killer cells for myeloma immunotherapy. Neoplasma. 2018.

90. Leivas A, Perez-Martinez A, Blanchard MJ, Martin-Clavero E, Fernandez L, Lahuerta JJ, et al. Novel treatment strategy with autologous activated and expanded natural killer cells plus anti-myeloma drugs for multiple myeloma. Oncoimmunology. 2016;5(12):e1250051.

91. Yi Q, Szmania S, Freeman J, Qian J, Rosen NA, Viswamitra S, et al. Optimizing dendritic cell-based immunotherapy in multiple myeloma: intranodal injections of idiotype-pulsed CD40 ligand-matured vaccines led to induction of type-1 and cytotoxic T-cell immune responses in patients. British journal of haematology. 2010;150(5):554-64.

92. Jung SH, Lee HJ, Lee YK, Yang DH, Kim HJ, Rhee JH, et al. A phase I clinical study of autologous dendritic cell therapy in patients with relapsed or refractory multiple myeloma. Oncotarget. 2017;8(25):41538-48.

93. Anguille S, Van de Velde AL, Smits EL, Van Tendeloo VF, Juliusson G, Cools N, et al. Dendritic cell vaccination as postremission treatment to prevent or delay relapse in acute myeloid leukemia. Blood. 2017;130(15):1713-21.

94. Kitawaki T, Kadowaki N, Fukunaga K, Kasai Y, Maekawa T, Ohmori K, et al. Cross-priming of CD8(+) T cells in vivo by dendritic cells pulsed with autologous apoptotic leukemic cells in immunotherapy for elderly patients with acute myeloid leukemia. Experimental hematology. 2011;39(4):424-33.e2.

95. ClinicalTrials.gov. DC Vaccination for Post-remission Therapy in AML [NCT02405338]. Bethesda, MD: NIH U.S. National Library of Medicine; 2015.

96. Phillips JH, Lanier LL. Dissection of the lymphokine-activated killer phenomenon. Relative contribution of peripheral blood natural killer cells and T lymphocytes to cytolysis. The Journal of experimental medicine. 1986;164(3):814-25.

97. Rosenberg SA, Lotze MT, Muul LM, Leitman S, Chang AE, Ettinghausen SE, et al. Observations on the Systemic Administration of Autologous Lymphokine-Activated Killer Cells and Recombinant Interleukin-2 to Patients with Metastatic Cancer. New England Journal of Medicine. 1985;313(23):1485-92.

98. Takei F. LAK cell therapy of AML: not to be lost in translation. Experimental hematology. 2011;39(11):1045-6.

99. Schmeel FC, Schmeel LC, Gast SM, Schmidt-Wolf IGH. Adoptive Immunotherapy Strategies with Cytokine-Induced Killer (CIK) Cells in the Treatment of Hematological Malignancies. International Journal of Molecular Sciences. 2014;15(8):14632-48.

100. Maude SL, Teachey DT, Porter DL, Grupp SA. CD19-targeted chimeric antigen receptor T-cell therapy for acute lymphoblastic leukemia. Blood. 2015;125(26):4017-23.

101. Calmes-Miller J. FDA Approves Second CAR T-cell Therapy. Cancer discovery. 2018;8(1):5-6.

102. Guo B, Chen M, Han Q, Hui F, Dai H, Zhang W, et al. CD138-directed adoptive immunotherapy of chimeric antigen receptor (CAR)-modified T cells for multiple myeloma. Journal of Cellular Immunotherapy. 2016;2(1):28-35.

103. Ali SA, Shi V, Maric I, Wang M, Stroncek DF, Rose JJ, et al. T cells expressing an anti-B-cell maturation antigen chimeric antigen receptor cause remissions of multiple myeloma. Blood. 2016;128(13):1688-700.

104. Gogishvili T, Danhof S, Prommersberger S, Rydzek J, Schreder M, Brede C, et al. SLAMF7-CAR T cells eliminate myeloma and confer selective fratricide of SLAMF7(+) normal lymphocytes. Blood. 2017;130(26):2838-47.

105. Tasian SK. Acute myeloid leukemia chimeric antigen receptor T-cell immunotherapy: how far up the road have we traveled? Therapeutic advances in hematology. 2018;9(6):135-48.

106. Ajina A, Maher J. Prospects for combined use of oncolytic viruses and CAR T-cells. J Immunother Cancer. 2017;5(1):90.

107. Noonan KA, Huff CA, Davis J, Lemas MV, Fiorino S, Bitzan J, et al. Adoptive transfer of activated marrow-infiltrating lymphocytes induces measurable antitumor immunity in the bone marrow in multiple myeloma. Science translational medicine. 2015;7(288):288ra78.

108. ClinicalTrials.gov. Tadalafil and Lenalidomide Maintenance With or Without Activated Marrow Infiltrating Lymphocytes (MILs) in High Risk Myeloma [NCT01858558]. Bethesda, MD: NIH U.S. National Library of Medicine; 2013.

109. ClinicalTrials.gov. Adoptive Immunotherapy With Activated Marrow Infiltrating Lymphocytes and Cyclophosphamide Graft-Versus-Host Disease Prophylaxis in Patients With Relapse of Hematologic Malignancies After Allogeneic Hematopoietic Cell Transplantation [NCT02342613]. Bethesda, MD: NIH U.S. National Library of Medicine; 2015.

110. Belardelli F, Ferrantini M, Proietti E, Kirkwood JM. Interferon-alpha in tumor immunity and immunotherapy. Cytokine & growth factor reviews. 2002;13(2):119-34.

111. Schaar CG, Kluin-Nelemans HC, Te Marvelde C, le Cessie S, Breed WP, Fibbe WE, et al. Interferon-alpha as maintenance therapy in patients with multiple myeloma. Annals of oncology : official journal of the European Society for Medical Oncology. 2005;16(4):634-9.

112. Anguille S, Lion E, Willemen Y, Van Tendeloo VF, Berneman ZN, Smits EL. Interferon-alpha in acute myeloid leukemia: an old drug revisited. Leukemia. 2011;25(5):739-48.

113. Mo XD, Wang Y, Zhang XH, Xu LP, Yan CH, Chen H, et al. Interferon-alpha Is Effective for Treatment of Minimal Residual Disease in Patients with t(8;21) Acute Myeloid Leukemia After Allogeneic Hematopoietic Stem Cell Transplantation: Results of a Prospective Registry Study. The oncologist. 2018.

114. Lopez-Girona A, Mendy D, Ito T, Miller K, Gandhi AK, Kang J, et al. Cereblon is a direct protein target for immunomodulatory and antiproliferative activities of lenalidomide and pomalidomide. Leukemia. 2012;26(11):2326-35.

115. Corral LG, Haslett PA, Muller GW, Chen R, Wong LM, Ocampo CJ, et al. Differential cytokine modulation and T cell activation by two distinct classes of thalidomide analogues that are potent inhibitors of TNF-alpha. Journal of immunology (Baltimore, Md : 1950). 1999;163(1):380-6.

116. Henry JY, Labarthe MC, Meyer B, Dasgupta P, Dalgleish AG, Galustian C. Enhanced cross-priming of naive CD8+ T cells by dendritic cells treated by the IMiDs(R) immunomodulatory compounds lenalidomide and pomalidomide. Immunology. 2013;139(3):377-85.

117. Chang DH, Liu N, Klimek V, Hassoun H, Mazumder A, Nimer SD, et al. Enhancement of ligand-dependent activation of human natural killer T cells by lenalidomide: therapeutic implications. Blood. 2006;108(2):618-21.

118. Zhu D, Corral LG, Fleming YW, Stein B. Immunomodulatory drugs Revlimid (lenalidomide) and CC-4047 induce apoptosis of both hematological and solid tumor cells through NK cell activation. Cancer immunology, immunotherapy : CII. 2008;57(12):1849-59.

119. Le Roy A, Prebet T, Castellano R, Goubard A, Riccardi F, Fauriat C, et al. Immunomodulatory Drugs Exert Anti-Leukemia Effects in Acute Myeloid Leukemia by Direct and Immunostimulatory Activities. Frontiers in immunology. 2018;9:977.

120. Blum W, Klisovic RB, Becker H, Yang X, Rozewski DM, Phelps MA, et al. Dose escalation of lenalidomide in relapsed or refractory acute leukemias. Journal of clinical oncology : official journal of the American Society of Clinical Oncology. 2010;28(33):4919-25.

121. Fehniger TA, Uy GL, Trinkaus K, Nelson AD, Demland J, Abboud CN, et al. A phase 2 study of high-dose lenalidomide as initial therapy for older patients with acute myeloid leukemia. Blood. 2011;117(6):1828-33.

122. Podoltsev NA, Stahl M, Zeidan AM, Gore SD. Selecting initial treatment of acute myeloid leukaemia in older adults. Blood reviews. 2017;31(2):43-62.

123. Heninger E, Krueger TE, Lang JM. Augmenting antitumor immune responses with epigenetic modifying agents. Frontiers in immunology. 2015;6:29.

124. Orskov AD, Treppendahl MB, Skovbo A, Holm MS, Friis LS, Hokland M, et al. Hypomethylation and up-regulation of PD-1 in T cells by azacytidine in MDS/AML patients: A rationale for combined targeting of PD-1 and DNA methylation. Oncotarget. 2015;6(11):9612-26.

125. Boddu P, Kantarjian H, Garcia-Manero G, Allison J, Sharma P, Daver N. The emerging role of immune checkpoint based approaches in AML and MDS. Leukemia & lymphoma. 2018;59(4):790-802.

126. Ansell SM, Lesokhin AM, Borrello I, Halwani A, Scott EC, Gutierrez M, et al. PD-1 blockade with nivolumab in relapsed or refractory Hodgkin's lymphoma. The New England journal of medicine. 2015;372(4):311-9.

127. Lesokhin AM, Ansell SM, Armand P, Scott EC, Halwani A, Gutierrez M, et al. Nivolumab in Patients With Relapsed or Refractory Hematologic Malignancy: Preliminary Results of a Phase Ib Study. Journal of clinical oncology : official journal of the American Society of Clinical Oncology. 2016;34(23):2698-704.

128. ClinicalTrials.gov. Study of Lenalidomide and Dexamethasone With or Without Pembrolizumab (MK-3475) in Participants With Newly Diagnosed Treatment Naive Multiple Myeloma (MK-3475-185/KEYNOTE-185) [NCT02579863]. Bethesda, MD: NIH U.S. National Library of Medicine; 2015.

129. ClinicalTrials.gov. Study of Pomalidomide and Low Dose Dexamethasone With or Without Pembrolizumab (MK-3475) in Refractory or Relapsed and Refractory Multiple Myeloma (rrMM) (MK-3475-183/KEYNOTE-183) [NCT02576977]. Bethesda, MD: NIH U.S. National Library of Medicine; 2015.

130. Daver NG, Basu S, Garcia-Manero G, Cortes JE, Ravandi F, Jabbour E, et al. Phase IB/II study of nivolumab with azacytidine (AZA) in patients (pts) with relapsed AML. Journal of Clinical Oncology. 2017;35(15_suppl):7026-.

131. ClinicalTrials.gov. An Open-Label Phase II Study of Nivolumab (BMS-936558) in Combination With 5-azacytidine (Vidaza) or Nivolumab With Ipilimumab in Combination With 5-azacytidine for the Treatment of Patients With Refractory/ Relapsed Acute Myeloid Leukemia [NCT02397720]. Bethesda, MD: NIH U.S. National Library of Medicine; 2015.

132. Laubach JP, Paba Prada CE, Richardson PG, Longo DL. Daratumumab, Elotuzumab, and the Development of Therapeutic Monoclonal Antibodies in Multiple Myeloma. Clinical pharmacology and therapeutics. 2017;101(1):81-8.

133. Hoyos V, Borrello I. The immunotherapy era of myeloma: monoclonal antibodies, vaccines, and adoptive T-cell therapies. Blood. 2016;128(13):1679-87.

134. Acheampong DO, Adokoh CK, Asante DB, Asiamah EA, Barnie PA, Bonsu DOM, et al. Immunotherapy for acute myeloid leukemia (AML): a potent alternative therapy. Biomedicine & pharmacotherapy = Biomedecine & pharmacotherapie. 2018;97:225-32.

135. Jurcic JG. Clinical Studies with Bismuth-213 and Actinium-225 for Hematologic Malignancies. Current radiopharmaceuticals. 2018.

136. Xie LH, Biondo M, Busfield SJ, Arruda A, Yang X, Vairo G, et al. CD123 target validation and preclinical evaluation of ADCC activity of anti-CD123 antibody CSL362 in combination with NKs from AML patients in remission. Blood cancer journal. 2017;7(6):e567.

137. He SZ, Busfield S, Ritchie DS, Hertzberg MS, Durrant S, Lewis ID, et al. A Phase 1 study of the safety, pharmacokinetics and anti-leukemic activity of the anti-CD123 monoclonal antibody CSL360 in relapsed, refractory or high-risk acute myeloid leukemia. Leukemia & lymphoma. 2015;56(5):1406-15.

138. Parrish C, Scott GB, Migneco G, Scott KJ, Steele LP, Ilett E, et al. Oncolytic reovirus enhances rituximab-mediated antibody-dependent cellular cytotoxicity against chronic lymphocytic leukaemia. Leukemia. 2015;29(9):1799-810.

139. Kelly E, Russell SJ. History of oncolytic viruses: genesis to genetic engineering. Molecular therapy : the journal of the American Society of Gene Therapy. 2007;15(4):651-9.

140. Garber K. China approves world's first oncolytic virus therapy for cancer treatment. Journal of the National Cancer Institute. 2006;98(5):298-300.

141. Randazzo BP, Tal-Singer R, Zabolotny JM, Kesari S, Fraser NW. Herpes simplex virus 1716, an ICP 34.5 null mutant, is unable to replicate in CV-1 cells due to a translational block that can be overcome by coinfection with SV40. The Journal of general virology. 1997;78 (Pt 12):3333-9.

142. Liu BL, Robinson M, Han ZQ, Branston RH, English C, Reay P, et al. ICP34.5 deleted herpes simplex virus with enhanced oncolytic, immune stimulating, and anti-tumour properties. Gene therapy. 2003;10(4):292-303.

143. Lorence RM, Rood PA, Kelley KW. Newcastle disease virus as an antineoplastic agent: induction of tumor necrosis factor-alpha and augmentation of its cytotoxicity. Journal of the National Cancer Institute. 1988;80(16):1305-12.

144. Stojdl DF, Lichty B, Knowles S, Marius R, Atkins H, Sonenberg N, et al. Exploiting tumor-specific defects in the interferon pathway with a previously unknown oncolytic virus. Nature medicine. 2000;6(7):821-5.

145. Moehler M, Blechacz B, Weiskopf N, Zeidler M, Stremmel W, Rommelaere J, et al. Effective infection, apoptotic cell killing and gene transfer of human hepatoma cells but not primary hepatocytes by parvovirus H1 and derived vectors. Cancer gene therapy. 2001;8(3):158-67.

146. Shafren DR, Au GG, Nguyen T, Newcombe NG, Haley ES, Beagley L, et al. Systemic therapy of malignant human melanoma tumors by a common cold-producing enterovirus, coxsackievirus a21. Clinical cancer

research : an official journal of the American Association for Cancer Research. 2004;10(1 Pt 1):53-60.

147. Hashiro G, Loh PC, Yau JT. The preferential cytotoxicity of reovirus for certain transformed cell lines. Archives of virology. 1977;54(4):307-15.

148. Grote D, Russell SJ, Cornu TI, Cattaneo R, Vile R, Poland GA, et al. Live attenuated measles virus induces regression of human lymphoma xenografts in immunodeficient mice. Blood. 2001;97(12):3746-54.

149. Breitbach CJ, Arulanandam R, De Silva N, Thorne SH, Patt R, Daneshmand M, et al. Oncolytic vaccinia virus disrupts tumor-associated vasculature in humans. Cancer research. 2013;73(4):1265-75.

150. Ilkow CS, Marguerie M, Batenchuk C, Mayer J, Ben Neriah D, Cousineau S, et al. Reciprocal cellular cross-talk within the tumor microenvironment promotes oncolytic virus activity. Nature medicine. 2015;21(5):530-6.

151. Bauzon M, Hermiston T. Armed therapeutic viruses - a disruptive therapy on the horizon of cancer immunotherapy. Frontiers in immunology. 2014;5:74.

152. Newcombe NG, Johansson ES, Au G, Lindberg AM, Barry RD, Shafren DR. Enterovirus capsid interactions with decay-accelerating factor mediate lytic cell infection. Journal of virology. 2004;78(3):1431-9.

153. Kanerva A, Mikheeva GV, Krasnykh V, Coolidge CJ, Lam JT, Mahasreshti PJ, et al. Targeting adenovirus to the serotype 3 receptor increases gene transfer efficiency to ovarian cancer cells. Clinical cancer research : an official journal of the American Association for Cancer Research. 2002;8(1):275-80.

154. Dmitriev I, Krasnykh V, Miller CR, Wang M, Kashentseva E, Mikheeva G, et al. An adenovirus vector with genetically modified fibers demonstrates expanded tropism via utilization of a coxsackievirus and adenovirus receptor-independent cell entry mechanism. Journal of virology. 1998;72(12):9706-13.

155. Kaufman HL, Kohlhapp FJ, Zloza A. Oncolytic viruses: a new class of immunotherapy drugs. Nature reviews Drug discovery. 2015;14(9):642-62.

156. Harle P, Sainz B, Jr., Carr DJ, Halford WP. The immediate-early protein, ICP0, is essential for the resistance of herpes simplex virus to interferon-alpha/beta. Virology. 2002;293(2):295-304.

157. Fiola C, Peeters B, Fournier P, Arnold A, Bucur M, Schirrmacher V. Tumor selective replication of Newcastle disease virus: association with defects of tumor cells in antiviral defence. International journal of cancer. 2006;119(2):328-38.

158. Balachandran S, Barber GN. Defective translational control facilitates vesicular stomatitis virus oncolysis. Cancer cell. 2004;5(1):51-65.

159. Hummel JL, Safroneeva E, Mossman KL. The role of ICP0-Null HSV-1 and interferon signaling defects in the effective treatment of breast adenocarcinoma. Molecular therapy : the journal of the American Society of Gene Therapy. 2005;12(6):1101-10.

160. Obuchi M, Fernandez M, Barber GN. Development of recombinant vesicular stomatitis viruses that exploit defects in host defense to augment specific oncolytic activity. Journal of virology. 2003;77(16):8843-56.

161. Sadler AJ, Williams BR. Structure and function of the protein kinase R. Current topics in microbiology and immunology. 2007;316:253-92.

162. Christian SL, Zu D, Licursi M, Komatsu Y, Pongnopparat T, Codner DA, et al. Suppression of IFN-induced transcription underlies IFN defects generated by activated Ras/MEK in human cancer cells. PloS one. 2012;7(9):e44267.

163. Strong JE, Coffey MC, Tang D, Sabinin P, Lee PW. The molecular basis of viral oncolysis: usurpation of the Ras signaling pathway by reovirus. The EMBO journal. 1998;17(12):3351-62.

164. He B, Gross M, Roizman B. The gamma(1)34.5 protein of herpes simplex virus 1 complexes with protein phosphatase 1alpha to dephosphorylate the alpha subunit of the eukaryotic translation initiation factor 2 and preclude the shutoff of protein synthesis by double-stranded RNA-activated protein kinase. Proceedings of the National Academy of Sciences of the United States of America. 1997;94(3):843-8.

165. Dobbelstein M. Replicating adenoviruses in cancer therapy. Current topics in microbiology and immunology. 2004;273:291-334.

166. Bischoff JR, Kirn DH, Williams A, Heise C, Horn S, Muna M, et al. An adenovirus mutant that replicates selectively in p53-deficient human tumor cells. Science (New York, NY). 1996;274(5286):373-6.

167. Ries S, Korn WM. ONYX-015: mechanisms of action and clinical potential of a replication-selective adenovirus. British journal of cancer. 2002;86(1):5-11.

168. Dorer DE, Nettelbeck DM. Targeting cancer by transcriptional control in cancer gene therapy and viral oncolysis. Advanced drug delivery reviews. 2009;61(7-8):554-71.

169. Furuhata S, Ide H, Miura Y, Yoshida T, Aoki K. Development of a prostate-specific promoter for gene therapy against androgen-independent prostate cancer. Molecular therapy : the journal of the American Society of Gene Therapy. 2003;7(3):366-74.

170. Kawashima T, Kagawa S, Kobayashi N, Shirakiya Y, Umeoka T, Teraishi F, et al. Telomerase-specific replication-selective virotherapy for human cancer. Clinical cancer research : an official journal of the American Association for Cancer Research. 2004;10(1 Pt 1):285-92.

171. Oh E, Hong J, Kwon OJ, Yun CO. A hypoxia- and telomerase-responsive oncolytic adenovirus expressing secretable trimeric TRAIL triggers tumour-specific apoptosis and promotes viral dispersion in TRAIL-resistant glioblastoma. Scientific reports. 2018;8(1):1420.

172. Toda M, Rabkin SD, Kojima H, Martuza RL. Herpes simplex virus as an in situ cancer vaccine for the induction of specific anti-tumor immunity. Human gene therapy. 1999;10(3):385-93.

173. Diaz RM, Galivo F, Kottke T, Wongthida P, Qiao J, Thompson J, et al. Oncolytic immunovirotherapy for melanoma using vesicular stomatitis virus. Cancer research. 2007;67(6):2840-8.

174. Cai J, Lin Y, Zhang H, Liang J, Tan Y, Cavenee WK, et al. Selective replication of oncolytic virus M1 results in a bystander killing effect that is potentiated by Smac mimetics. Proceedings of the National Academy of Sciences of the United States of America. 2017;114(26):6812-7.

175. Arulanandam R, Batenchuk C, Varette O, Zakaria C, Garcia V, Forbes NE, et al. Microtubule disruption synergizes with oncolytic virotherapy by inhibiting interferon translation and potentiating bystander killing. Nature communications. 2015;6:6410.

176. Woller N, Gurlevik E, Ureche CI, Schumacher A, Kuhnel F. Oncolytic viruses as anticancer vaccines. Frontiers in oncology. 2014;4:188.

177. Bhat R, Dempe S, Dinsart C, Rommelaere J. Enhancement of NK cell antitumor responses using an oncolytic parvovirus. International journal of cancer. 2011;128(4):908-19.

178. Raulet DH, Gasser S, Gowen BG, Deng W, Jung H. Regulation of ligands for the NKG2D activating receptor. Annual review of immunology. 2013;31:413-41.

179. Paolini R, Bernardini G, Molfetta R, Santoni A. NK cells and interferons. Cytokine & growth factor reviews. 2015;26(2):113-20.

180. Zamai L, Ahmad M, Bennett IM, Azzoni L, Alnemri ES, Perussia B. Natural killer (NK) cell-mediated cytotoxicity: differential use of TRAIL and Fas ligand by immature and mature primary human NK cells. The Journal of experimental medicine. 1998;188(12):2375-80.

181. Le Boeuf F, Selman M, Son HH, Bergeron A, Chen A, Tsang J, et al. Oncolytic Maraba Virus MG1 as a Treatment for Sarcoma. International journal of cancer. 2017;141(6):1257-64.

182. Jiang H, Rivera-Molina Y, Gomez-Manzano C, Clise-Dwyer K, Bover L, Vence LM, et al. Oncolytic Adenovirus and Tumor-Targeting Immune Modulatory Therapy Improve Autologous Cancer Vaccination. Cancer research. 2017;77(14):3894-907.

183. Bergman I, Griffin JA, Gao Y, Whitaker-Dowling P. Treatment of implanted mammary tumors with recombinant vesicular stomatitis virus targeted to Her2/neu. International journal of cancer. 2007;121(2):425-30.

184. Duffy MR, Fisher KD, Seymour LW. Making Oncolytic Virotherapy a Clinical Reality: The European Contribution. Human gene therapy. 2017;28(11):1033-46.

185. Donnelly OG, Errington-Mais F, Prestwich R, Harrington K, Pandha H, Vile R, et al. Recent clinical experience with oncolytic viruses. Current pharmaceutical biotechnology. 2012;13(9):1834-41.

186. Adair RA, Roulstone V, Scott KJ, Morgan R, Nuovo GJ, Fuller M, et al. Cell carriage, delivery, and selective replication of an oncolytic virus in tumor in patients. Science translational medicine. 2012;4(138):138ra77.

187. Warner SG, O'Leary MP, Fong Y. Therapeutic oncolytic viruses: clinical advances and future directions. Current opinion in oncology. 2017;29(5):359-65.

188. Russell SJ, Federspiel MJ, Peng KW, Tong C, Dingli D, Morice WG, et al. Remission of disseminated cancer after systemic oncolytic virotherapy. Mayo Clinic proceedings. 2014;89(7):926-33.

189. Li L, You LS, Mao LP, Jin SH, Chen XH, Qian WB. Combing oncolytic adenovirus expressing Beclin-1 with chemotherapy agent doxorubicin synergistically enhances cytotoxicity in human CML cells in vitro. Acta pharmacologica Sinica. 2018;39(2):251-60.

190. Castleton A, Dey A, Beaton B, Patel B, Aucher A, Davis DM, et al. Human mesenchymal stromal cells deliver systemic oncolytic measles virus to treat acute lymphoblastic leukemia in the presence of humoral immunity. Blood. 2014;123(9):1327-35.

191. Tumilasci VF, Oliere S, Nguyen TL, Shamy A, Bell J, Hiscott J. Targeting the apoptotic pathway with BCL-2 inhibitors sensitizes primary chronic lymphocytic leukemia cells to vesicular stomatitis virus-induced oncolysis. Journal of virology. 2008;82(17):8487-99.

192. Esfandyari T, Tefferi A, Szmidt A, Alain T, Zwolak P, Lasho T, et al. Transcription factors down-stream of Ras as molecular indicators for targeting malignancies with oncolytic herpes virus. Molecular oncology. 2009;3(5-6):464-8.

193. Calton CM, Kelly KR, Anwer F, Carew JS, Nawrocki ST. Oncolytic Viruses for Multiple Myeloma Therapy. Cancers. 2018;10(6).

194. Bartee E, Bartee MY, Bogen B, Yu XZ. Systemic therapy with oncolytic myxoma virus cures established residual multiple myeloma in mice. Molecular therapy oncolytics. 2016;3:16032.

195. Sborov DW, Nuovo GJ, Stiff A, Mace T, Lesinski GB, Benson DM, Jr., et al. A phase I trial of single-agent reolysin in patients with relapsed multiple

myeloma. Clinical cancer research : an official journal of the American Association for Cancer Research. 2014;20(23):5946-55.

196. ClinicalTrials.gov. VSV-hIFNbeta-NIS in Treating Patients With Relapsed or Refractory Multiple Myeloma, Acute Myeloid Leukemia, or T-cell Lymphoma [NCT03017820]. Bethesda, MD: NIH U.S. National Library of Medicine; 2017.

197. Naik S, Nace R, Barber GN, Russell SJ. Potent systemic therapy of multiple myeloma utilizing oncolytic vesicular stomatitis virus coding for interferon-beta. Cancer gene therapy. 2012;19(7):443-50.

198. Dispenzieri A, Tong C, LaPlant B, Lacy MQ, Laumann K, Dingli D, et al. Phase I trial of systemic administration of Edmonston strain of measles virus genetically engineered to express the sodium iodide symporter in patients with recurrent or refractory multiple myeloma. Leukemia. 2017;31(12):2791-8.

199. ClinicalTrials.gov. UARK 2014-21 A Phase II Trial of Oncolytic Virotherapy by Systemic Administration of Edmonston Strain of Measles Virus [NCT02192775]. Bethesda, MD: NIH U.S. Nationl Library of Medicine; 2014.

200. Lilly CL, Villa NY, Lemos de Matos A, Ali HM, Dhillon JS, Hofland T, et al. Ex Vivo Oncolytic Virotherapy with Myxoma Virus Arms Multiple Allogeneic Bone Marrow Transplant Leukocytes to Enhance Graft versus Tumor. Molecular therapy oncolytics. 2017;4:31-40.

201. Deng H, Tang N, Stief AE, Mehta N, Baig E, Head R, et al. Oncolytic virotherapy for multiple myeloma using a tumour-specific double-deleted vaccinia virus. Leukemia. 2008;22(12):2261-4.

202. Au GG, Lincz LF, Enno A, Shafren DR. Oncolytic Coxsackievirus A21 as a novel therapy for multiple myeloma. British journal of haematology. 2007;137(2):133-41.

203. Senac JS, Doronin K, Russell SJ, Jelinek DF, Greipp PR, Barry MA. Infection and killing of multiple myeloma by adenoviruses. Human gene therapy. 2010;21(2):179-90.

204. Fernandes MS, Gomes EM, Butcher LD, Hernandez-Alcoceba R, Chang D, Kansopon J, et al. Growth inhibition of human multiple myeloma cells by an oncolytic adenovirus carrying the CD40 ligand transgene. Clinical cancer research : an official journal of the American Association for Cancer Research. 2009;15(15):4847-56.

205. Shen W, Patnaik MM, Ruiz A, Russell SJ, Peng KW. Immunovirotherapy with vesicular stomatitis virus and PD-L1 blockade enhances therapeutic outcome in murine acute myeloid leukemia. Blood. 2016;127(11):1449-58.

206. Hall K, Scott KJ, Rose A, Desborough M, Harrington K, Pandha H, et al. Reovirus-mediated cytotoxicity and enhancement of innate immune

responses against acute myeloid leukemia. BioResearch open access. 2012;1(1):3-15.

207. Samudio I, Rezvani K, Shaim H, Hofs E, Ngom M, Bu L, et al. UV-inactivated HSV-1 potently activates NK cell killing of leukemic cells. Blood. 2016;127(21):2575-86.

208. Madlambayan GJ, Bartee E, Kim M, Rahman MM, Meacham A, Scott EW, et al. Acute myeloid leukemia targeting by myxoma virus in vivo depends on cell binding but not permissiveness to infection in vitro. Leukemia research. 2012;36(5):619-24.

209. Wei X, Liu L, Wang G, Li W, Xu K, Qi H, et al. Potent antitumor activity of the Ad5/11 chimeric oncolytic adenovirus combined with interleukin-24 for acute myeloid leukemia via induction of apoptosis. Oncology reports. 2015;33(1):111-8.

210. Zhang LF, Tan DQ, Jeyasekharan AD, Hsieh WS, Ho AS, Ichiyama K, et al. Combination of vaccine-strain measles and mumps virus synergistically kills a wide range of human hematological cancer cells: Special focus on acute myeloid leukemia. Cancer letters. 2014;354(2):272-80.

211. Dermody TSP, J.S.L.; Sherry, B. . Orthoreovirus. In: Knipe DMH, P.M., editor. Fields Virology. 2. Philadelphia, PA: Lippincott, Williams, & Wilkins; 2013. p. 1304-46.

212. Lemay G. Transcriptional and translational events during reovirus infection. Biochemistry and cell biology = Biochimie et biologie cellulaire. 1988;66(8):803-12.

213. Shatkin AJ, Sipe JD, Loh P. Separation of ten reovirus genome segments by polyacrylamide gel electrophoresis. Journal of virology. 1968;2(10):986-91.

214. Rosen L, Hovis JF, Mastrota FM, Bell JA, Huebner RJ. Observations on a newly recognized virus (Abney) of the reovirus family. American journal of hygiene. 1960;71:258-65.

215. Smakman N, van den Wollenberg DJ, Borel Rinkes IH, Hoeben RC, Kranenburg O. Sensitization to apoptosis underlies KrasD12-dependent oncolysis of murine C26 colorectal carcinoma cells by reovirus T3D. Journal of virology. 2005;79(23):14981-5.

216. Ikeda Y, Nishimura G, Yanoma S, Kubota A, Furukawa M, Tsukuda M. Reovirus oncolysis in human head and neck squamous carcinoma cells. Auris, nasus, larynx. 2004;31(4):407-12.

217. Berger AK, Hiller BE, Thete D, Snyder AJ, Perez E, Jr., Upton JW, et al. Viral RNA at Two Stages of Reovirus Infection Is Required for the Induction of Necroptosis. Journal of virology. 2017;91(6).

218. Clarke P, Meintzer SM, Gibson S, Widmann C, Garrington TP, Johnson GL, et al. Reovirus-induced apoptosis is mediated by TRAIL. Journal of virology. 2000;74(17):8135-9.

219. Kominsky DJ, Bickel RJ, Tyler KL. Reovirus-induced apoptosis requires both death receptor- and mitochondrial-mediated caspase-dependent pathways of cell death. Cell death and differentiation. 2002;9(9):926-33.

220. Kominsky DJ, Bickel RJ, Tyler KL. Reovirus-induced apoptosis requires mitochondrial release of Smac/DIABLO and involves reduction of cellular inhibitor of apoptosis protein levels. Journal of virology. 2002;76(22):11414-24.

221. Knowlton JJ, Dermody TS, Holm GH. Apoptosis induced by mammalian reovirus is beta interferon (IFN) independent and enhanced by IFN regulatory factor 3- and NF-kappaB-dependent expression of Noxa. Journal of virology. 2012;86(3):1650-60.

222. Thirukkumaran C, Shi ZQ, Thirukkumaran P, Luider J, Kopciuk K, Spurrell J, et al. PUMA and NF-kB Are Cell Signaling Predictors of Reovirus Oncolysis of Breast Cancer. PloS one. 2017;12(1):e0168233.

223. Barton ES, Forrest JC, Connolly JL, Chappell JD, Liu Y, Schnell FJ, et al. Junction adhesion molecule is a receptor for reovirus. Cell. 2001;104(3):441-51.

224. Sugano Y, Takeuchi M, Hirata A, Matsushita H, Kitamura T, Tanaka M, et al. Junctional adhesion molecule-A, JAM-A, is a novel cell-surface marker for long-term repopulating hematopoietic stem cells. Blood. 2008;111(3):1167-72.

225. Kelly KR, Espitia CM, Zhao W, Wendlandt E, Tricot G, Zhan F, et al. Junctional adhesion molecule-A is overexpressed in advanced multiple myeloma and determines response to oncolytic reovirus. Oncotarget. 2015;6(38):41275-89.

226. Xu PP, Sun YF, Fang Y, Song Q, Yan ZX, Chen Y, et al. JAM-A overexpression is related to disease progression in diffuse large B-cell lymphoma and downregulated by lenalidomide. Scientific reports. 2017;7(1):7433.

227. Goetsch L, Haeuw JF, Beau-Larvor C, Gonzalez A, Zanna L, Malissard M, et al. A novel role for junctional adhesion molecule-A in tumor proliferation: modulation by an anti-JAM-A monoclonal antibody. International journal of cancer. 2013;132(6):1463-74.

228. Zhao C, Lu F, Chen H, Zhao X, Sun J, Chen H. Dysregulation of JAM-A plays an important role in human tumor progression. International journal of clinical and experimental pathology. 2014;7(10):7242-8.

229. Maginnis MS, Forrest JC, Kopecky-Bromberg SA, Dickeson SK, Santoro SA, Zutter MM, et al. Beta1 integrin mediates internalization of mammalian reovirus. Journal of virology. 2006;80(6):2760-70.

230. Alain T, Kim TS, Lun X, Liacini A, Schiff LA, Senger DL, et al. Proteolytic disassembly is a critical determinant for reovirus oncolysis. Molecular therapy : the journal of the American Society of Gene Therapy. 2007;15(8):1512-21.

231. Golden JW, Linke J, Schmechel S, Thoemke K, Schiff LA. Addition of exogenous protease facilitates reovirus infection in many restrictive cells. Journal of virology. 2002;76(15):7430-43.

232. Downward J. Targeting RAS signalling pathways in cancer therapy. Nature reviews Cancer. 2003;3(1):11-22.

233. Marcato P, Shmulevitz M, Pan D, Stoltz D, Lee PW. Ras transformation mediates reovirus oncolysis by enhancing virus uncoating, particle infectivity, and apoptosis-dependent release. Molecular therapy : the journal of the American Society of Gene Therapy. 2007;15(8):1522-30.

234. Errington F, Steele L, Prestwich R, Harrington KJ, Pandha HS, Vidal L, et al. Reovirus activates human dendritic cells to promote innate antitumor immunity. Journal of immunology (Baltimore, Md : 1950). 2008;180(9):6018-26.

235. Levy DE, Marie IJ, Durbin JE. Induction and function of type I and III interferon in response to viral infection. Current opinion in virology. 2011;1(6):476-86.

236. Rojas M, Arias CF, Lopez S. Protein kinase R is responsible for the phosphorylation of eIF2alpha in rotavirus infection. Journal of virology. 2010;84(20):10457-66.

237. Steele L, Errington F, Prestwich R, Ilett E, Harrington K, Pandha H, et al. Pro-inflammatory cytokine/chemokine production by reovirus treated melanoma cells is PKR/NF-kappaB mediated and supports innate and adaptive anti-tumour immune priming. Molecular cancer. 2011;10:20.

238. Prestwich RJ, Errington F, Steele LP, Ilett EJ, Morgan RS, Harrington KJ, et al. Reciprocal human dendritic cell-natural killer cell interactions induce antitumor activity following tumor cell infection by oncolytic reovirus. Journal of immunology (Baltimore, Md : 1950). 2009;183(7):4312-21.

239. Johansson C, Wetzel JD, He J, Mikacenic C, Dermody TS, Kelsall BL. Type I interferons produced by hematopoietic cells protect mice against lethal infection by mammalian reovirus. The Journal of experimental medicine. 2007;204(6):1349-58.

240. Morin MJ, Warner A, Fields BN. Reovirus infection in rat lungs as a model to study the pathogenesis of viral pneumonia. Journal of virology. 1996;70(1):541-8.

241. Gauvin L, Bennett S, Liu H, Hakimi M, Schlossmacher M, Majithia J, et al. Respiratory infection of mice with mammalian reoviruses causes systemic infection with age and strain dependent pneumonia and encephalitis. Virology journal. 2013;10:67.

242. Loken SD, Norman K, Hirasawa K, Nodwell M, Lester WM, Demetrick DJ. Morbidity in immunosuppressed (SCID/NOD) mice treated with reovirus (dearing 3) as an anti-cancer biotherapeutic. Cancer biology & therapy. 2004;3(8):734-8.

243. Kim M, Garant KA, zur Nieden NI, Alain T, Loken SD, Urbanski SJ, et al. Attenuated reovirus displays oncolysis with reduced host toxicity. British journal of cancer. 2011;104(2):290-9.

244. Finberg R, Weiner HL, Fields BN, Benacerraf B, Burakoff SJ. Generation of cytolytic T lymphocytes after reovirus infection: role of S1 gene. Proceedings of the National Academy of Sciences of the United States of America. 1979;76(1):442-6.

245. Gujar SA, Pan DA, Marcato P, Garant KA, Lee PW. Oncolytic virus-initiated protective immunity against prostate cancer. Molecular therapy : the journal of the American Society of Gene Therapy. 2011;19(4):797-804.

246. Prestwich RJ, Errington F, Ilett EJ, Morgan RS, Scott KJ, Kottke T, et al. Tumor infection by oncolytic reovirus primes adaptive antitumor immunity. Clinical cancer research : an official journal of the American Association for Cancer Research. 2008;14(22):7358-66.

247. Prestwich RJ, Ilett EJ, Errington F, Diaz RM, Steele LP, Kottke T, et al. Immune-mediated antitumor activity of reovirus is required for therapy and is independent of direct viral oncolysis and replication. Clinical cancer research : an official journal of the American Association for Cancer Research. 2009;15(13):4374-81.

248. Minuk GY, Paul RW, Lee PW. The prevalence of antibodies to reovirus type 3 in adults with idiopathic cholestatic liver disease. J Med Virol. 1985;16(1):55-60.

249. Tai JH, Williams JV, Edwards KM, Wright PF, Crowe JE, Jr., Dermody TS. Prevalence of reovirus-specific antibodies in young children in Nashville, Tennessee. The Journal of infectious diseases. 2005;191(8):1221-4.

250. Ilett EJ, Prestwich RJ, Kottke T, Errington F, Thompson JM, Harrington KJ, et al. Dendritic cells and T cells deliver oncolytic reovirus for tumour killing despite pre-existing anti-viral immunity. Gene therapy. 2009;16(5):689-99.

251. Ilett EJ, Barcena M, Errington-Mais F, Griffin S, Harrington KJ, Pandha HS, et al. Internalization of oncolytic reovirus by human dendritic cell carriers protects the virus from neutralization. Clinical cancer research : an official journal of the American Association for Cancer Research. 2011;17(9):2767-76.

252. Ilett E, Kottke T, Donnelly O, Thompson J, Willmon C, Diaz R, et al. Cytokine conditioning enhances systemic delivery and therapy of an oncolytic virus. Molecular therapy : the journal of the American Society of Gene Therapy. 2014;22(10):1851-63.

253. Berkeley RA, Steele LP, Mulder AA, van den Wollenberg DJM, Kottke TJ, Thompson J, et al. Antibody-Neutralized Reovirus Is Effective in Oncolytic Virotherapy. Cancer immunology research. 2018;6(10):1161-73.

254. Yue Z, Shatkin AJ. Double-stranded RNA-dependent protein kinase (PKR) is regulated by reovirus structural proteins. Virology. 1997;234(2):364-71.

255. Stanifer ML, Kischnick C, Rippert A, Albrecht D, Boulant S. Reovirus inhibits interferon production by sequestering IRF3 into viral factories. Scientific reports. 2017;7(1):10873.

256. Comins C, Spicer J, Protheroe A, Roulstone V, Twigger K, White CM, et al. REO-10: a phase I study of intravenous reovirus and docetaxel in patients with advanced cancer. Clinical cancer research : an official journal of the American Association for Cancer Research. 2010;16(22):5564-72.

257. Lolkema MP, Arkenau HT, Harrington K, Roxburgh P, Morrison R, Roulstone V, et al. A phase I study of the combination of intravenous reovirus type 3 Dearing and gemcitabine in patients with advanced cancer. Clinical cancer research : an official journal of the American Association for Cancer Research. 2011;17(3):581-8.

258. Karapanagiotou EM, Roulstone V, Twigger K, Ball M, Tanay M, Nutting C, et al. Phase I/II trial of carboplatin and paclitaxel chemotherapy in combination with intravenous oncolytic reovirus in patients with advanced malignancies. Clinical cancer research : an official journal of the American Association for Cancer Research. 2012;18(7):2080-9.

259. ClinicalTrials.gov. Viral Immunotherapy in Relapsed/Refractory Multiple Myeloma (MUKeleven) [NCT03015922]. Bethesda, MD: NIH U.S. National Library of Medicine; 2017.

260. White CL, Twigger KR, Vidal L, De Bono JS, Coffey M, Heinemann L, et al. Characterization of the adaptive and innate immune response to intravenous oncolytic reovirus (Dearing type 3) during a phase I clinical trial. Gene therapy. 2008;15(12):911-20.

261. Samson A, Scott KJ, Taggart D, West EJ, Wilson E, Nuovo GJ, et al. Intravenous delivery of oncolytic reovirus to brain tumor patients immunologically primes for subsequent checkpoint blockade. Science translational medicine. 2018;10(422).

262. Vidal L, Pandha HS, Yap TA, White CL, Twigger K, Vile RG, et al. A phase I study of intravenous oncolytic reovirus type 3 Dearing in patients with advanced cancer. Clinical cancer research : an official journal of the American Association for Cancer Research. 2008;14(21):7127-37.

263. Forsyth P, Roldan G, George D, Wallace C, Palmer CA, Morris D, et al. A phase I trial of intratumoral administration of reovirus in patients with histologically confirmed recurrent malignant gliomas. Molecular therapy : the journal of the American Society of Gene Therapy. 2008;16(3):627-32.

264. Noonan AM, Farren MR, Geyer SM, Huang Y, Tahiri S, Ahn D, et al. Randomized Phase 2 Trial of the Oncolytic Virus Pelareorep (Reolysin) in Upfront Treatment of Metastatic Pancreatic Adenocarcinoma. Molecular therapy : the journal of the American Society of Gene Therapy. 2016;24(6):1150-8.

265. Karnad AB, Haigentz M, Miley T, Coffey M, Gill G, Mita M. Abstract C22: A phase II study of intravenous wild-type reovirus (Reolysin®) in combination with paclitaxel plus carboplatin in patients with platinum refractory metastatic and/or recurrent squamous cell carcinoma of the head and neck. Molecular Cancer Therapeutics. 2011;10(11 Supplement):C22-C.

266. Galanis E, Markovic SN, Suman VJ, Nuovo GJ, Vile RG, Kottke TJ, et al. Phase II trial of intravenous administration of Reolysin((R)) (Reovirus Serotype-3-dearing Strain) in patients with metastatic melanoma. Molecular therapy : the journal of the American Society of Gene Therapy. 2012;20(10):1998-2003.

267. Mahalingam D, Fountzilas C, Moseley J, Noronha N, Tran H, Chakrabarty R, et al. A phase II study of REOLYSIN((R)) (pelareorep) in combination with carboplatin and paclitaxel for patients with advanced malignant melanoma. Cancer chemotherapy and pharmacology. 2017;79(4):697-703.

268. ClinicalTrials.gov. Wild-type Reovirus in Combination With Carfilzomib and Dexamethasone in Treating Patients With Relapsed or Refractory Multiple Myeloma [NCT02101944]. Bethesda, MD: NIH U.S. National Library of Medicine; 2014.

269. ClinicalTrials.gov. Wild-Type Reovirus, Bortezomib, and Dexamethasone in Treating Patients With Relapsed or Refractory Multiple Myeloma [NCT02514382]. Bethesda, MD: NIH U.S. National Library of Medicine; 2015.

270. Villalona-Calero MA, Lam E, Otterson GA, Zhao W, Timmons M, Subramaniam D, et al. Oncolytic reovirus in combination with chemotherapy in metastatic or recurrent non-small cell lung cancer patients with KRAS-activated tumors. Cancer. 2016;122(6):875-83.

271. Mita AC, Argiris A, Coffey M, Gill G, Mita M. Abstract C70: A phase 2 study of intravenous administration of REOLYSIN® (reovirus type 3 dearing) in combination with paclitaxel (P) and carboplatin (C) in patients with squamous cell carcinoma of the lung. Molecular Cancer Therapeutics. 2013;12(11 Supplement):C70-C.

272. Bradbury PA, Morris DG, Nicholas G, Tu D, Tehfe M, Goffin JR, et al. Canadian Cancer Trials Group (CCTG) IND211: A randomized trial of

pelareorep (Reolysin) in patients with previously treated advanced or metastatic non-small cell lung cancer receiving standard salvage therapy. Lung cancer (Amsterdam, Netherlands). 2018;120:142-8.

273. Eigl BJ, Winquist E, Tu D, Hotte SJ, Canil CM, Gregg RW, et al. A randomized phase II study of pelareorep (REO) plus docetaxel vs. docetaxel alone in patients with metastatic castration resistant prostate cancer (mCRPC): Canadian Cancer Trials Group study IND 209. Journal of Clinical Oncology. 2017;35(15_suppl):5021-.

274. Bernstein VE, S.; Dent, S. F.; Gelmon, K. A.; Dhesy-Thind, S. K.; Mates, M.; Salim, M.; Panasci, L.; Song, X.; Clemons, M.; Tu, D.; Hagerman, L. J.; Seymour, L., editor A randomized (RCT) phase II study of oncolytic reovirus (pelareorep) plus standard weekly paclitaxel (P) as therapy for metastatic breast cancer (mBC) [Abstract nr CT131]. American Association for Cancer Research Annual Meeting 2017; 2017; Washington, DC: Cancer Res 2017;77 (13 Suppl).

275. Rossmann MG, Arnold E, Erickson JW, Frankenberger EA, Griffith JP, Hecht HJ, et al. Structure of a human common cold virus and functional relationship to other picornaviruses. Nature. 1985;317(6033):145-53.

276. Tuthill TJ, Groppelli E, Hogle JM, Rowlands DJ. Picornaviruses. Current topics in microbiology and immunology. 2010;343:43-89.

277. Hyypia T, Kallajoki M, Maaronen M, Stanway G, Kandolf R, Auvinen P, et al. Pathogenetic differences between coxsackie A and B virus infections in newborn mice. Virus research. 1993;27(1):71-8.

278. Xiao C, Bator CM, Bowman VD, Rieder E, He Y, Hebert B, et al. Interaction of coxsackievirus A21 with its cellular receptor, ICAM-1. Journal of virology. 2001;75(5):2444-51.

279. Shafren DR, Dorahy DJ, Ingham RA, Burns GF, Barry RD. Coxsackievirus A21 binds to decay-accelerating factor but requires intercellular adhesion molecule 1 for cell entry. Journal of virology. 1997;71(6):4736-43.

280. van de Stolpe A, van der Saag PT. Intercellular adhesion molecule-1. Journal of molecular medicine (Berlin, Germany). 1996;74(1):13-33.

281. Hopkins AM, Baird AW, Nusrat A. ICAM-1: targeted docking for exogenous as well as endogenous ligands. Advanced drug delivery reviews. 2004;56(6):763-78.

282. Xia YF, Liu LP, Zhong CP, Geng JG. NF-kappaB activation for constitutive expression of VCAM-1 and ICAM-1 on B lymphocytes and plasma cells. Biochemical and biophysical research communications. 2001;289(4):851-6.

283. Heicappell R, Podlinski J, Buszello H, Ackermann R. Cell surface expression and serum levels of intercellular adhesion molecule-1 in renal cell carcinoma. Urological research. 1994;22(1):9-15.

284. Johnson JP, Stade BG, Holzmann B, Schwable W, Riethmuller G. De novo expression of intercellular-adhesion molecule 1 in melanoma correlates with increased risk of metastasis. Proceedings of the National Academy of Sciences of the United States of America. 1989;86(2):641-4.

285. Schwaeble W, Kerlin M, Meyer zum Buschenfelde KH, Dippold W. De novo expression of intercellular adhesion molecule 1 (ICAM-1, CD54) in pancreas cancer. International journal of cancer. 1993;53(2):328-33.

286. Maeda K, Kang SM, Sawada T, Nishiguchi Y, Yashiro M, Ogawa Y, et al. Expression of intercellular adhesion molecule-1 and prognosis in colorectal cancer. Oncology reports. 2002;9(3):511-4.

287. Molica S, Dattilo A, Mannella A, Levato D, Levato L. Expression on leukemic cells and serum circulating levels of intercellular adhesion molecule-1 (ICAM-1) in B-cell chronic lymphocytic leukemia: implications for prognosis. Leukemia research. 1995;19(8):573-80.

288. Miele ME, Bennett CF, Miller BE, Welch DR. Enhanced metastatic ability of TNF-alpha-treated malignant melanoma cells is reduced by intercellular adhesion molecule-1 (ICAM-1, CD54) antisense oligonucleotides. Experimental cell research. 1994;214(1):231-41.

289. Johnson JP, Stade BG, Hupke U, Holzmann B, Riethmuller G. The melanoma progression-associated antigen P3.58 is identical to the intercellular adhesion molecule, ICAM-1. Immunobiology. 1988;178(3):275-84.

290. Triantafilou K, Orthopoulos G, Vakakis E, Ahmed MA, Golenbock DT, Lepper PM, et al. Human cardiac inflammatory responses triggered by Coxsackie B viruses are mainly Toll-like receptor (TLR) 8-dependent. Cellular microbiology. 2005;7(8):1117-26.

291. Wang JP, Asher DR, Chan M, Kurt-Jones EA, Finberg RW. Cutting Edge: Antibody-mediated TLR7-dependent recognition of viral RNA. Journal of immunology (Baltimore, Md : 1950). 2007;178(6):3363-7.

292. Huhn MH, McCartney SA, Lind K, Svedin E, Colonna M, Flodstrom-Tullberg M. Melanoma differentiation-associated protein-5 (MDA-5) limits early viral replication but is not essential for the induction of type 1 interferons after Coxsackievirus infection. Virology. 2010;401(1):42-8.

293. Wang JP, Cerny A, Asher DR, Kurt-Jones EA, Bronson RT, Finberg RW. MDA5 and MAVS mediate type I interferon responses to coxsackie B virus. Journal of virology. 2010;84(1):254-60.

294. Richer MJ, Lavallee DJ, Shanina I, Horwitz MS. Toll-like receptor 3 signaling on macrophages is required for survival following coxsackievirus B4 infection. PloS one. 2009;4(1):e4127.

295. Lowenstein CJ, Hill SL, Lafond-Walker A, Wu J, Allen G, Landavere M, et al. Nitric oxide inhibits viral replication in murine myocarditis. The Journal of clinical investigation. 1996;97(8):1837-43.

296. Vella C, Festenstein H. Coxsackievirus B4 infection of the mouse pancreas: the role of natural killer cells in the control of virus replication and resistance to infection. The Journal of general virology. 1992;73 (Pt 6):1379-86.

297. Anderson DR, Carthy CM, Wilson JE, Yang D, Devine DV, McManus BM. Complement component 3 interactions with coxsackievirus B3 capsid proteins: innate immunity and the rapid formation of splenic antiviral germinal centers. Journal of virology. 1997;71(11):8841-5.

298. Kemball CC, Harkins S, Whitton JL. Enumeration and functional evaluation of virus-specific CD4+ and CD8+ T cells in lymphoid and peripheral sites of coxsackievirus B3 infection. Journal of virology. 2008;82(9):4331-42.

299. Klingel K, Schnorr JJ, Sauter M, Szalay G, Kandolf R. beta2-microglobulin-associated regulation of interferon-gamma and virus-specific immunoglobulin G confer resistance against the development of chronic coxsackievirus myocarditis. The American journal of pathology. 2003;162(5):1709-20.

300. Slifka MK, Pagarigan R, Mena I, Feuer R, Whitton JL. Using recombinant coxsackievirus B3 to evaluate the induction and protective efficacy of CD8+ T cells during picornavirus infection. Journal of virology. 2001;75(5):2377-87.

301. Annels NE, Arif M, Simpson GR, Denyer M, Moller-Levet C, Mansfield D, et al. Oncolytic Immunotherapy for Bladder Cancer Using Coxsackie A21 Virus. Molecular therapy oncolytics. 2018;9:1-12.

302. Pereira M, Pereira HG. COE VIRUS PROPERTIES AND PREVALENCE IN GREAT BRITAIN. The Lancet. 1959;274(7102):539-41.

303. Au GG. Control of Cancer Progression by Virotherapy. Newcastle, Australia: University of Newcastle; 2004.

304. Au GG, Beagley LG, Haley ES, Barry RD, Shafren DR. Oncolysis of malignant human melanoma tumors by Coxsackieviruses A13, A15 and A18. Virology journal. 2011;8:22.

305. Pandha H, Harrington K, Ralph C, Melcher A, Grose M, Shafren D. Phase I/II storm study: Intravenous delivery of a novel oncolytic immunotherapy agent, Coxsackievirus A21, in advanced cancer patients. J Immunother Cancer. 2015;3(Suppl 2):P341.

306. Mukherjee A, Morosky SA, Delorme-Axford E, Dybdahl-Sissoko N, Oberste MS, Wang T, et al. The coxsackievirus B 3C protease cleaves MAVS and TRIF to attenuate host type I interferon and apoptotic signaling. PLoS pathogens. 2011;7(3):e1001311.

307. Lind K, Svedin E, Domsgen E, Kapell S, Laitinen OH, Moll M, et al. Coxsackievirus counters the host innate immune response by blocking type III interferon expression. Journal of General Virology. 2016;97(6):1368-80.

308. Kemball CC, Harkins S, Whitmire JK, Flynn CT, Feuer R, Whitton JL. Coxsackievirus B3 inhibits antigen presentation in vivo, exerting a profound and selective effect on the MHC class I pathway. PLoS pathogens. 2009;5(10):e1000618.

309. Viralytics Ltd. Clinical Trials - Phase 1 KEYNOTE-200. Sydney, Australia: Viralytics Ltd; 2018. Available from: https://www.viralytics.com/our-pipeline/clinical-trials/clinical-trials-phase-i-storm/.

310. Ann W. Silk HLK, Mark Faries, Steven O'Day, Nashat Gabrail, Janice Mehnert, Jennifer Bryan, Jacqueline Norrell, Azra Haider, Praveen K. Bommareddy, Darren Shafren, Mark Grose and Andrew Zloza. CAPRA: A Phase Ib study of intratumoral oncolytic Coxsackievirus A21 (CVA21) and systemic pembrolizumab in advanced melanoma patients. Society for Immunotherapy of Cancer – 32nd Annual Meeting. 2017.

311. Brendan Curti JR, Mark Faries, Robert H.I Andtbacka, Sigrun Hallmeyer, Mark Grose, Roberta Karpathy, Darren R. Shafren. . A phase Ib study of intratumoral CAVATAK (Coxsackievirus A21) and ipilimumab in patients with advanced melanoma Society for Immunotherapy of Cancer (SITC) - 31st Annual Meeting National Harbor, MD2016.

312. ClinicalTrials.gov. CAVATAK® and Ipilimumab in Uveal Melanoma Metastatic to the Liver (VLA-024 CLEVER) (CLEVER) [NCT03408587]. Bethesda, MD: NIH U.S. National Library of Medicine; 2018.

313. Andtbacka RH, Curti BD, Hallmeyer S, Feng Z, Paustian C, Bifulco C, et al. Phase II calm extension study: Coxsackievirus A21 delivered intratumorally to patients with advanced melanoma induces immune-cell infiltration in the tumor microenvironment. Journal for ImmunoTherapy of Cancer. 2015;3(2):P343.

314. Pandha HA, N.; Simpson, G.; Iqbal, A.; Mansfield, D.; Sandhu, S. S.; Melcher, A. A.; Harrington, K. J.; Davies, B.; Au, G. G.; Grose, M.; Mostafid, H.; Shafren, D. Phase I/II CANON study: Oncolytic immunotherapy for the treatment of Non-Muscle Invasive Bladder Cancer using intravesical Coxsackievirus A21. Society for Immunotherapy of Cancer (SITC) - 31st Annual Meeting National Harbor, MD2016.

315. ClinicalTrials.gov. CVA21 and Pembrolizumab in NSCLC & Bladder Cancer (VLA-009 STORM/ KEYNOTE-200) (STORM) [NCT02043665]. Bethesda, MD: NIH U.S. National Library of Medicine; 2014.

316. ClinicalTrials.gov. Pembrolizumab + CVA21 in Advanced NSCLC [NCT02824965]. Bethesda, MD: NIH U.S. National Library of Medicine; 2016.

317. Ramakrishnan MA. Determination of 50% endpoint titer using a simple formula. World Journal of Virology. 2016;5(2):85-6.

318. Kelly KR, Espitia CM, Mahalingam D, Oyajobi BO, Coffey M, Giles FJ, et al. Reovirus therapy stimulates endoplasmic reticular stress, NOXA

induction, and augments bortezomib-mediated apoptosis in multiple myeloma. Oncogene. 2012;31(25):3023-38.

319. Stiff A, Caserta E, Sborov DW, Nuovo GJ, Mo X, Schlotter SY, et al. Histone Deacetylase Inhibitors Enhance the Therapeutic Potential of Reovirus in Multiple Myeloma. Molecular cancer therapeutics. 2016;15(5):830-41.

320. Thirukkumaran CM, Shi ZQ, Luider J, Kopciuk K, Gao H, Bahlis N, et al. Reovirus as a viable therapeutic option for the treatment of multiple myeloma. Clinical cancer research : an official journal of the American Association for Cancer Research. 2012;18(18):4962-72.

321. Thirukkumaran CM, Shi ZQ, Luider J, Kopciuk K, Gao H, Bahlis N, et al. Reovirus modulates autophagy during oncolysis of multiple myeloma. Autophagy. 2013;9(3):413-4.

322. ClinicalTrials.gov. Wild-type Reovirus in Combination With Carfilzomib and Dexamethasone in Treating Patients With Relapsed or Refractory Multiple Myeloma [NCT02101944]. Bethesda, MD: NIH U.S. National Library of Medicine; 2014.

323. Thirukkumaran CM, Shi ZQ, Luider J, Kopciuk K, Bahlis N, Neri P, et al. Reovirus as a successful ex vivo purging modality for multiple myeloma. Bone marrow transplantation. 2014;49(1):80-6.

324. Manier S, Sacco A, Leleu X, Ghobrial IM, Roccaro AM. Bone marrow microenvironment in multiple myeloma progression. Journal of biomedicine & biotechnology. 2012;2012:157496.

325. Clements DR, Sterea AM, Kim Y, Helson E, Dean CA, Nunokawa A, et al. Newly recruited CD11b+, GR-1+, Ly6C(high) myeloid cells augment tumor-associated immunosuppression immediately following the therapeutic administration of oncolytic reovirus. Journal of immunology (Baltimore, Md : 1950). 2015;194(9):4397-412.

326. Zamarin D, Ricca JM, Sadekova S, Oseledchyk A, Yu Y, Blumenschein WM, et al. PD-L1 in tumor microenvironment mediates resistance to oncolytic immunotherapy. The Journal of clinical investigation. 2018;128(4):1413-28.

327. Hossain DM, Pal SK, Moreira D, Duttagupta P, Zhang Q, Won H, et al. TLR9-Targeted STAT3 Silencing Abrogates Immunosuppressive Activity of Myeloid-Derived Suppressor Cells from Prostate Cancer Patients. Clinical cancer research : an official journal of the American Association for Cancer Research. 2015;21(16):3771-82.

328. Mirjacic Martinovic K, Srdic-Rajic T, Babovic N, Dzodic R, Jurisic V, Konjevic G. Decreased expression of pSTAT, IRF-1 and DAP10 signalling molecules in peripheral blood lymphocytes of patients with metastatic melanoma. Journal of clinical pathology. 2016;69(4):300-6.

329. Okuma Y, Hosomi Y, Nakahara Y, Watanabe K, Sagawa Y, Homma S. High plasma levels of soluble programmed cell death ligand 1 are prognostic for reduced survival in advanced lung cancer. Lung cancer (Amsterdam, Netherlands). 2017;104:1-6.

330. Schmielau J, Finn OJ. Activated granulocytes and granulocyte-derived hydrogen peroxide are the underlying mechanism of suppression of t-cell function in advanced cancer patients. Cancer research. 2001;61(12):4756-60.

331. Carlo-Stella C, Guidetti A, Di Nicola M, Lavazza C, Cleris L, Sia D, et al. IFN-gamma enhances the antimyeloma activity of the fully human anti-human leukocyte antigen-DR monoclonal antibody 1D09C3. Cancer research. 2007;67(7):3269-75.

332. Koziner B, Dengra C, Cisneros M, Glancszpigel R. Double-blind prospective randomized comparison of interferon gamma-1b versus placebo after autologous stem cell transplantation. Acta haematologica. 2002;108(2):66-73.

333. Salmasinia D, Chang M, Wingard JR, Hou W, Moreb JS. Combination of IFN-alpha/Gm-CSF as a Maintenance Therapy for Multiple Myeloma Patients After Autologous Stem Cell Transplantation (ASCT): A Prospective Phase II Study. Clinical Medicine Insights Oncology. 2010;4:117-25.

334. Yoo EM, Trinh KR, Tran D, Vasuthasawat A, Zhang J, Hoang B, et al. Anti-CD138-targeted interferon is a potent therapeutic against multiple myeloma. Journal of interferon & cytokine research : the official journal of the International Society for Interferon and Cytokine Research. 2015;35(4):281-91.

335. Mitsiades CS, Treon SP, Mitsiades N, Shima Y, Richardson P, Schlossman R, et al. TRAIL/Apo2L ligand selectively induces apoptosis and overcomes drug resistance in multiple myeloma: therapeutic applications. Blood. 2001;98(3):795-804.

336. Lincz LF, Yeh TX, Spencer A. TRAIL-induced eradication of primary tumour cells from multiple myeloma patient bone marrows is not related to TRAIL receptor expression or prior chemotherapy. Leukemia. 2001;15(10):1650-7.

337. Gillies SD, Lan Y, Hettmann T, Brunkhorst B, Sun Y, Mueller SO, et al. A low-toxicity IL-2-based immunocytokine retains antitumor activity despite its high degree of IL-2 receptor selectivity. Clinical cancer research : an official journal of the American Association for Cancer Research. 2011;17(11):3673-85.

338. Tyler KL, Squier MK, Rodgers SE, Schneider BE, Oberhaus SM, Grdina TA, et al. Differences in the capacity of reovirus strains to induce apoptosis are determined by the viral attachment protein sigma 1. Journal of virology. 1995;69(11):6972-9.

339. McClain ME, Spendlove RS. Multiplicity reactivation of reovirus particles after exposure to ultraviolet light. Journal of bacteriology. 1966;92(5):1422-9.

340. Winzler C, Rovere P, Rescigno M, Granucci F, Penna G, Adorini L, et al. Maturation stages of mouse dendritic cells in growth factor-dependent long-term cultures. The Journal of experimental medicine. 1997;185(2):317-28.

341. Pierre P, Turley SJ, Gatti E, Hull M, Meltzer J, Mirza A, et al. Developmental regulation of MHC class II transport in mouse dendritic cells. Nature. 1997;388(6644):787-92.

342. Cella M, Engering A, Pinet V, Pieters J, Lanzavecchia A. Inflammatory stimuli induce accumulation of MHC class II complexes on dendritic cells. Nature. 1997;388(6644):782-7.

343. Germain RN. MHC-dependent antigen processing and peptide presentation: providing ligands for T lymphocyte activation. Cell. 1994;76(2):287-99.

344. Bhat P, Leggatt G, Waterhouse N, Frazer IH. Interferon-gamma derived from cytotoxic lymphocytes directly enhances their motility and cytotoxicity. Cell death & disease. 2017;8(6):e2836.

345. Ghanekar SA, Nomura LE, Suni MA, Picker LJ, Maecker HT, Maino VC. Gamma interferon expression in CD8(+) T cells is a marker for circulating cytotoxic T lymphocytes that recognize an HLA A2-restricted epitope of human cytomegalovirus phosphoprotein pp65. Clinical and diagnostic laboratory immunology. 2001;8(3):628-31.

346. Bradley LM, Yoshimoto K, Swain SL. The cytokines IL-4, IFN-gamma, and IL-12 regulate the development of subsets of memory effector helper T cells in vitro. Journal of immunology (Baltimore, Md : 1950). 1995;155(4):1713-24.

347. Bradley LM, Dalton DK, Croft M. A direct role for IFN-gamma in regulation of Th1 cell development. Journal of immunology (Baltimore, Md : 1950). 1996;157(4):1350-8.

348. Thirukkumaran CM, Luider JM, Stewart DA, Cheng T, Lupichuk SM, Nodwell MJ, et al. Reovirus oncolysis as a novel purging strategy for autologous stem cell transplantation. Blood. 2003;102(1):377-87.

349. Hadac EM, Kelly EJ, Russell SJ. Myeloma xenograft destruction by a nonviral vector delivering oncolytic infectious nucleic acid. Molecular therapy : the journal of the American Society of Gene Therapy. 2011;19(6):1041-7.

350. Muguruma Y, Yahata T, Warita T, Hozumi K, Nakamura Y, Suzuki R, et al. Jagged1-induced Notch activation contributes to the acquisition of bortezomib resistance in myeloma cells. Blood cancer journal. 2017;7(12):650.

351. Voorhees PM, Chen Q, Kuhn DJ, Small GW, Hunsucker SA, Strader JS, et al. Inhibition of interleukin-6 signaling with CNTO 328 enhances the activity of bortezomib in preclinical models of multiple myeloma. Clinical cancer research : an official journal of the American Association for Cancer Research. 2007;13(21):6469-78.

352. Zheng Y, Cai Z, Wang S, Zhang X, Qian J, Hong S, et al. Macrophages are an abundant component of myeloma microenvironment and protect myeloma cells from chemotherapy drug-induced apoptosis. Blood. 2009;114(17):3625-8.

353. Farrell ML, Reagan MR. Soluble and Cell-Cell-Mediated Drivers of Proteasome Inhibitor Resistance in Multiple Myeloma. Frontiers in endocrinology. 2018;9:218.

354. Roecklein BA, Torok-Storb B. Functionally distinct human marrow stromal cell lines immortalized by transduction with the human papilloma virus E6/E7 genes. Blood. 1995;85(4):997-1005.

355. Tang J, Zhou H, Wang C, Fei X, Zhu L, Huang Y, et al. Cell adhesion downregulates the expression of Homer1b/c and contributes to drug resistance in multiple myeloma cells. Oncology reports. 2016;35(3):1875-83.

356. Furukawa M, Ohkawara H, Ogawa K, Ikeda K, Ueda K, Shichishima-Nakamura A, et al. Autocrine and Paracrine Interactions between Multiple Myeloma Cells and Bone Marrow Stromal Cells by Growth Arrest-specific Gene 6 Cross-talk with Interleukin-6. The Journal of biological chemistry. 2017;292(10):4280-92.

357. Xu X, Liu J, Shen C, Ding L, Zhong F, Ouyang Y, et al. The role of ubiquitin-specific protease 14 (USP14) in cell adhesion-mediated drug resistance (CAM-DR) of multiple myeloma cells. European journal of haematology. 2017;98(1):4-12.

358. de la Puente P, Muz B, Gilson RC, Azab F, Luderer M, King J, et al. 3D tissue-engineered bone marrow as a novel model to study pathophysiology and drug resistance in multiple myeloma. Biomaterials. 2015;73:70-84.

359. Wang X, Feng X, Wang J, Shao N, Ji C, Ma D, et al. Bortezomib and IL-12 produce synergetic anti-multiple myeloma effects with reduced toxicity to natural killer cells. Anti-cancer drugs. 2014;25(3):282-8.

360. Berger U, Engelich G, Maywald O, Pfirrmann M, Hochhaus A, Reiter A, et al. Chronic myeloid leukemia in the elderly: long-term results from randomized trials with interferon alpha. Leukemia. 2003;17(9):1820-6.

361. Bohn JP, Gastl G, Steurer M. Long-term treatment of hairy cell leukemia with interferon-alpha: still a viable therapeutic option. Memo. 2016;9:63-5.

362. Patel MR, Jacobson BA, Ji Y, Drees J, Tang S, Xiong K, et al. Vesicular stomatitis virus expressing interferon-beta is oncolytic and

promotes antitumor immune responses in a syngeneic murine model of non-small cell lung cancer. Oncotarget. 2015;6(32):33165-77.

363. Li H, Peng KW, Dingli D, Kratzke RA, Russell SJ. Oncolytic measles viruses encoding interferon beta and the thyroidal sodium iodide symporter gene for mesothelioma virotherapy. Cancer gene therapy. 2010;17(8):550-8.

364. Sterman DH, Recio A, Carroll RG, Gillespie CT, Haas A, Vachani A, et al. A phase I clinical trial of single-dose intrapleural IFN-beta gene transfer for malignant pleural mesothelioma and metastatic pleural effusions: high rate of antitumor immune responses. Clinical cancer research : an official journal of the American Association for Cancer Research. 2007;13(15 Pt 1):4456-66.

365. Katsoulidis E, Kaur S, Platanias LC. Deregulation of Interferon Signaling in Malignant Cells. Pharmaceuticals (Basel, Switzerland). 2010;3(2):406-18.

366. Danziger O, Pupko T, Bacharach E, Ehrlich M. Interleukin-6 and Interferon-alpha Signaling via JAK1-STAT Differentially Regulate Oncolytic versus Cytoprotective Antiviral States. Frontiers in immunology. 2018;9:94.

367. Mittal SK, Roche PA. Suppression of antigen presentation by IL-10. Current opinion in immunology. 2015;34:22-7.

368. Mittal SK, Cho KJ, Ishido S, Roche PA. Interleukin 10 (IL-10)-mediated Immunosuppression: MARCH-I INDUCTION REGULATES ANTIGEN PRESENTATION BY MACROPHAGES BUT NOT DENDRITIC CELLS. The Journal of biological chemistry. 2015;290(45):27158-67.

369. van Rhee F, Szmania SM, Dillon M, van Abbema AM, Li X, Stone MK, et al. Combinatorial efficacy of anti-CS1 monoclonal antibody elotuzumab (HuLuc63) and bortezomib against multiple myeloma. Molecular cancer therapeutics. 2009;8(9):2616-24.

370. Garg TK, Szmania SM, Khan JA, Hoering A, Malbrough PA, Moreno-Bost A, et al. Highly activated and expanded natural killer cells for multiple myeloma immunotherapy. Haematologica. 2012;97(9):1348-56.

371. Adair RA, Scott KJ, Fraser S, Errington-Mais F, Pandha H, Coffey M, et al. Cytotoxic and immune-mediated killing of human colorectal cancer by reovirus-loaded blood and liver mononuclear cells. International journal of cancer. 2013;132(10):2327-38.

372. Sherbenou DW, Mark TM, Forsberg P. Monoclonal Antibodies in Multiple Myeloma: A New Wave of the Future. Clinical lymphoma, myeloma & leukemia. 2017;17(9):545-54.

373. Schwartz C, Palissot V, Aouali N, Wack S, Brons NH, Leners B, et al. Valproic acid induces non-apoptotic cell death mechanisms in multiple myeloma cell lines. International journal of oncology. 2007;30(3):573-82.

374. Neri P, Tagliaferri P, Di Martino MT, Calimeri T, Amodio N, Bulotta A, et al. In vivo anti-myeloma activity and modulation of gene expression profile induced by valproic acid, a histone deacetylase inhibitor. British journal of haematology. 2008;143(4):520-31.

375. Kaiser M, Zavrski I, Sterz J, Jakob C, Fleissner C, Kloetzel PM, et al. The effects of the histone deacetylase inhibitor valproic acid on cell cycle, growth suppression and apoptosis in multiple myeloma. Haematologica. 2006;91(2):248-51.

376. Wu X, Tao Y, Hou J, Meng X, Shi J. Valproic acid upregulates NKG2D ligand expression through an ERK-dependent mechanism and potentially enhances NK cell-mediated lysis of myeloma. Neoplasia (New York, NY). 2012;14(12):1178-89.

377. Kojima H, Shinohara N, Hanaoka S, Someya-Shirota Y, Takagaki Y, Ohno H, et al. Two distinct pathways of specific killing revealed by perforin mutant cytotoxic T lymphocytes. Immunity. 1994;1(5):357-64.

378. Seki N, Brooks AD, Carter CR, Back TC, Parsoneault EM, Smyth MJ, et al. Tumor-specific CTL kill murine renal cancer cells using both perforin and Fas ligand-mediated lysis in vitro, but cause tumor regression in vivo in the absence of perforin. Journal of immunology (Baltimore, Md : 1950). 2002;168(7):3484-92.

379. Jennings VA, Ilett EJ, Scott KJ, West EJ, Vile R, Pandha H, et al. Lymphokine-activated killer and dendritic cell carriage enhances oncolytic reovirus therapy for ovarian cancer by overcoming antibody neutralization in ascites. International journal of cancer. 2014;134(5):1091-101.

380. Gujar SA, Marcato P, Pan D, Lee PW. Reovirus virotherapy overrides tumor antigen presentation evasion and promotes protective antitumor immunity. Molecular cancer therapeutics. 2010;9(11):2924-33.

381. Goodyear OC, Pratt G, McLarnon A, Cook M, Piper K, Moss P. Differential pattern of CD4+ and CD8+ T-cell immunity to MAGE-A1/A2/A3 in patients with monoclonal gammopathy of undetermined significance (MGUS) and multiple myeloma. Blood. 2008;112(8):3362-72.

382. Goodyear OC, Pearce H, Pratt G, Moss P. Dominant responses with conservation of T-cell receptor usage in the CD8+ T-cell recognition of a cancer testis antigen peptide presented through HLA-Cw7 in patients with multiple myeloma. Cancer immunology, immunotherapy : CII. 2011;60(12):1751-61.

383. Noto H, Takahashi T, Makiguchi Y, Hayashi T, Hinoda Y, Imai K. Cytotoxic T lymphocytes derived from bone marrow mononuclear cells of multiple myeloma patients recognize an underglycosylated form of MUC1 mucin. International immunology. 1997;9(5):791-8.

384. Ocadlikova D, Kryukov F, Mollova K, Kovarova L, Buresdova I, Matejkova E, et al. Generation of myeloma-specific T cells using dendritic

cells loaded with MUC1- and hTERT- drived nonapeptides or myeloma cell apoptotic bodies. Neoplasma. 2010;57(5):455-64.

385. Lu ZY, Condomines M, Tarte K, Nadal L, Delteil MC, Rossi JF, et al. B7-1 and 4-1BB ligand expression on a myeloma cell line makes it possible to expand autologous tumor-specific cytotoxic T cells in vitro. Experimental hematology. 2007;35(3):443-53.

386. Blotta S, Tassone P, Prabhala RH, Tagliaferri P, Cervi D, Amin S, et al. Identification of novel antigens with induced immune response in monoclonal gammopathy of undetermined significance. Blood. 2009;114(15):3276-84.

387. Parrish C, Scott GB, Coffey M, Melcher A, Errington-Mais F, Cook G. Combination Therapy with Reovirus and Immunomodulatory Drugs Induces Direct Oncolytic and Immune-Mediated Killing of Multiple Myeloma Cells and Overcomes Stromal-Mediated Microenvironmental Protection. Blood. 2014;124(21):4778-.

388. El-Sherbiny YM, Holmes TD, Wetherill LF, Black EV, Wilson EB, Phillips SL, et al. Controlled infection with a therapeutic virus defines the activation kinetics of human natural killer cells in vivo. Clinical and experimental immunology. 2015;180(1):98-107.

389. Atanackovic D, Luetkens T, Kroger N. Coinhibitory molecule PD-1 as a potential target for the immunotherapy of multiple myeloma. Leukemia. 2014;28(5):993-1000.

390. Badros A, Hyjek E, Ma N, Lesokhin A, Dogan A, Rapoport AP, et al. Pembrolizumab, pomalidomide, and low-dose dexamethasone for relapsed/refractory multiple myeloma. Blood. 2017;130(10):1189-97.

391. ClinicalTrials.gov. Intratumoral CAVATAK (CVA21) and Pembrolizumab in Patients With Advanced Melanoma (VLA-011 CAPRA) [NCT02565992]. Bethesda, MD: NIH U.S. National Library of Medicine; 2015.

392. Kelly KR, Espitia CM, Zhao W, Wu K, Visconte V, Anwer F, et al. Oncolytic reovirus sensitizes multiple myeloma cells to anti-PD-L1 therapy. Leukemia. 2018;32(1):230-3.

393. Mostafa AA, Meyers DE, Thirukkumaran CM, Liu PJ, Gratton K, Spurrell J, et al. Oncolytic Reovirus and Immune Checkpoint Inhibition as a Novel Immunotherapeutic Strategy for Breast Cancer. Cancers. 2018;10(6).

394. Samson A, Bentham MJ, Scott K, Nuovo G, Bloy A, Appleton E, et al. Oncolytic reovirus as a combined antiviral and anti-tumour agent for the treatment of liver cancer. Gut. 2018;67(3):562-73.

395. Viralytics Ltd. Our Pipeline - Pre-Clinical Studies. Sydney, Australia: Viralytics Ltd; 2018. Available from: https://www.viralytics.com/our-pipeline/pre-clinical-studies/.

396. Kato H, Takeuchi O, Mikamo-Satoh E, Hirai R, Kawai T, Matsushita K, et al. Length-dependent recognition of double-stranded ribonucleic acids by retinoic acid-inducible gene-I and melanoma differentiation-associated gene 5. The Journal of experimental medicine. 2008;205(7):1601-10.

397. Shafren DR, Dorahy DJ, Greive SJ, Burns GF, Barry RD. Mouse cells expressing human intercellular adhesion molecule-1 are susceptible to infection by coxsackievirus A21. Journal of virology. 1997;71(1):785-9.

398. Paton-Hough J, Chantry AD, Lawson MA. A review of current murine models of multiple myeloma used to assess the efficacy of therapeutic agents on tumour growth and bone disease. Bone. 2015;77:57-68.

399. Radl J, De Glopper ED, Schuit HR, Zurcher C. Idiopathic paraproteinemia. II. Transplantation of the paraprotein-producing clone from old to young C57BL/KaLwRij mice. Journal of immunology (Baltimore, Md : 1950). 1979;122(2):609-13.

400. Dallas SL, Garrett IR, Oyajobi BO, Dallas MR, Boyce BF, Bauss F, et al. Ibandronate reduces osteolytic lesions but not tumor burden in a murine model of myeloma bone disease. Blood. 1999;93(5):1697-706.

401. van den Akker TW, Radl J, Franken-Postma E, Hagemeijer A. Cytogenetic findings in mouse multiple myeloma and Waldenstrom's macroglobulinemia. Cancer genetics and cytogenetics. 1996;86(2):156-61.

402. Radl J, Croese JW, Zurcher C, Van den Enden-Vieveen MH, de Leeuw AM. Animal model of human disease. Multiple myeloma. The American journal of pathology. 1988;132(3):593-7.

403. Goel A, Carlson SK, Classic KL, Greiner S, Naik S, Power AT, et al. Radioiodide imaging and radiovirotherapy of multiple myeloma using VSV(Delta51)-NIS, an attenuated vesicular stomatitis virus encoding the sodium iodide symporter gene. Blood. 2007;110(7):2342-50.

404. Oyajobi BO, Munoz S, Kakonen R, Williams PJ, Gupta A, Wideman CL, et al. Detection of myeloma in skeleton of mice by whole-body optical fluorescence imaging. Molecular cancer therapeutics. 2007;6(6):1701-8.

405. Ziegler SF, Ramsdell F, Alderson MR. The activation antigen CD69. Stem cells (Dayton, Ohio). 1994;12(5):456-65.

406. Parrish C. Immune Dysfunction in Myeloma: Characterisation and Generation of IL-17-secreting Lymphocytes and Immune Manipulation using Oncolytic Virotherapy. Leeds: University of Leeds; 2016.

407. Sallusto F, Geginat J, Lanzavecchia A. Central memory and effector memory T cell subsets: function, generation, and maintenance. Annual review of immunology. 2004;22:745-63.

408. Navabi S, Doroudchi M, Tashnizi AH, Habibagahi M. Natural Killer Cell Functional Activity After 4-1BB Costimulation. Inflammation. 2015;38(3):1181-90.

409. Barao I. The TNF receptor-ligands 4-1BB-4-1BBL and GITR-GITRL in NK cell responses. Frontiers in immunology. 2012;3:402.

410. Wolfl M, Kuball J, Ho WY, Nguyen H, Manley TJ, Bleakley M, et al. Activation-induced expression of CD137 permits detection, isolation, and expansion of the full repertoire of CD8+ T cells responding to antigen without requiring knowledge of epitope specificities. Blood. 2007;110(1):201-10.

411. Agata Y, Kawasaki A, Nishimura H, Ishida Y, Tsubata T, Yagita H, et al. Expression of the PD-1 antigen on the surface of stimulated mouse T and B lymphocytes. International immunology. 1996;8(5):765-72.

412. Chikuma S. Basics of PD-1 in self-tolerance, infection, and cancer immunity. International journal of clinical oncology. 2016;21(3):448-55.

413. Krummel MF, Allison JP. CD28 and CTLA-4 have opposing effects on the response of T cells to stimulation. The Journal of experimental medicine. 1995;182(2):459-65.

414. Walunas TL, Lenschow DJ, Bakker CY, Linsley PS, Freeman GJ, Green JM, et al. CTLA-4 can function as a negative regulator of T cell activation. Immunity. 1994;1(5):405-13.

415. Blackburn SD, Shin H, Haining WN, Zou T, Workman CJ, Polley A, et al. Coregulation of CD8+ T cell exhaustion by multiple inhibitory receptors during chronic viral infection. Nature immunology. 2009;10(1):29-37.

416. Crawford A, Wherry EJ. The diversity of costimulatory and inhibitory receptor pathways and the regulation of antiviral T cell responses. Current opinion in immunology. 2009;21(2):179-86.

417. Denton NL, Chen CY, Scott TR, Cripe TP. Tumor-Associated Macrophages in Oncolytic Virotherapy: Friend or Foe? Biomedicines. 2016;4(3).

418. Chavez-Galan L, Olleros ML, Vesin D, Garcia I. Much More than M1 and M2 Macrophages, There are also CD169(+) and TCR(+) Macrophages. Frontiers in immunology. 2015;6:263.

419. Wang C, Yu X, Cao Q, Wang Y, Zheng G, Tan TK, et al. Characterization of murine macrophages from bone marrow, spleen and peritoneum. BMC immunology. 2013;14:6.

420. Ciavarra RP, Buhrer K, Van Rooijen N, Tedeschi B. T cell priming against vesicular stomatitis virus analyzed in situ: red pulp macrophages, but neither marginal metallophilic nor marginal zone macrophages, are required for priming CD4+ and CD8+ T cells. Journal of immunology (Baltimore, Md : 1950). 1997;158(4):1749-55.

421. Asosingh K, Radl J, Van Riet I, Van Camp B, Vanderkerken K. The 5TMM series: a useful in vivo mouse model of human multiple myeloma. The hematology journal : the official journal of the European Haematology Association. 2000;1(5):351-6.

422. Lwin ST, Edwards CM, Silbermann R. Preclinical animal models of multiple myeloma. BoneKEy reports. 2016;5:772.

423. Turner PV, Brabb T, Pekow C, Vasbinder MA. Administration of substances to laboratory animals: routes of administration and factors to consider. Journal of the American Association for Laboratory Animal Science : JAALAS. 2011;50(5):600-13.

424. Vaha-Koskela MJ, Kallio JP, Jansson LC, Heikkila JE, Zakhartchenko VA, Kallajoki MA, et al. Oncolytic capacity of attenuated replicative semliki forest virus in human melanoma xenografts in severe combined immunodeficient mice. Cancer research. 2006;66(14):7185-94.

425. Tseng JC, Levin B, Hurtado A, Yee H, Perez de Castro I, Jimenez M, et al. Systemic tumor targeting and killing by Sindbis viral vectors. Nature biotechnology. 2004;22(1):70-7.

426. Peng KW, Frenzke M, Myers R, Soeffker D, Harvey M, Greiner S, et al. Biodistribution of oncolytic measles virus after intraperitoneal administration into Ifnar-CD46Ge transgenic mice. Human gene therapy. 2003;14(16):1565-77.

427. Naik S, Nace R, Federspiel MJ, Barber GN, Peng KW, Russell SJ. Curative one-shot systemic virotherapy in murine myeloma. Leukemia. 2012;26(8):1870-8.

428. Lawson MA, McDonald MM, Kovacic N, Hua Khoo W, Terry RL, Down J, et al. Osteoclasts control reactivation of dormant myeloma cells by remodelling the endosteal niche. Nature communications. 2015;6:8983.

429. Pessoa de Magalhaes RJ, Vidriales MB, Paiva B, Fernandez-Gimenez C, Garcia-Sanz R, Mateos MV, et al. Analysis of the immune system of multiple myeloma patients achieving long-term disease control by multidimensional flow cytometry. Haematologica. 2013;98(1):79-86.

430. Parker SE, Sears DW. H-2 restriction and serotype crossreactivity of anti-reovirus cytotoxic T lymphocytes (CTL). Viral immunology. 1990;3(1):77-87.

431. Finberg R, Spriggs DR, Fields BN. Host immune response to reovirus: CTL recognize the major neutralization domain of the viral hemagglutinin. Journal of immunology (Baltimore, Md : 1950). 1982;129(5):2235-8.

432. Li X, Wang P, Li H, Du X, Liu M, Huang Q, et al. The Efficacy of Oncolytic Adenovirus Is Mediated by T-cell Responses against Virus and Tumor in Syrian Hamster Model. Clinical cancer research : an official journal of the American Association for Cancer Research. 2017;23(1):239-49.

433. Benson DM, Jr., Bakan CE, Mishra A, Hofmeister CC, Efebera Y, Becknell B, et al. The PD-1/PD-L1 axis modulates the natural killer cell versus multiple myeloma effect: a therapeutic target for CT-011, a novel monoclonal anti-PD-1 antibody. Blood. 2010;116(13):2286-94.

434. Beldi-Ferchiou A, Lambert M, Dogniaux S, Vély F, Vivier E, Olive D, et al. PD-1 mediates functional exhaustion of activated NK cells in patients with Kaposi sarcoma. Oncotarget. 2016;7(45):72961-77.

435. Liu Y, Cheng Y, Xu Y, Wang Z, Du X, Li C, et al. Increased expression of programmed cell death protein 1 on NK cells inhibits NK-cell-mediated anti-tumor function and indicates poor prognosis in digestive cancers. Oncogene. 2017;36(44):6143-53.

436. Katayama Y, Tachibana M, Kurisu N, Oya Y, Terasawa Y, Goda H, et al. Oncolytic Reovirus Inhibits Immunosuppressive Activity of Myeloid-Derived Suppressor Cells in a TLR3-Dependent Manner. Journal of immunology (Baltimore, Md : 1950). 2018;200(8):2987-99.

437. Shim KG, Zaidi S, Thompson J, Kottke T, Evgin L, Rajani KR, et al. Inhibitory Receptors Induced by VSV Viroimmunotherapy Are Not Necessarily Targets for Improving Treatment Efficacy. Molecular therapy : the journal of the American Society of Gene Therapy. 2017;25(4):962-75.

438. Ilett E, Kottke T, Thompson J, Rajani K, Zaidi S, Evgin L, et al. Prime-boost using separate oncolytic viruses in combination with checkpoint blockade improves anti-tumour therapy. Gene therapy. 2017;24(1):21-30.

439. Bar-On Y, Charpak-Amikam Y, Glasner A, Isaacson B, Duev-Cohen A, Tsukerman P, et al. NKp46 Recognizes the Sigma1 Protein of Reovirus: Implications for Reovirus-Based Cancer Therapy. Journal of virology. 2017;91(19).

440. Brown MC, Holl EK, Boczkowski D, Dobrikova E, Mosaheb M, Chandramohan V, et al. Cancer immunotherapy with recombinant poliovirus induces IFN-dominant activation of dendritic cells and tumor antigen-specific CTLs. Science translational medicine. 2017;9(408).

441. Durham NM, Mulgrew K, McGlinchey K, Monks NR, Ji H, Herbst R, et al. Oncolytic VSV Primes Differential Responses to Immuno-oncology Therapy. Molecular therapy : the journal of the American Society of Gene Therapy. 2017;25(8):1917-32.

442. Gauvrit A, Brandler S, Sapede-Peroz C, Boisgerault N, Tangy F, Gregoire M. Measles virus induces oncolysis of mesothelioma cells and allows dendritic cells to cross-prime tumor-specific CD8 response. Cancer research. 2008;68(12):4882-92.

443. Veinalde R, Grossardt C, Hartmann L, Bourgeois-Daigneault MC, Bell JC, Jager D, et al. Oncolytic measles virus encoding interleukin-12 mediates potent antitumor effects through T cell activation. Oncoimmunology. 2017;6(4):e1285992.

444. Racanelli V, Leone P, Frassanito MA, Brunetti C, Perosa F, Ferrone S, et al. Alterations in the antigen processing-presenting machinery of transformed plasma cells are associated with reduced recognition by CD8+

T cells and characterize the progression of MGUS to multiple myeloma. Blood. 2010;115(6):1185-93.

445. Leone P, Berardi S, Frassanito MA, Ria R, De Re V, Cicco S, et al. Dendritic cells accumulate in the bone marrow of myeloma patients where they protect tumor plasma cells from CD8+ T-cell killing. Blood. 2015;126(12):1443-51.

446. Kurotaki D, Uede T, Tamura T. Functions and development of red pulp macrophages. Microbiology and immunology. 2015;59(2):55-62.

447. Kim CC, Nelson CS, Wilson EB, Hou B, DeFranco AL, DeRisi JL. Splenic red pulp macrophages produce type I interferons as early sentinels of malaria infection but are dispensable for control. PloS one. 2012;7(10):e48126.

448. Kurotaki D, Kon S, Bae K, Ito K, Matsui Y, Nakayama Y, et al. CSF-1-dependent red pulp macrophages regulate CD4 T cell responses. Journal of immunology (Baltimore, Md : 1950). 2011;186(4):2229-37.

449. Clements DR, Murphy JP, Sterea A, Kennedy BE, Kim Y, Helson E, et al. Quantitative Temporal in Vivo Proteomics Deciphers the Transition of Virus-Driven Myeloid Cells into M2 Macrophages. Journal of proteome research. 2017;16(9):3391-406.

450. Tan DQ, Zhang L, Ohba K, Ye M, Ichiyama K, Yamamoto N. Macrophage response to oncolytic paramyxoviruses potentiates virus-mediated tumor cell killing. European journal of immunology. 2016;46(4):919-28.

451. Muthana M, Giannoudis A, Scott SD, Fang HY, Coffelt SB, Morrow FJ, et al. Use of macrophages to target therapeutic adenovirus to human prostate tumors. Cancer research. 2011;71(5):1805-15.

452. Muthana M, Rodrigues S, Chen YY, Welford A, Hughes R, Tazzyman S, et al. Macrophage delivery of an oncolytic virus abolishes tumor regrowth and metastasis after chemotherapy or irradiation. Cancer research. 2013;73(2):490-5.

453. Fulci G, Dmitrieva N, Gianni D, Fontana EJ, Pan X, Lu Y, et al. Depletion of peripheral macrophages and brain microglia increases brain tumor titers of oncolytic viruses. Cancer research. 2007;67(19):9398-406.

454. Liu YP, Suksanpaisan L, Steele MB, Russell SJ, Peng KW. Induction of antiviral genes by the tumor microenvironment confers resistance to virotherapy. Scientific reports. 2013;3:2375.

455. Binsfeld M, Muller J, Lamour V, De Veirman K, De Raeve H, Bellahcene A, et al. Granulocytic myeloid-derived suppressor cells promote angiogenesis in the context of multiple myeloma. Oncotarget. 2016;7(25):37931-43.

456. Chesi M, Mirza NN, Garbitt VM, Sharik ME, Dueck AC, Asmann YW, et al. IAP antagonists induce anti-tumor immunity in multiple myeloma. Nature medicine. 2016;22(12):1411-20.

457. Zhang L, Bi E, Hong S, Qian J, Zheng C, Wang M, et al. CD4(+) T cells play a crucial role for lenalidomide in vivo anti-tumor activity in murine multiple myeloma. Oncotarget. 2015;6(34):36032-40.

458. Hong S, Qian J, Yang J, Li H, Kwak LW, Yi Q. Roles of Idiotype-Specific T Cells in Myeloma Cell Growth and Survival: Th1 and CTL Cells Are Tumoricidal While Th2 Cells Promote Tumor Growth. Cancer research. 2008;68(20):8456-64.

459. Skelding KA, Barry RD, Shafren DR. Systemic targeting of metastatic human breast tumor xenografts by Coxsackievirus A21. Breast cancer research and treatment. 2009;113(1):21-30.

460. Peters JM, Ansari MQ. Multiparameter flow cytometry in the diagnosis and management of acute leukemia. Archives of pathology & laboratory medicine. 2011;135(1):44-54.

461. Stark GR, Kerr IM, Williams BR, Silverman RH, Schreiber RD. How cells respond to interferons. Annual review of biochemistry. 1998;67:227-64.

462. Darnell JE, Jr., Kerr IM, Stark GR. Jak-STAT pathways and transcriptional activation in response to IFNs and other extracellular signaling proteins. Science (New York, NY). 1994;264(5164):1415-21.

463. Ratanatharathorn V, Uberti J, Karanes C, Lum LG, Abella E, Dan ME, et al. Phase I study of alpha-interferon augmentation of cyclosporine-induced graft versus host disease in recipients of autologous bone marrow transplantation. Bone marrow transplantation. 1994;13(5):625-30.

464. Grigg A, Kannan K, Schwarer AP, Spencer A, Szer J. Chemotherapy and granulocyte colony stimulating factor-mobilized blood cell infusion followed by interferon-alpha for relapsed malignancy after allogeneic bone marrow transplantation. Internal medicine journal. 2001;31(1):15-22.

465. Yang J, Ikezoe T, Nishioka C, Nobumoto A, Yokoyama A. IL-1beta inhibits self-renewal capacity of dormant CD34(+)/CD38(-) acute myelogenous leukemia cells in vitro and in vivo. International journal of cancer. 2013;133(8):1967-81.

466. Margolin K, Forman SJ. Immunotherapy with interleukin-2 after hematopoietic cell transplantation for hematologic malignancy. The cancer journal from Scientific American. 2000;6 Suppl 1:S33-8.

467. Givon T, Slavin S, Haran-Ghera N, Michalevicz R, Revel M. Antitumor effects of human recombinant interleukin-6 on acute myeloid leukemia in mice and in cell cultures. Blood. 1992;79(9):2392-8.

468. Lee S, Margolin K. Cytokines in Cancer Immunotherapy. Cancers. 2011;3(4):3856-93.

469. Long EO, Kim HS, Liu D, Peterson ME, Rajagopalan S. Controlling natural killer cell responses: integration of signals for activation and inhibition. Annual review of immunology. 2013;31:227-58.

470. Sloan KE, Eustace BK, Stewart JK, Zehetmeier C, Torella C, Simeone M, et al. CD155/PVR plays a key role in cell motility during tumor cell invasion and migration. BMC cancer. 2004;4:73.

471. Morimoto K, Satoh-Yamaguchi K, Hamaguchi A, Inoue Y, Takeuchi M, Okada M, et al. Interaction of cancer cells with platelets mediated by Necl-5/poliovirus receptor enhances cancer cell metastasis to the lungs. Oncogene. 2008;27(3):264-73.

472. Deguine J, Breart B, Lemaitre F, Di Santo JP, Bousso P. Intravital imaging reveals distinct dynamics for natural killer and CD8(+) T cells during tumor regression. Immunity. 2010;33(4):632-44.

473. Marcus A, Gowen BG, Thompson TW, Iannello A, Ardolino M, Deng W, et al. Recognition of tumors by the innate immune system and natural killer cells. Advances in immunology. 2014;122:91-128.

474. Greiner J, Ringhoffer M, Taniguchi M, Li L, Schmitt A, Shiku H, et al. mRNA expression of leukemia-associated antigens in patients with acute myeloid leukemia for the development of specific immunotherapies. International journal of cancer. 2004;108(5):704-11.

475. Siegal FP, Kadowaki N, Shodell M, Fitzgerald-Bocarsly PA, Shah K, Ho S, et al. The nature of the principal type 1 interferon-producing cells in human blood. Science (New York, NY). 1999;284(5421):1835-7.

476. Cella M, Jarrossay D, Facchetti F, Alebardi O, Nakajima H, Lanzavecchia A, et al. Plasmacytoid monocytes migrate to inflamed lymph nodes and produce large amounts of type I interferon. Nature medicine. 1999;5(8):919-23.

477. Boyette LB, Macedo C, Hadi K, Elinoff BD, Walters JT, Ramaswami B, et al. Phenotype, function, and differentiation potential of human monocyte subsets. PloS one. 2017;12(4):e0176460.

478. Shaw GM, Levy PC, LoBuglio AF. Human monocyte antibody-dependent cell-mediated cytotoxicity to tumor cells. The Journal of clinical investigation. 1978;62(6):1172-80.

479. Yeap WH, Wong KL, Shimasaki N, Teo EC, Quek JK, Yong HX, et al. CD16 is indispensable for antibody-dependent cellular cytotoxicity by human monocytes. Scientific reports. 2016;6:34310.

480. Dale DC, Boxer L, Liles WC. The phagocytes: neutrophils and monocytes. Blood. 2008;112(4):935-45.

481. Liu YJ. IPC: professional type 1 interferon-producing cells and plasmacytoid dendritic cell precursors. Annual review of immunology. 2005;23:275-306.

482. Shortman K, Sathe P, Vremec D, Naik S, O'Keeffe M. Plasmacytoid dendritic cell development. Advances in immunology. 2013;120:105-26.

483. Vogel K, Thomann S, Vogel B, Schuster P, Schmidt B. Both plasmacytoid dendritic cells and monocytes stimulate natural killer cells early during human herpes simplex virus type 1 infections. Immunology. 2014;143(4):588-600.

484. Le Bon A, Etchart N, Rossmann C, Ashton M, Hou S, Gewert D, et al. Cross-priming of CD8+ T cells stimulated by virus-induced type I interferon. Nature immunology. 2003;4(10):1009-15.

485. Spadaro F, Lapenta C, Donati S, Abalsamo L, Barnaba V, Belardelli F, et al. IFN-alpha enhances cross-presentation in human dendritic cells by modulating antigen survival, endocytic routing, and processing. Blood. 2012;119(6):1407-17.

486. Kadowaki N, Ho S, Antonenko S, Malefyt RW, Kastelein RA, Bazan F, et al. Subsets of human dendritic cell precursors express different toll-like receptors and respond to different microbial antigens. The Journal of experimental medicine. 2001;194(6):863-9.

487. Bao M, Liu YJ. Regulation of TLR7/9 signaling in plasmacytoid dendritic cells. Protein & cell. 2013;4(1):40-52.

488. Li G, Li X, Wu H, Yang X, Zhang Y, Chen L, et al. CD123 targeting oncolytic adenoviruses suppress acute myeloid leukemia cell proliferation in vitro and in vivo. Blood cancer journal. 2014;4:e194.

489. Johansson ES, Xing L, Cheng RH, Shafren DR. Enhanced cellular receptor usage by a bioselected variant of coxsackievirus a21. Journal of virology. 2004;78(22):12603-12.

490. Newcombe NG, Beagley LG, Christiansen D, Loveland BE, Johansson ES, Beagley KW, et al. Novel role for decay-accelerating factor in coxsackievirus A21-mediated cell infectivity. Journal of virology. 2004;78(22):12677-82.

491. Ruby J, Bluethmann H, Peschon JJ. Antiviral Activity of Tumor Necrosis Factor (TNF) Is Mediated via p55 and p75 TNF Receptors. The Journal of experimental medicine. 1997;186(9):1591-6.

492. Elankumaran S, Chavan V, Qiao D, Shobana R, Moorkanat G, Biswas M, et al. Type I interferon-sensitive recombinant newcastle disease virus for oncolytic virotherapy. Journal of virology. 2010;84(8):3835-44.

493. Brun J, McManus D, Lefebvre C, Hu K, Falls T, Atkins H, et al. Identification of genetically modified Maraba virus as an oncolytic rhabdovirus. Molecular therapy : the journal of the American Society of Gene Therapy. 2010;18(8):1440-9.

494. Beug ST. Smac mimetics and innate immune stimuli synergize to promote tumor death. 2014;32(2):182-90.

495. Cai J, Lin Y, Zhang H, Liang J, Tan Y, Cavenee WK, et al. Selective replication of oncolytic virus M1 results in a bystander killing effect that is potentiated by Smac mimetics. Proceedings of the National Academy of Sciences of the United States of America. 2017;114(26):6812-7.

496. Errington F, White CL, Twigger KR, Rose A, Scott K, Steele L, et al. Inflammatory tumour cell killing by oncolytic reovirus for the treatment of melanoma. Gene therapy. 2008;15(18):1257-70.

497. Leng Y, Qiu L, Hou J, Zhao Y, Zhang X, Yang S, et al. Phase II open-label study of recombinant circularly permuted TRAIL as a single-agent treatment for relapsed or refractory multiple myeloma. Chinese journal of cancer. 2016;35(1):86.

498. Yang T, Lan J, Huang Q, Chen X, Sun X, Liu X, et al. Embelin sensitizes acute myeloid leukemia cells to TRAIL through XIAP inhibition and NF-kappaB inactivation. Cell biochemistry and biophysics. 2015;71(1):291-7.

499. Dijk M, Murphy E, Morrell R, Knapper S, O'Dwyer M, Samali A, et al. The Proteasome Inhibitor Bortezomib Sensitizes AML with Myelomonocytic Differentiation to TRAIL Mediated Apoptosis. Cancers. 2011;3(1):1329-50.

500. Jurcic JG. What happened to anti-CD33 therapy for acute myeloid leukemia? Current hematologic malignancy reports. 2012;7(1):65-73.

501. Diermayr S, Himmelreich H, Durovic B, Mathys-Schneeberger A, Siegler U, Langenkamp U, et al. NKG2D ligand expression in AML increases in response to HDAC inhibitor valproic acid and contributes to allorecognition by NK-cell lines with single KIR-HLA class I specificities. Blood. 2008;111(3):1428-36.

502. Poggi A, Catellani S, Garuti A, Pierri I, Gobbi M, Zocchi MR. Effective in vivo induction of NKG2D ligands in acute myeloid leukaemias by all-trans-retinoic acid or sodium valproate. Leukemia. 2009;23(4):641-8.

503. Sohlberg E, Pfefferle A, Andersson S, Baumann BC, Hellstrom-Lindberg E, Malmberg KJ. Imprint of 5-azacytidine on the natural killer cell repertoire during systemic treatment for high-risk myelodysplastic syndrome. Oncotarget. 2015;6(33):34178-90.

504. Raneros AB, Puras AM, Rodriguez RM, Colado E, Bernal T, Anguita E, et al. Increasing TIMP3 expression by hypomethylating agents diminishes soluble MICA, MICB and ULBP2 shedding in acute myeloid leukemia, facilitating NK cell-mediated immune recognition. Oncotarget. 2017;8(19):31959-76.

505. Vasu S, He S, Cheney C, Gopalakrishnan B, Mani R, Lozanski G, et al. Decitabine enhances anti-CD33 monoclonal antibody BI 836858-mediated natural killer ADCC against AML blasts. Blood. 2016;127(23):2879-89.

506. Yao Y, Zhou J, Wang L, Gao X, Ning Q, Jiang M, et al. Increased PRAME-specific CTL killing of acute myeloid leukemia cells by either a novel histone deacetylase inhibitor chidamide alone or combined treatment with decitabine. PloS one. 2013;8(8):e70522.

507. van den Ancker W, Ruben JM, Westers TM, Wulandari D, Bontkes HJ, Hooijberg E, et al. Priming of PRAME- and WT1-specific CD8(+) T cells in healthy donors but not in AML patients in complete remission: Implications for immunotherapy. Oncoimmunology. 2013;2(4):e23971.

508. Batenchuk C, Le Boeuf F, Stubbert L, Falls T, Atkins HL, Bell JC, et al. Non-replicating rhabdovirus-derived particles (NRRPs) eradicate acute leukemia by direct cytolysis and induction of antitumor immunity. Blood cancer journal. 2013;3:e123.

509. Carreno BM, Collins M. The B7 family of ligands and its receptors: new pathways for costimulation and inhibition of immune responses. Annual review of immunology. 2002;20:29-53.

510. Tel J, Smits EL, Anguille S, Joshi RN, Figdor CG, de Vries IJ. Human plasmacytoid dendritic cells are equipped with antigen-presenting and tumoricidal capacities. Blood. 2012;120(19):3936-44.

511. Bernhard CA, Ried C, Kochanek S, Brocker T. CD169+ macrophages are sufficient for priming of CTLs with specificities left out by cross-priming dendritic cells. Proceedings of the National Academy of Sciences of the United States of America. 2015;112(17):5461-6.

512. Beauvillain C, Delneste Y, Scotet M, Peres A, Gascan H, Guermonprez P, et al. Neutrophils efficiently cross-prime naive T cells in vivo. Blood. 2007;110(8):2965-73.

513. Mouries J, Moron G, Schlecht G, Escriou N, Dadaglio G, Leclerc C. Plasmacytoid dendritic cells efficiently cross-prime naive T cells in vivo after TLR activation. Blood. 2008;112(9):3713-22.

514. Schlecht G, Garcia S, Escriou N, Freitas AA, Leclerc C, Dadaglio G. Murine plasmacytoid dendritic cells induce effector/memory CD8+ T-cell responses in vivo after viral stimulation. Blood. 2004;104(6):1808-15.

515. Vance RE, Jamieson AM, Cado D, Raulet DH. Implications of CD94 deficiency and monoallelic NKG2A expression for natural killer cell development and repertoire formation. Proceedings of the National Academy of Sciences of the United States of America. 2002;99(2):868-73.

516. Zhang L. PD-1/PD-L1 interactions inhibit antitumor immune responses in a murine acute myeloid leukemia model. 2009;114(8):1545-52.

517. Ghosh A, Wolenski M, Klein C, Welte K, Blazar BR, Sauer MG. Cytotoxic T cells reactive to an immunodominant leukemia-associated antigen can be specifically primed and expanded by combining a specific priming step with nonspecific large-scale expansion. Journal of immunotherapy (Hagerstown, Md : 1997). 2008;31(2):121-31.

518. Nakajima H, Oka Y, Tsuboi A, Tatsumi N, Yamamoto Y, Fujiki F, et al. Enhanced tumor immunity of WT1 peptide vaccination by interferon-beta administration. Vaccine. 2012;30(4):722-9.

519. Scholer A, Hugues S, Boissonnas A, Fetler L, Amigorena S. Intercellular adhesion molecule-1-dependent stable interactions between T cells and dendritic cells determine CD8+ T cell memory. Immunity. 2008;28(2):258-70.

520. Deeths MJ, Mescher MF. ICAM-1 and B7-1 provide similar but distinct costimulation for CD8+ T cells, while CD4+ T cells are poorly costimulated by ICAM-1. European journal of immunology. 1999;29(1):45-53.

521. Bhella D. The role of cellular adhesion molecules in virus attachment and entry. Philosophical transactions of the Royal Society of London Series B, Biological sciences. 2015;370(1661):20140035.

522. Tardif MR, Tremblay MJ. Presence of host ICAM-1 in human immunodeficiency virus type 1 virions increases productive infection of CD4+ T lymphocytes by favoring cytosolic delivery of viral material. Journal of virology. 2003;77(22):12299-309.

523. Crozat K, Beutler B. TLR7: A new sensor of viral infection. Proceedings of the National Academy of Sciences of the United States of America. 2004;101(18):6835-6.

524. Eng HL, Hsu YY, Lin TM. Differences in TLR7/8 activation between monocytes and macrophages. Biochemical and biophysical research communications. 2018;497(1):319-25.

525. Thomann S, Boscheinen JB, Vogel K, Knipe DM, DeLuca N, Gross S, et al. Combined cytotoxic activity of an infectious, but non-replicative herpes simplex virus type 1 and plasmacytoid dendritic cells against tumour cells. Immunology. 2015;146(2):327-38.

526. Hamalainen S, Nurminen N, Ahlfors H, Oikarinen S, Sioofy-Khojine AB, Frisk G, et al. Coxsackievirus B1 reveals strain specific differences in plasmacytoid dendritic cell mediated immunogenicity. Journal of medical virology. 2014;86(8):1412-20.

527. Guillerme JB, Boisgerault N, Roulois D, Menager J, Combredet C, Tangy F, et al. Measles virus vaccine-infected tumor cells induce tumor antigen cross-presentation by human plasmacytoid dendritic cells. Clinical cancer research : an official journal of the American Association for Cancer Research. 2013;19(5):1147-58.

528. Cao H, Dai P, Wang W, Li H, Yuan J, Wang F, et al. Innate immune response of human plasmacytoid dendritic cells to poxvirus infection is subverted by vaccinia E3 via its Z-DNA/RNA binding domain. PloS one. 2012;7(5):e36823.

529. Diaz-Rodriguez Y, Cordeiro P, Belounis A, Herblot S, Duval M. In vitro differentiated plasmacytoid dendritic cells as a tool to induce anti-

leukemia activity of natural killer cells. Cancer immunology, immunotherapy : CII. 2017;66(10):1307-20.

530. Rickmann M, Krauter J, Stamer K, Heuser M, Salguero G, Mischak-Weissinger E, et al. Elevated frequencies of leukemic myeloid and plasmacytoid dendritic cells in acute myeloid leukemia with the FLT3 internal tandem duplication. Annals of hematology. 2011;90(9):1047-58.

531. Goswami M, Prince G, Biancotto A, Moir S, Kardava L, Santich BH, et al. Impaired B cell immunity in acute myeloid leukemia patients after chemotherapy. Journal of translational medicine. 2017;15(1):155.

532. Torelli GF, Guarini A, Palmieri G, Breccia M, Vitale A, Santoni A, et al. Expansion of cytotoxic effectors with lytic activity against autologous blasts from acute myeloid leukaemia patients in complete haematological remission. British journal of haematology. 2002;116(2):299-307.

533. Braciak TA, Wildenhain S, Roskopf CC, Schubert IA, Fey GH, Jacob U, et al. NK cells from an AML patient have recovered in remission and reached comparable cytolytic activity to that of a healthy monozygotic twin mediated by the single-chain triplebody SPM-2. Journal of translational medicine. 2013;11:289.

534. Sieber S, Wirth L, Cavak N, Koenigsmark M, Marx U, Lauster R, et al. Bone marrow-on-a-chip: Long-term culture of human haematopoietic stem cells in a three-dimensional microfluidic environment. Journal of tissue engineering and regenerative medicine. 2018;12(2):479-89.

535. Huang X, Zhu B, Wang X, Xiao R, Wang C. Three-dimensional co-culture of mesenchymal stromal cells and differentiated osteoblasts on human bio-derived bone scaffolds supports active multi-lineage hematopoiesis in vitro: Functional implication of the biomimetic HSC niche. International journal of molecular medicine. 2016;38(4):1141-51.

536. Kreiter S, Diken M, Selmi A, Diekmann J, Attig S, Hüsemann Y, et al. FLT3 Ligand Enhances the Cancer Therapeutic Potency of Naked RNA Vaccines. Cancer research. 2011;71(19):6132-42.

537. Maraskovsky E, Daro E, Roux E, Teepe M, Maliszewski CR, Hoek J, et al. In vivo generation of human dendritic cell subsets by Flt3 ligand. Blood. 2000;96(3):878-84.

538. Tel J, Sittig SP, Blom RA, Cruz LJ, Schreibelt G, Figdor CG, et al. Targeting uptake receptors on human plasmacytoid dendritic cells triggers antigen cross-presentation and robust type I IFN secretion. Journal of immunology (Baltimore, Md : 1950). 2013;191(10):5005-12.

539. Tel J, Aarntzen EH, Baba T, Schreibelt G, Schulte BM, Benitez-Ribas D, et al. Natural human plasmacytoid dendritic cells induce antigen-specific T-cell responses in melanoma patients. Cancer research. 2013;73(3):1063-75.

540. Fischer K, Tognarelli S, Roesler S, Boedicker C, Schubert R, Steinle A, et al. The Smac Mimetic BV6 Improves NK Cell-Mediated Killing of Rhabdomyosarcoma Cells by Simultaneously Targeting Tumor and Effector Cells. Frontiers in immunology. 2017;8:202.

541. de Graaf JF, de Vor L, Fouchier RAM, van den Hoogen BG. Armed oncolytic viruses: A kick-start for anti-tumor immunity. Cytokine & growth factor reviews. 2018;41:28-39.

542. Nguyen A, Ho L, Wan Y. Chemotherapy and Oncolytic Virotherapy: Advanced Tactics in the War against Cancer. Frontiers in oncology. 2014;4:145.

543. Wan S, Pestka S, Jubin RG, Lyu YL, Tsai YC, Liu LF. Chemotherapeutics and radiation stimulate MHC class I expression through elevated interferon-beta signaling in breast cancer cells. PloS one. 2012;7(3):e32542.

544. Bourgeois-Daigneault MC, St-Germain LE, Roy DG, Pelin A, Aitken AS, Arulanandam R, et al. Combination of Paclitaxel and MG1 oncolytic virus as a successful strategy for breast cancer treatment. Breast cancer research : BCR. 2016;18(1):83.

Appendix

Appendix

List of manufacturers and suppliers

Abcam	330 Cambridge Science Park Cambridge, CB4 0FL, UK
Alpha Laboratories	40 Parham Drive, Eastleigh Hampshire, SO50 4NU, UK
ATCC	American Type Culture Collection (ATCC), 10801 University Boulevard, Manassas, VA 20110 USA
BD Biosciences Manufacturer of BD Falcon brand	2350 Qume Drive San Jose, CA 95131, USA
Beckman Coulter (UK) Ltd.	Biomedical Research, Oakley Court, Kingsmead Business Park, London Road, High Wycombe, Bucks., HP11 1JU, UK
BioLegend	9729 Pacific Heights Blvd San Diego, CA 92121, USA
Bio-Rad Lab Ltd.	Bio-Rad Laboratories Ltd., Bio-Rad House, Maxted Road, Hemel Hempstead, Hertfordshire, HP2 7DX, UK
eBioscience Ltd	2nd Floor, Titan Court, 3 Bishop Square, Hatfield, AL10 9NA,UK
Fresenius Kabi AS	Else-Kröner-Straße 1 61352 Bad Homburg Germany

Fisher Scientific UK Ltd. Supplier of Eppendorf	Bishop Meadow Road, Loughborough, Leicestershire, LE11 5RG, UK
GeneTex®, Inc.	2456 Alton Parkway, Irvine, CA 92606, USA
Integrated DNA Technologies, Inc	8180 N. McCormick Blvd. Skokie, Illinois 60076, USA
Greiner Bio-One GmBH	Bad Haller Str. 32 4550 Kremsmünster, Austria
Mabtech	Box 1233, SE-131 28 Nacka Strand, Sweden
MBL International	15A Constitution Way Woburn, MA 01801, USA
Merck Millipore (UK) Ltd.	Suite 3 & 5. Building 6. Croxley Green Business Park, Watford, WD18 8YH, UK
Miltenyi Biotec GmBH	Friedrich-Ebert-Straße 68, 51429 Bergisch Gladbach, Germany
Molecular Devices	3860 N First Street San Jose, CA 95134, USA
National Health Service Blood and Transplant	Bridle Path, Leeds, LS15 7TW, UK
Nuaire	Western Industrial Estate Caerphilly, CF83 1NA, UK
Oncolytics Biotech Inc.	1167 Kensington Crescent NW Calgary, AB, Canada
PBL Assay Science	131 Ethel Road West, Suite 6 Piscataway, NJ 08854, USA

PeproTech	Princeton Business Park 5 Crescent Avenue, P.O. Box 275 Rocky Hill, NJ 08553, USA
Perkin Elmer	Kelvin Close, Birchwood Science Park, Risley, Warrington, Cheshire WA3 7PB, UK
Qiagen Ltd.	Boundary Court, Gatwick Road, Crawley, West Sussex, RH10 2AX, UK
R & D Systems Europe Ltd.	19 Barton Lane, Abingdon Science Park, Abingdon,OX14 3NB, UK
Sanyo	Sanyo Gallenkamp Plc., Monarch Way, Belton Park, Loughborough, LE11 5XG, UK
Sera Laboratories Intl Ltd	Unit 44 Bolney Grange Business Park Haywards Heath, RH17 5PB, UK
Sigma-Aldrich Ltd. Supplier of Corning Costar	3050 Spruce St. St. Louis, MO 63103, USA
Thermo Fisher Scientific Supplier of Oxoid, Gibco, Invitrogen, Evos, Nunc, Applied Biosystems, and Life Technologies brands	Unit 5, The Ringway Centre, Edison Rd., Basingstoke, Hampshire, RG21 6YH, UK
UVP Llc.	2066 W. 11th St. Upland, CA 91786, USA
Viralytics Ltd.	Suite 305, Level 3, 66 Hunter Street Sydney NSW 2000 Australia

ELISA antibodies

Human ELISA antibodies

Target molecule	Species of origin	Clone	Role	Dilution	Coating buffer/blocking solution
IFN-α (pan)	Mouse	MT1/3/5	Capture	1:250	PBS
IFN-α (pan)	Mouse	MT2/4/6	Detection	1:1000	10% FBS in PBS
IFN-γ	Mouse	NIB42	Capture	1:250	100nM $NaHCO_3$ in ddH2O
IFN-γ	Mouse	4S.B3	Dilution	1:500	10% FBS in PBS

IFN-α: Mabtech, IFN-γ: BD Biosciences

Murine ELISA antibodies

Target Molecule	Species of origin	Clone	Role	Dilution	Coating buffer/blocking solution
IFN-γ	Rat	R4-6A2	Capture	1:500	100nM $NaHCO_3$ in ddH2O
IFN-γ	Rat	XMG1.2	Detection	1:500	10% (v/v) FCS in PBS

Source: BD Biosciences

Human ELISA standards

Cytokine	Top standard concentration	Manufacturer
IFN-α	2000 pg/mL	R&D Systems
IFN-γ	10 000 pg/mL	BD Biosciences

Murine ELISA standards

Cytokine	Top standard concentration	Manufacturer
IFN-γ	10 000 pg/mL	R&D Systems

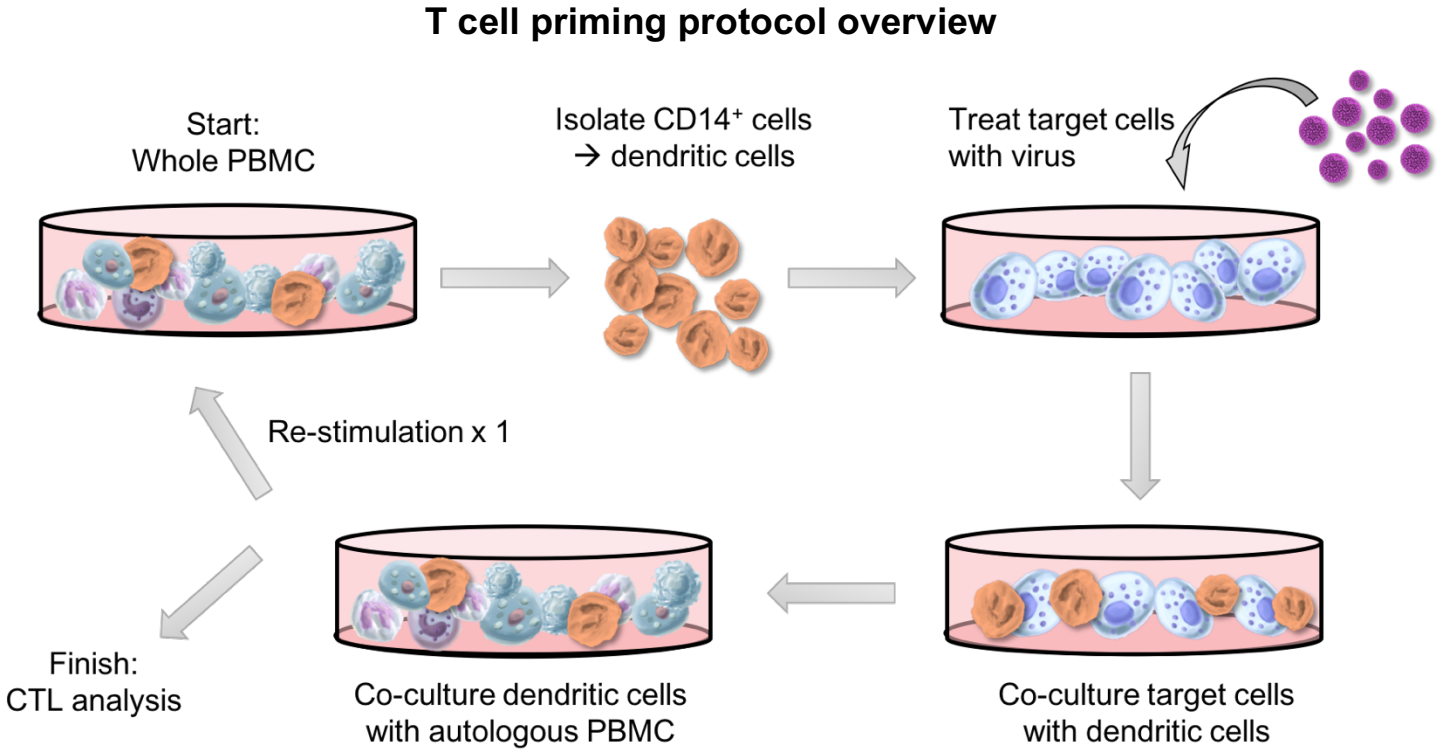

Figure A-1: Illustration of CTL priming protocol.

PBMC were isolated from healthy donors and approx. 25% were used for the generation of dendritic cells (DC) and remaining PBMC were frozen. DC were generated by isolating $CD14^+$ cells and culturing them in the presence of GM-CSF and IL-4 for 5 days. Simultaneously, target cells were either left untreated, or treated with virus for 24 hrs. DC were then loaded with untreated or treated target cells, respectively, by co-culture for 48 hrs. Tumour-loaded DC were then co-cultured with autologous PBMC (thawed from frozen). Then, a round of re-stimulation was initiated with loading of new target cells onto freshly generated DC. After 7 days of culture, CTLs were re-stimulated with fresh tumour-loaded DC, and following culture for another 6 days, primed CTLs were analysed using ^{51}Cr release assays and flow cytometry-based assays.